The Pennsylvania State University

The Graduate School

College of Agricultural Sciences

SPATIAL AND TEMPORAL VARIABILITY OF NITROGEN TRANSPORT IN RIPARIAN ZONE SEEPS

A Dissertation in

Agricultural and Biological Engineering

by

Mark R. Williams

Submitted in Partial Fulfillment
of the Requirements
for the Degree of

Doctor of Philosophy

August 2013

The dissertation of Mark R. Williams was reviewed and approved* by the following:

Herschel A. Elliott
Professor of Agricultural and Biological Engineering
Dissertation Adviser, Chair of Committee

Anthony R. Buda
Hydrologist, USDA-ARS PSWMRU
Special Member

James M. Hamlett
Associate Professor of Agricultural and Biological Engineering

Kamini Singha
Associate Professor of Hydrologic Science and Engineering

Curtis J. Dell
Soil Scientist, USDA-ARS PSWMRU

Paul H. Heinemann
Professor of Agricultural and Biological engineering
Head of the Department of Agricultural and Biological Engineering

*Signatures are on file in the Graduate School

ABSTRACT

Excess nitrate-nitrogen (NO_3-N) in terrestrial and aquatic ecosystems has resulted in numerous water quality problems throughout the U.S., which emphasizes the need to develop effective management plans to deal with NO_3-N pollution, especially in agricultural catchments. Emergent groundwater-fed seeps have been identified as a potentially significant source of water and NO_3-N to streams in headwater catchments, yet few studies have evaluated NO_3-N transport in seeps and their influence on downstream water quality. To address this need, four studies were undertaken to better understand the role of seeps in FD36 and RS, two small (0.40 and 0.45 ha, respectively) agricultural headwater catchments located in the Ridge and Valley physiographic region of central Pennsylvania.

The first study (Chapter 2) examined spatial and temporal variations in NO_3-N concentration and transport potential in shallow groundwater of three seep and adjacent non-seep areas in the riparian zone. Results showed that NO_3-N concentrations within the seep areas were significantly greater than NO_3-N concentrations in the non-seep areas. Water table depth was also more spatially variable in the seep areas compared to the non-seep areas, which indicated less uniform flow, shorter residence times for groundwater, and greater potential for NO_3-N delivery to the stream from seep areas.

The second study (Chapter 3) used electrical resistivity imaging (ERI) to visualize seep zone formation in order to enhance our understanding of the chemical-hydrologic interactions in the riparian zone. ERI data showed large, localized decreases in resistivity within a seep area following a series of three precipitation events, which suggested that groundwater was upwelling through discontinuities in the fragipan. The non-seep area showed no such response. The changes in resistivity within the seep area coincided with increased NO_3-N concentrations. Results

showed that seeps were highly dynamic and responsive to precipitation events compared to non-seep areas, and subsurface hydrologic processes in seep zones could significantly affect NO_3-N concentrations in the groundwater being delivered to the stream.

The third study (Chapter 4) was intended to improve our understanding of spatial patterns in stream NO_3-N concentrations during baseflow and stormflow conditions, and to determine if seeps contributed to the patterns observed in stream chemistry. Semi-variogram analysis showed that stream NO_3-N concentrations were spatially dependent during baseflow conditions. Spatial patterns in stream NO_3-N concentrations were positively correlated with the number of flowing seeps in the monitored reach. Additionally, stream reaches with seep inputs had increased stream NO_3-N concentrations relative to areas with no seep inputs. These results suggest that seeps are an important source of NO_3-N in headwater agricultural catchments and play a key role in determining stream NO_3-N concentrations.

The final study (Chapter 5) was undertaken to quantify factors that influenced seep NO_3-N concentrations, such as NO_3-N retention and/or removal along seep surface flow pathways and N application rates throughout the catchment, and to determine the relationship between seep and stream water quality. Results showed that in FD36, NO_3-N concentrations generally decreased downseep and that NO_3-N retention within these seeps varied seasonally, with most of the retention occuring during in the summer. Only minimal NO_3-N retention was observed in seeps within the RS catchment. Seasonal variation in seep NO_3-N retention was related to both discharge and air temperature in FD36. However, the effects of N application rates throughout the catchment played a more significant role in determining NO_3-N concentrations in seep water in both catchments. In both FD36 and RS, seep NO_3-N concentrations were significantly correlated with stream NO_3-N concentration at the catchment outlet.

The results of this research highlight the need for management practices that decrease NO_3-N concentrations in seep discharge (i.e., changes in N application rates) or enhance NO_3-N

retention and/or removal within seep surface flow paths (i.e., riparian zone wetlands or bioreactors) in order to improve stream water quality in agricultural streams. Future studies are needed to improve our ability to identify seepage inputs to streams, as well as to predict where seepage zones are likely to occur on the landscape. Seeps should be considered critical source areas for NO_3-N delivery to streams since they have been shown to contribute higher fluxes of water and nutrients to streams relative to the surrounding riparian zone. Overall, the four studies in this dissertation demonstrated that seeps exert a strong influence on streamflow generation and NO_3-N fluxes in headwater catchments. Dissertation results also showed that an improved understanding of seep formation, hydrology, and biogeochemistry is necessary for evaluating the potential effectiveness of management practices aimed at improving stream water quality in headwater catchments.

TABLE OF CONTENTS

LIST OF FIGURES

LIST OF TABLES

ACKNOWLEDGEMENTS

This Ph. D. dissertation is the culmination of my hard work and long hours over the past nine years (2004-2013) at Penn State University. During my time at Penn State, I have obtained three degrees, learned how to design and conduct sound research projects, collaborated with some of the top scientists and engineers in the field, and collected thousands of soil and water samples. I have not only grown professionally, but also personally as a husband, colleague, and friend. I could not have done this all on my own. I would like to thank the people who have provided me with support, advice, and guidance throughout my journey.

I would first like to extend my sincerest thanks to Dr. John Schmidt for his contributions to the design of this project and his thoughtful advice during the initial stages of sample collection. I would also like to thank my committee members: Dr. Herschel Elliott, Dr. Anthony Buda, Dr. James Hamlett, Dr. Kamini Singha, and Dr. Curtis Dell. I truly appreciate your willingness to be actively involved in my research and I am grateful for your support and guidance. In addition, I would like to thank the Department of Agricultural and Biological Engineering and Dr. Paul Heinemann for offering me the financial support to complete my graduate studies at Penn State. In addition, I would like to acknowledge Dr. Elizabeth Boyer for her assistance with sample analysis and her interest in this project.

I would like to extend a very warm thank you to all of the research scientists and technicians at the USDA-Agricultural Research Service in University Park, PA and Klingerstown, PA. In particular, I would like to thank Michael Reiner and Todd Strohecker for all of their help in collecting and processing over 6,000 water samples. Rain, snow, freezing-cold, or extreme heat, they were always willing to offer assistance. Over the past three years, Klingerstown and FD36 have been my second home and I am sure going to miss it. I would also

like to thank Sarah Fishel for her help in collecting samples and her assistance in the laboratory. Without her help, I think I would still be sitting in the laboratory doing Murphy-Riley extractions and washing bottles.

I would like to express my deepest gratitude to my parents who throughout the years have supported and loved me. Without your support and love, none of this would have been possible. Lastly, I would like to thank my wife Rachel. You have been by my side through the good times and bad times. Whether it was late night talks about statistics, trips to Klingerstown in the rain, or all of the pairs of jeans I ruined working in the laboratory, you have always been there for me and I am forever thankful for your constant support. Your friendship and love have shaped who I am today.

CHAPTER 1

Introduction and Literature Review

Located at the interface between terrestrial and aquatic ecosystems, riparian zones function as areas of transition that are often distinguished by hydrology, vegetation, and soils (*Swanson et al., 1982; Lowrance et al., 1985*). Hence, riparian zones are complex environments that exhibit a high degree of spatial and temporal variability with respect to hydrological and biogeochemical processes. The overall goal of this research project was to better understand how groundwater-fed seeps affect nitrogen (N) transport in riparian zones and ultimately N delivery to streams. To accomplish this goal, four studies were completed in two central Pennsylvania agricultural headwater catchments (FD36 and RS) in order to evaluate seep area formation, hydrology, and biogeochemistry.

This first chapter provides the rationale for the current research project and highlights previous work and information on riparian zones, seeps, and N transport. Following the literature review, chapter two examines the spatial and temporal variation of N concentrations in shallow groundwater within three seep and adjacent non-seep areas of the riparian zone. Chapter three describes the visualization of subsurface flow pathways using electrical resistivity imaging (ERI). Chapter four presents results from a study evaluating spatial patterns in stream N concentrations during baseflow and precipitation events and describes how seeps contribute to the patterns observed in stream chemistry. Chapter five quantifies N retention and transport in seep-fed surface flow pathways and examines potential relationships between N application rates throughout the catchment, seeps, and stream water quality. The final chapter, chapter six, summarizes the principal findings of this research and discusses the importance of understanding

dynamic hydrologic processes and the implications of these processes on watershed N management.

Excess Nutrients in the Environment

In order to maintain profitable crop production, manure and commercial fertilizers are often applied on agricultural lands. Manure and fertilizers provide plants with essential nutrients, such as N and phosphorus (P), which are required for their growth and development. In many instances, however, nutrient additions to agricultural systems have overwhelmed natural nutrient cycles. Globally, more nutrients are added as fertilizers than are removed as produce (*Carpenter et al., 1998*). Excess nutrients that are transported from agricultural lands can become environmental contaminants and result in the eutrophication and degradation of surface water bodies (*Carpenter et al., 1998; Correll, 1998; Daniel et al., 1998; Boesch et al., 2001*).

Eutrophication caused by excessive inputs of nutrients is the most common impairment of surface waters in the U.S. (*U.S. EPA, 2008*). Impairment is measured as the area of surface water not suitable for designated uses such as drinking, irrigation, industry, recreation, or fishing. Across the U.S., eutrophication accounts for approximately 50% of the impaired lake area and 60% of impaired rivers (*U.S. EPA, 2008*). It is also the most widespread pollution problem of U.S. estuaries (*NRCS, 2003*). An increased incidence of nuisance algal blooms and proliferation of aquatic weeds is often evidence of eutrophication. Not only are algal blooms and aquatic weeds aesthetically unappealing, but their death and decomposition can cause anoxia (i.e., no oxygen) and hypoxia (i.e., low oxygen) in stratified waters. Low levels of dissovled oxygen can result in significant losses of fish and shellfish resources (*Baden et al., 1990; Hansson and Rudstam, 1990*), which negatively impacts recreational and commercial fishing.

Table 1.1 Pennsylvania nitrogen, phosphorus, and sediment loads delivered to the Chesapeake Bay in 2009.

Sector	Nitrogen	Phosphorus	Sediment
	(kg yr^{-1})		(metric ton yr^{-1})
Agriculture	27,211,000	797,700	813,600
Forest	10,311,000	280,500	226,300
Point Source	5,815,000	533,600	7,500
Urban/Developed	3,047,000	171,800	119,000
Septic	1,495,000	0	0
Air Deposition to Water	490,000	18,600	0
Total	**48,370,000**	**1,802,000**	**1,167,000**

Values adapted from the PA Chesapeake Bay Watershed Implementation Plan (*PA DEP, 2010*)

Reducing nutrient inputs has been the focus of extensive restoration projects during the past 25 years in many watersheds, including that of the Chesapeake Bay. Compared to nutrient management plans for the Chesapeake Bay in 1985, however, Pennsylvania has only achieved 28%, 46%, and 42% of its N, P, and sediment reduction goals, respectively (*PA DEP, 2010*). The majority of the N and sediment delivered to the Chesapeake Bay via Pennsylvania waterways is from agricultural sources (Table 1.1). Insufficient progress toward nutrient reduction goals and continued poor water quality in the Chesapeake Bay has prompted the U.S. Environmental Protection Agency (U.S. EPA) to establish the Chesapeake Bay Total Maximum Daily Load (TMDL). The TMDL is designed to ensure that all pollution control measures needed to fully restore the Bay and its tidal rivers are in place by 2025, with at least 60% of the actions completed by 2017. To meet the goals set by the EPA, Pennsylvania needs to achieve an additional 13.4, 0.55, and 258 million kg reduction in N, P, and sediment loads, respectively (*PA DEP, 2010*). The attainment of these water quality goals will largely rely on nutrient and sediment reductions by the agriculture sector, as well as the development of effective and viable remedial strategies that minimize pollutant losses from agricultural landscapes.

Riparian Zones for Controlling Nonpoint Pollution

Excessive nutrient inputs and the resultant impacts on water quality have motivated research aimed at developing best management practices (BMPs) that are able to intercept and attenuate nutrients. The establishment and conservation of riparian zones has emerged as the most widely used BMP by state and federal resource agencies in agricultural landscapes to help improve water quality (*NRCS, 2003; Bernhardt et al., 2005*). Since 2002, a total of 6,240 km of riparian zones have been re-established along waterways in Pennsylvania (*PA DEP, 2010*). The effectiveness of riparian zones as BMPs arises mainly from their positioning on the landscape (Figure 1.1). Nutrients from agricultural upland areas must be transported through the riparian zone in either surface runoff or in groundwater; therefore, the riparian zone creates a "buffer" between the nutrient source and the stream channel.

In studies documenting riparian zone nutrient attenuation, the percent difference in nutrient concentration between the influent and effluent of the riparian zone is often calculated

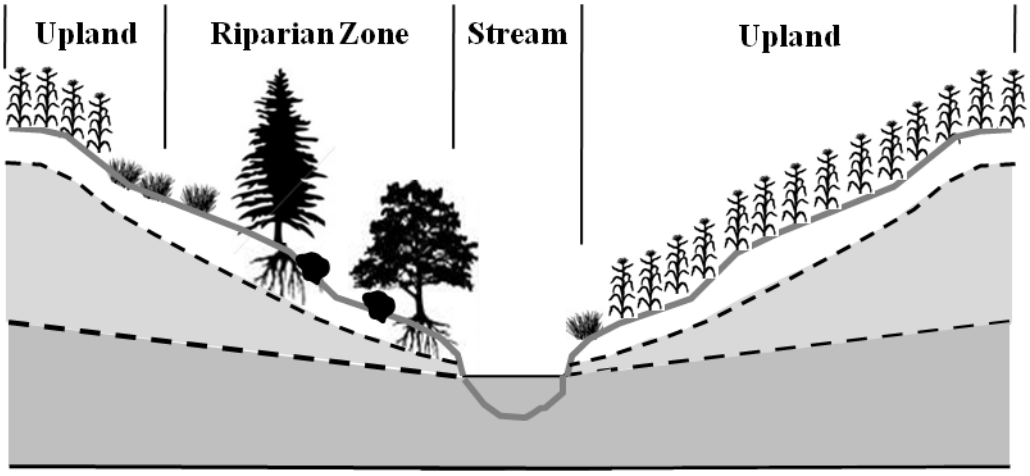

Figure 1.1

Cross-section identifying the position of the upland, riparian zone, and stream channel relative to one another within the landscape. Riparian zones act as a buffer between the upland agricultural area and the stream channel because nutrients have to be transported through the riparian zone before they enter the stream.

(*Hill, 1996*). Alternatively, the percent difference in nutrient concentration between the terminus of a control riparian zone to that of a test riparian zone can also be calculated. Peterjohn and Correll (1984) found that 90% to 98% of the nitrate-N (NO_3-N) was removed along a 19 m and a 50 m transect in a deciduous riparian forest. Jordan et al. (1993) also observed greater than 95% removal of NO_3-N in a deciduous riparian forest adjacent to agricultural land in the Delmarva Peninsula, Maryland. In Georgia, groundwater NO_3-N inputs from cropland that varied seasonally from 2 to 6 mg L^{-1} declined rapidly to less than 0.5 mg L^{-1} within a bottomland hardwood forest (*Lowrance et al., 1984*). At a second site in the same watershed, Lowrance (1992) reported a 94% decrease in NO_3-N within a 55 m wide riparian zone. Jacobs and Gilliam (1985) found that NO_3-N declined greater than 90% in shallow groundwater flow from cropland through a riparian area in North Carolina.

Over the years, numerous studies similar to those summarized above have been conducted on riparian zones with different widths, hydrology, and vegetation types. A complete review of riparian zone studies and their findings is beyond the scope of this introductory chapter; however, Mayer et al. (2007) conducted a meta-analysis of 88 peer-reviewed riparian zone studies to determine how N retention and/or removal (i.e., riparian zone effectiveness) was related to the characteristics of the riparian zone (Table 1.2). The authors concluded that N removal effectiveness varied widely among studies. While wide riparian zones (> 50 m) more consistently removed significant portions of N than narrow riparian zones (0 – 25 m), riparian zones of various vegetation types were equally effective at removing N. They also concluded that subsurface removal of N was efficient, but did not appear to be related to riparian zone width. Conversely, surface removal of N was partly related to riparian zone width. These results suggest that riparian zone width is an important consideration in managing N in watersheds. However, the inconsistent effects of riparian zone width and vegetation on N removal reflect the fact that soil

Table 1.2 Percent effectiveness of riparian zones at removing N based on width, hydrology, and vegetation type.

Riparian Zone Variable	n	Mean Removal Effectiveness (% ± 1 SE)
All Studies	88	67.5 ± 4.0
Width Category		
0 – 25 m	45	57.9 ± 6.0
26 – 50 m	24	71.4 ± 7.8
> 50 m	19	85.2 ± 4.8
Flow Pathway		
Surface	23	41.6 ± 7.1
Subsurface	65	76.7 ± 4.3
Vegetation Type		
Forest	31	72.2 ± 6.9
Forested Wetland	7	85.0 ± 5.2
Herbaceous/Forest	43	79.5 ± 7.3
Wetland	7	72.3 ± 12

Values adapted from Mayer et al. (2007)

type, hydrology (e.g., flow pathways), and subsurface biogeochemistry (e.g., organic carbon supply, N inputs) also are important factors governing N removal.

The overarching conclusion that can be drawn from the vast riparian zone literature is that riparian zone effectiveness is highly variable and inconsistent. As the results of Mayer et al. (2007) suggest, other factors, such as hydrology, may play a more important role in determining riparian zone nutrient removal effectiveness compared to the traditional parameters of width and vegetation type. Knowledge of hydrology is essential to understanding riparian zone biogeochemistry (*Correll and Weller, 1989; Hill, 1990; McDowell et al., 1992; Gilliam, 1994*) and although its importance is recognized, hydrology is often not thoroughly investigated in studies of nutrient transport through riparian zones (*Hill, 1996*). Additional research is therefore needed to improve the understanding of riparian zone hydrology and to better characterize how surface and subsurface flow pathways influence stream water quality.

Surface water, Groundwater, and their Interaction

Over the past two decades, researchers and conservationists have worked diligently to develop BMPs to intercept and attenuate nutrients before they enter surface water bodies. While there has been some success, the effectiveness of these BMPs has varied (*Mayer et al., 2007*). Nutrients are typically transported from the agricultural source to the surface water body with the movement of water; therefore, in order to increase BMP efficacy, it is important to identify and understand hydrologic processes. In general, there are four major pathways for water and nutrient transport through the riparian zone to a surface water body (Figure 1.2). Water and nutrients may move laterally along a shallow confining layer or bedrock (Figure 1.2a), or they may move into deeper and longer groundwater flow pathways if a confining layer is absent (Figure 1.2b). During and following precipitation events, water can also be transported across the land surface via faster flow pathways such as surface runoff (Figure 1.2c). Additionally, water and nutrients moving through the shallow subsurface may emerge onto the surface as either a seep or spring (Figure 1.2d).

The major problem that has challenged researchers and hindered the success of many BMPs is that the transport of water and nutrients from agricultural sources to surface water is typically through a combination of these four major flow pathways. Hydrologic processes can also vary among seasons, in response to precipitation events, and spatially across the landscape. The high degree of spatial and temporal variability in hydrologic processes can alter the location, timing, and duration of N transport from the source to the stream, which makes the design and placement of BMPs difficult. Emergent groundwater seeps, in many ways, embody the spatial and temporal variability of hydrologic processes observed in the riparian zone. Water and N are transported in both surface and subsurface hydrologic components in seeps. Discharge from seeps can be intermittent and originate from both shallow and deep groundwater flow paths. Seeps also

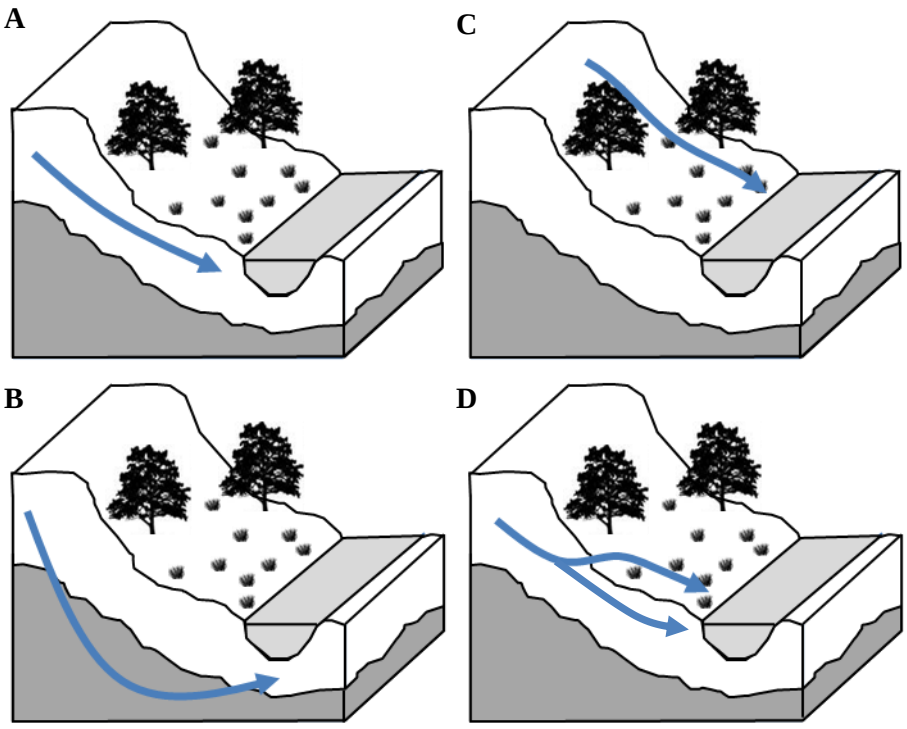

Figure 1.2

Major water and nutrient flow pathways through the riparian zone: a) shallow groundwater flow; b) deep groundwater flow; c) surface runoff; and d) spring and seepage flow.

change rapidly in response to precipitation events by expanding and contracting in size. While seeps are only one of the major flow pathways of water and nutrients through the riparian zone, their ever-changing characteristics makes them an ideal candidate for studying how dynamic hydrologic processes affect nutrient transport.

Occurrence and Hydrology of Seeps

Seeps can be found in many watersheds across the U.S. (*Pionke et al., 1988*) and are often the predominant source of streamflow in headwater streams (*O'Driscoll and DeWalle, 2010*). They may occur as simple point sources that emerge at a single location and only gain groundwater at this emergence point. Seep discharge may interact with vegetation and sediments

as it flows to the stream channel or it may infiltrate back into the subsurface before entering the stream. Alternatively, groundwater seepage may emerge at multiple locations along the length of the seep. It is also likely that a mixture of discrete point inputs, return flows, and new seepage inputs exist along a single seep (Figure 1.3).

The formation of seep areas in the riparian zone typically takes place in watersheds where substantial percolation occurs seasonally and the downslope transmission capacity of the subsurface flow system is restricted due to geologic, geometric, or hydrologic properties (*Pionke et al., 1988*). Geologic, geometric, and hydrologic properties that result in seep formation include low or decreased downslope water table gradients (e.g., decreasing land slope without increased water storage) (*Pionke et al., 1988*), small cross-sectional areas (e.g., slope break or reduced aquifer thickness) (*Stein et al., 2004*), and reduced permeability (e.g., downgradient shifts from coarser to finer textured soils or geologic deposits) (*Vidon and Hill, 2004*). While these properties establish a large-scale control on the extent and location of seeps, individual or a short series of.

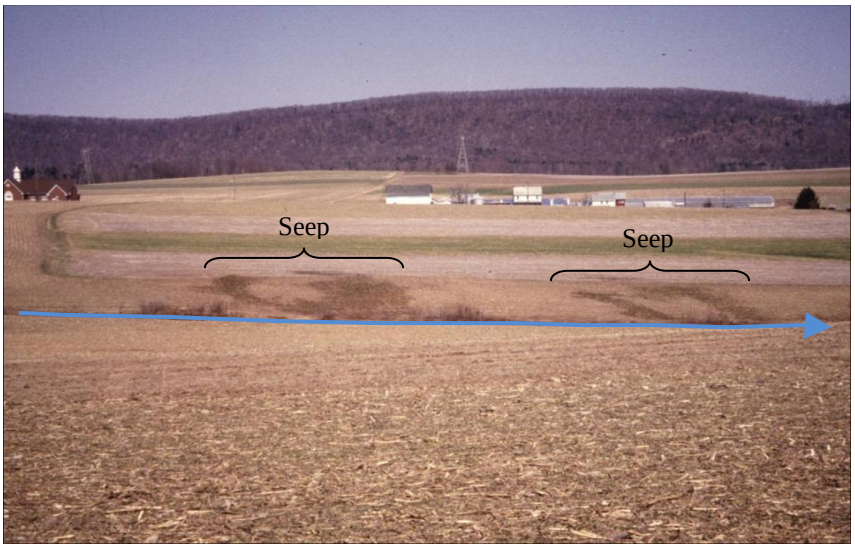

Figure 1.3

Seeps located in a central Pennsylvania headwater catchment following a precipitation event. The blue line indicates the location of the stream channel, which flows from left to right.

precipitation events can also serve to generate new seeps or expand existing seepage zones.

Seep hydrologic processes are often hard to quantify due to the complexities and difficulties associated with accurate discharge measurements in shallow, ill-defined seep channels (*Hill, 1996; O'Driscoll and DeWalle, 2010*). Several studies, however, have successfully measured seep discharge (*Baedke and Krothe, 2001; Amit et al., 2002; Gentry and Burbey, 2004*). Monitoring of seep discharge and evaluation of hydrographs can provide information on aquifer properties, such as transmissivity or specific yield, and flow pathways that may be supplying water to a seep. It also is useful for determining seep contributions to streamflow. In some instances, seep discharge can constitute more than 95% of streamflow in between precipitation events (*Srinivasan et al., 2002*).

Spatial and temporal patterns in stream and seep hydrologic processes in response to precipitation have also been observed and characterized in a small headwater catchment in the northeastern U.S. (*Pionke et al., 1988*). This research has resulted in a conceptual model that details the hydrologic sources of stream flow during an event and the contributions of seeps. During a typical event, the source of stream flow cycles from (1) baseflow dominated to (2) rainfall-diluted baseflow to (3) surface-runoff-dominated flow to (4) a progressively subsurface-discharge-dominated flow, which then drains back to (5) normal baseflow (*Pionke et al., 1988*). It is evident from this model that seeps play an important role in headwater catchment hydrology. Not only do seeps generate streamflow between precipitation events (i.e., baseflow), but they also affect streamflow during precipitation events. Seeps can discharge subsurface waters to the land surface, which can then drain to the stream, and can also be major surface runoff producers. Additionally, expanding seeps during a precipitation event may interact with previously unsaturated areas, which impart a different chemical signature than that of the initial contributing area. Both the expanding seep and the ratio of seepage to surface runoff can result in concomitant changes in stream water quality.

The study by Pionke et al. (1988) highlights the importance of seep hydrologic processes; yet, few studies have documented the relationship between hydrologic flow pathways in seeps and water quality. The spatial and temporal patterns in seep water flow pathways likely have a significant impact on stream water quality. Water and N flowing across the surface or in deep groundwater flow pathways may bypass the riparian zone, whereas water and N moving in shallow groundwater may interact with riparian zone sediments and vegetation where the N can be retained or removed. A better understanding of the chemical-hydrologic interactions in seeps is therefore needed for more effective BMP design and placement in agricultural headwater catchments.

Nutrient Dynamics in Seeps

While riparian zones have been commonly shown to reduce N in groundwater by 90% or more, significant variability in N removal efficiency has been documented (*Hill, 1996; Mayer et al., 2007*). Inconsistencies in nutrient removal efficiency may be due to differences in hydrologic flow pathways through the riparian zone. Previous research has indicated that riparian zones are highly effective in removing nutrients from shallow groundwater flow pathways that increase interaction with organic-rich surface soils favoring denitrification and plant uptake (*Peterjohn and Correll, 1984; Haycock and Burt, 1993*). In contrast, in landscapes where a shallow confining layer is absent, groundwater can be transported along deep, slower flow pathways through the riparian zone. Nutrient removal in these riparian zones has been shown to be less effective and dependent on interactions with sufficient supplies of electron donors such as organic carbon and reduced forms of sulfur or iron (*Bohlke and Denver, 1995; Devito et al., 2000; Puckett and Cowdery, 2002; Puckett and Hughes, 2005*). Lastly, overland flow produced by groundwater discharge has resulted in inconsistent nutrient removal (Table 1.3). Some studies of

Table 1.3 Summary of studies that document headwater channel, seep, or spring NO_3-N changes along surface flow paths in a variety of geographic settings.

Reference	NO_3-N conc. change	Sampling technique
Steinheimer et al., 1998	NO_3 gain	Upstream-downstream sampling
Warwick and Hill, 1988	NS NO_3 loss[a]	Tracer enrichment experiments
Hill, 1990	NS NO_3 loss	Spring flow through wetlands, upstream-downstream sampling
Rutherford and Nguyen, 2004	NO_3 loss	Wetland enclosures, tracer injections
Brusch and Nillson, 1993	NO_3 loss	Spring flow through wetlands, upstream-downstream sampling
Peterson et al., 2001	NO_3 loss	Headwater channels, N isotope injections
Burns et al., 1998	NO_3 loss	Spring flow through wetlands, upstream-downstream sampling

[a] NS = not significant

Table adapted from O'Driscoll and DeWalle (2010)

overland flow pathways have reported substantial removal of nutrients (*Brusch and Nilsson, 1993; Rutherford and Nguyen, 2004*), whereas others have found ineffective nutrient removal (*Warwick and Hill, 1988; Hill, 1990; Angier et al., 2002, 2005*).

Seeps often have both shallow and deep groundwater hydrologic components as well as overland flow; therefore, they may function both as a conduit and barrier to fluxes of nutrients in surface runoff and groundwater flowing from upland agricultural sources toward the stream. This creates the potential for significant spatial and temporal variability of nutrient inputs to streams (*West et al., 2001*). Few published studies have documented the variability in surface and groundwater nutrient cycling and retention along seeps; however, several recent studies have begun to explore this area. O'Driscoll and DeWalle (2010) investigated the function of seeps in an Appalachian forested watershed as a source or sink of NO_3-N to the stream. They found that at

the top of the seep (i.e., emergence point) concentrations of NO_3-N were relatively stable year-round. Seep top groundwater had higher median annual NO_3-N concentrations than seep bottom waters (i.e., where the seep enters the stream channel) (0.51 and 0.35 mg L^{-1}, respectively), which suggested an annual retention of NO_3-N by seeps. Overall, the study found a high positive correlation between seep bottom NO_3-N and stream outlet NO_3-N concentrations, indicating that seep processes are linked with stream NO_3-N concentrations.

A tracer study conducted in New Zealand by Rutherford and Nguyen (2004) provides further insight into seep nutrient retention and hydrologic processes. Their tracer results showed that approximately 24% of NO_3-N could be removed along a 1.5-m long flow pathway and that removal efficiency decreased during higher discharge periods because more of the downseep flow was moving along rapid surface flow pathways as opposed to slower, subsurface pathways. The tracer concentration data indicated that NO_3-N diffusion from high concentration surface waters to low concentration groundwater may have played an important role in downseep losses of N. Subsurface residence times on the order of 1 day were deemed sufficient to achieve significant NO_3-N reductions. This suggested that downseep NO_3-N concentration bypass events likely occurred when surface flow pathways dominated the seep discharge. Vertical exchange between surface water, soil water, and groundwater allowed seep water to spend more time in the subsurface environment, thereby increasing the potential for biotic assimilation of N or denitrification, as suggested by Gold et al. (2001) and Rosenblatt et al. (2001).

Spatial and temporal variability in nutrient transport and retention has also been characterized in terms of ‘hotspots’ and ‘hot moments’ (*McClain et al., 2003*). Hotspots are defined as regions that exhibit disproportionately high reaction rates relative to the surrounding area (matrix). Hot moments are defined as short periods of time that display disproportionately high reaction rates relative to longer intervening time periods. McCain et al. (2003) proposed that these phenomena, which are localized in space and time, have large impacts on the fluxes of

solutes and thus are critical to furthering our understanding of nutrient cycling. Research indicates that the development of biogeochemical hotspots and/or hot moments in riparian systems is generally governed by subtle changes in electron accepter and donor availability, redox conditions, and hydrologic conditions. Although limited in space and time, biogeochemical hotspots and hot moments have the ability to alter annual catchment nutrient budgets (*Gold et al., 2001; McClain et al., 2003; Vidon and Hill, 2004; Groffman et al., 2009*). Furthermore, transport hot phenomena are also critical to developing accurate annual nutrient budgets across the stream, riparian zone, and upland continuum (*Wigington et al., 2003*). Often, transport hot moments are associated with episodic hydrological events that occur in response to rainfall or snowmelt. Transport hotspots generally occur where the water table is closer to the land surface and where groundwater fluxes can be much larger and of longer duration. Seeps exhibit characteristics that favor both biogeochemical and transport-driven hotspots and moments. Dynamic hydrologic conditions, favorable redox potential, and potentially large fluxes of electron donors and acceptors all occur within a seep. Understanding the spatial and temporal patterns in seep nutrient retention and the relationship between hydrologic flow pathway and water quality is therefore critical to managing catchment nutrient budgets. Although seeps are a very small part of a catchment, they have the potential to exert major controls on streamflow chemistry and hydrology. Identifying and quantifying seep processes is an important step in understanding how landscape-level hydrologic dynamics contribute to whole catchment hydrologic and solute responses.

Research Objectives

The information that is presented in subsequent chapters is an extension of previous work on seep hydrologic processes and their influence on nutrient transport and stream water quality.

The specific objectives of the research project are shown in Table 1.4. Through a unique study design, the characterization and quantification of flow pathways for water and nutrient transport in riparian zone seeps of two small agricultural headwater catchments was completed with a high degree of spatial and temporal resolution. The information gained from this research can be used to consider which existing BMPs might be most effective at addressing NO_3-N emanating from emergent seeps. Since this project focused on processes and pathways that controlled nutrient transport, the information gained is applicable to many other sub-catchments within the Chesapeake Bay.

Table 1.4 Research objectives by chapter.

Chapter	Objective
2	a. Investigate the shallow groundwater dynamics and identify key hydrologic flow pathways within both seep and non-seep areas of the riparian zone b. Determine the relationship between subsurface hydrologic characteristics and N concentration within seep and non-seep areas c. Examine the N transport potential from both areas of the riparian zone
3	a. Investigate chemical and hydrologic interactions within a seep and adjacent area without a seep using standard hydrometric techniques b. Examine these interactions in the context of observed subsurface hydrologic responses visualized with ERI c. Use the results from objectives (a) and (b) to develop a conceptual model of seep zone formation, subsurface flow pathways, and N transport in the riparian zone
4	a. Quantify the variability of N concentration in two agricultural headwater streams b. Determine if spatial patterns of stream N concentrations are influenced by seeps c. Examine the controls of baseflow and stormflow on in-stream N variability
5	a. Determine the relationship between agricultural N management and seep NO_3-N concentrations b. Quantify NO_3-N retention within seeps and identify potential factors that influence NO_3-N retention c. Examine seep contributions to stream water NO_3-N concentrations at the catchment outlet
6	a. Summarize the finding and conclusions from the previous chapters b. Discuss the importance of seeps to watershed N management c. Evaluate the potential efficacy of BMPs in catchments with seeps

References

Amit, H., V. Lyakhovsky, A. Katz, A. Starinsky, and A. Burg. 2002. Interpretation of spring recession curves. *Groundwater* 40:543-551.

Angier, J.T., G.W. McCarty, and K.L. Prestegaard. 2005. Hydrology of a first-order riparian zone and stream, mid-Atlantic coastal plain, Maryland. *J. Hydrol.* 309:149-166.

Angier, J.T., G.W. McCarty, C.P. Rice, and K. Bialek. 2002. Influence of a riparian wetland on nitrate and herbicides exported from a field applied with agrochemicals. *Journal of Agriculture and Food Chemistry* 50:4424-4429.

Baden, S.P., L. Pihl, and R. Rosenberg. 1990. Effects of oxygen depletion on the ecology, blood physiology, and fishery of the Norway lobster Nephrops norvegicus. *Marine Ecological Progress Series* 67:141-155.

Baedke, S.J., and N.C. Krothe. 2001. Derivation of effective hydraulic parameters of a karst aquifer from discharge hydrograph analysis. *Water Resour. Res.* 37:13-19.

Bernhardt, E.S., M.A. Palmer, J.D. Allen, G. Alexander, K. Barnas, S. Brooks, J. Carr, S. Clayton, C. Dahm, J. Follstad-Shah, D. Galat, S. Gloss, P. Goodwin, D. Hart, B. Hassett, R. Jenkinson, S. Katz, G.M. Kondolf, P.S. Lake, J.L. Meyer, T.K. O'Donnell, L Pagano, B. Powell, and E. Sudduth. 2005. Synthesizing U.S. river restoration efforts. *Science* 308: 636-637.

Boesch, D.F., R.B. Brinsfield, and R.E. Magnien. 2001. Chesapeake Bay eutrophication: Scientific understanding, ecosystem restoration, and challenges for agriculture. *J. Environ. Qual.* 30: 303-320.

Bohlke, J.K., and J.M. Denver. 1995. Combined use of groundwater dating, chemical, and isotopic analysis to resolve the history and fate of nitrogen contamination in two agricultural watersheds, Atlantic coastal plain, Maryland. *Water Resour. Res.* 31: 2319-2339.

Brusch, W., and B. Nilsson. 1993. Nitrate transformation and water movement in a wetland area. *Hydrobiologia* 251: 103-111.

Burns, D.A., P.S. Murdoch, G.B. Lawrence, and R.L. Michel. 1998. Effects of groundwater springs on NO_3^- concentration during summer in Catskill Mountain streams. *Water Resour. Res.* 34:1987-1996.

Carpenter, S.R., N.F. Caraco, D.L. Correll, R.W. Howarth, A.N. Sharpley, and V.H. Smith. 1998. Nonpoint pollution of surface waters with phosphorus and nitrogen. *Ecol. Appl.* 8: 559-568.

Correll, D.L. 1998. The role of phosphorus in the eutrophication of receiving waters: A review. *J. Environ. Qual.* 27: 261-266.

Correll, D.L. and D.E. Weller. 1989. Factors limiting processes in freshwater wetlands: An agricultural primary stream riparian forest. p. 9-23. *In* R.R. Sharitz and J.W. Gibbons (ed.) Freshwater wetlands and wildlife. Conf. 8603101. DOE Symp. Sur. U.S. Dep. of Energy, Washington, DC.

Daniel, T.C., A.N. Sharpley, and J.L. Lemunyon. 1998. Agricultural phosphorus and eutrophication: A symposium overview. *J. Environ. Qual.* 27:251-257.

Devito, K.J., D. Fitzgerald, A.R. Hill, and R. Aravena. 2000. Nitrate dynamics in relation to lithology and hydrologic flow path in a river riparian zone. *J. Environ. Qual.* 29:1075-1084.

Gentry, W.M., and T.J. Burbey. 2004. Characterization of groundwater flow from spring discharge in a crystalline rock environment. *J. Am. Water Resour. Assoc.* 40:1205-1217.

Gilliam, J.W. 1994. Riparian wetlands and water quality. *J. Environ. Qual.* 23: 896-900.

Gold, A.J., P.M. Groffman, K. Addy, D.Q. Kellogg, M. Stolt, and A.E. Rosenblatt. 2001. Landscape attributes as controls on groundwater nitrate removal capacity of riparian zones. *J. Am. Water Res. Assoc*. 37:1457-1464.

Groffman, P.M., K. Butterbach-Bahl, W. Fulweiler, A.J. Gold, J. Morse, E. Stander, C. Tague, C. Tonitto, and P. Vidon. 2009. Incorporating spatially and temporally explicit phenomena (hotspots and hot moments) in denitrification models. *Biogeochemistry* 93: 49-77.

Hansson, S., and L.G. Rudstam. 1990. Eutrophication and Baltic fish communities. *Ambio* 19:123-125.

Haycock, N.E., and T.P. Burt. 1993. Role of floodplain sediments in reducing the nitrate concentration of subsurface runoff: a case study in the Cotswold, UK. *Hydrol. Process.* 7:287-295.

Hill, A.R. 1990. Groundwater flow paths in relation to nitrogen chemistry in the near-stream zone. *Hydrobiologia* 206:39-52.

Hill, A.R. 1996. Nitrate removal in stream riparian zones. *J. Environ. Qual.* 25: 743-755.

Jacobs, T.C., and J.W. Gilliam. 1985. Riparian losses of nitrate from agricultural drainage waters. *J. Environ. Qual.* 14: 472-478.

Jordan, T.E., D.L. Correll, and D.E. Weller. 1993. Nutrient interception by a riparian forest receiving inputs from adjacent cropland. *J. Environ. Qual.* 22:467-473.

Lowrance, R.R. 1992. Groundwater nitrate and denitrification in a coastal riparian forest. *J. Environ. Qual.* 21:401-405.

Lowrance, R.R., R. Leonard, and J. Sheridan. 1985. Managing riparian ecosystems to control nonpoint pollution. *J. Soil Water Conserv.* 40: 87-91.

Lowrance, R.R., R. Todd, J. Fail, O. Hendrickson, R. Leonard, and L. Asmussen. 1984. Riparian forests as nutrient filters in agricultural watersheds. *Bioscience* 34:374-377.

Mayer, P.M., S.K. Reynolds Jr., M.D. McCutchen, and T.J. Canfield. 2007. Meta-analysis of nitrogen removal in riparian buffers. *J. Environ. Qual.* 36: 1172-1180.

McClain, M.E., E.W. Boyer. C.L. Dent, S.E. Gergel, N.B. Grimm, P.M. Groffman, S.C. Hart, J.W. Harvey, C.A. Johnson, E. Mayorga, W.H. McDowell, and G. Pinay. 2003. Biogeochemical hotspots and hot moments at the interface of terrestrial and aquatic ecosystems. *Ecosystems* 6:301-312.

McDowell, W.H., W.B. Bowden, and C.E. Asbury. 1992. Riparian nitrogen dynamics in two geomorphologically distinct tropical rain forest watersheds: Subsurface solute patterns. *Biogeochemistry* 18: 53-75.

National Resources Conservation Service. 2003. National handbook of conservation practices. USDA, Washington, DC.

O'Driscoll, M.A., and D.R. DeWalle. 2010. Seeps regulate stream nitrate concentration in forested Appalachian catchments. *J. Environ. Qual.* 39:420-431.

Pennsylvania Department of Environmental Protection. 2010. Pennsylvania watershed implementation plan. Harrisburg, PA.

Peterjohn, W.T., and D.L. Correll. 1984. Nutrient dynamics in an agricultural watershed: observations on the role of a riparian forest. *Ecology* 65:1466-1475.

Peterson, B.J., W.M. Wolheim, P.J. Mulholland, J.R. Webster, J.L. Meyer, J.L. Tank, E. Marti, W.B. Bowden, H.M. Valett, A.E. Hershey, W.H. McDowell, W.K. Dodds, S.K. Hamilton, S. Gregory, and D.D. Morrall. 2001. Control of nitrogen export from watersheds by headwater streams. *Science* 292:86-90.

Pionke, H.B., J.R. Hoover, R.R. Schnabel, W.J. Gburek, J.B. Urban, and A.S. Rogowski. 1988. Chemical-hydrologic interactions in the near-stream zone. *Water Resour. Res.* 24:1101-1110.

Puckett, L.J., and T.K. Cowdery. 2002. Transport and fate of nitrate in a glacial outwash aquifer in relation to groundwater age, land use practices, and redox processes. *J. Environ. Qual.* 31:782-796.

Puckett, L.J., and W.B. Hughes. 2005. Transport and fate of nitrate and pesticides: hydrogeology and riparian zone processes. *J. Environ. Qual.* 34:2278-2292.

Rosenblatt, E., A.J. Gold, H.P. Stolt, P.M. Groffman, and D.Q. Kellogg. 2001. Identifying riparian sinks for watershed nitrate using soil surveys. *J. Environ. Qual.* 30: 1596-1604.

Rutherford, J.C., and M.L. Nguyen. 2004. Nitrate removal in riparian wetlands: interactions between surface flow and soils. *J. Environ. Qual.* 33:1133-1143.

Srinivasan, M.S., W.J. Gburek, and J.M. Hamlett. 2002. Dynamics of stormflow generation - a hillslope-scale field study in east-central Pennsylvania, USA. *Hydrol. Process.* 16:649-665.

Steinheimer, T.R., K.D. Scoggin, and L.A. Kramer. 1998. Agricultural chemical movement through a field-size watershed in Iowa: Subsurface hydrology and nitrate losses in discharge. *Environ. Sci. Technol.* 32:1048-1052.

Swanson, F.J., S.V. Gregory, J.R. Sedell, and A.G. Campbell. 1982. Land-water interactions: The riparian zone. p. 267-291. *In* R.L. Edmonds (ed.) Analysis of coniferous forest ecosystems in the western United States. US/IBP Synthesis Ser. 14. Hutchinson Ross Publ. Co., Stroudsburg, PA.

U.S. Environmental Protection Agency. 2008. National water quality inventory: 2008. Washington, DC.

Vidon, P.G.F., and A.R. Hill. 2004. Landscape controls on nitrate removal in stream riparian zones. *Water Resour. Res.* 40:1-14.

Warwick, J., and A.R. Hill. 1988. Nitrate depletion in the riparian zone of a small woodland stream. *Hydrobiologia* 157:231-240.

West, A.J., S.E. Findlay, D.A. Burns, K.C. Weathers, and C.M. Lovett. 2001. Catchment-scale variation in the nitrate concentration of groundwater seeps in the Catskill Mountains, New York, USA. *Water Air Soil Poll.* 132:389-400.

Wigington, P.J., S.M. Griffith, J.A. Field, J.E. Baham, W.R. Horwath, J. Owen, J.H. Davis, S.C. Rain, and J.J. Steiner. 2003. Nitrate removal effectiveness of a riparian buffer along a small agricultural stream in western Oregon. *J. Environ. Qual.* 32: 162-170.

CHAPTER 2

Groundwater Flow Path Dynamics and Nitrogen Transport Potential in the Riparian Zone of an Agricultural Headwater Catchment

Abstract

Stream riparian zones are often thought of as areas that provide natural remediation for groundwater contaminants, especially agricultural nitrogen (N). While denitrification and vegetative uptake tend to be efficient processes in slow moving shallow groundwater, these N removal mechanisms decrease in effectiveness as faster flows through soil macropores and other preferential flow pathways become dominant. The objective of our study was to characterize N concentration variability and hydrologic transport pathways through shallow groundwater draining areas of the riparian zone with and without emergent groundwater seeps. The study was conducted within FD36, an agricultural headwater catchment in the Ridge and Valley physiographic region of central Pennsylvania. Three seep and adjacent non-seep areas were instrumented with a field of 40 piezometers installed in a grid pattern (1.5-m spacing) at both 20- and 60-cm depths. The piezometers were monitored seasonally for a period of two years (Oct. 2010 – May 2012). Results showed that water table depths within seep areas were variable and some regions in the seep areas exhibited positive vertical hydraulic gradients of 5 to 10 cm. Non-seep areas were characterized by a uniform water table surface and were hydrostatic. Discharge of groundwater onto the land surface was also common in seep areas, but was not observed in non-seep areas. Ammonium-N (NH_4-N) concentrations were mostly low (< 0.1 mg L^{-1}) and relatively similar between seep and non-seep areas at each of the three study sites. In contrast,

nitrate-N (NO_3-N) concentrations in seep areas were significantly greater than the non-seep areas at two of the study sites. A two-component mixing model indicated that groundwater in seep areas of FD36 was primarily (53% - 75%) comprised of water from a shallow fractured aquifer (6-m deep monitoring wells), which was high in NO_3-N concentration. Non-seep areas, however, were comprised (58% - 82%) of perched water on top of the fragipan (1-m deep monitoring wells) that was likely recharged locally in the riparian zone and was low in NO_3-N concentration. Higher NO_3-N concentrations, variable water table elevation, and groundwater emergence onto the land surface in seep areas provided evidence that preferential flow paths were an important pathway for water and N in these areas of the riparian zone. Thus, the potential for N delivery to the stream in FD36 was much greater from seep areas compared to non-seep areas. To increase N removal efficiency in catchments with seeps, management practices that target seep areas need to be developed.

Introduction

Nitrogen (N) is one of the most common agricultural contaminants found in groundwater and surface water around the world (*Craig and Weil, 1993; Tesoriero et al., 2000*). Due to its high solubility, N is easily transported in water from agricultural fields to nearby waterways (*Lowrance et al., 1983; Crum et al., 1990; Simmons et al., 1992*). Excess N loading of groundwater and surface water is of concern because it can create conditions that lead to negative impacts on water quality (*e.g., Correll, 1998*). For example, eutrophication caused by excessive inputs of nutrients, such as N, is the most common impairment of surface waters in the U.S. (*U.S. EPA, 2008*). Insufficient progress toward N reduction goals and continued poor water quality in many surface water bodies emphasizes the need to develop management plans to deal with N pollution from agricultural landscapes.

Riparian corridors are often considered to be effective sites for remediation of agricultural N (*Peterjohn and Correll, 1984; Jordan et al., 1993*), especially those located along first-order streams (*Peterson et al., 2001*). Indeed, a meta-analysis by Mayer et al. (2007) demonstrated the influence of riparian zones on the supply, transport, and fate of solutes in headwater catchments. Despite setting aside vegetated riparian zones along waterways in these headwater settings, significant N loads are still measured at watershed outlets (*e.g., Koerkle, 1992*). Guidelines for N mitigation measures in riparian zones have typically focused on factors such as width and vegetation (*Mayer et al., 2007*), but limited consideration has been given to hydrologic factors that affect N transport and removal in the riparian zone (*Hill, 1996; Angier and McCarty, 2008*). Since water is the medium of transport for N, hydrological processes and properties of the riparian zone have an impact on N transport and delivery to streams. For instance, the transmissivity of riparian sediments can influence N dynamics, as groundwater residence time within the subsurface affects N behavior (*Jacinthe et al., 1998; Rutherford and Nyugen, 2004*). Differences in flow paths can also affect groundwater (*Calver, 1990*) and contaminant delivery patterns (*Harvey and Nuttle, 1995; Angier et al., 2001*).

Most conceptual models of riparian zone hydrology in agricultural catchments assume uniform, lateral subsurface flow from an upland field, through the riparian zone, and ultimately to a stream (*Jordan et al., 1993; Bosch et al., 1994*). These models suggest a scenario in which there is sufficient contact time between groundwater and the soil matrix to facilitate N removal. While many riparian zones have sediment layers with high N removal potential (*Groffman et al., 1992*), the presence of environmental conditions suitable for N removal (e.g., soils high in organic carbon, anaerobic conditions, vegetation) alone may be insufficient to remove N from groundwater if flow paths deviate from uniform lateral flow. Recent research has suggested that much of the groundwater may travel through preferential subsurface flow paths, even in the presence of an aquiclude (e.g., fragipan) occurring at shallow depth (*Hill et al., 2000; Angier et*

al., 2005). Preferential subsurface flow can result in N-laden groundwater that effectively bypasses the remediation capacity of the riparian zone (*Hill, 1996; McGlynn and McDonnell, 2003; Vidon et al., 2010*).

One example of preferential flow in the riparian zone is the presence of groundwater-sustained wetlands, slope wetlands, springs, or emergent groundwater seeps (hereafter referred to as seeps). These groundwater discharge zones often serve as a primary source of streamflow in headwater catchments (*Pionke et al., 1988; Rutherford and Nyugen, 2004; O'Driscoll and DeWalle, 2010; Shabaga and Hill, 2010*). Several characteristics of seeps, such as visible zones of groundwater emergence and the rapid discharge of groundwater, suggest that in these areas preferential flow may play a substantial role in determining the quantity and chemistry of water being delivered to the stream. Evidence of this was reported in a study by Devito et al. (2000), in which groundwater upwelling areas showed consistently elevated nitrate-N (NO_3-N) concentrations (up to 20 mg L^{-1}) relative to neighboring inactive areas with low (< 1 mg L^{-1}) concentrations. Similarly, preferential flow paths have been shown to play a major role in NO_3-N leaching in agricultural landscapes (*Di and Cameron, 2002*). Thus, information on spatial and temporal N variations across the riparian zone are needed in order to determine where zones of N delivery may occur, predict what conditions (hydrological, biogeochemical) might increase or decrease stream N loading, and possibly adjust agricultural management practices.

We report here the results of a study examining spatial and temporal patterns of groundwater and N transport at three paired study sites within the riparian zone of FD36, a small agricultural headwater catchment in central Pennsylvania. Each study site included an area with an emergent groundwater seep and an adjacent area without a seep (i.e., non-seep) in order to contrast hydrological and biogeochemical processes within different areas of the riparian zone. The objectives of this study were to (1) investigate the shallow groundwater dynamics and identify key hydrologic flow pathways within both seep and non-seep areas of the riparian zone;

(2) determine the relationship between subsurface hydrologic characteristics and N concentrations within seep and non-seep areas; and (3) examine the N transport potential from both areas of the riparian zone.

Materials and Methods

Site Location and Characteristics

FD36 (40 ha) is a headwater catchment within the non-glaciated, folded and faulted, Appalachian Ridge and Valley physiographic region (Figure 2.1). Located approximately 40 km north of Harrisburg, Pennsylvania, FD36 is one of 15 sub-catchments that form WE-38, a primary research site of the USDA – Agricultural Research Service since 1968 (see Bryant et al. (2011) for a detailed history of the site). The climate is temperate and humid with annual precipitation averaging 1080 mm yr^{-1} and mean annual air temperatures of 8 to 10°C (*Gburek and Sharpley, 1998; Buda et al., 2011*). Since 1996, stream discharge has been monitored every 5 min at four locations with recording H-flumes. Previous research in FD36 has shown that groundwater provides the majority (60% – 80%) of the annual streamflow (*Gburek et al., 1996; Pionke et al., 1996*) and that surface and subsurface flow systems are predominately self-contained at the catchment-scale (*Gburek and Folmar, 1999*).

The dominant land use in FD36 is agriculture (56%) with forested woodlots (30%) and meadow/pasture (13%) comprising the remainder of the catchment. The common crop rotations in FD36 include three- to four-year sequences of corn, small grains, hay, and soybeans. Crops are planted on upslope fields and the riparian zone is planted with grasses. Most fertilizers and manures (dairy and swine) are applied for corn during the fall and spring. Application rates over the study period ranged from 0 to 200 kg N ha^{-1} in individual fields across the catchment. Two contrasting soil groups are found within FD36 (*Needelman et al., 2002*). Well-drained residual

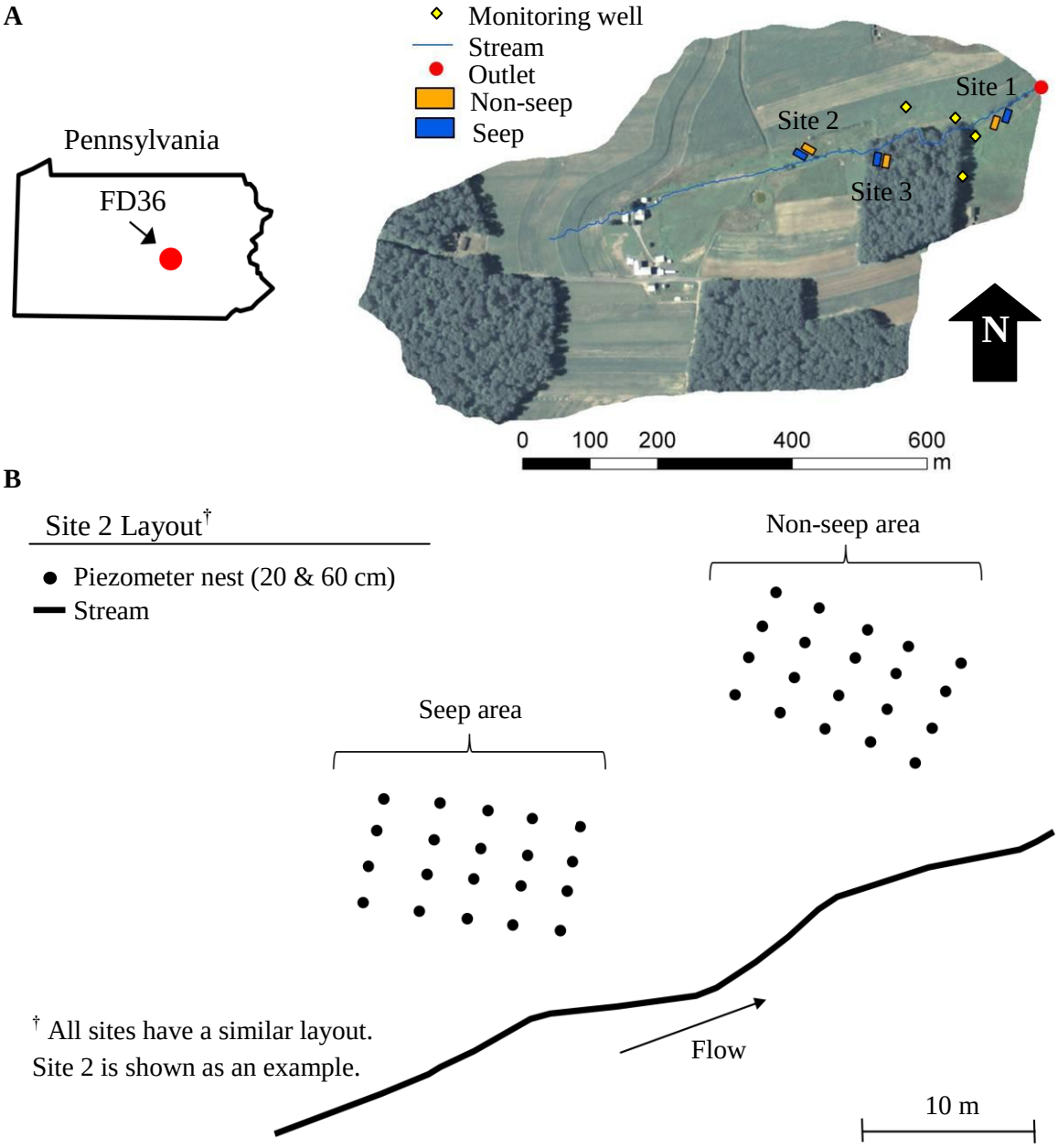

Figure 2.1

(A) Aerial photo of FD36, an agricultural headwater catchment located in central Pennsylvania, with three study sites marked. FD36 is a sub-catchment of East Mahantango Creek, which flows into the Susquehanna River and ultimately the Chesapeake Bay. (B) Instrumentation at study site 2. One study area was located where an emergent groundwater seep was present (seep area). The other area was located where there were no seeps (non-seep area). Site 2 is shown, but all three study sites have identical instrumentation.

soils that are typically stony, silt loams (Leck Kill, Calvin, Berks series) line the hillslopes, while colluvial soils (Albrights and Hustontown series) are distributed along the stream and valley floor. The Albrights and Hustontown soils in the riparian zone have a moderately well-developed fragipan beginning at a depth of 0.5 to 0.7 m and have low permeability. Slopes in FD36 range from 1% to 20%. The steepest slopes are found on the midslopes (~20%), while gentler slopes occur on the shoulders and on the footslopes.

Three study sites within the riparian zone of FD36 were chosen for intensive monitoring of subsurface hydrology and N transport potential (Figure 2.1). The study sites were chosen to represent areas of the riparian zone downslope of the three main land uses within the catchment (i.e., agriculture [site 2], forest [site 3], and meadow/pasture [site 1]). At each study site, monitoring was conducted in a zone of emergent groundwater seepage (seep area), as well as in an adjacent region without an emergent groundwater seep (non-seep area) (Figure 2.1). Both seep and non-seep areas at all three study sites were instrumented identically with five transects (6-m long) of nested piezometers (Figure 2.1), which were installed perpendicular to the flow of water in the riparian zone. Each piezometer transect contained four pairs of piezometers installed at depths of 20 and 60 cm with a spacing of 1.5 m between pairs of piezometers. All piezometers were screened at the bottom 8 cm. The depths of the piezometers were chosen to best represent the soil properties at the study sites (20 cm – Ap horizon boundary; 60 cm – top of fragipan). In addition, four pairs of monitoring wells (1- and 6-m deep) were installed outside of the study sites and were sampled concurrently with the piezometers (Figure 2.1). All monitoring wells were screened at the bottom 0.5 m. The shallow wells (1 m) sampled perched water above the fragipan that is likely recharged locally. In contrast, the deep wells (6 m) sampled a fractured aquifer below the fragipan that provides the majority of streamflow in FD36 (*Pionke and Urban, 1985; Schnabel et al., 1993; Lindsey et al, 2003*).

Field Sampling and Laboratory Analysis

Water samples were collected from the piezometers at each study site as well as the monitoring wells on nine occasions between October 2010 and May 2012. Sample collection immediately followed precipitation events in order to ensure that water samples could be collected from the non-seep areas within each site. Within one week following a precipitation event, approximately one well volume of water was removed from the piezometers using a peristaltic pump. Then, two days later, the depth of the water table was measured in both the 20- and 60-cm deep piezometers at each site and water samples were collected in 125 mL plastic (HDPE) bottles. On return to the laboratory, water samples were filtered (0.45 μm) and then later analyzed with a Lachat QuikChem FIA+ autoanalyzer (QuikChem Methods FIA+ 8000 Series, Lachat Instruments, Loveland, Colorado) to determine concentrations of NO_3-N, ammonium-N (NH_4-N), and chloride (Cl^-). Total N was determined on unfiltered samples following alkaline persulfate digestion (*Patton and Kryskalla, 2003*). Concentrations of dissolved inorganic-N (NO_3-N + NH_4-N) comprised, on average, 95% of total N. Thus, the main focus of this paper is on NO_3-N and NH_4-N.

Statistics and Data Analysis

To determine spatial patterns of shallow groundwater flow, ordinary kriging was used to interpolate water table depth measurements within each study site. In addition, Moran's *I* was calculated to examine spatial autocorrelation in water table depth within seep and non-seep areas for all sampling dates (*O'Sullivan and Unwin, 2010*). Statistical significance of spatial autocorrelation was completed with a Monte Carlo simulation, which randomly shuffled the observed water table depth values on a single sampling date and recalculated Moran's *I* to determine a sampling distribution. Differences in water table depth and N concentration within a

single site (i.e., seep area vs. non-seep area) were evaluated by ANOVA. Pairwise comparisons were made using Tukey's Studentized Range (HSD) test in order to separate treatment means. Furthermore, the least squares estimation method was performed to obtain Pearson correlation coefficients to measure the strength of linear relationship between NH_4-N concentration, NO_3-N concentration, Cl^- concentration, and water table depth within a site.

A two-component mixing model (*Hill, 1991*) was used to ascertain the relative contributions of perched water above the fragipan (1-m deep wells) and groundwater from the fractured aquifer (6-m deep wells) to seep and non-seep areas. Chloride was used to separate these two water sources because it is non-reactive and serves as an ideal conservative tracer of water flow pathways (*Davis et al., 2006*). The model was calculated as $Q_{Fractured}/Q_{Piezometer} = (C_{Piezometer} - C_{Perched})/(C_{Fractured} - C_{Perched})$, where $Q_{Fractured}/Q_{Piezometer}$ is the proportion of groundwater from the fractured aquifer to seep and non-seep areas, $C_{Piezometer}$ is the Cl^- concentration of the 60-cm deep piezometers, $C_{Fractured}$ is the Cl^- concentration of the 6-m deep monitoring wells, and $C_{Perched}$ is the Cl^- concentration of the 1-m deep monitoring wells. All statistical analyses were completed in *R* statistical software package (*R Foundation for Statistical Computing, 2011*). A probability level of 0.05 was used to evaluate statistical significance in all analyses.

Results

Piezometer N Concentration

Ammonium-N concentration measured in piezometers comprised a relatively small fraction (1% - 5%) of the total inorganic N (NH_4-N + NO_3-N) in seep and non-seep areas at all three study sites. On most sampling dates, mean NH_4-N concentrations were 0.1 mg L^{-1} or less (data not shown). The highest mean NH_4-N concentration for all three sites occurred on May 31,

2012 in which concentrations averaged 0.3 mg L^{-1}. In contrast to piezometer NH_4-N concentrations, piezometer NO_3-N concentrations varied spatially within each site as well as temporally throughout the study period (Figure 2.2). Mean NO_3-N concentration was significantly greater in seep areas compared to non-seep areas in sites 1 and 2, but not in site 3 ($p < 0.03$) (Figure 2.2). Nitrate-N concentrations in the seep areas averaged 1.9, 2.6, and 1.3 mg L^{-1} in sites 1, 2, and 3, respectively, and NO_3-N concentrations did not vary significantly by depth (Figure 2.2). Depth, however, was a significant factor affecting NO_3-N concentrations in non-seep areas of sites 1 and 3. Mean NO_3-N concentration at the 60-cm depth was significantly greater than mean NO_3-N concentration at the 20-cm depth ($p < 0.01$) (Figure 2.2).

Temporal patterns in piezometer NO_3-N concentrations at site 1, which was downslope of a pasture/meadow land use, were relatively stable over the study period in both seep and non-seep areas, except on Aug. 31, 2011 when mean NO_3-N concentrations of 5.9 and 4.2 mg L^{-1}, respectively, were measured. Site 2, which was downslope of cropped fields, exhibited the most variability in NO_3-N concentration over the study period compared to sites 1 and 3, especially in the seep area (Figure 2.2). Nitrate-N concentration in the seep area of site 2 ranged between 1.3 and 5.0 mg L^{-1} over the study period. The non-seep area in site 2 was also the only area that was dry (i.e., water table depth > 60 cm) on several sampling dates (3 out of 9 sampling dates; 33%). The seep and non-seep areas in site 3, the forested site, showed little variability in NO_3-N concentrations compared to sites 1 and 2.

Monitoring Well N Concentration

Similar to NH_4-N concentrations measured in piezometers, NH_4-N concentrations in the four monitoring wells were low and were often less than 0.1 mg L^{-1} (data not shown). Mean NH_4-N concentrations were between 0.1 and 0.3 mg L^{-1} for all monitoring wells and NH_4-N

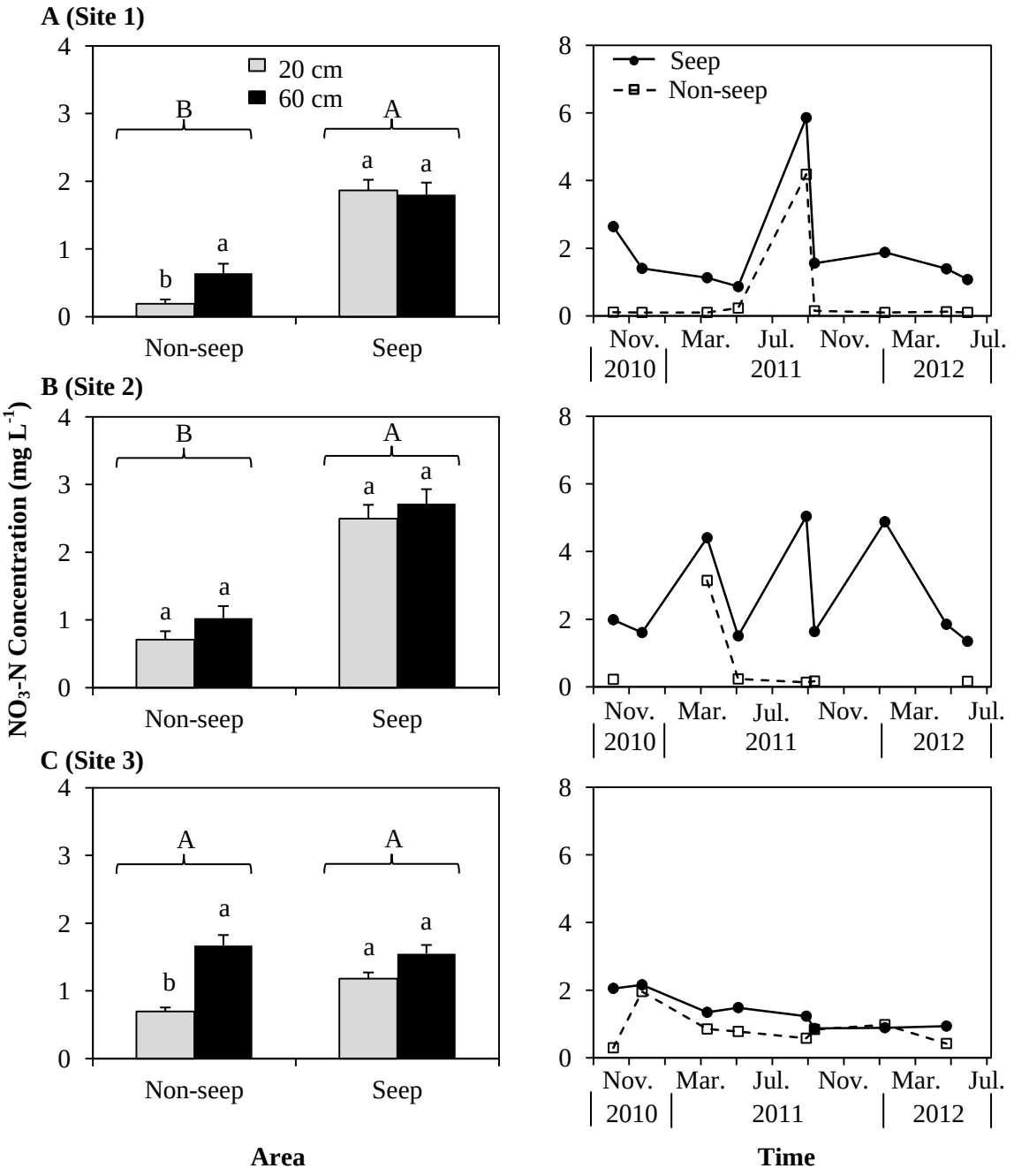

Figure 2.2

Mean groundwater NO_3-N concentration measured from piezometers in seep and non-seep areas of three riparian zone study sites in FD36. (A) Site 1; (B) Site 2; and (C) Site 3. Lower case letters denote statistical significance ($p < 0.05$) between depths (20 and 60 cm) within each seep or non-seep area. Upper case letters denote statistical significance ($p < 0.05$) between seep and non-seep areas. Differences in concentration among sites were not analyzed. Error bars represent standard error. Temporal patterns were based on mean NO_3-N concentrations from both 20- and 60-cm depths.

concentrations did not vary by depth. In contrast, NO_3-N concentrations in the monitoring wells ranged from 0.2 to 11.1 mg L^{-1} over the study period (Table 2.1). Mean NO_3-N concentration in groundwater perched on top of the fragipan (1-m deep wells) was significantly less than mean NO_3-N concentration in the fractured aquifer (6-m deep wells) at all four of the monitoring well locations ($p = 0.02$). The mean NO_3-N concentration of 1- and 6-m deep monitoring wells was 0.6 and 5.7 mg L^{-1}, respectively (Table 2.1). The north side of the stream in FD36 tended to have higher NO_3-N concentrations compared to NO_3-N concentrations on the south side of the stream (Table 2.1), which was likely due to differences in N application rates to cropped fields (*Williams, unpublished data*). The relative position of the monitoring wells (i.e., hillslope vs. riparian zone), however, did not appear to influence NO_3-N concentration (Table 2.1).

Groundwater Flow Paths and Patterns

Water table depth observed in 20- and 60-cm deep piezometers throughout the study period at all three sites revealed that groundwater flow in FD36 was generally perpendicular to

Table 2.1 Mean and range of monitoring well groundwater NO_3-N concentration in FD36 between October 2010 and May 2012.

Well	Description[†]	Depth	NO_3-N concentration	
			Mean	Range
		m	mg L^{-1}	
1	North hillslope	1	0.2	0.2-0.3
		6	9.4	6.6-11.1
2	North riparian zone	1	1.6	0.2-4.4
		6	4.5	3.3-5.4
3	South riparian zone	1	0.2	0.2-0.4
		6	4.6	3.1-5.2
4	South hillslope	1	0.2	0.2-0.4
		6	4.2	4.0-4.7

[†] Location of monitoring wells as noted in Figure 2.1.

the stream. Site 2 tended to have a water table depth that was closer to the land surface compared to sites 1 and 3; however, mean water table depth did not differ significantly among sites (Table 2.2). Within each site, mean water table depth in seep and non-seep areas was also not significantly different on any sampling date; although, the water table in seep areas was typically closer to the land surface (Table 2.2). While mean water table depth was similar between seep and non-seep areas within each site, water table depth was substantially more variable in seep

Table 2.2 Water table depth and variability in seep and non-seep areas of three riparian zone study sites in FD36 from October 2010 to May 2012.

		Site 1			Site 2			Site 3		
Date	**Area**[†]	**n**[‡]	**Mean ± Std. Dev.**	**Range**	**n**[‡]	**Mean ± Std. Dev.**	**Range**	**n**[‡]	**Mean ± Std. Dev.**	**Range**
			cm			cm			cm	
2010										
Oct. 5	S	16	22 ± 18*	50	20	11 ± 15*	43	n/a	n/a[§]	n/a
	NS	14	36 ± 14	43	20	26 ± 5	16	n/a	n/a	n/a
Nov. 23	S	10	44 ± 9	29	7	45 ± 10	26	14	36 ± 16*	56
	NS	4	52 ± 1	3	0			19	37 ± 6	17
2011										
Mar. 14	S	20	10 ± 21*	50	20	-1 ± 7*	27	20	10 ± 17*	56
	NS	20	15 ± 11	39	20	7 ± 3	12	20	8 ± 7	22
May 6	S	17	24 ± 23*	52	20	4 ± 14*	45	20	4 ± 12*	48
	NS	14	36 ± 14	43	20	6 ± 7	29	20	14 ± 14	36
Aug. 30	S	18	19 ± 13*	40	20	19 ± 7*	30	9	26 ± 11*	50
	NS	20	24 ± 2	8	18	38 ± 8	25	5	46 ± 2	6
Sept. 13	S	19	19 ± 16*	38	20	10 ± 8*	20	20	30 ± 16*	55
	NS	20	13 ± 4	13	17	28 ± 5	16	19	25 ± 9	31
2012										
Jan. 11	S	15	41 ± 8	30	7	45 ± 13	35	20	24 ± 16*	58
	NS	15	47 ± 4	14	0			20	25 ± 8	23
Apr. 25	S	16	24 ± 17*	51	7	37 ± 10	29	20	5 ± 12*	34
	NS	19	25 ± 13	40	0			20	17 ± 6	23
May 31	S	20	10 ± 12*	33	19	1 ± 3*	16	20	1 ± 10*	35
	NS	20	9 ± 3	10	20	3 ± 3	15	20	11 ± 6	21

[†] S = Seep; NS = Non-seep
[‡] Number of 60-cm deep piezometers that had a measurable water depth (max. = 20).
[§] Site 3 was not instrumented until after the Oct. 5, 2010 sampling date.
* Visible discharge of groundwater onto the land surface was observed.

areas compared to non-seep areas (Table 2.2). For instance, on Nov. 23, 2010, mean water table depth in the seep and non-seep areas at site 3 was similar (36 and 37 cm, respectively), yet the range in depth was more than three times greater in the seep area compared to the non-seep area (56 and 17 cm, respectively). The high degree of variability in seep area water table depths resulted in some regions where the water table was higher than the land surface even though the mean depth was well below the surface. Groundwater discharge onto the land surface was therefore observed within the seep area at all three sites on several occasions, whereas no exfiltration was observed in the non-seep areas (Table 2.2).

While hydraulic head measurements from nested piezometers were variable throughout the study, the general groundwater flow pattern was consistent within each site. All three non-seep areas were relatively hydrostatic (i.e., no vertical gradient), which indicated that lateral groundwater flow predominated in these areas. In contrast, seep areas consistently had regions with positive vertical gradients (Figure 2.3). Regions in seep areas with positive vertical gradients of 5 to 10 cm coincided with visible surface saturation and water table elevations that were closer to the surface relative to other, hydrostatic, regions of the seep area. Thus, it is likely that the regions of seep areas with a positive vertical gradient represented a likely pathway of groundwater discharge to the surface. Analysis of spatial autocorrelation with Moran's *I* showed that spatial patterns in water table depth were vastly different between seep and non-seep areas. At all three sites, water table depths in the non-seep areas were positively autocorrelated ($p < 0.05$) on greater than 75% of the sampling dates. This suggested that groundwater flow was relatively uniform across the non-seep areas (Figure 2.3). On the other hand, water table depths in all three seep areas were not significantly different from a random pattern on the majority (75 – 100%) of sampling dates ($p > 0.05$), which further confirmed that groundwater flow in seep areas was highly variable (Figure 2.3). Water table depth in all three seep areas was only positively autocorrelated on dates when the mean water table depth was near the land surface.

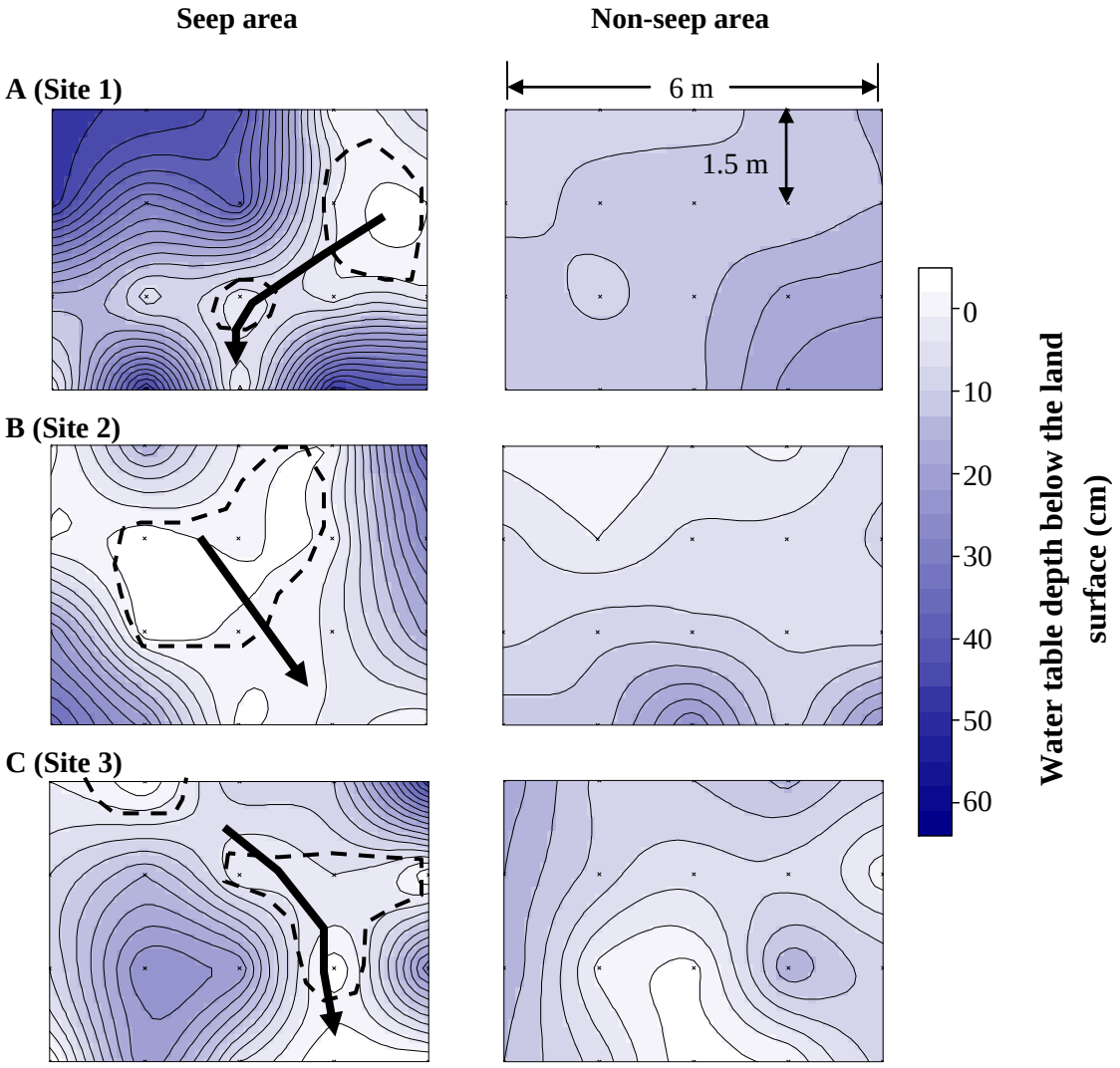

Figure 2.3

Spatial distribution of water table depth in seep (left column) and non-seep (right column) areas of three riparian zone study sites in FD36 on Mar. 14, 2011. (A) Site 1; (B) Site 2; and (C) Site 3. Water table depths were interpolated with ordinary kriging. The land surface is located at 0 cm. Water table depths were measured from the 60-cm deep piezometers in each area, which are labeled with an *x* in the figure. The stream channel is located below all three study sites; thus, groundwater flow is from the top of the image toward the bottom of the image for all areas. Highlighted (dashed) areas on the seep figures indicate regions where positive vertical hydraulic gradients were observed throughout the study. Arrows indicate seep surface flow paths that were the result of groundwater upwelling.

Relationship between N Concentration and Hydrology

Seep areas in all three study sites had significantly greater Cl^- concentrations in piezometers compared to non-seep areas ($p < 0.001$) (Table 2.3). On average, Cl^- concentrations in seep areas were 1.5 to 2.0 times greater in seep areas compared to non-seep areas. Piezometer Cl^- concentrations within seep areas were also significantly greater at the 60-cm depth compared to the 20-cm depth (Table 2.3). Chloride concentrations in monitoring wells also varied significantly by depth ($p < 0.001$) (Table 2.3). Using the monitoring well Cl^- concentrations as end-members in a two-component mixing model, the contribution of groundwater from the fractured aquifer (6-m deep wells) to seep and non-seep areas was calculated (Figure 2.4). In all three study sites, the majority of groundwater in seep areas appeared to originate from the fractured aquifer, whereas, in the non-seep areas, the majority of water was from perched groundwater on top of the fragipan. The fractured aquifer comprised 69%, 53%, and 75% of the groundwater in seep areas at sites 1, 2, and 3, respectively (Figure 2.4). In contrast, it only

Table 2.3 Mean Cl^- concentration from piezometers in seep and non-seep areas of three riparian zone study sites, as well as mean monitoring well Cl^- concentration.

		Piezometer Cl^- conc.						Monitoring well Cl^- conc.	
Area	**Depth**	**Site 1**		**Site 2**		**Site 3**		**Depth**	**All wells**
	cm	mg L^{-1}						m	mg L^{-1}
Seep	20	5.5b[†]	A[‡]	4.2b	A	5.6b	A	1.0	1.5b
	60	6.0a		5.3a		6.6a		6.0	7.7a
Non-seep	20	2.5a	B	3.3a	B	3.9a	B		
	60	2.7a		3.6a		4.3a			

[†] Lower case letters denote statistical significance ($p < 0.05$) between depths (20 and 60 cm) within each seep or non-seep area.
[‡] Upper case letters denote statistical significance ($p < 0.05$) between seep and non-seep areas. Differences in concentration among sites were not analyzed.

comprised 18%, 32%, and 42% of groundwater in the non-seep areas of sites 1, 2, and 3, respectively (Figure 2.4).

Piezometer NO_3-N and Cl^- concentrations were positively correlated at sites 1 and 2, but not at site 3 (R^2 = 0.67 and 0.43, respectively) (Table 2.4, Figure 2.5). Similarly, piezometer NO_3-N concentrations at sites 1 and 2 were significantly correlated with water table depth (Table 2.4, Figure 2.5). Piezometer Cl^- concentrations and water table depths, however, were significantly correlated at all three sites (R^2 = -0.20, -0.39, and -0.33, respectively) (Table 2.4, Figure 2.5). Ammonium-N concentrations in piezometers were not related to NO_3-N concentrations, Cl^- concentrations, or water table depths at any of the three sites.

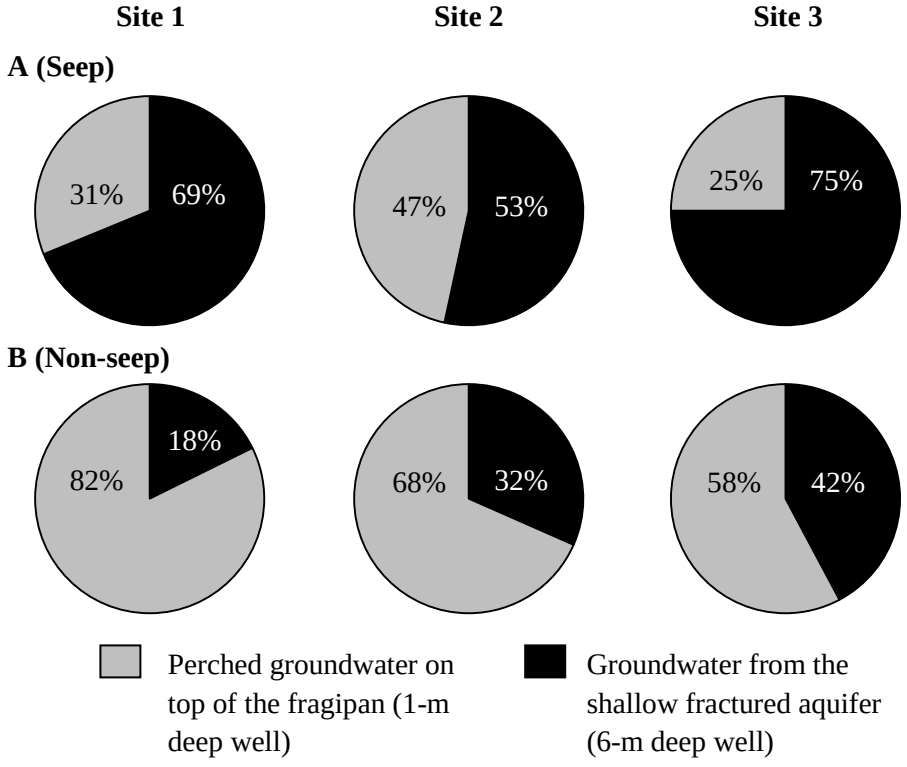

Figure 2.4

Mean percentage of groundwater that was attributed to either perched groundwater on top of the fragipan or the shallow fractured aquifer. Percentages were calculated from mean piezometer (20- and 60-cm depths) and monitoring well Cl^- concentrations with a two component mixing model. (A) Seep area; (B) Non-seep area.

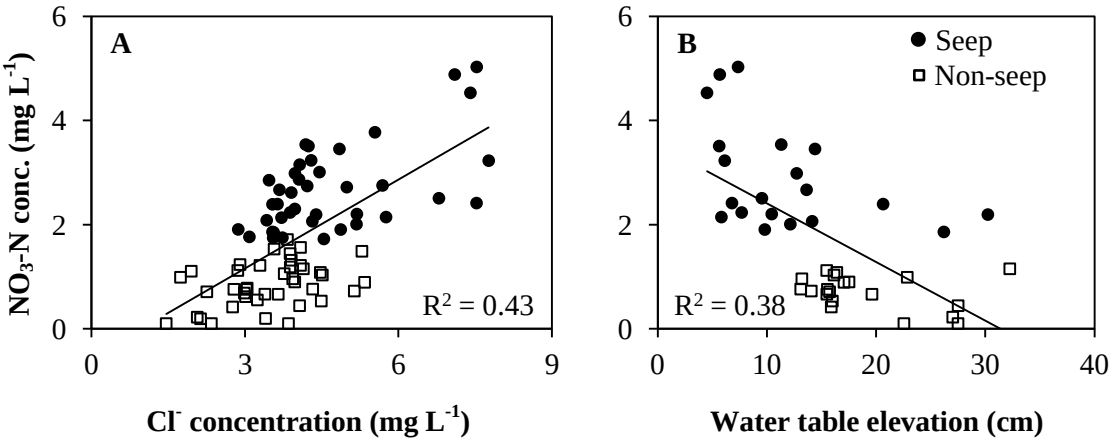

Figure 2.5

Mean Cl^- concentration (A) and water table depth (B) measured in piezometers at site 2 compared with mean NO_3-N concentration during the study period ($p < 0.001$ and $p = 0.004$, respectively). Both 20- and 60-cm deep piezometers were used in the analysis of Cl^- concentration vs. NO_3-N, whereas only the 60-cm deep piezometers were used for the water table depth vs. NO_3-N because the 20-cm deep piezometers were often dry. Site 2 was chosen as an example; data for all three study sites are shown in Table 2.4.

Table 2.4 Pearson correlation coefficients and p values (in parentheses) for correlations among piezometer NH_4-N concentration, NO_3-N concentration, Cl^- concentration, and water table depth from three riparian zone seep areas in FD36. Italics indicate correlation is significant at $p < 0.05$.

		NH_4-N	**NO_3-N**	**Cl^-**
		mg L^{-1}		
			Site 1	
NO_3-N	mg L^{-1}	-0.12 (0.187)		
Cl^-	mg L^{-1}	-0.05 (0.244)	*0.67 (<0.001)*	
Water table depth	cm	-0.01 (0.563)	*-0.27 (0.001)*	*-0.20 (0.004)*
			Site 2	
NO_3-N	mg L^{-1}	0.01 (0.730)		
Cl^-	mg L^{-1}	0.00 (0.909)	*0.42 (<0.001)*	
Water table depth	cm	0.06 (0.118)	*-0.38 (<0.001)*	*-0.39 (<0.001)*
			Site 3	
NO_3-N	mg L^{-1}	0.01 (0.776)		
Cl^-	mg L^{-1}	-0.03 (0.165)	0.04 (0.084)	
Water table depth	cm	0.07 (0.092)	-0.03 (0.269)	*-0.33 (<0.001)*

Seep area NH_4-N, NO_3-N, and Cl^- concentrations in piezometers were also compared to N concentrations in the groundwater discharged onto the land surface (Figure 2.6). At all three study sites, NH_4-N concentrations were similar between surface seep discharge and piezometer concentration (Figure 2.6). Surface seep discharge NO_3-N concentrations and piezometer NO_3-N concentrations were similar at sites 1 and 2. However, at site 3, surface seep discharge NO_3-N concentrations were significantly greater than piezometer NO_3-N concentrations ($p = 0.02$) (Figure 2.6). Chloride concentrations were not different between piezometer and surface seep discharge at any of the three sites.

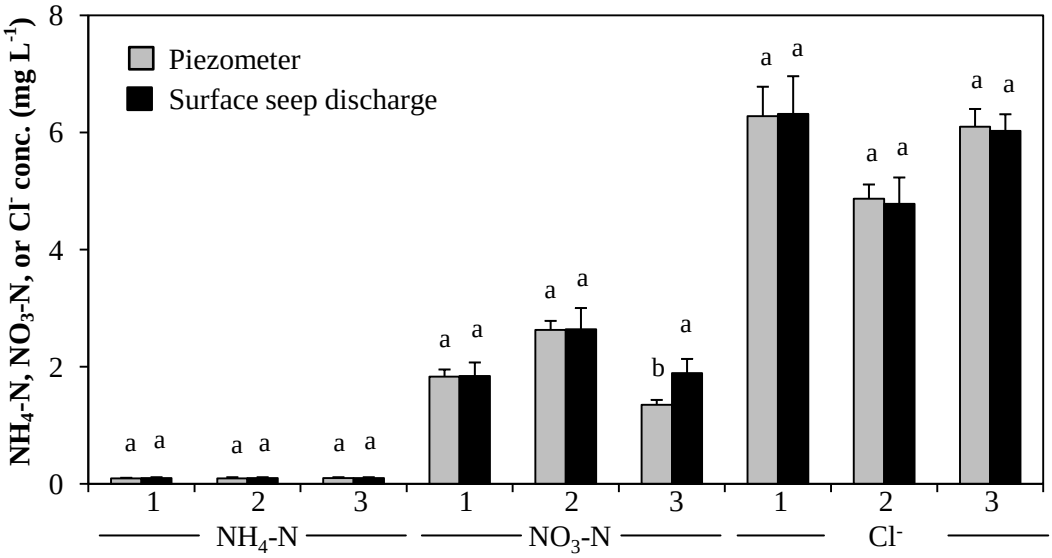

Figure 2.6

Comparison of mean NH_4-N, NO_3-N, and Cl^- concentrations in piezometers and surface seep discharge from three seep areas in the riparian zone of FD36. Surface seep discharge was collected (when present) on the same day as samples were taken from piezometers as part of a separate study in FD36 (*Chapter 5*). Error bars represent standard error. Lower case letters denote statistical significance ($p < 0.05$) between groundwater and surface discharge within each site and nutrient.

Discussion

Hydrology of Seep and Non-seep Areas of the Riparian Zone

Water table depths were measured in nested piezometers at three sites in FD36 to investigate groundwater flow paths and patterns in seep and non-seep areas of the riparian zone. Results showed that non-seep areas were characterized by a water table that was relatively uniform, whereas seep areas were characterized by a water table that was highly variable. In addition, regions of the seep areas exhibited positive (i.e., upward) vertical gradients and discharge of groundwater onto the land surface that corresponded with the location of seep surface flow paths. No vertical movement of groundwater was observed in the non-seep areas. A comparison of water table patterns in seep and non-seep areas of the riparian zone in FD36 indicated that the hydrology of these areas was substantially different. Specifically, groundwater flow in non-seep areas of the riparian zone was predominately lateral flow through the soil matrix. Seep areas, however, showed evidence for groundwater upwelling and preferential flow paths through the subsurface.

Spatial patterns of water table depth in the non-seep areas of FD36 were typical of groundwater flow in riparian zones underlain by a restrictive soil layer (*Hill, 1996*). That is, groundwater flow was mainly in a lateral direction through the shallow subsurface. Analysis of spatial autocorrelation in the non-seep areas showed that water table depths were clustered (i.e., positive autocorrelation), which indicated that water table depths in piezometers were dependent on their spatial location. Combined with visual observations, these data demonstrated that groundwater flow was uniform across the monitored area and resulted from a consistent downward gradient toward the stream channel. In these hydrogeologic settings, the limited thickness of the soil above the fragipan (or other soil restrictive layers) can often result in groundwater inputs that are small and seasonally variable (*Pinay et al., 1993; Jordan et al.,*

1993). For example, the non-seep area in site 2 became hydrologically disconnected from the upland on several occasions throughout the study and exhibited fluctuations in water table elevation of over 0.5 m. Therefore, contributions of groundwater to streamflow from non-seep areas are likely variable and dependent on several factors such as rainfall depth from a single event or series of events, and antecedent soil moisture.

In contrast to the non-seep areas, positive vertical gradients in nested piezometers and visible exfiltration of groundwater in the seep areas of the riparian zone in FD36 documented the importance of groundwater upwelling in these areas. Indeed, several studies have indicated that vertical discharge can predominate in riparian environments (*Devito et al., 2000; Angier et al., 2002*), even in the presence of a restrictive layer (*Angier et al., 2005*). Once discharged onto the land surface, groundwater often was transported in small rivulets across the seep area toward the stream channel. Highly variable water table depths also suggested that groundwater upwelling occurred at discrete locations within a seep area. These observations indicated that localized regions within a seep area were likely locations of preferential groundwater flow. Preferential flow can occur due to macropores, animal burrows, soil pipes, or discontinuities in soil layers (*Allaire et al., 2009*). While the exact mechanism for preferential flow was difficult to determine, a two-component mixing model suggested that the fractured aquifer system, which has the highest NO_3-N concentrations (*Pionke and Urban, 1985; Schnabel et al., 1993; Lindsey et al., 2003*), contributed groundwater to seepage zones during and after storm events. This implies that groundwater from the fractured aquifer was transported vertically upward through the fragipan in seep areas, whereas in non-seep areas, perched water above the fragipan was the primary source of groundwater. Seep area contributions to streamflow are therefore likely based on longer-term factors, such as seasonal or annual groundwater recharge.

Influence of Hydrology on N Concentrations in Seep and Non-seep Areas

Nitrogen concentrations among study sites in FD36 were more similar than was initially expected. Based on land use and N management above the three study sites, we expected that a site below agricultural land (site 2) would have substantially higher N concentration compared to a site below a pasture/meadow (site 1) and a forested area (site 3). While the observed trend was similar to what we anticipated (site 2 > 1 > 3), the magnitude of concentration differences between the three sites was relatively small. Mean NO_3-N concentration in seep areas of all three sites only ranged from 1 to 3 mg L^{-1}. Temporal patterns in NO_3-N concentration suggest that land management may still play an important role in the timing of N delivery to the stream. For example, the peaks in seep area NO_3-N concentration occurred in both the early-spring and late-summer at site 2. Manure is applied during the spring before planting and during the late fall (typically November) above site 2. Therefore, the seasonal peaks in NO_3-N concentration were likely tied to the timing of manure application to cropped fields upslope of site 2. In contrast, no manure or fertilizer was applied to the pasture/meadow above site 3, which had seasonally invariable NO_3-N concentrations in the seep area throughout the study period.

Sampling of piezometers in this study also only represented several snapshots in time. If samples were collected at multiple times during and following a storm event or immediately after manure application, greater differences in N concentration would have likely been observed among sites. It is also important to note that we were unable to determine the location or extent of the contributing area draining to each site. Groundwater patterns suggest that seep areas are fed by groundwater from the fractured aquifer, whereas non-seep areas appear to be more locally controlled (e.g., water that is perched above the fragipan). Depending on the extent of the contributing area, N concentrations could vary greatly due to differences in management practices or land use. In addition to land use, the ratio of groundwater from the fractured aquifer to perched

water above the fragipan in seep areas varied throughout the study period. At sites 1 and 2, results suggested that NO_3-N concentration was dependent on the amount of groundwater from the fractured aquifer; thus, the timing of sample collection in relation to a storm event, the size of the storm, and the antecedent conditions prior to the storm event likely played a role in the NO_3-N concentrations that we observed.

Within each study site, NO_3-N concentrations in non-seep areas were low compared to seep areas and averaged less than 0.7 mg L^{-1}. This finding is consistent with previous studies in which riparian zones underlain by a fragipan or other impermeable layer are effective in removing NO_3-N from shallow groundwater (*e.g., Peterjohn and Correll, 1984; Jordan et al., 1993*). Shallow lateral subsurface flow paths maximize the interaction between groundwater and riparian soils and vegetation. Longer residence times in the riparian zone promote NO_3-N removal via denitrification and vegetative uptake (*Vidon and Hill, 2004*). While NO_3-N removal was not observed along groundwater flow paths in non-seep areas during this study, it is possible that the majority of NO_3-N removal occurred at the upland-riparian zone interface (*Hill et al., 2000*) and the low NO_3-N concentrations reflected the effectiveness of the riparian zone in removing N in shallow groundwater. Differences in NO_3-N concentrations were however observed at all three non-seep areas between depths. Near the surface (20 cm), mean NO_3-N concentration was less compared to mean NO_3-N concentration deeper in the soil profile (60 cm). In contrast, mean Cl^- concentrations were not different between the two depths. Changes in the NO_3-N to Cl^- ratio with depth in the non-seep areas suggests that NO_3-N removal in non-seep areas may be more efficient in near-surface riparian soils that are typically higher in organic material (*Addy et al., 1999*).

Groundwater upwelling through preferential flow paths in seep areas of site 1 and 2 resulted in higher NO_3-N concentrations compared to non-seep areas. At both sites, NO_3-N concentrations were significantly correlated with water table depth. Areas within the seep where

the water table was closer to the land surface (i.e., areas of groundwater upwelling) had higher NO_3-N concentrations than areas where the water table elevation was deeper. Preferential flow paths have been shown to decrease residence times of groundwater (*Su et al., 2001*), which could limit interaction with riparian zone soils. In many instances, preferential flow paths have been shown to increase the potential for NO_3-N leaching down through the soil profile (*e.g., Di and Cameron, 2002*). In this case, however, they served as foci for discharging groundwater. Similar NO_3-N concentrations between depths in the seep areas at sites 1 and 2 suggest that groundwater was being transported quickly toward the surface with minimal NO_3-N removal occurring in near-surface soils. Nitrate-N concentrations, however, were similar in seep and non-seep areas at site 3; although, patterns in water table depth suggested that groundwater upwelling occurred in the seep area similar to the seep areas in sites 1 and 2. Nitrate-N concentration in seep surface flow paths have been shown to be correlated with dissolved organic carbon (DOC) concentrations (*O'Driscoll and DeWalle, 2010*). Dissolved organic carbon concentrations are often higher in forested areas compared to agricultural areas due to leaf litter inputs (*Boyer and Groffman, 1996*). While DOC was not measured as part of this study, it is possible that higher DOC concentrations in the soil at site 3 resulted in greater NO_3-N removal and decreased NO_3-N concentrations in the seep area relative to sites 1 and 2.

N Transport Potential in Seep and Non-seep Areas

The combination of preferential flow paths, discharge of groundwater onto the land surface, and longer periods of saturation in seep areas of the riparian zone in FD36 suggest that the potential for N delivery, especially NO_3-N, to streams is much greater in seep areas compared to non-seep areas. Preferential flow paths in seep areas resulted in upwelling of groundwater from below the fragipan, which had higher NO_3-N concentrations than the water perched above it.

Once the groundwater reached the surface, it was transported in small rivulets towards the stream channel. Research has shown that NO_3-N retention and/or removal can occur along seep surface pathways (*Blackwell et al., 1999; Rutherford and Nguyen, 2004; O'Driscoll and DeWalle, 2010*), but in many instances groundwater bypasses the N mitigating benefits of the riparian zone (*Warwick and Hill, 1988; Hill, 1990*). High NO_3-N concentrations observed in seep areas therefore have the potential to be delivered to the stream without any significant remediation. Visual observations also indicate that seep areas in FD36 are saturated for a greater portion of the year compared to non-seep areas. The total volume of groundwater delivered to the stream from seep areas is therefore likely much greater than adjacent non-seep areas of similar size, which tend to be dry for extended periods of time throughout the year. Even if a seep and an adjacent non-seep area had similar NO_3-N concentrations, such as site 3, NO_3-N loads would be expected to be much higher from the seep area due to the potential for larger volumes of groundwater to be delivered to the stream. Few studies, however, have focused on seeps and their effect on stream water quality. Future research should examine hydrologic processes in seeps, as results from this study show that N concentrations and transport potential are strongly influenced by the hydrology of the riparian zone. Management practices aimed at improving stream water quality in FD36 and other headwater agricultural catchments with seeps, should target seep areas since the potential for NO_3-N delivery is much greater compared to adjacent non-seep areas.

Conclusions

The results of this study showed that the potential for NO_3-N transport to the stream in FD36 is greater from seep areas of the riparian zone compared to areas without seeps (non-seep areas). Spatial patterns in water table depth indicated that groundwater flow paths in non-seep areas were dominated by uniform, lateral flow through the subsurface. Lateral subsurface flow is

characterized by longer residence times in which groundwater can interact with riparian soils and vegetation, which promote N removal and uptake. In contrast, water table depths in seep areas were highly variable with some regions having positive upward vertical gradients, which suggested that groundwater upwelling via preferential flow was an important pathway for groundwater discharge in seep areas. Preferential flow paths limit N removal because groundwater typically has short residence times within the subsurface. In seep and non-seep areas at two of the three study sites, NO_3-N concentrations were significantly correlated with water table depths. Groundwater from the fractured aquifer, which had higher NO_3-N concentration, was also the primary source of water to seep areas at all three study sites. Thus, groundwater flow paths in the riparian zone of FD36 played a significant role in the NO_3-N transport potential of these areas. Future research should examine hydrologic processes in areas of the riparian zone that differ hydrologically, such as seep and non-seep areas, to better understand how groundwater flow paths influence N transport. Results from this study show that management practices aimed at improving stream water quality in FD36 and other headwater agricultural catchments with seeps, should target these areas since the potential for NO_3-N delivery is much greater compared to adjacent areas without seeps.

References

Addy, K.L., A.J. Gold, P.M. Groffman, and P.A. Jacinthe. 1999. Ground water nitrate removal in subsoil of forested and mowed riparian buffer zones. *J. Envrion. Qual.* 28:962-970.

Allaire, S.E., S. Roulier, and A.J. Cessna. 2009. Quantifying preferential flow in soils: a review of different techniques. *J. Hydrol.* 378:179-204.

Angier, J.T., and G.W. McCarty. 2008. Variations in baseflow nitrate flux in a first order stream and riparian zone. *J. Am. Water Resour. Assoc.* 44:367-380.

Angier, J.T., G.W. McCarty, and K.L. Prestegaard. 2005. Hydrology of a first-order riparian zone and stream, mid-Atlantic Coastal Plain Maryland. *J. Hydrol.* 309:149-166.

Angier, J.T., G.W. McCarty, T.J. Gish, and C.S.T. Daughtry. 2001. Impact of a first-order riparian zone on nitrogen removal and export from an agricultural ecosystem. *The Sci. World* 1. 2: 642-651.

Blackwell, M.S.A., D.V. Hogan, and E. Maltby. 1999. The use of conveniently and alternatively located buffer zones for the removal of nitrate from diffuse agricultural run-off. *Water Sci. Technol.* 39:157-164.

Bosch, D.D., R.K. Hubbard, L.T. West, and R.R. Lowrance. 1994. Subsurface flow patterns in a riparian buffer system. *Trans. ASAE* 37:1783-1790.

Boyer, J.N., and P.M. Groffman. 1996. Bioavailability of water extractable organic carbon fractions in forest and agricultural soil profiles. *Soil Biol. Biochem.* 28:783-790.

Bryant, R.B., T.L. Veith, G.W. Feyereisen, A.R. Buda, C.D. Church, G.J. Folmar, J.P. Schmidt, C.J. Dell, and P.J.A. Kleinman. 2011. U.S. Department of Agriculture Agricultural Research Service Manhantango creek watershed, Pennsylvania, United States: phsiography and history. *Water Resour. Res.* 47: DOI: 10.1029/2010WR010056.

Buda, A.R., T.L. Veith, G.J. Folmar, G.W. Feyereisen, R.B. Bryant, C.D. Church, J.P. Schmidt, C.J. Dell, and P.J.A. Kleinman. 2011. U.S. Department of Agriculture Agricultural Research Service Manhantango creek watershed, Pennsylvania, United States: long-term precipitation database. *Water Resour. Res.* 47: DOI: 10.1029/2010WR010058.

Calver, A. 1990. Stream head migration: an indicator of runoff processes on chalklands. *Catena* 17:399-408.

Correll, D.L. 1998. The role of phosphorus in the eutrophication of receiving waters: A review. *J. Environ. Qual.* 27:261-266.

Craig, J.P., and R.R. Weil. 1993. Nitrate leaching to a shallow mid-Atlantic coastal plain aquifer as influenced by conventional no-till and low-input sustainable grain production systems. *Water. Sci. Technol.* 28:691-700.

Crum, J.R., F.J. Pierce, M.L. Vitosh, and B.D. Knezek. 1990. Potential nitrogen contamination of groundwater as affected by soil, water, and land use relationships. Institute of Water Research, MI.

Davis, S.N., G.M. Thomson, H.W. Bently, and G. Stiles. 2006. Groundwater tracers: a short review. *Groundwater*. 18:14-23.

Devito, K.J., D. Fitzgerald, A.R. Hill, and R. Aravena. 2000. Nitrate dynamics in relation to lithology and hydrologic flow path in a river riparian zone. *J. Environ. Qual.* 29:1075-1084.

Di, H.J., and K.C. Cameron. 2002. Nitrate leaching in temperate agroecosystems: sources, factors, and mitigating strategies. *Nutrient Cycling in Agroecosystems* 46:237-256.

Gburek, W.J., and A.N. Sharpley. 1998. Hydrologic controls on phosphorus loss from upland agricultural watersheds. *J. Environ. Qual.* 27:267-277.

Gburek, W.J., A.N. Sharpley, and H.B. Pionke. 1996. Identification of critical source areas for phosphorus export from agricultural catchments. *In: Advances in hillslope processes*. M.G. Anderson and S.M. Brooks (Editors) Vol. 1. John Wiley and Sons, New York, NY, pp. 263-282.

Gburek, W.J., and G.J. Folmar. 1999. Patterns of contaminant transport in a layered fractured aquifer. *J. Contam. Hydrol.* 37:87-109.

Groffman, P.M., A.J. Gold, and R.C. Simmons. 1992. Nitrate dynamics in riparian forests: microbial studies. *J. Environ. Qual.* 21:666-671.

Harvey, J.W., and W.K. Nuttle. 1995. Fluxes of water and solute in a coastal wetland sediment. 2. Effect of macropores on solute exchange with surface water. *J. Hydrol.* 164:109-125.

Hill, A.R. 1991. A groundwater nitrogen budget for a headwater swamp in an area of permanent groundwater discharge. *Biogeochemistry*. 14:209-224.

Hill, A.R. 1990. Groundwater flow paths in relation to nitrogen chemistry in the near-stream zone. *Hydrobiologia* 206:39-52.

Hill, A.R. 1996. Nitrate removal in stream riparian zones. *J. Environ. Qual.* 25: 743-755.

Hill, A.R., K.J. Devito, S. Campangnolo, and K. Sanmugadas. 2000. Substrate denitrification in a forest riparian zone: interactions between hydrology and supplies of nitrate and organic carbon. *Biogeochemistry* 51:193-223.

Jacinthe, P.A., P.M. Groffman, A.J. Gold, and A. Mosier. 1998. Patchiness in microbial nitrogen transformations in groundwater in a riparian forest. *J. Environ. Qual.* 27:156-164.

Jordan, T.E., D.L. Correll, and D.E. Weller. 1993. Nutrient interception by a riparian forest receiving inputs from adjacent cropland. *J. Environ. Qual.* 22:467-473.

Koerkle, E.H. 1992. Effects of nutrient management on surface water quality in a small watershed in Pennsylvania. p. 193-207, *In*: The Natural Rural Clean Water Program Symposium, Sept. 1992, Orlando, FL. ORD EPA/625/R-92/006. US EPA, Washington DC.

Lindsey, B.D., S.W. Phillips, C.A. Donnelly, G.K. Speiran, L.N. Plummer, J.K. Bohlke, M.J. Focazio, W.C. Burton, and E. Busenberg. 2003. Residence times and nitrate transport in groundwater discharging to streams in the Chesapeake Bay watershed. U.S. Geological Survey Water Resources Investigations Report 03-4035.

Lowrance, R.R., R.L. Todd, and L.E. Asmussen. 1983. Waterborne nutrient budgets for the riparian zone of an agricultural watershed. *Ag. Ecosys. Environ*. 10:371-384.

Mayer, P.M., S.K. Reynolds Jr., M.D. McCutchen, and T.J. Canfield. 2007. Meta-analysis of nitrogen removal in riparian buffers. *J. Environ. Qual.* 36: 1172-1180.

McGlynn, B.L., and J.J. McDonnell. 2003. Quantifying the relative contributions of riparian and hillslope zones to catchment runoff. *Water Resour. Res*. 39:1310-1330.

Needlelman, B.A. 2002. Surface runoff hydrology and phosphorus transport along two agricultural hillslopes with contrasting soils. Ph.D. Thesis. The Pennsylvania State University, University Park, PA.

O'Driscoll, M.A., and D.R. DeWalle. 2010. Seeps regulate stream nitrate concentration in forested Appalachian catchments. *J. Environ. Qual.* 39:420-431.

O'Sullivan, D. and J.J. Unwin. 2010. Geographic Information Analysis. John Wiley & Sons, Inc. New York, NY.

Patton, C.J., and J.R. Kryskalla. 2003. Methods of analysis by the U.S. Geological Survey National Water Quality Laboratory: evaluation of alkaline persulfate digestion as an alternative to Kjeldahl digestion for determination of total dissolved nitrogen and phosphorus in water. U.S. Geological Survey water resources investigations report 03-4174, 33 p.

Peterjohn, W.T., and D.L. Correll. 1984. Nutrient dynamics in an agricultural watershed: observations on the role of a riparian forest. *Ecology* 65:1466-1475.

Peterson, B.J., W.M. Wolheim, P.J. Mulholland, J.R. Webster, J.L. Meyer, J.L. Tank, E. Marti, W.B. Bowden, H.M. Valett, A.E. Hershey, W.H. McDowell, W.K. Dodds, S.K. Hamilton, S. Gregory, and D.D. Morrall. 2001. Control of nitrogen export from watersheds by headwater streams. *Science* 292:86-90.

Pinay, G., L. Rogues, and A. Fabre. 1993. Spatial and temporal patterns of denitrification in a riparian forest. *J. Appl. Ecol.* 30:581-591.

Pionke, H.B., and J.B. Urban. 1985. Effect of agriculture land use on ground-water quality in a small Pennsylvania watershed. *Groundwater*. 23:68-80.

Pionke, H.B., J.R. Hoover, R.R. Schnabel, W.J. Gburek, J.B. Urban, and A.S. Rogowski. 1988. Chemical-hydrologic interactions in the near-stream zone. *Water Resour. Res.* 24:1101-1110.

Pionke, H.B., W.J. Gburek, and R.R. Schnabel. 1996. Flow and nutrient transport patterns for an agricultural hill-land watershed. *Water Resour. Res.* 32:1795-1804.

R Development Core Team. 2011. R: a language and environment for statistical computing. R Foundation for Statistical Computing, Vienna, Austria.

Rutherford, J.C., and M.L. Nguyen. 2004. Nitrate removal in riparian wetlands: interactions between surface flow and soils. *J. Environ. Qual.* 33:1133-1143.

Schnabel, R.R., J.B. Urban, and W.J. Gburek. 1993. Hydrologic controls in nitrate, sulfate, and chloride concentrations. *J. Environ. Qual.* 22:589-596.

Shabaga, J.A., and A.R. Hill. 2010. Groundwater-fed surface flow path hydrodynamics and nitrate removal in three riparian zones in southern Ontario, Canada. *J. Hydrol.* 388:52-64.

Simmons, R.C., A.J. Gold, and P.M. Groffman. 1992. Nitrate dynamics in riparian forests: groundwater studies. *J. Environ. Qual.* 21:659-665.

Su, G.W., J.T. Geller, K. Pruess, and J.R. Hunt. 2001. Solute transport along preferential flow paths in unsaturated fractures. *Water Resour. Res.* 37:2481-2491.

Tesoriero, A.J., H. Liebsecher, and S.E. Cox. 2000. Mechanisms and rate of denitrification in an agricultural watershed: electron and mass balance along groundwater flow paths. *Water Resour. Res.* 36:1545-1559.

U.S. Environmental Protection Agency. 2008. National water quality inventory: 2008. Washington, DC.

Vidon, P., and A.R. Hill. 2004. Landscape controls on nitrate removal in stream riparian zones. *Water Resour. Res*. 40: DOI: 10.1029/2003WR002473.

Vidon, P., C. Allen, D. Burns, T.P. Duval, N. Gurwick, S. Inamdar, R. Lowrance, J. Okay, D. Scott, and S. Sebestyen. 2010. Hot spots and hot moments in riparian zones: potential for improved water quality management. *J. Am. Water. Resour. Assoc.* 46:278-298.

Warwick, J., and A.R. Hill. 1988. Nitrate depletion in the riparian zone of a small woodland stream. *Hydrobiologia* 157:231-240.

CHAPTER 3

Imaging Riparian Seepage Zones Using Electrical Resistivity: Linking Hydrology and Nitrogen Transport

Abstract

The activation of subsurface seepage in response to precipitation events represents a potentially important pathway of nitrogen (N) delivery to streams in agricultural catchments. In this study, we used electrical resistivity imaging (ERI) and shallow piezometers to elucidate how seep and non-seep areas within the riparian zone responded to a series of three precipitation events that occurred over a one-month period (mid-April to mid-May, 2012). Two study areas were established on soils possessing a fragipan (0.6-m deep) in FD36, an agricultural catchment (40 ha) in the Ridge and Valley physiographic region of central Pennsylvania. On six occasions, ERI data were collected across 32 electrodes (0.5 m spacing) in both areas. A network of 40 piezometers in each area (20- and 60-cm deep) was also monitored for water table depth and N chemistry. Soil conditions prior to the rainfall events were dry (soil water content (Θ) = 21%); however, the first rainfall event (41 mm) was sufficient to activate subsurface discharge within the seep area. The non-seep area showed no such response. Specifically, ERI data showed large, localized decreases in resistivity (30% - 40%) within the seep area, suggesting groundwater was upwelling via preferential flow pathways through the fragipan. After the second and third events (100 mm total), both seep and non-seep areas were saturated (Θ = 47%), with overland flow visible within the seep area. The activation and expansion of the seep zone coincided with significant changes in seep discharge N concentration. Nitrate-N concentrations averaged 1.4 mg

L^{-1} when the subsurface initially became hydrologically active, but increased to 5.0 mg L^{-1} as upwelling groundwater expanded the seep zone. Upon saturation, seep nitrate-N concentration returned to 1.3 mg L^{-1}. Mean NO_3-N concentration in the non-seep area was 0.2 mg L^{-1}. Results from ERI and hydrometric monitoring of the riparian zone show that seep areas are highly dynamic and responsive to rainfall events compared to non-seep areas, and that subsurface hydrologic processes in seep zones can significantly affect N concentrations in the groundwater being delivered to the stream.

Introduction

Streamflow in headwater catchments is often sustained by seeps or seepage zones, which supply a source of groundwater during low-flow periods between rainfall and snowmelt events. In these settings, groundwater from seeps can often account for 50% to 80% of annual stream discharge (*Srinivasan et al., 2002; O'Driscoll and DeWalle, 2010; Morley et al., 2011*). Seep zones are also dynamic and responsive during precipitation events, both expanding and then contracting rapidly (*Pionke et al., 1988*). These expansions and contractions of the seep zone are, in part, due to activation of subsurface groundwater flow pathways, which can change the quantity and chemistry of groundwater being delivered to the stream. To date, our understanding of chemical and hydrological interactions in seeps has been hampered by an inability to describe and quantify seep zone formation over space and time. Improved characterization of hydrological processes in emergent groundwater seeps is therefore critical to characterizing their role in generating streamflow and influencing water quality.

In headwater catchments, riparian zone seeps are commonly found where substantial percolation occurs annually or seasonally, and where the downslope transmission capacity of the subsurface flow system is restricted due to low hydraulic gradients (*Pionke et al., 1988*), small

cross sectional areas (*Stein et al., 2004*), or decreased permeability (*Vidon and Hill, 2004*). While these properties establish a large-scale control on the extent and location of seep zones, precipitation events can serve to generate new seeps or expand existing seeps over short time scales. Hence, recent investigations of seep discharge have suggested that multiple flow pathways may be responsible for variations in seep flow during and following precipitation events. For example, studies in Virginia and New York found that seep baseflow was generated from a regional groundwater flow system (e.g., shallow aquifers) and discharge was maintained even during periods of prolonged drought (*Burns et al., 1998; Gentry and Burbey, 2004*). The authors also found that increased seep discharge identified on hydrograph peaks was the result of rapid flow through a local groundwater flow system (e.g., infiltration of rainwater, soil water, and perched water on top of aquicludes) that was formed within a small radius of the seep orifice.

The activation of seepage zones has the potential to be a significant source of nitrogen (N) to streams, especially nitrate-N (NO_3-N), in agricultural landscapes (*e.g., Chapter 2*). In many non-glaciated areas in the northeastern U.S., catchments are underlain by bedrock that is severely weathered at a shallow depth as a result of stress-relief fracturing (*Gburek and Folmar, 1999*). This highly conductive fractured layer can support lateral saturated flows that contribute directly to seeps and influence both hydrology and water quality within these catchments (*Lindsey et al., 2003*). Indeed, water quality within these fractured aquifers has been shown to be affected directly by the overlying and immediately upgradient land use. Pionke and Urban (1985) found that NO_3-N concentrations representing a fractured aquifer (10 – 60 m deep) in central Pennsylvania were lowest beneath forest (0.7 mg L^{-1}) and highest under cropland (4.7 mg L^{-1}). In the same catchment, Schnabel et al. (1993) found that the fractured aquifer had high NO_3-N concentrations due to agricultural N inputs compared to a deeper flow system (> 60 m deep), which had low NO_3-N concentrations. The authors also showed that stream NO_3-N concentrations during baseflow were influenced by groundwater contributions from the fractured aquifer.

Subsurface hydrologic processes have typically been characterized using local observation methods, such as time-domain reflectometry (TDR) and monitoring well networks (*Oberdorster et al., 2010; Williams, Chapter 2*). For example, on the coastal plain of Maryland, Angier et al. (2005) examined spatial and temporal differences in subsurface hydrology and groundwater flow direction within a riparian zone using piezometer transects. Hill (1990) and Hill et al. (2000) also investigated the interaction between groundwater flow paths and water chemistry in the riparian zone of a small headwater catchment near Toronto, Ontario using transects of nested piezometers that extended from the perimeter of the riparian zone to the stream. In addition, Williams (Chapter 2) monitored groundwater flow patterns and NO_3-N concentrations in three seep and adjacent non-seep areas of a riparian zone using a gridded network of piezometers. While piezometers and other local observation methods provide point verification of subsurface hydrologic processes and N transport (*Hill, 1990; Hill et al., 2000*), they ultimately lack spatial resolution and often fail to represent the extensive spatial coverage of the processes being studied (*Ward et al., 2010*).

Recently, several studies have shown that electrical resistivity imaging (ERI) is a useful technology for visualizing the impacts of soil state variables and soil physical properties on subsurface hydrologic processes (*Besson et al., 2010*). Electrical resistivity has been applied to investigate water uptake by corn roots and its impact on soil water content (*Michot et al., 2003*) and to describe the structural heterogeneity of ploughed soils (*Besson et al., 2004; Seger et al., 2009*). Groundwater flow and solute infiltration in the vadose zone have been described by electrical monitoring during tracer experiments (*Slater et al., 2000; Kemna et al., 2002; Vanderborght et al., 2005; Cassiani et al., 2006*). Ward et al. (2010) also used ERI to visualize the spatial and temporal dynamics of hyporheic exchange along a headwater stream. Therefore, combining ERI with local observation methods (i.e., monitoring well network and TDR) has the potential to increase our ability to characterize chemical-hydrologic interactions in seeps and

better understand the role of seeps on N dynamics within the riparian zones of headwater agricultural catchments.

In this study, we apply standard hydrometric measurements and ERI to examine seep zone formation, subsurface discharge, and N transport potential following a series of three precipitation events in a central Pennsylvania agricultural headwater catchment. These events transitioned the landscape from a dry to a wet state and allowed us to track the activation of seep zones. Our objectives were to (1) investigate chemical and hydrologic interactions within a seep and in an adjacent area without a seep using standard hydrometric techniques; (2) examine these interactions in the context of observed subsurface hydrologic responses visualized with ERI; and (3) use the results from objectives (1) and (2) to develop a conceptual model of seep zone formation, subsurface flow pathways, and N transport in the riparian zone of this catchment.

Materials and Methods

Site Location and Characteristics

The study was conducted in FD36 (0.40 ha) a small headwater catchment located approximately 40 km north of Harrisburg, Pennsylvania within the non-glaciated, folded and faulted, Appalachian Ridge and Valley physiographic region. FD36 is one of 15 sub-catchments that form WE-38, a primary research site of the USDA – Agricultural Research Service for over 40 years (see Bryant et al. (2011) for a detailed history of the site). The climate is temperate and humid with annual precipitation averaging 1080 mm yr^{-1} and mean annual air temperatures of 8 to 10°C (*Gburek and Sharpley, 1998; Buda et al., 2011*). Previous research in FD36 has shown that groundwater from a fractured aquifer provides the majority (60% – 80%) of the annual streamflow (*Pionke and Urban, 1985; Schnabel et al., 1993; Lindsey et al, 2003*) and that surface and subsurface flow systems are predominately self-contained at the catchment scale (*Gburek and*

Folmar, 1999). Two contrasting soil groups are also found within FD36 (*Needelman et al., 2002*). Well-drained residual soils that are typically stony, silt loams (Leck Kill, Calvin, and Berks series) line the hillslopes, while colluvial soils (Albrights and Hustontown series) are distributed along the stream and valley floor. The Albrights and Hustontown soils in the riparian zone have a moderately well-developed fragipan beginning at a depth of 0.5 to 0.7 m and have low permeability.

Two adjacent sites on the north hillslope in FD36 were chosen for intensive monitoring of subsurface flow processes and N transport (Figure 3.1). One study site was located where an emergent groundwater seep was commonly observed (seep area), while the other study site was an area without an emergent groundwater seep (non-seep area). The seep was selected because it flowed consistently, was active during storm events, and was easily paired with an adjacent, less active area without an emergent seep. Both seep and non-seep sites were instrumented identically with five transects of piezometers (6-m long) (Figure 3.1). Each piezometer transect contained four pairs of piezometers installed at depths of 20 and 60 cm with a spacing of 1.5 m between pairs of piezometers. All piezometers were screened at the bottom 8 cm. The depths of the piezometers were chosen to best represent the soil properties at the study sites (20 cm – Ap horizon boundary; 60 cm – top of fragipan). A 4-m deep piezometer was also located at the base of each seep and non-seep area in order to get an approximate water table depth when the water table was greater than 60 cm from the land surface (i.e., the depth of the piezometers within each site). Time-domain reflectometry (TDR) access tubes (1-m deep) were installed at both study sites (Figure 3.1) in order to monitor soil water content. In addition, four pairs of monitoring wells (1- and 6-m deep) throughout FD36 were sampled concurrently with the piezometers. All monitoring wells were screened at the bottom 0.5 m. The shallow monitoring wells (1 m) sampled perched groundwater above the fragipan. In contrast, the deep monitoring wells (6 m) sampled water in the fractured aquifer.

Field Sampling and Laboratory Analysis

Water samples were collected from piezometers at both study sites on six occasions between April 21, 2012 and May 21, 2012. This time period coincided with a series of three precipitation events that transitioned the riparian zone from a dry (soil moisture (Θ) = 21%) to a wet state (Θ = 50%). Prior to collecting water samples from each piezometer, the depth of the water table was recorded and the piezometers were purged using a peristalitic pump. Water samples were collected in 125 mL plastic (HDPE) bottles, transported on ice back to the laboratory, and then stored at 4°C until analysis. Soil water content was measured concurrently with sample collection at 20 cm intervals using a TDR probe. All water samples were filtered (0.45 µm) and then analyzed with a Lachat QuikChem FIA+ autoanalyzer (QuikChem Methods FIA+ 8000 Series, Lachat Instruments, Loveland, Colorado) to determine concentrations of NO_3-N, ammonium-N (NH_4-N), and chloride (Cl^-). Total N was determined on unfiltered samples following alkaline persulfate digestion (*Patton and Kryskalla, 2003*). Since NO_3-N comprised, on average, 95% of total N, the main focus of this paper is on NO_3-N.

Statistics and Data Analysis

Ordinary kriging was used to interpolate spatial patterns of water table depth and NO_3-N concentration within each study site (*O'Sullivan and Unwin, 2010*). We first created a grid of unsampled locations at one-third the spacing of the piezometers (0.5 m) and overlaid it on top of the piezometer network at each study site. This grid served as the locations onto which the interpolation was completed. Variograms were fit to the observed data in order to determine the relationship between data points within the piezometer network. Ordinary kriging was then performed to estimate the values at unknown (i.e., unsampled) locations within each site and the

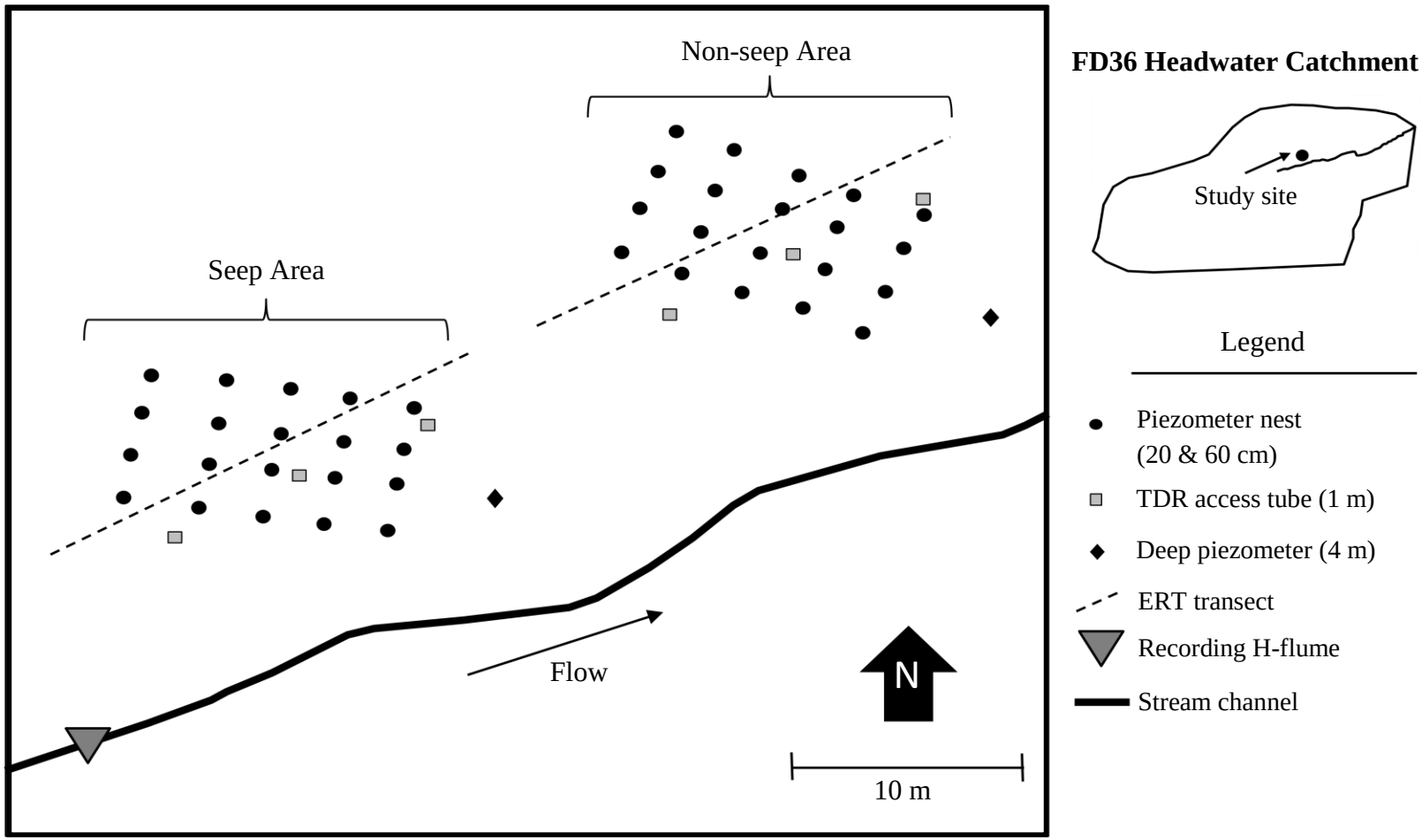

Figure 3.1

Instrumentation at the study site in FD36. One study site is located where an emergent groundwater seep is present (seep area). The other site is an area without an emergent groundwater seep (non-seep area). FD36 is a sub-catchment of WE-38, which has been a primary research site of the USDA-Agricultural Research Service for over 40 years. The water leaving WE-38 flows into East Mahantango Creek, which is a tributary of the Susquehanna River and ultimately the Chesapeake Bay.

results were plotted on a contour map. All spatial analysis was completed in *R* statistical package (*R Foundation for Statistical Computing, 2011*).

Following the methods described by Williams (Chapter 2), a two-component mixing model was used to ascertain the relative contributions of perched water above the fragipan (1-m deep monitoring wells) and groundwater from the fractured aquifer (6-m deep monitoring wells) in seep and non-seep areas. Briefly, the model was calculated as $Q_{Fractured}/Q_{Piezometer} = (C_{Piezometer} - C_{Perched})/(C_{Fractured} - C_{Perched})$, where $Q_{Fractured}/Q_{Piezometer}$ is the proportion of groundwater from the fractured aquifer to seep and non-seep areas, $C_{Piezometer}$ is the Cl^- concentration of the 60-cm deep piezometers, $C_{Fractured}$ is the Cl^- concentration of the 6-m deep monitoring wells, and $C_{Perched}$ is the Cl^- concentration of the 1-m deep monitoring wells.

Electrical Resistivity Imaging

Electrical resistivity imaging (ERI) is a geophysical method that can be used to estimate the spatial and temporal distribution of subsurface electrical resistivity (i.e., reciprocal of electrical conductivity). ERI data were collected following the methods of Ward et al. (2010). Briefly, ERI data were collected at the seep and non-seep areas with an IRIS Syscal Pro Resistivity Meter using a dipole-dipole geometry with 259 quadripoles collected across 32 electrodes set at 0.5 m spacing (Figure 3.1). ERI data collection was completed on the same dates as the piezometer sampling. During sampling, replicate measurements were collected and averaged twice by the instrument for data within 3% difference of one another. If this quality threshold was not met, a third measurement was included in the average. The average standard deviation between replicate measurements was 0.17 Ωm (0.04%). Inversion of ERI data was completed using EarthImager2D (Advanced Geosciences, Inc.). Background (pre-storm) data

were used as a baseline for comparison of data collected during subsequent time steps. Inversion results produced a root mean square error of less than 3% (mean: 2.5%) for all time steps.

Results

Water Table Dynamics and Seep Area Formation

The 90-d period prior to the start of the study (Apr. 21, 2012) was drier than the recent 5-yr (2007 – 2011) average recorded at the rain gauge within FD36. Precipitation within FD36 totaled 76 mm from Jan. 20 to Apr. 20, 2012. In comparison, the 5-yr mean precipitation within FD36 over the same period was 170 mm. Due to the dry antecedent conditions, the depth of the shallow water table at the start of the study period was greater than 60 cm in both seep and non-seep areas. A 4-m deep piezometer at each study area (Figure 3.1) showed that the water table was located approximately 68 and 159 cm below the surface in the seep and non-seep areas, respectively. Following this unseasonably dry period, a series of three significant precipitation events occurred between Apr. 21 and May 21, 2012, with a cumulative rainfall depth totaling 141 mm (Figure 3.2a). The first storm event (storm 1) occurred on Apr. 22, 2012 and had a rainfall depth of 41 mm. Storm 2 (28 mm) and storm 3 (45 mm) occurred on May 8 and May 15, respectively. Stream discharge increased in response to each of the storm events (Figure 3.2b).

On Apr. 23, 1 d after the first storm, the water table depth remained relatively unchanged in the non-seep area of the riparian zone (154-cm deep) (Figure 3.3). Within the seep area, however, the water table rose to a mean depth of 45 cm in 35% (7 out of 20) of the piezometers. The rise in the water table occurred within a topographic low region of the seep area (Figure 3.3). Three-days after storm 1 (Apr. 25), the water table in the seep area continued to rise and the saturated area continued to expand, indicating there was a time lag between the precipitation event and the seep zone response. The mean water table depth in the seep area was 36 cm in

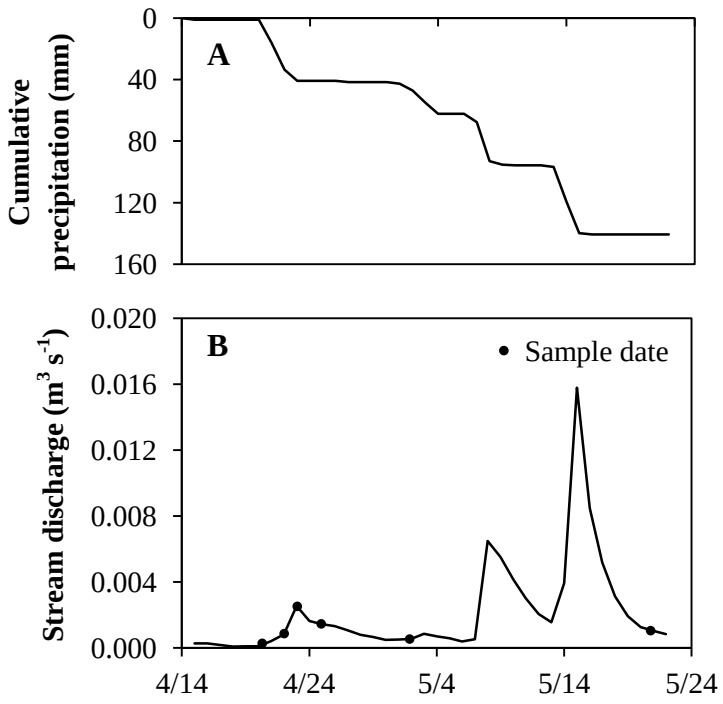

Figure 3.2

(A) Cumulative precipitation measured at a rain gauge approximately 100 m south-west of the study site in FD36. (B) Daily average stream discharge measured at a recording H-flume in FD36 from April 14, 2012 to May 22, 2012 with sample dates labeled.

40% (8 out of 20) of the piezometers (Figure 3.3). Between Apr. 25 and May 2 an additional 6 mm of rain fell in FD36. While the mean water table elevation in the seep area did not change during this time, the seep zone expanded to 55% (11 out of 20) of the piezometers (Figure 3.3). No such response was observed in the non-seep area (water table depth = 155 cm). Storms 2 and 3 resulted in substantial changes to the water table in both seep and non-seep areas. On May 21, mean water table depths were 1 and 13 cm in the seep and non-seep area, respectively (Figure 3.3). Exfiltration of groundwater onto the land surface was visible in the seep area. The water table depth was generally uniform in both seep and non-seep areas, except for one piezometer on the outside edge of the seep area in which the water table remained greater than 60 cm. Following

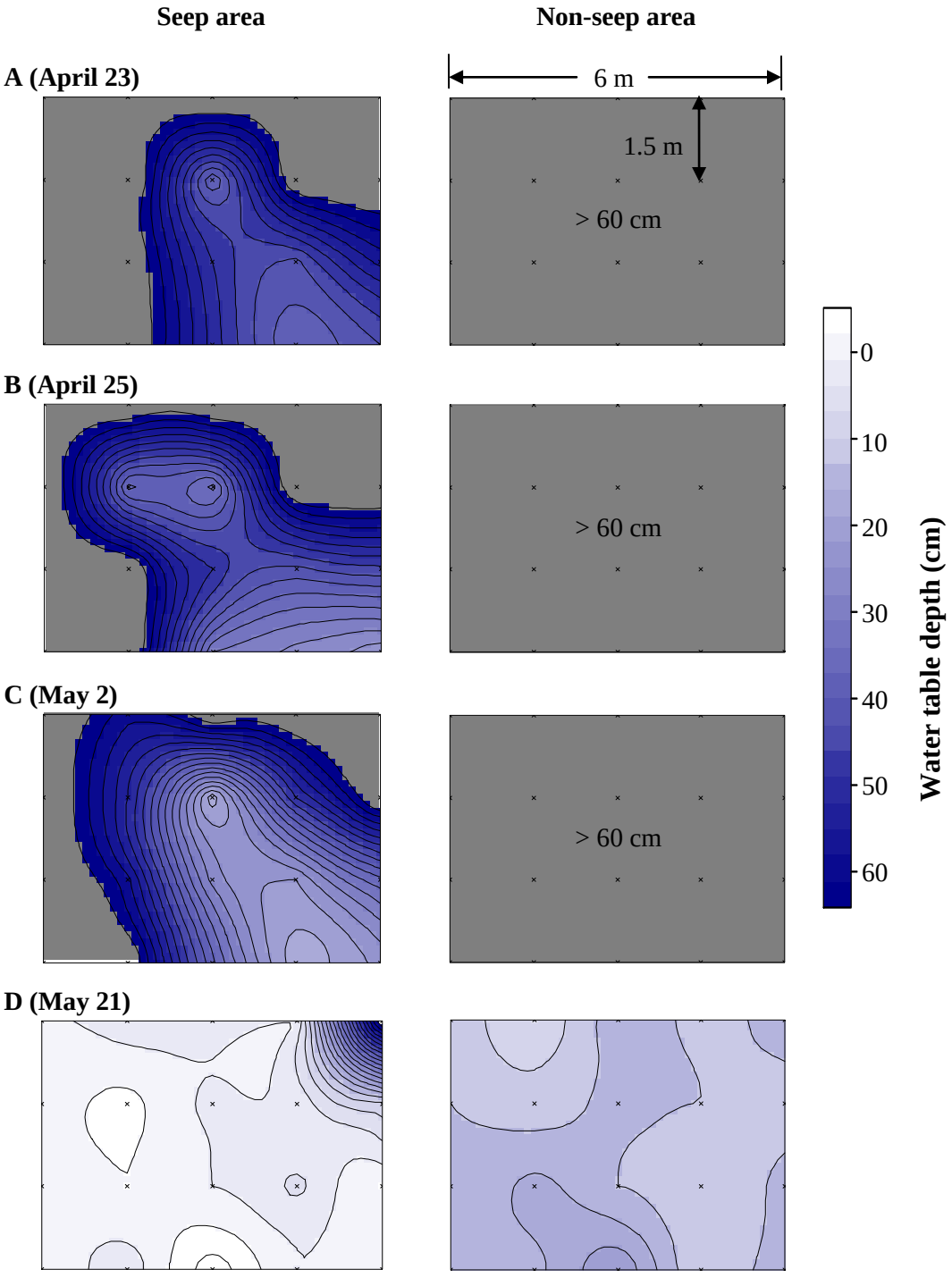

Figure 3.3

(A-D) Depth of the water table below the land surface. (A) Apr. 23; (B) Apr. 25; (C) May 2; (D) May 21. The left column is the seep area and the right column is the non-seep area. Depths were measured from the 60 cm piezometers in each area. On Apr. 21 and 22, the water table was > 60 cm in both areas (not shown).

storms 2 and 3, there were differences between the water table depth measured in the 60-cm deep piezometers and the deep piezometers at each site. Water table depths in the deep piezometers were -39 (i.e., 39 cm above the land surface) and 41 cm in the seep and non-seep area, respectively, indicating artesian conditions were present in the seep area.

Water Chemistry: NO_3-N and Cl^-

The NO_3-N transport potential within the non-seep area was low compared to the seep area since the non-seep area remained inactive for the majority of the study period (Table 3.1). Activation of subsurface flow and seep zone expansion, however, substantially influenced NO_3-N concentrations in the seep area (Table 3.1, Figure 3.4). Following storm 1 (Apr. 23), the mean

Table 3.1 Nitrate-N and Cl^- concentration in piezometers at the study sites in FD36 from April 23 to May 21, 2012. No samples were collected on April 21 or 22.

				NO_3-N		**Cl^-**	
Date	**Depth**	**Site**	**n**[†]	**Mean**	**Range**	**Mean**	**Range**
	cm			mg L^{-1}			
April 23	20	Non-seep	0				
		Seep	0				
	60	Non-seep	0				
		Seep	7	1.4	0.6-2.3	4.2	3.6-6.9
April 25	20	Non-seep	0				
		Seep	0				
	60	Non-seep	0				
		Seep	8	1.9	1.3-3.1	5.6	3.2-12.1
May 2	20	Non-seep	0				
		Seep	4	5.0	2.7-6.2	3.9	3.8-4.0
	60	Non-seep	0				
		Seep	11	4.2	0.9-11.3	7.3	3.9-13.9
May 21	20	Non-seep	20	0.2	0.1-0.5	2.2	1.3-3.3
		Seep	20	1.4	0.2-3.6	2.7	1.2-4.0
	60	Non-seep	20	0.2	0.1-0.5	2.3	1.2-3.5
		Seep	19	1.3	0.2-2.9	2.8	1.2-3.7

[†] n is the number of water samples collected at each site (max. = 20).

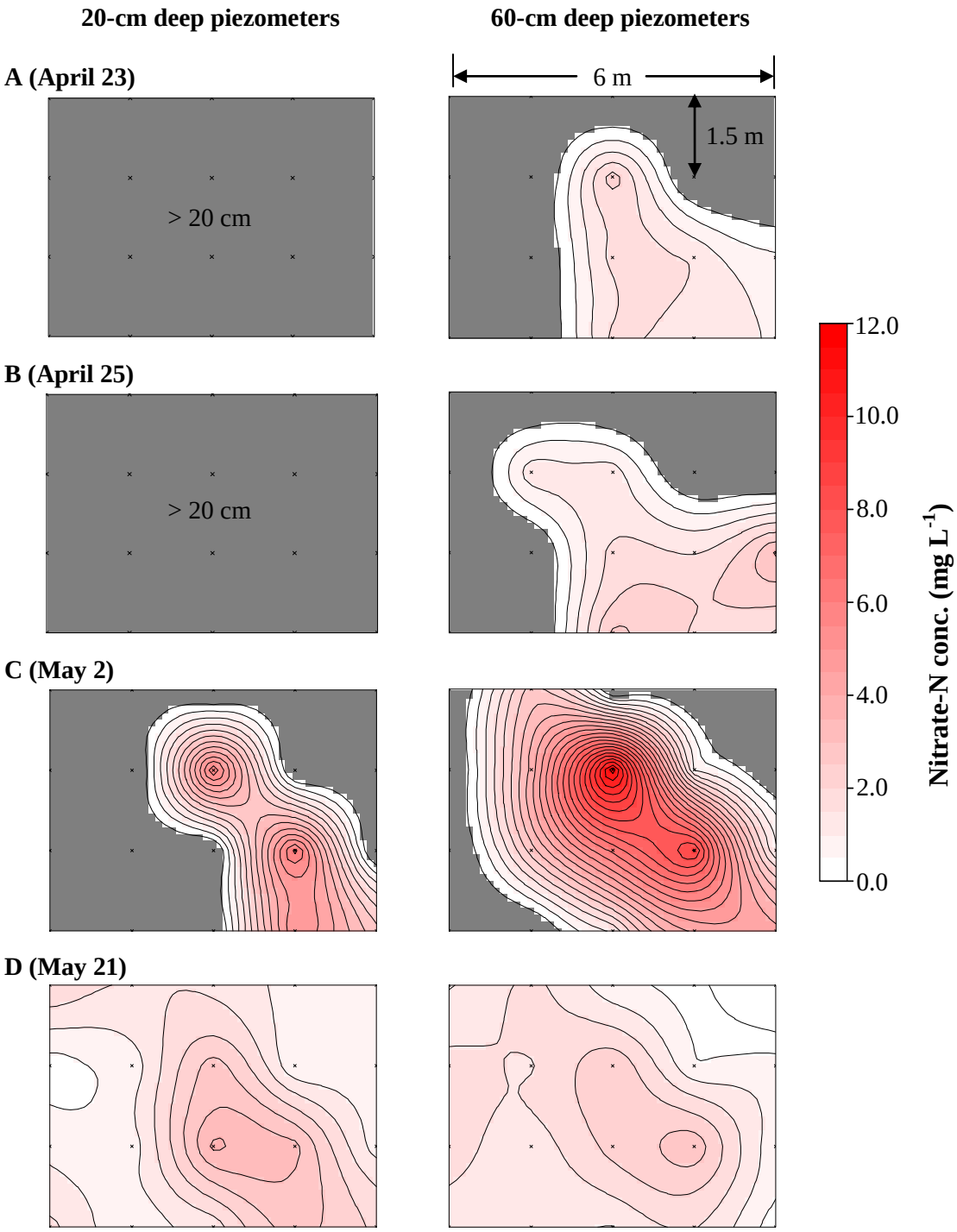

Figure 3.4

Spatial patterns of NO_3-N concentration measured in seep area piezometers in FD36. The left and right columns are NO_3-N concentrations in the 20 cm and 60 cm piezometers, respectively. (A) Apr. 23; (B) Apr. 25; (C) May 2; (D) May 21. No water samples were collected on Apr. 21 and 22.

NO_3-N concentration in the seep area was 1.4 mg L^{-1}. As the water table continued to rise after storm 1, mean NO_3-N concentrations in the seep increased to 1.9 mg L^{-1} on Apr. 25 and then to 5.0 mg L^{-1} on May 2. Nitrate-N concentrations were spatially variable in the seep area and ranged from 0.9 to 11.3 mg L^{-1} (Table 3.1). In general, NO_3-N concentrations in the 60-cm deep piezometers tended to be greater in areas where the water table was closest to the land surface (i.e., areas of groundwater upwelling) (Figure 3.4). Nitrate-N concentrations observed in the 20-cm deep piezometers were less (mean = 4.2 mg L^{-1}) than NO_3-N concentrations in the 60-cm deep piezometers on May 2 (Table 3.1). When the seep area became fully saturated (May 21), NO_3-N concentrations decreased to 1.4 and 1.3 mg L^{-1} in the 20- and 60-cm deep piezometers, respectively (Table 3.1, Figure 3.4). Nitrate-N concentrations, however, remained higher at both depths within the initial seep zone activation area as shown at the beginning of the sampling period on Apr. 23 (Figure 3.4). Mean NO_3-N concentration in the non-seep area was 0.2 mg L^{-1}.

Chloride concentrations throughout the study period were also monitored to track potential sources of water to the seep and non-seep areas. Overall, Cl^- concentrations followed a similar pattern to NO_3-N concentrations in both areas (Table 3.1). Mean seep area Cl^- concentration following storm 1 was 4.2 mg L^{-1} (60-cm deep piezometers) and increased to 5.6 and 7.3 mg L^{-1} on Apr. 25 and May 2, respectively, as the seep zone expanded. Chloride concentrations in the 60-cm deep piezometers were similar in the seep (2.8 mg L^{-1}) and non-seep (2.3 mg L^{-1}) areas following storm 3 ($p > 0.05$; Table 3.1). Comparing NO_3-N and Cl^- concentrations collected in piezometers to those measured in groundwater perched on top of the fragipan (1-m deep monitoring wells) and in the fractured aquifer (6-m deep monitoring wells), suggests that the source of water to the seep area changed as the seep zone expanded (Figure 3.5). When the seep area initially became active (Apr. 23 and 25), groundwater from the fractured aquifer comprised 43% and 66% of the water in the seep area, respectively (Figure 3.5). However, as the seep zone expanded (May 2), groundwater from the fractured aquifer became the

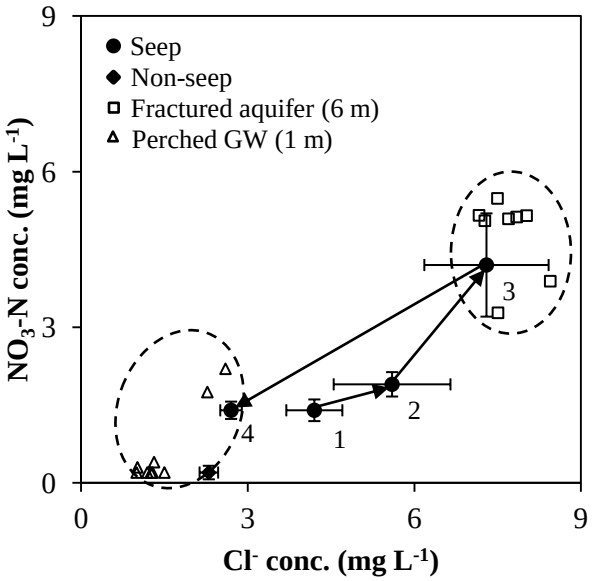

Figure 3.5

Changes in mean seep and non-seep Cl^- and NO_3-N concentrations during and following a series of precipitation events compared to fractured aquifer (deep GW) and perched groundwater (shallow GW) concentrations. Data for deep and shallow groundwater is from Williams (Chapter 2). For the seep data: 1 = Apr. 23; 2 = Apr. 25; 3 = May 2; and 4 = May 21. The non-seep concentration is from May 21. Error bars represent ± 1 standard error.

predominant source of water to the seep area (~93%). As the seep area approached full saturation (May 21), groundwater perched on top of the fragipan, which had much lower NO_3-N and Cl^- concentrations compared to fractured aquifer, became an important source to the seep area and comprised 81% of the water. Subsurface water in the non-seep area was largely derived from perched groundwater on top of the fragipan (~87%) throughout the four-week monitoring period (Figure 3.5).

Imaging Subsurface Hydrologic Processes with Electrical Resistivity

Electrical resistivity values for both seep and non-seep areas on Apr. 21 (i.e., pre-storm or background) were between 150 and 650 Ωm, which fall within a typical range of values for soils

and sediments (10 – 1,000 Ωm, *Loke, 2001*) (Figure 3.6, Figure 3.7). A layer of higher resistivity (400 – 650 Ωm) between 60 and 160 cm was present in the non-seep area, with lower resistivity values near the land surface (200 – 300 Ωm) (Figure 3.6). Based on previous soil survey data from FD36 (*Needelman et al., 2002*), the layer of higher resistivity corresponded with the location of a fragipan within the soil profile. The depth and location of the fragipan in the seep area was not as clearly defined as in the non-seep area (Figure 3.7). The seep area was characterized by pockets of higher resistivity (400 – 650 Ωm) within the top 80 cm of the soil profile and low resistivity values (150 – 250 Ωm) between 120 and 160 cm (Figure 3.7). The antecedent conditions on Apr. 21 were dry in both areas with soil water content in the upper 20 cm ranging from 17% to 22% in the seep area and 14% to 17% in the non-seep areas (Table 3.2). Soil water content of approximately 40% is representative of saturated conditions in these areas based on the depth of the water table in the deep piezometer at each site. All changes in resistivity in subsequent time steps were assumed to be due to variation in soil water content.

Minimal changes in resistivity (0% - 3%) occurred prior to the end of storm 1 (Apr. 22) in the non-seep area (Figure 3.6). Following storm 1 (Apr. 23), resistivity in the top 60 cm of the non-seep area decreased between 10% and 25%, which corresponded with a mean increase in soil water content of 8% (Table 3.2). Declines in resistivity in the non-seep area relative to pre-storm conditions persisted through May 2 with the vertical migration of water from the surface to deeper in the soil profile visible with ERI (Figure 3.6). Resistivity in the non-seep area further decreased following storm 3 in the top 80 cm of the soil profile (Figure 3.6). Decreases in resistivity of 60% were observed across the entire transect in the non-seep area as the top 80 cm approached saturation (mean $\Theta = 46\%$).

Similar to the non-seep area, small decreases in resistivity (0% - 5%) were observed in the seep area prior to the end of storm 1 (Figure 3.7). One day following storm 1 (Apr. 23), resistivity between 0 to 60 cm and 120 and 160 cm in the seep area decreased between 25%

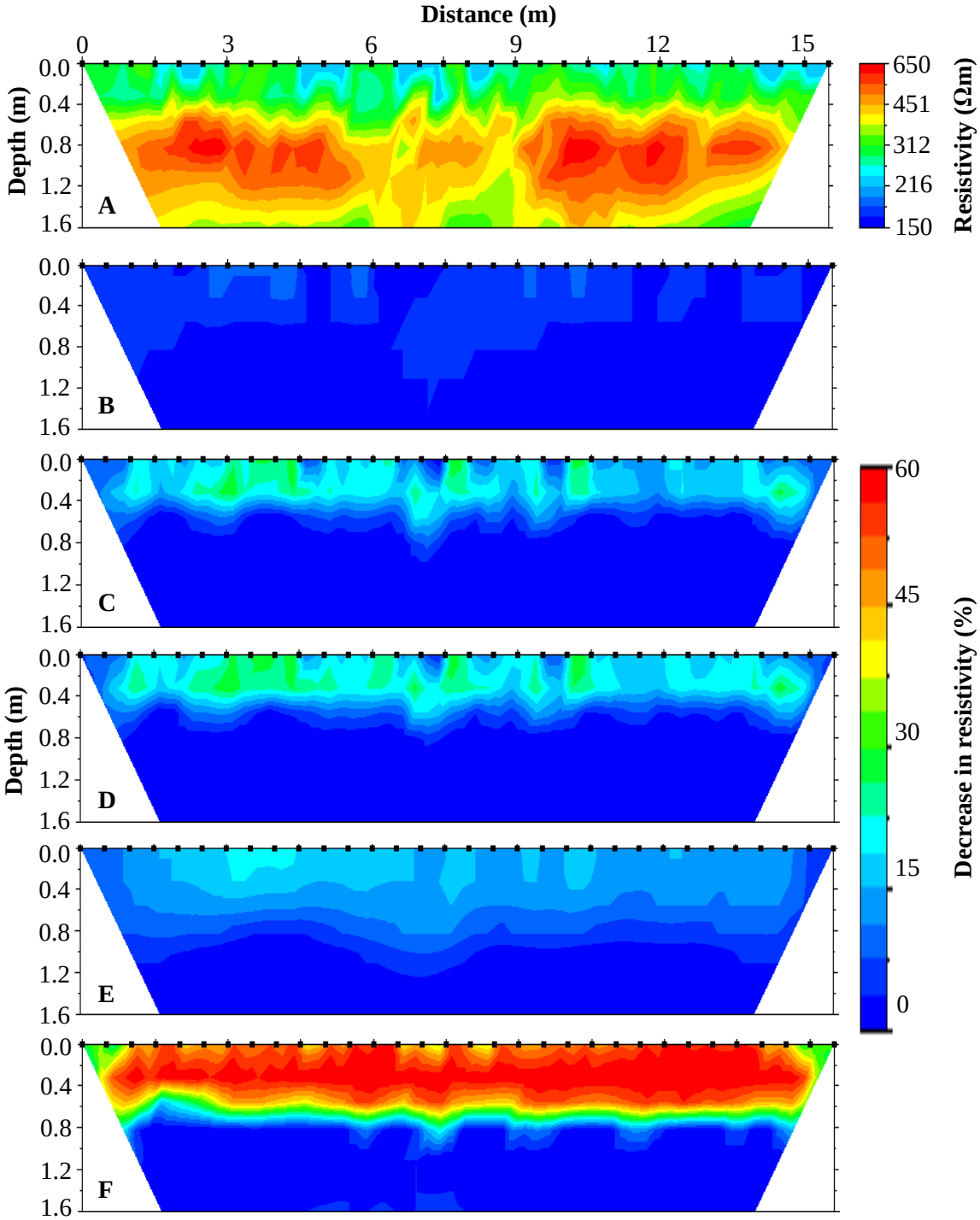

Figure 3.6

(A) Electrical resistivity measured in the non-seep area on April 21, 2012. Data were collected before a series of three precipitation events and were used as a comparion for subsequent time steps. (B-F) Change in electrical resistivity relative to background conditions (April 21, 2012). (B) April 22,2012 (C) April 23, 2012 (D) April 25, 2012 (E) May 2, 2012 (F) May 21, 2012.

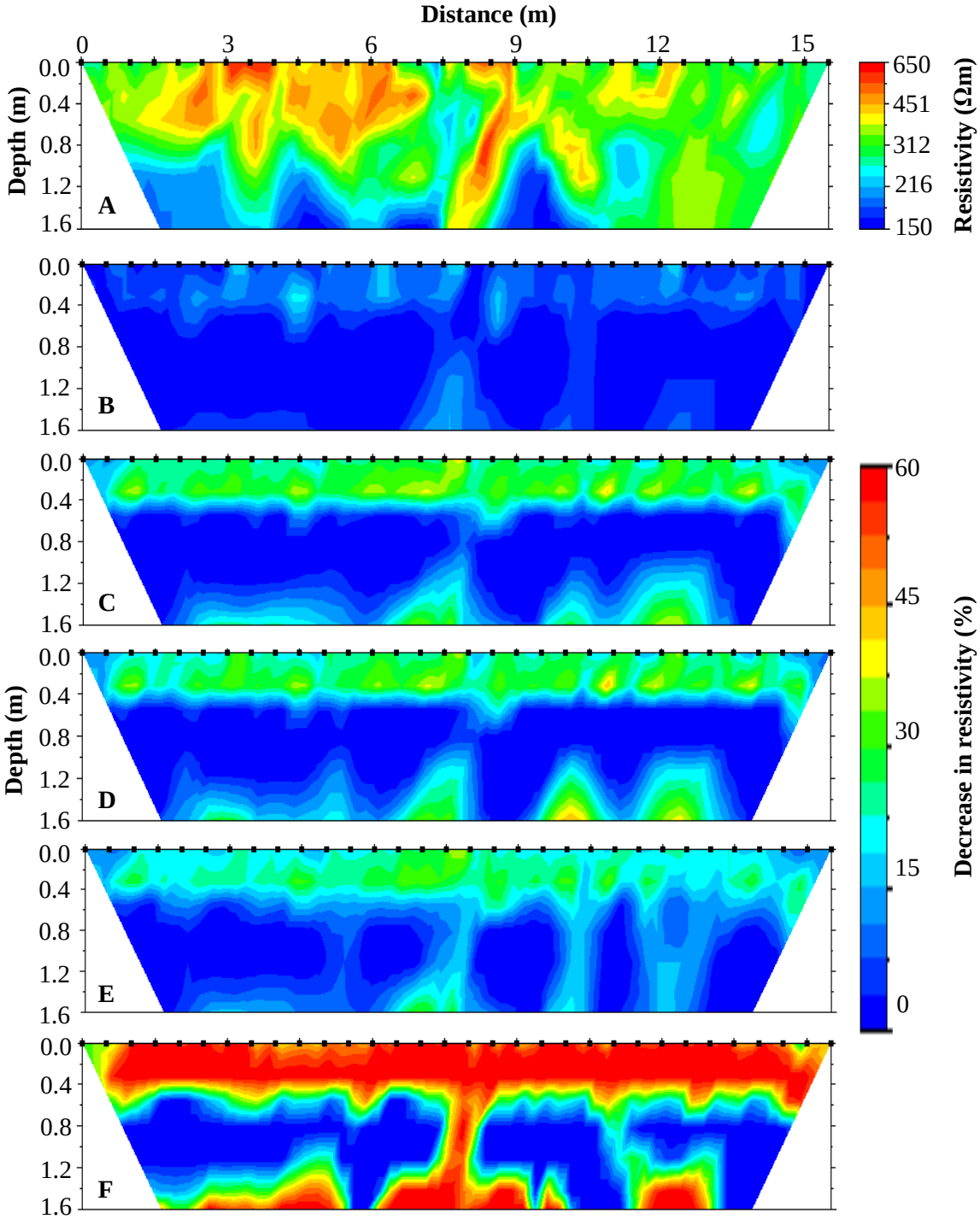

Figure 3.7

(A) Electrical resistivity measured in the seep area on April 21, 2012. Data were collected before a series of three precipitation events and were used as a comparion for subsequent time steps. (B-F) Change in electrical resistivity relative to background conditions (April 21, 2012). (B) April 22,2012 (C) April 23, 2012 (D) April 25, 2012 (E) May 2, 2012 (F) May 21, 2012.

and 40%. This corresponded with an overall mean increase of 18% in soil water content in the seep site as measured with TDR (Table 3.2). While the decrease in resistivity was relatively uniform in the top 60 cm of the seep area, decreases with depth occurred at localized areas along the ERI transect (i.e., at 7, 10, and 12 m) (Figure 3.7). Resistivity values in the seep area remained relatively unchanged between Apr. 23 and Apr. 25; however, on May 2, ERI data showed decreases in resistivity of 10% to 20% in localized regions that spanned the entire soil

Table 3.2 Soil water content at the study sites in FD36 from April 21 to May 21, 2012. Soil water content was measured at 20-cm depth intervals with TDR. See Figure 3.1 for locations of TDR access tubes.

Site	TDR position	Depth (cm)	Volumetric soil water content (%)					
			Apr. 21	Apr. 22	Apr. 23	Apr. 25	May 2	May 21
Seep	Left	20	17	23	34	30	21	48
		40	20	22	50	43	38	49
		60	38	50	52	50	46	53
		80	49	56	51	50	49	51
	Middle	20	17	18	44	42	40	49
		40	21	28	49	51	50	50
		60	41	56	56	51	51	51
		80	48	54	53	48	48	48
	Right	20	22	27	36	31	18	40
		40	24	25	28	28	23	51
		60	26	29	32	24	24	47
		80	32	35	46	35	32	47
Non-seep	Left	20	16	21	28	26	19	40
		40	15	18	20	16	23	47
		60	18	21	20	18	22	50
		80	19	26	27	24	24	41
	Middle	20	17	21	24	28	18	41
		40	15	22	21	19	28	50
		60	19	24	24	23	26	46
		80	29	30	31	27	27	42
	Right	20	14	19	28	23	15	43
		40	20	23	28	25	25	50
		60	20	28	29	25	25	49
		80	23	29	29	25	25	50

profile in the vertical direction. Following storm 3 (May 21), large decreases in resistivity (60%) were observed across the entire transect in the seep area, similar to changes in the non-seep area (Figure 3.7). Large decreases in resistivity were also observed at a depth of 120 – 160 cm and in a vertical pattern at several localized regions across the monitored seep area (i.e., at 7 and 11 m).

Discussion

Riparian Zone Hydrology and Seep Area Formation

The riparian zone in FD36 is underlain at shallow depth by a fragipan (~60 cm), which has been shown to affect surface runoff generation (*e.g., Gburek et al., 2006; Buda et al., 2009*). Fragipans and other confining layers are common across Pennsylvania (*Ciolkosz et al., 2000*) and the eastern U.S. (*Grossman and Carlisle, 1969*) and are often considered relatively impermeable; thus, limiting the downward movement of water. Groundwater flow in landscapes with a fragipan is therefore assumed to move laterally along the fragipan surface before discharging to the stream (*Jordan et al., 1993; Hill, 1996; Bosch et al., 1998*). In these settings, upland areas of the catchment are often considered to be recharge zones and the stream a discharge point. Within many models of riparian zone hydrology, however, consideration has not been given to the riparian zone regarding the effects of vertical movement (e.g., infiltration and exfiltration) of groundwater (*Angier et al., 2005*). Results from FD36 suggest that in seep areas, even in the presence of a fragipan at a shallow depth, much of the groundwater travels through the fragipan, and is delivered to the surface via preferential subsurface flow paths.

Several studies have indicated that vertical groundwater movement via recharge (*O'Connell, 1998; Sharratt, 2001*) or discharge (*Devito et al., 2000; Angier et al., 2002*) is common in riparian zones, even in those with a restrictive layer. However, characterizing preferential flow and other rapid transport flow pathways is difficult when using standard

hydrometric techniques (*Oberdorster et al., 2010*). Local observation methods, such as TDR and monitoring well networks, only sample part of the total soil volume and as a result, their ability to represent the observed transport may be limited. In this study, we combined standard hydrometric measurements with ERI in order to improve our concept of riparian zone hydrology in FD36. Electrical resistivity data provided a distributed assessment of groundwater transport in the riparian zone, a data set that is impossible to collect using traditional and invasive point measurements. It also illuminated the spatial and temporal dynamics of groundwater transport by allowing us to 'see' the heterogeneity that existed in subsurface flow pathways. While previous research in FD36 has documented positive vertical gradients and groundwater upwelling in several seep areas throughout the catchment (*Williams, Chapter 2*), we were able to confirm with ERI that groundwater moved vertically through the fragipan in localized regions within a seep area following a series of three precipitation events. We were also able to visualize with ERI the connection between the shallow fractured aquifer below the fragipan and the seepage zone. While the nature of the preferential flow pathway through the fragipan of the seep area could not be determined with ERI, fractures in the fragipan, macropores, or the uneven distribution of the fragipan extent (i.e., heterogeneity) within the riparian zone are possible explanations for preferential flow paths through the fragipan (*Day et al., 1998; Allaire et al., 2009*).

Electrical resistivity imaging has the potential to more accurately quantify subsurface hydrologic processes and provide more spatially complete data than could be collected with standard methods; however, it remains challenging to correctly interpret and identify processes when ERI data are the only source of information (*Koch et al., 2009*). Complementary evidence from hydrometric measurements is therefore necessary for a more comprehensive interpretation of subsurface flow paths. In the riparian zone of FD36, water chemistry data aided in the interpretation of ERI results. The groundwater perched on top of the fragipan and in the shallow fractured aquifer below the fragipan in FD36 was previously shown to have different

concentrations of NO_3-N and Cl^- that could be used to resolve the relative importance of these sources of groundwater in seep and non-seep areas (*Williams, Chapter 2*). In this study, NO_3-N and Cl^- concentrations increased over the course of three precipitation events, indicating that groundwater from the shallow fractured aquifer, which has higher NO_3-N concentrations, became more important over time as the riparian zone wetted up and the seep zone expanded. Indeed, Burns et al. (1998) also found that groundwater discharging from seeps in the Catskill Mountains of New York originated from varying sources of water depending on the season and seep discharge rate. In comparison, the NO_3-N and Cl^- concentrations of the non-seep area in FD36 were similar to those measured in perched groundwater at saturation, which suggested that in these areas of the riparian zone, groundwater flow is limited to lateral movement through the shallow subsurface system above the fragipan and is mostly disconnected from groundwater below the fragipan. Therefore, the combination of hydrometric and ERI results in FD36 demonstrate that the characteristics of the fragipan appear to control the location of seep areas in the riparian zone.

Results from standard hydrometric measurements and ERI in the riparian zone of FD36 in this study were in agreement. That is, piezometric, water chemistry, and ERI data all provided evidence of groundwater upwelling in seep areas and lateral flow on top of the fragipan in non-seep areas. Other studies, however, have found that observed spatial ERI patterns do not conform to the subsurface processes supported by previous hydrometric research (*e.g., Koch et al., 2009*). The joint interpretation of hydrometric data and ERI in these situations has the potential to provide new ideas about the possible functioning of a local hydrologic system, allow for reinterpretation of preconceived hydrologic processes, and generate research questions and hypotheses.

Linking Hydrology and Nitrogen Transport

Stream riparian zones often present conditions (e.g., soils high in organic carbon, anaerobic conditions, and wide vegetated corridors) that are considered favorable for NO_3-N removal (*Emmet et al., 1994; Peterson et al., 2001*). Significant groundwater NO_3-N, however, may nevertheless be transported through the riparian zone to the stream (*Hill et al., 2000; McCarty and Angier, 2001*). Therefore, knowledge of hydrology has been deemed essential to further understand riparian zone chemistry (*Hill, 1996*). In the non-seep area in FD36, NO_3-N concentrations were low (0.2 mg L^{-1}) following storm 3 (May 21). Electrical resistivity data showed that lateral subsurface flow on top of the fragipan was the primary pathway for NO_3-N transport in non-seep areas. Low NO_3-N concentrations in non-seep areas in FD36 are consistent with many other studies in which riparian zones underlain by a fragipan or other impermeable layer are effective in removing NO_3-N from groundwater (*e.g., Peterjohn and Correll, 1984*). These shallow lateral flow paths often maximize the interaction with riparian soils and vegetation, which promotes denitrification and vegetative uptake. While NO_3-N removal was not observed within the non-seep area, it is possible that the majority of NO_3-N removal occurred at the upland-riparian zone interface (*Hill et al., 2000*) and the NO_3-N concentrations that were measured in the piezometers reflected the effectiveness of the riparian zone in removing N along this flow path.

Differences in NO_3-N concentration between the seep and non-seep study areas in FD36 highlight how subtle differences in hydrology can influence groundwater quality and transport potential. Nitrate-N concentrations measured in the seep area were 8 to 25 times greater than NO_3-N concentrations measured in the non-seep area. Electrical resistivity showed that groundwater was upwelling through the fragipan via preferential flow paths in the seep area and as a result, likely had limited interaction with the surface riparian soils and minimal reductions in

NO_3-N. Preferential flow paths have been shown to reduce the residence time of water and N in the soil and facilitate leaching of NO_3-N down through the soil profile (*e.g., Jarvis, 2007*). While preferential flow paths are typically thought to enhance infiltration (recharge), in this case, they also served as foci for discharging groundwater through the fragipan. Some NO_3-N removal may have occurred in seep areas as the groundwater moved upward towards the land surface. Nitrate-N concentrations were slightly less in the 20-cm deep piezometers compared to the 60-cm deep piezometers in the seep area. In addition, following storm 3, NO_3-N concentration in the seep area was substantially less compared to NO_3-N concentration after storm 1. One likely explanation is that the higher NO_3-N concentrations from the fractured aquifer were diluted by low NO_3-N concentration groundwater perched on top of the fragipan (*Hill, 1990; Bohlke and Denver, 1995*). High NO_3-N concentration groundwater may however still be delivered to the stream via surface flow pathways in seep areas. Once groundwater is discharged onto the surface in seep areas, it can move rapidly across the surface in shallow rivulets to the stream with minimal opportunities for NO_3-N removal (*Warwick and Hill, 1988: Rutherford and Nyugen, 2004; O'Driscoll and DeWalle, 2010*).

Conceptual Model of Groundwater and Nitrogen Transport in the Riparian Zone of FD36

Electrical resistivity and hydrometric data collected in seep and non-seep areas of the riparian zone of FD36 demonstrate the considerable range in hydrologic and N transport processes that can occur in riparian zones. A conceptual model suggesting the chemical-hydrologic interactions in seep and non-seep areas of the riparian zone in FD36 is presented in Figure 3.8. The non-seep area in FD36 functions similar to previous models of groundwater and N transport in riparian zones underlain by a restrictive layer (*e.g., Hill, 1996*). Results show that the non-seep area likely remains hydrologically inactive for the majority of the year, except after

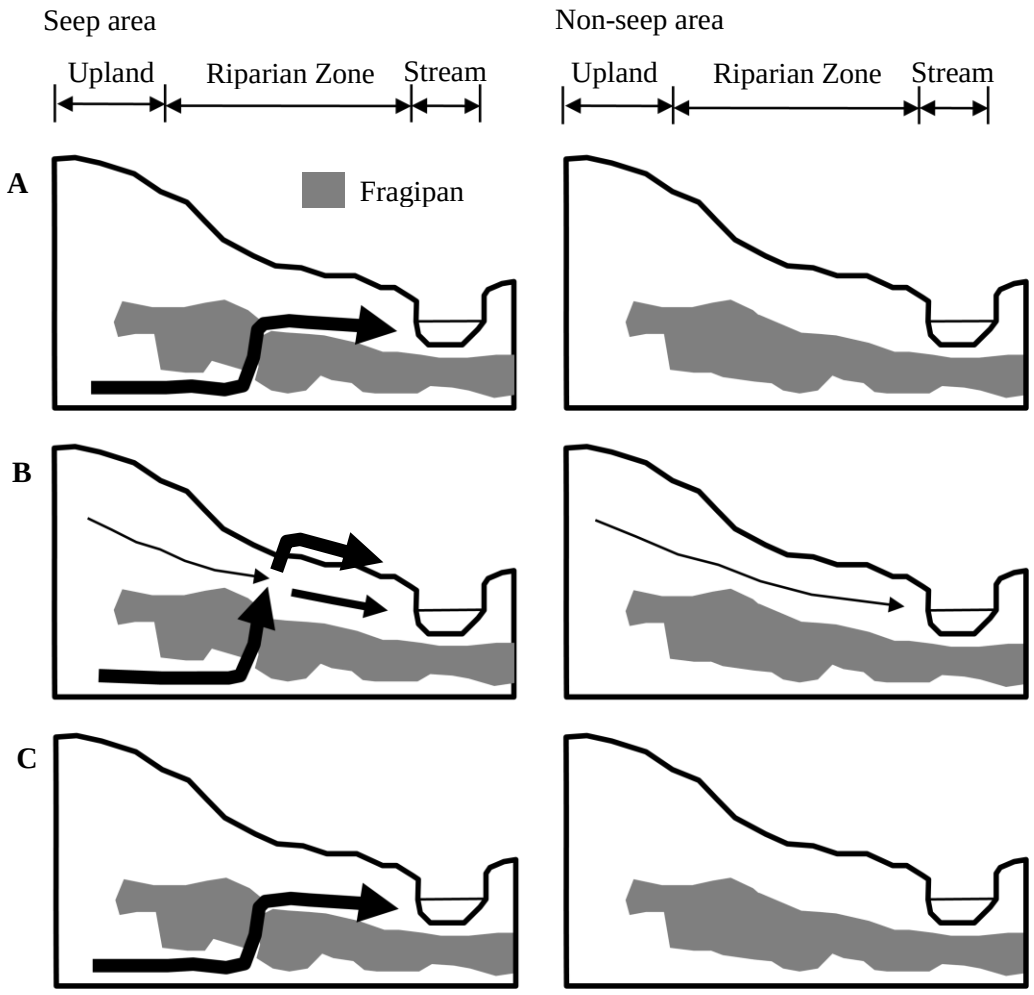

Figure 3.8

Conceptual diagram of groundwater and N transport in the seep and non-seep areas of the riparian zone in FD36. Arrows represent groundwater flow paths and the thickness of the arrows is the relative NO_3-N concentration (i.e., thick arrow = higher concentration). (A) Seep area expansion; (B) Saturation; and (C) Seep area contraction.

a large precipitation event, series of events (as shown in the current study), or even snowmelt. During these times, groundwater flows laterally along the surface of the fragipan and ultimately discharges to the stream channel. Thus, the hydrogeologic setting in the non-seep area restricts water movement to a local flow system that can become hydrologically disconnected from the uplands and exhibit considerable fluctuations in water table depth and extent of surface saturation (*Lowrance, 1992; Jordan et al., 1993*). The potential for the non-seep area of the riparian zone to

remove NO_3-N is high, due to increased interaction with riparian soils and vegetation as groundwater moves laterally toward the stream.

In comparison to the non-seep area, the seep area of the riparian zone in FD36 is much more complex in terms of hydrology and N transport. Electrical resistivity results highlight the role of preferential flow pathways in connecting deeper groundwater from the fractured aquifer system to surface seepage zones. While the nature of the preferential flow paths (i.e., fractures, macropores, etc.) could not be determined with ERI, upwelling groundwater in these localized regions creates an area of the riparian zone that is hydrologically dynamic. In seep areas, only a relatively small amount of precipitation (41 mm) was required to activate groundwater flow. The size of the saturated area and the amount of water table rise will depend on the event duration and intensity, but the seep area will remain active until another event or series of events continues to expand the seep area or the groundwater drains to the stream during dry conditions. As the seep area becomes active, NO_3-N removal potential is low due to rapid flows through riparian zone soils via preferential flow paths. At saturation, however, groundwater flow in the seep area was found to be a mixture of sources, which results in the dilution of NO_3-N concentrations under these conditions. While this study was focused primarily on seep zone activation and expansion, results from other studies suggest that that seeps will remain active following precipitation events and continue to supply baseflow to the stream (*Srinivasan et al., 2002; O'Driscoll and DeWalle, 2010*). During seep area contraction, NO_3-N concentrations will likely increase as groundwater from the shallow fractured aquifer becomes the predominant source of water in the seep area.

Conclusions

Results of this study show that in FD36, riparian zone hydrology exerts a strong influence on the chemistry of groundwater being delivered to the stream. During a series of three

precipitation events, monitoring of water table fluctuations and NO_3-N concentrations in nested piezometers showed that seep areas were more dynamic (i.e., rapid water table rise) and transported groundwater higher in NO_3-N concentration compared to non-seep areas of the riparian zone. The interpretation of these results was further enhanced with the use of ERI, which elucidated differences in subsurface hydrologic processes occurring within the seep and non-seep areas. In FD36, preferential flow paths through the fragipan where inferred using evidence from hydrometric measurements and simple mixing models, and then confirmed using data from ERI. These preferential flow paths likely resulted in shorter groundwater residence times in the subsurface, which decreased the NO_3-N removal potential compared to slower, lateral groundwater flow paths in non-seep areas of the riparian zone. This study also demonstrates the utility of ERI as a valuable tool to understand the hydrology and chemistry of riparian zone seeps. While ERI is clearly useful in riparian zone research, it may not be feasible to image the entire riparian zone, even within a small catchment like FD36. Therefore, future studies should focus on better ways to identify zones of seepage in the riparian zone that may contribute higher fluxes of water and N to streams.

References

Allaire, S.E., S. Roulier, and A.J. Cessna. 2009. Quantifying preferential flow in soils: a review of different techniques. *J. Hydrol.* 378:179-204.

Angier, J.T., G.W. McCarty, and K.L. Prestegaard. 2005. Hydrology of a first-order riparian zone and stream, mid-Atlantic coastal plain, Maryland. *J. Hydrol.* 309:149-166.

Angier, J.T., G.W. McCarty, C.P. Rice, and K. Bialek. 2002. Influence of a riparian wetland on nitrate and herbicides exported from a field applied with agrochemicals. *Journal of Agriculture and Food Chemistry*. 50:4424-4429.

Besson, A., I. Cousin, A. Samouelian, H. Boizard, and G. Richard. 2004. Structural heterogeneity of the soil tilled layer as characterized by 2D electrical resistivity surveying. *Soil Till. Res.* 79:239-249.

Besson, A., I. Cousin, H. Bourennane, B. Nicoullaud, C. Pasquier, G. Richard, A. Dorigny, and D. King. 2010. The spatial and temporal organization of soil water at the field scale as described by electrical resistivity measurements. *Eur. J. Soil. Sci.* 61:120-132.

Bohlke, J.K., and J.M. Denver. 1995. Combined use of groundwater dating, chemical, and isotopic analysis to resolve the history and fate of nitrate contamination in two agricultural watersheds, Atlantic coastal plain, Maryland. *Water Resour. Res.* 31:2319-2339.

Bosch, D.D., R.K. Hubbard, L.T. West, and R.R. Lowrance. 1998. Subsurface flow patterns in a riparian buffer system. *Trans. ASAE* 37:1783-1790.

Bryant, R.B., T.L. Veith, G.W. Feyereisen, A.R. Buda, C.D. Church, G.J. Folmar, J.P. Schmidt, C.J. Dell, and P.J.A. Kleinman. 2011. U.S. Department of Agriculture Agricultural Research Service Mahantango creek watershed, Pennsylvania, United States: phsiography and history. *Water Resour. Res.* 47: DOI: 10.1029/2010WR010056.

Buda, A.R., P.J.A. Kleinman, M.S. Srinivasan, R.B. Bryant, and G.W. Feyereisen. 2009. Factors influencing surface runoff generation from two agricultural hillslopes in central Pennsylvania. *Hydrol. Process.* 23:1295-1312.

Buda, A.R., T.L. Veith, G.J. Folmar, G.W. Feyereisen, R.B. Bryant, C.D. Church, J.P. Schmidt, C.J. Dell, and P.J.A. Kleinman. 2011. U.S. Department of Agriculture Agricultural Research Service Manhantango creek watershed, Pennsylvania, United States: long-term precipitation database. *Water Resour. Res.* 47: DOI: 10.1029/2010WR010058.

Burns, D.A., P.S. Murdoch, and G.B. Lawrence. 1998. Effect of groundwater springs on NO3-concentrations during summer in Catskill Mountain streams. *Water Resour. Res.* 34:1987-1996.

Cassiani, G., V. Bruno, A. Villa, N. Fusi, and A.M. Binley. 2006. A saline trace test monitored via time-lapse surface electrical resistivity tomography. *J. Appl. Geophys.* 59:244-259.

Ciolkosz, E.J., and W.J. Waltman. 2000. Pennsylvania's fragipans. The Pennsylvania State University Agronomy Series Number 147. University Park, PA.

Day, R.L., M.A. Calmon, J.M. Stiteler, J.D. Jabro, and R.L. Cunningham. 1998. Water balance and flow patterns in a fragipan using in situ soil block. *Soil Sci.* 163:517-528.

Devito, K.J., D. Fitzgerald, A.R. Hill, and R. Aravena. 2000. Nitrate dynamics in relation to lithology and hydrologic flow path in a river riparian zone. *J. Environ. Qual.* 29:1075-1084.

Emmett, B.A., J.A. Hudson, P.A. Coward, and B. Reynolds. 1994. The impact of a riparian wetland on stream water quality in a recently afforested upland catchment. *J. Hydrol.* 162:337-353.

Gburek, W.J., and A.N. Sharpley. 1998. Hydrologic controls on phosphorus loss from upland agricultural watersheds. *J. Environ. Qual.* 27:267-277.

Gburek, W.J., and G.J. Folmar. 1999. Patterns of contaminant transport in a layered fractured aquifer. *J. Contam. Hydrol.* 37:87-109.

Gburek, W.J., B.A. Needelman, M.S. Srinivasan. 2006. Fragipan controls on runoff generation: hydropedological implications at landscape and watershed scales. *Geoderma* 131:330-344.

Gentry, W.M., and T.J. Burbey. 2004. Characterization of groundwater flow from spring discharge in a crystalline rock environment. *J. Am. Water Resour. Assoc.* 40:1205-1217.

Grossman, R.B., and F.J. Carlisle. 1969. Fragipans of the eastern United States. *Adv. Agron.* 21:237-239.

Hill, A.R. 1990. Groundwater flow paths in relation to nitrogen chemistry in the near-stream zone. *Hydrobiologia* 206:39-52.

Hill, A.R. 1996. Nitrate removal in stream riparian zones. *J. Environ. Qual.* 25: 743-755.

Hill, A.R., K.J. Devito, S. Campangnolo, and K. Sanmugadas. 2000. Substrate denitrification in a forest riparian zone: interactions between hydrology and supplies of nitrate and organic carbon. *Biogeochemistry* 51:193-223.

Jarvis, N.J. 2007. A review of non-equilibrium water flow and solute transport in soil macropores: principles, controlling factors and consequences for water quality. *Eur. J. Soil Sci.* 58:523-546.

Jordan, T.E., D.L. Correll, and D.E. Weller. 1993. Nutrient interception by a riparian forest receiving inputs from adjacent cropland. *J. Environ. Qual.* 22:467-473.

Kemna, A., J. Vanderborght, B. Kulessa, and H. Vereecken. 2002. Imaging and characterization of subsurface solute transport using electrical resistivity tomography (ERT) and equivalent transport models. *J. Hydrol.* 267:125-146.

Koch, K., J. Wenninger, S. Uhlenbrook, and M. Bonell. 2009. Joint interpretation of hydrological and geophysical data: electrical resistivity tomography results from a process hydrological research site in the Black Forest Mountains, Germany. *Hydrol. Process.* 23:1501-1513.

Lindsey, B.D., S.W. Phillips, C.A. Donnelly, G.K. Speiran, L.N. Plummer, J.K. Bohlke, M.J. Focazio, W.C. Burton, and E. Busenberg. 2003. Residence times and nitrate transport in groundwater discharging to streams in the Chesapeake Bay watershed. U.S. Geological Survey Water Resources Investigations Report 03-4035.

Loke, M.H. 2001. Tutorial: 2-D and 3-D electrical imaging surveys. Course notes for USGS workshop 2-D and 3-D inversion and modeling of surface and borehole resistivity data. Torrs, CT.

Lowrance, R.R. 1992. Groundwater nitrate and denitrification in a coastal riparian forest. *J. Environ. Qual.* 21:401-405.

McCarty, G.W., and J.T. Angier. 2001. Impact of preferential flow pathways on ability of riparian wetlands to mitigate agricultural pollution. Proc. 2nd International Preferential Flow Symposium. ASAE. 2001; 53-56. Honolulu, HI.

Michot, D., Y. Benderitter, A. Dorigny, B. Nicoullaud, D. King, and A. Tabbagh. 2003. Spatial and temporal monitoring of soil water content with an irrigated corn crop cover using surface electrical resistivity tomography. *Water Resour. Res.* 39:1138-1144.

Morley, T.R., A.S. Reeve, and A.J.K Calhoun. 2011. The role of headwater wetlands in altering streamflow and chemistry in a Maine, USA catchment. *J. Am. Water. Resour. Assoc.* 47:337-349.

Needlelman, B.A. 2002. Surface runoff hydrology and phosphorus transport along two agricultural hillslopes with contrasting soils. Ph.D. Thesis. The Pennsylvania State University, University Park, PA.

Oberdorster, C., J. Vanderborght, A. Kemna, and H. Vereecken. 2010. Investigating preferential flow processes in a forest soil using time-domain reflectometry and electrical resistivity tomography. *Vadose Zone J.* 9:350-361.

O'Connell, M. 1998. Combined hydrologic and geochemical study of storm and seasonal delivery of solutes to streamflows. PhD. Thesis, University of Maryland, College Park.

O'Driscoll, M.A., and D.R. DeWalle. 2010. Seeps regulate stream nitrate concentration in forested Appalachian catchments. *J. Environ. Qual.* 39:420-431.

O'Sullivan, D. and J.J. Unwin. 2010. Geographic Information Analysis. John Wiley & Sons, Inc. New York, NY.

Patton, C.J., and J.R. Kryskalla. 2003. Methods of analysis by the U.S. Geological Survey National Water Quality Laboratory: evaluation of alkaline persulfate digestion as an alternative to Kjeldahl digestion for determination of total dissolved nitrogen and phosphorus in water. U.S. Geological Survey water resources investigations report 03-4174, 33 p.

Peterjohn, W.T., and D.L. Correll. 1984. Nutrient dynamics in an agricultural watershed: observations on the role of a riparian forest. *Ecology* 65:1466-1475.

Peterson, B.J., W.M. Wolheim, P.J. Mulholland, J.R. Webster, J.L. Meyer, J.L. Tank, E. Marti, W.B. Bowden, H.M. Valett, A.E. Hershey, W.H. McDowell, W.K. Dodds, S.K. Hamilton, S. Gregory, and D.D. Morrall. 2001. Control of nitrogen export from watersheds by headwater streams. *Science* 292:86-90.

Pionke, H.B., and J.B. Urban. 1985. Effect of agriculture land use on ground-water quality in a small Pennsylvania watershed. *Groundwater*. 23:68-80.

Pionke, H.B., J.R. Hoover, R.R. Schnabel, W.J. Gburek, J.B. Urban, and A.S. Rogowski. 1988. Chemical-hydrologic interactions in the near-stream zone. *Water Resour. Res.* 24:1101-1110.

R Development Core Team. 2011. R: a language and environment for statistical computing. R Foundation for Statistical Computing, Vienna, Austria.

Rutherford, J.C., and M.L. Nguyen. 2004. Nitrate removal in riparian wetlands: interactions between surface flow and soils. *J. Environ. Qual.* 33:1133-1143.

Schnabel, R.R., J.B. Urban, and W.J. Gburek. 1993. Hydrologic controls in nitrate, sulfate, and chloride concentrations. *J. Environ. Qual.* 22:589-596.

Seger, M., I. Cousin, A. Frison, H. Boizard, and G. Richard. 2009. Characterization of the structural heterogeneity of the soil tilled layer by using in situ 2D and 3D electrical resistivity measurements. *Soil Till. Res.* 103:387-398.

Sharratt, B.S. 2001. Groundwater recharge during spring thaw in the prairie pothole region via large, unfrozen preferential pathways. Proc. 2nd International Preferential Flow Symposium. ASAE. 2001; 49-52. Honolulu, HI.

Slater, L., A.M. Binley, W. Daily, and R. Johnson. 2000. Cross-hole electrical imaging of a controlled saline tracer injection. *J. Appl. Geophys.* 44:85-102.

Srinivasan, M.S., W.J. Gburek, and J.M. Hamlett. 2002. Dynamics of stormflow generation - a hillslope-scale field study in east-central Pennsylvania, USA. *Hydrol. Process.* 16:649-665.

Stein, E.D., M. Mattson, A.E. Fetscher, and K.J. Halama. 2004. Influence of geologic setting on slope wetland dynamics. *Wetlands* 24:244-260.

Vanderborght, J., A. Kemna, H. Hardelauf, and H. Vereecken. 2005. Potential of electrical resistivity tomography to infer aquifer transport characteristics from tracer studies: a synthetic case study. *Water Resour. Res.* 41:1-23.

Vidon, P.G.F., and A.R. Hill. 2004. Landscape controls on nitrate removal in stream riparian zones. *Water Resour. Res.* 40:1-14.

Ward, A.S., M.N. Gooseff, and K. Singha. 2010. Imaging hyporheic zone solute transport using electrical resistivity. *Hydrol. Process.* 24:948-953.

Warwick, J., and A.R. Hill. 1988. Nitrate depletion in the riparian zone of a small woodland stream. *Hydrobiologia* 157:231-240.

CHAPTER 4

Influence of Riparian Seepage Zones on Nitrate Variability in Stream Water during Baseflow and Stormflow in Two Agricultural Headwater Catchments

Abstract

Surface seeps or seepage zones are one of the primary pathways of groundwater transport to headwater streams. While seeps have been recognized for their contributions to streamflow, there is little information on how seeps affect stream water quality. The objective of this study was to examine the influence of seeps on stream nitrate-nitrogen (NO_3-N) concentrations in FD36 and RS, two central Pennsylvania agricultural headwater catchments. From April 2009 to January 2012, stream water was sampled on 21 occasions (14 during baseflow; 7 during or following storm events) at 10-m intervals over stream reaches of 550 and 490 m in FD36 and RS, respectively. Nitrate concentrations in seep discharge were measured concurrent with stream water. Results showed NO_3-N concentrations in stream segments with seeps increased, on average, by 0.25 mg L^{-1}. In contrast, NO_3-N concentrations declined by 0.02 mg L^{-1} in stream segments with no seep inputs. The number of seep discharge locations was also positively correlated (R^2 = 0.82) to spatial patterns observed in stream NO_3-N concentration. Immediately following storm events, the influence of seeps on stream NO_3-N concentration was less compared to baseflow. The effect of seeps on stream NO_3-N concentration was likely diminished due to increased stream discharge and the addition of rainfall directly into the stream

during and immediately following the event. One day after a summer storm in FD36, however, an increase in the number of seeps and decreasing stream discharge, resulted in the greatest variability in stream water NO_3-N concentration recorded. These results suggest that seeps are significant sources of NO_3-N to the streams in FD36 and RS and play a key role in determining N fluxes from these catchments.

Introduction

Transfers of nitrogen (N) from terrestrial to aquatic ecosystems contribute to watershed impairment and can lead to eutrophication of coastal zones (where N is often the limiting nutrient) (*Carpenter et al., 1998*). Agriculture is an important source of N to surface waters (*Craig and Weil, 1993; Tesoriero et al., 2000*) and accounts for approximately 37% of the N load delivered to the Chesapeake Bay (*U.S. EPA, 2008*). Recent work by Peterson et al. (2001) and Alexander et al. (2007) point to the importance of headwater streams as major contributors of N to downstream (higher order) systems. Thus, identifying sources of N to headwater streams and evaluating the effects of these sources on water quality is essential for the attainment of downstream water quality goals.

In the Northeast U.S., groundwater-sustained wetlands, springs, or emergent groundwater seeps (hereafter referred to as seeps) represent a potentially significant source of water and N to many headwater streams. Burns et al. (1998) found that discharge from perennial seeps was the principal source of streamflow and nitrate-N (NO_3-N) in a forested headwater catchment in New York. Similarly, seep NO_3-N concentrations in a forested headwater catchment in Pennsylvania were linked with stream NO_3-N concentrations (*O'Driscoll and DeWalle, 2010*). In agricultural headwater catchments, recent work by Shabaga and Hill (2010) and Williams (Chapters 2 and 3) also suggest that seeps are a potential source of NO_3-N to streams.

Seeps often discharge groundwater to the surface in the riparian zone, which flows over land via concentrated flow paths before entering the stream at discrete points along the channel (*Pionke et al., 1988; Rutherford and Nyugen, 2004; O'Driscoll and DeWalle, 2010*). As a result, these point inputs can influence spatial patterns of N concentration in headwater streams similar to the effects of tributary inputs on higher order streams. Numerous studies have characterized the effects of tributaries and other point sources on in-stream variability of chemical constituents. For example, Haggard et al. (2001) examined the effect of point sources on water chemistry and nutrient retention during baseflow. The effects of wastewater treatment plant effluent on stream water quality have also been documented (*Marti et al., 2004*). In addition, the influence of tributaries on sediment transport (*e.g., Boyer et al., 2006*), stream organisms (*e.g., Fraser et al., 1995*), and water quality (*e.g., Scanlon et al., 2010*) has been studied extensively. Fewer studies, however, have looked at how seeps influence the variability of N in streams.

Semi-variogram analysis is a valuable tool for exploring the variability of nutrients, such as N, in terrestrial and aquatic ecosystems. This method has been used in a variety of fields including ecology (i.e., organism response to environmental heterogeneity), soil science (i.e., distribution of nutrient concentrations over an area), and geology (i.e., estimation of ore reserves). Semi-variograms quantify the strength, pattern, and extent of spatial dependence by examining how nutrient concentrations (or other data) co-vary as a function of the distance between sampling locations (*Cooper et al., 1997*). That is, semi-variograms can be used to quantify the distance over which data are spatially correlated (e.g., semi-variogram range) and are no longer considered spatially dependent (*Rossi et al., 1992*). The utility of semi-variograms in exploring longitudinal N variability in streams is that they can aid in the identification of potential causes of spatial patterns (*Legendre and Fortin, 1989; Rossi et al., 1992*).

Several recent studies have used semi-variogram analysis to quantify the variability of nutrients in higher order streams. Dent and Grimm (1999) found that nutrient concentrations were

extremely variable along a 10 km stream reach in Arizona. The authors concluded that N was consistently more spatially heterogeneous than phosphorus or conductivity. Within a large stream network in Maryland, Peterson et al. (2006) showed that the semi-variogram range and patterns of spatial correlation differed between chemical response variables, which were influenced by hydrologic and biogeochemical processes acting along a stream reach. Semi-variogram analysis has also been used extensively in studies aimed toward the prediction of nutrient concentrations at unmonitored locations within a stream network (*Gardener et al., 2003; Ver Hoef et al., 2006*). While most of these studies have been conducted at baseflow, the study by Dent and Grimm (1999) indicated that in-stream N variability can change with flow condition. They showed that flooding substantially decreased spatial variability in stream nutrient concentrations and increased the semi-variogram range. Distinguishing between different flows (i.e., baseflow vs. stormflow) is important because seeps are seen as a major contributor at baseflow, but less so during storms.

In this study, we examine the influence of groundwater-fed seeps on the longitudinal variation of N concentrations in FD36 and RS, two agricultural headwater streams, during baseflow and stormflow conditions. Specific study objectives were to (1) quantify the variability of N concentrations in two agricultural headwater streams; (2) determine if spatial patterns of stream N concentrations are influenced by seeps; and (3) examine the controls of baseflow and stormflow on in-stream N variability.

Materials and Methods

Site Location and Characteristics

The study was implemented in two headwater catchments (FD36 [40 ha] and RS [45 ha]) with seeps located within the Appalachian Ridge and Valley physiographic region of east-central Pennsylvania (Figure 4.1). FD36 and RS are sub-catchments of the WE-38 experimental

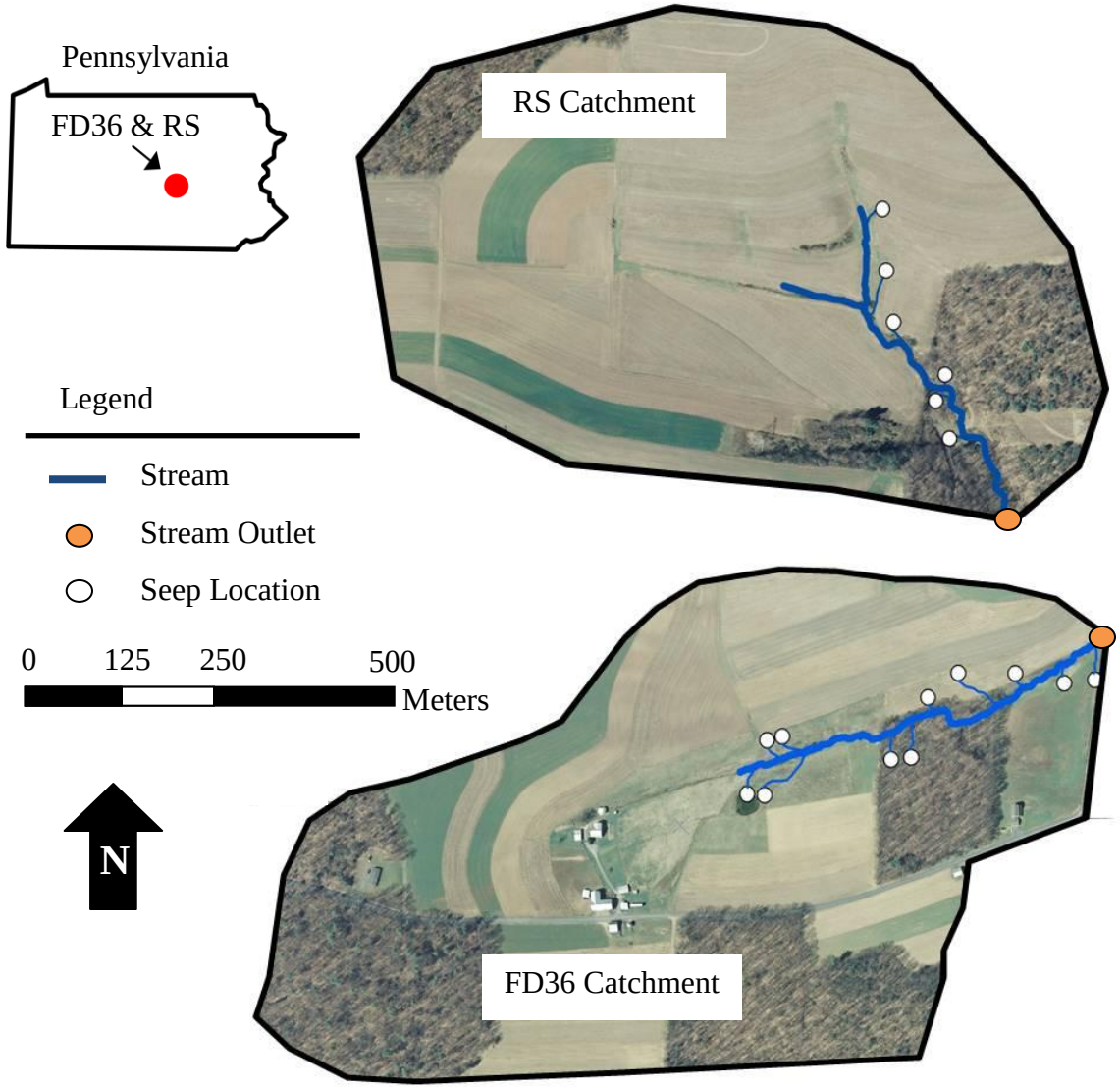

Figure 4.1

Aerial photo of FD36 and RS with locations of groundwater-fed seeps. FD36 and RS are sub-catchments of WE-38 (7.3 km^2), which is located in central Pennsylvania and has been a primary research site of the USDA-Agricultural Research Service for over 40 years.

watershed, which has been a key hydrologic and water quality research location of the USDA – Agricultural Research Service since 1968 (*Bryant et al., 2011*). Both watersheds feature well-drained residual soils on the hillslopes and somewhat poorly-drained soils along the valley floor (*Needelman et al., 2002*). The well-drained soils are typically stony, silt loams (Leck Kill, Calvin, Berks series), while the somewhat poorly-drained soils (Albrights and Hustontown series) have a

moderately-well developed fragipan beginning at a depth of 0.5 to 0.7 m and have low permeability. The dominant land use in FD36 and RS is agriculture, which comprises 56% and 75% of the land area in each catchment, respectively (Figure 4.1). The common crop rotations in FD36 and RS include three- to four-year sequences of corn, small grains, hay, and soybeans. Crops are planted on upslope fields in both catchments and the riparian zones in each catchment are variable in width and planted with grasses. Annual farmer surveys show that most N is applied during the spring and fall as commercial fertilizer, dairy manure, or swine manure. From 2007 through 2011, surveys showed that mean N application rate was significantly greater in RS (200 kg ha^{-1}) compared to mean N application rate in FD36 (133 kg ha^{-1}) ($p < 0.001$; Table 4.1).

The streams that drain the FD36 and RS catchments flow for most (if not all) of the year. The stream channel in FD36 follows a gentle gradient (3%) from the headwaters to the outlet, and flow rates range from about 5.8 x 10^{-3} m^3 s^{-1} at baseflow to 3.78 x 10^{-2} m^3 s^{-1} at stormflow. The stream channel in RS is much steeper than that of FD36, with a gradient of about 6%. Unlike FD36, the RS catchment is ungauged, but given the similarity in size, as well as in its soil and geologic characteristics, we expect the flows to be comparable. Both catchments contain numerous groundwater seeps, which is the focus of this study. Previous work by Williams (Chapters 2 and 3) highlights the potential importance of these seeps as sources of NO_3-N to agricultural headwater streams.

Stream and Seep Water Sampling

Stream study reaches were established in FD36 (550-m long) and RS (490-m long) in order to monitor variations in N concentrations in stream and seep water. In each study reach, stream and seep water were sampled on 21 occasions (14 at baseflow; 7 during or following storm events) between April 2009 and January 2012. On each sampling date, stream water was

Table 4.1 Nitrogen management data from FD36 and RS (2007 – 2011). Data were collected from annual surveys of farmers in both catchments. The amount of N applied in FD36 and RS was a combination of fertilizer, dairy manure, and swine manure. Nitrogen content in manure was determined using the Penn State Agronomy Guide (2011).

	FD36			RS		
Year	**N applied**	**Area**	**Mean N application rate**	**N applied**	**Area**	**Mean N application rate**
	kg	ha	kg ha^{-1}	kg	ha	kg ha^{-1}
2007	2182	15.4	142	3982	19.6	203
2008	2279	15.0	152	5796	27.3	212
2009	1773	12.8	139	4773	22.5	212
2010	1456	14.0	104	6011	28.2	213
2011	2148	15.3	140	4228	26.6	159

collected from the thalweg at 10-m intervals moving from the stream outlet upstream to the top of the reach. Sampling that coincided with storm events occurred within 12 hours of the end of the storm. For one of the summer storm events in FD36 (July 29, 2009), an additional set of stream water samples was collected 24 h after the event ceased. All stream water samples were collected in plastic (HDPE) bottles and stored at 4°C until they could by analyzed. In addition to stream water sampling, stream discharge was monitored continuously (5-min intervals) at the outlet of FD36 using a recording H-flume. As mentioned previously, stream discharge was not monitored in RS, but we anticipate that it would be similar to what is measured in FD36.

Within each stream reach, the locations of seep groundwater discharge were identified and sampled coincident with the longitudinal stream surveys described above (Figure 4.1). Seeps were defined as areas in which groundwater emerged onto the land surface and was transported via surface flow pathways to the stream channel. In order to be sampled, seeps had to have visible movement of water across the land surface and have a surface flow path longer than 1 m. Seep water samples were collected 0.5 m from the stream edge to ensure there was no mixing between seep and stream water. All seep water samples were collected in plastic (HPDE) bottles and stored at 4°C until analysis.

Water Quality Analysis

All water samples were analyzed for total N, NO_3-N, ammonium-N (NH_4-N), and chloride (Cl^-) concentrations. Concentrations of total N were determined for unfiltered samples following alkaline persulfate digestion (*Patton and Kryskalla, 2003*). For dissolved constituents, water samples were filtered (0.45 µm) and then analyzed with a Lachat QuikChem FIA+ autoanalyzer (QuikChem Methods FIA+ 8000 Series, Lachat Instruments, Loveland, CO) to determine concentrations of NH_4-N, NO_3-N, and Cl^-. Ammonium-N concentrations in both stream and seep water on all sampling dates were low and often below the analytical detection limit (0.1 mg L^{-1}); therefore, we chose not to report these values. Nitrate-N comprised 90% to 99% of total N on all sampling dates. Thus, the main focus of this paper is on NO_3-N.

Statistics and Data Analysis

Seep contributions to streamflow were estimated based on stream Cl^- concentrations. Chloride was used because it is non-reactive and serves as an ideal conservative tracer of water flow pathways (*Davis et al., 2006*). Seep contributions were calculated by $Q = [(C_2 - C_1)/(S - C_1)]100$, where Q is the contribution of a seep to streamflow (%), C_1 is the stream Cl^- concentration at a location upstream of the seep, C_2 is the stream Cl^- concentration 10 m downstream of C_1, and S is the Cl^- concentration of seep water entering between C_1 and C_2. Contributions from individual seeps on each date were added together to estimate total seep contributions for both catchments.

To determine the effects of seep inputs on NO_3-N concentrations, changes in NO_3-N concentrations were evaluated over each 10-m segment within a given stream reach. Briefly, the NO_3-N concentration at the upstream location was subtracted from the NO_3-N concentration measured at the adjacent downstream location. Stream segments with seep inputs were classified

as ‘seep’ and all other segments as ‘non-seep’. Seasonal means were then determined for each stream segment classification. Seasons were defined as spring (Mar. – May), summer (Jun. – Aug.), fall (Sept. – Nov.), and winter (Dec. – Feb.). Using a one sample t-test, we compared the mean seasonal change in stream water NO_3-N concentration for seep and non-seep segments to zero change in concentration. In addition, to determine the influence of seeps on spatial patterns of stream water NO_3-N, the least squares estimation method was performed to obtain a Pearson correlation coefficient to measure the strength of the linear relationship between the number of seeps discharging groundwater into the stream on each date and the semi-variogram range.

Analysis of variance (ANOVA) was used to assess differences in spatial patterns between FD36 and RS, stream and seep water NO_3-N concentrations within each catchment, and between baseflow and stormflow. Pairwise comparisons were made using Tukey’s Studentized Range test in order to separate means. All statistical analyses including ANOVA, semi-variogram calculation, and model fitting were completed in *R* statistical package (*R Foundation for Statistical Computing, 2011*). A probability level of 0.05 was used to evaluate statistical significance in all analyses.

Semi-variogram Analysis

Semi-variogram analysis is a valuable tool for quantifying the longitudinal (or spatial) variability of stream water chemistry (*Dent and Grimm, 1999*). As depicted in Figure 4.2, semi-variograms show how differences between data points change with increasing distance between them (referred to as the lag; *h*). When semi-variograms are plotted, semi-variance (γ) will not increase with increasing lag distance if data are spatially independent (Figure 4.2; Random model). If, however, data points closer together tend to be more similar than data points that are farther apart, semi-variance will increase with separation distance and the data are considered

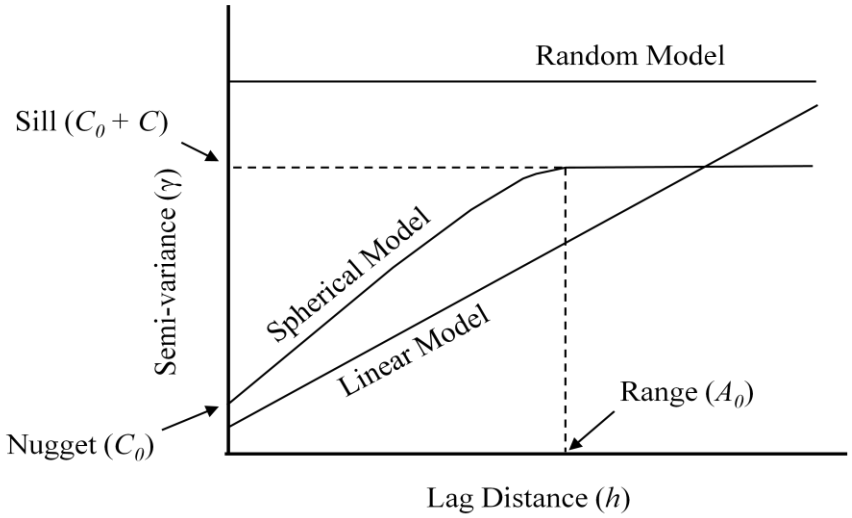

Figure 4.2

Semi-variogram models, showing the semi-variance (γ) as a function of increasing lag distance (h). For spatially independent data, semi-variance does not increase with lag (Random Model). For spatially dependent data, semi-variance may increase for all lags (Linear Model) or level off to an asymptote, called the sill (Spherical Model). The range or patch size indicates the distance over which data are spatially correlated. Figure adapted from Dent and Grimm (1999).

spatially dependent. In some instances semi-variance may increase for all lags, which suggests that points located further apart become continuously more different (Figure 4.2; Linear model). Semi-variance may also level off to an asymptote, called the sill (Figure 4.2; Spherical model). At the lag distance of the sill, called the range or patch size, data are no longer considered to be spatially dependent. Thus, the range denotes the lag distance over which data are spatially correlated (*Rossi et al., 1992*). The apparent y-intercept of a semi-variogram, called the nugget, is often greater than zero and represents either measurement error or variability at scales smaller than the sampling interval (*Rossi et al., 1992*). For more detailed information on semi-variogram use and terminology as applied to understanding stream chemistry variability, see Dent and Grimm (1999).

Semi-variogram analysis was used in this study to quantify spatial patterns in stream water NO_3-N concentrations along the stream reaches in FD36 and RS. Following the methods of Dent and Grimm (1999), downstream trends in NO_3-N concentration were removed using linear

regression and then the resultant regression residuals were used in the semi-variogram analysis. A lag interval of 10 m, which corresponded to our sampling interval, was used and we extended our analysis to a maximum lag of 200 m. The maximum lag was equivalent to 35% and 40% of the study reach in FD36 and RS, respectively. We then applied the technique of Cressie (1985) to determine the values of the sill, range, and nugget. Briefly, spherical models were fit to the semi-variogram using weighted least-squares analysis. In the spherical model (see Figure 4.2 for variable descriptions), if $h < A_0$, then $\gamma(h) = C_0 + C[1.5(h/A_0) - 0.5(h/A_0)^3]$, where h is the lag interval, A_0 is the range, $\gamma(h)$ is the semi-variance at lag h, C_0 is the nugget variance, and C is the structural variance (variance attributed to autocorrelation). If $h \geq A_0$, then $\gamma(h) = C_0 + C$.

Results

General Trends in Precipitation and Streamflow

Annual precipitation measured at the rain gauge in FD36 showed that rainfall amounts were similar in 2009 and 2010, but substantially greater in 2011. In 2009 and 2010, rainfall amounts were 887 and 914 mm, respectively, which was slightly less than the long-term mean rainfall of 1,080 mm in FD36 (*Buda et al., 2011*). The amount of rainfall nearly doubled in 2011, as 1,811 mm of rain was recorded. The large increase in rainfall in 2011 was caused by two large storm systems (remnants of Hurricane Irene [Aug. 27] and Tropical Storm Lee [Sept. 8]) that resulted in 645 mm of rain.

Stream discharge at the outlet of FD36 averaged 7.2×10^{-3} m^3 s^{-1} from April 2009 through January 2012 (Figure 4.3). Flow ranged from dry (i.e., no flow) to 0.4955 m^3 s^{-1}, with the lowest flow occurring in September 2010 and the highest flow occurring September 2011. On dates of stream surveys, stream discharge averaged 5.8×10^{-3} and 3.78×10^{-2} m^3 s^{-1} for baseflow and stormflow, respectively (Figure 4.3). Stream discharge during stormflow sampling ranged

from 5.0 x 10^{-3} to 0.1240 m^3 s^{-1}, whereas, stream discharge was relatively consistent during baseflow sampling (Figure 4.3).

Stream Water NO_3-N Concentration and Spatial Variability

Baseflow

Stream water NO_3-N concentrations over the study period were significantly less in FD36 compared to RS ($p < 0.001$). Nitrate-N concentrations in FD36 ranged from 1.6 to 6.1 mg L^{-1}, whereas in RS, NO_3-N concentrations ranged from 10.8 to 14.7 mg L^{-1} (Table 4.2). Nitrate-N concentrations were also significantly different among seasons in FD36 ($p = 0.005$), but not in RS (Figure 4.4a). In FD36, mean stream water NO_3-N concentrations were lower during the summer (1.5 mg L^{-1}) compared to the spring and fall (3.8 and 3.1 mg L^{-1}, respectively), and winter (5.8 mg L^{-1}). In both FD36 and RS, there was a strong linear relationship between NO_3-N concentration

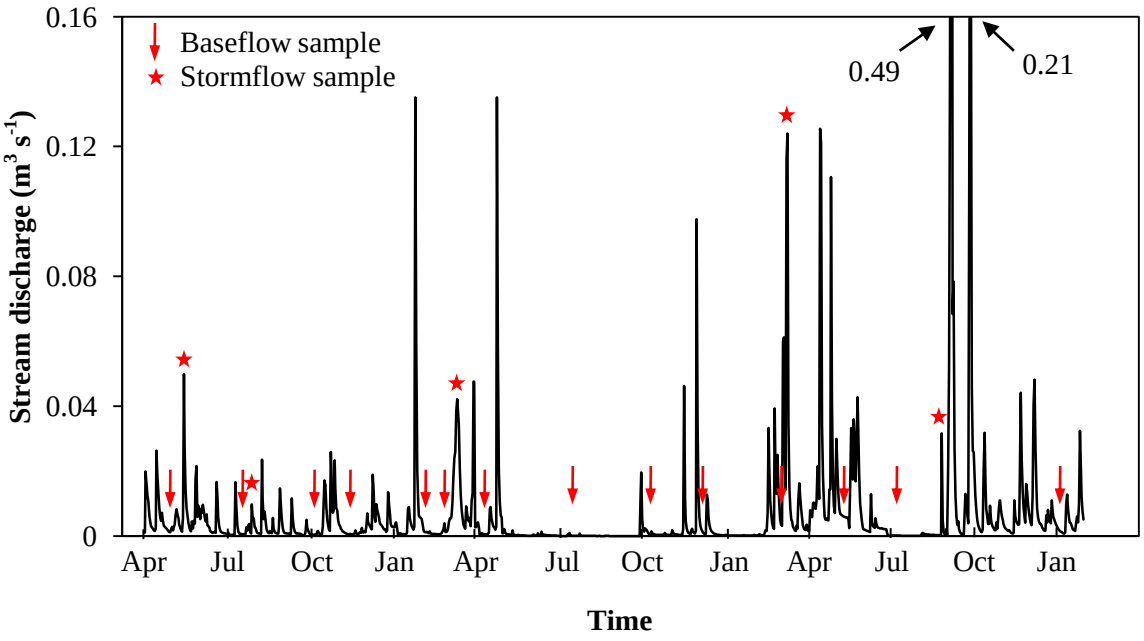

Figure 4.3

Daily average stream discharge at the outlet of FD36 from April 2009 through January 2012. Stream discharge was measured with a recording H-flume at 5-min intervals and averaged daily.

Table 4.2 Nitrate-N concentrations, downstream trends, and indices of spatial variability for stream water in FD36 and RS (April 2009 to January 2012). Highlighted rows indicate sampling dates that coincided with storm events.

	FD36						RS					
	Conc. and downstream trends		Spherical model parameters				Conc. and downstream trends		Spherical model parameters			
Date	**NO_3-N**	**$R^{2\dagger}$**	**Nugget‡**	**Sill§**	**Range$^{\infty}$**	**R^{2*}**	**NO_3-N**	**$R^{2\dagger}$**	**Nugget‡**	**Sill§**	**Range$^{\infty}$**	**R^{2*}**
	mg L^{-1}		C_0	$C_0 + C_1$	m		mg L^{-1}		C_0	$C_0 + C_1$	m	
2009												
Apr. 29	2.0	0.52	0.006	0.044	50	0.56	12.0	0.59	0.670	5.87	155	0.99
May 15	2.8	0.51	0.013	0.099	120	0.90	11.6	0.67	0.279	3.55	150	0.99
Jul. 22	1.6	0.85	0.032	0.175	71	0.88	13.8	0.64	0.886	7.44	159	0.99
Jul. 29	0.6	0.57	0.002	0.015	107	0.94	n/a	n/a	n/a	n/a	n/a	n/a
Jul. 30	1.9	0.49	-	-	-	0.91	14.3	0.58	-	-	-	0.95
Oct. 9	1.7	0.84	0.014	0.121	96	0.88	13.4	0.67	0.851	5.60	135	0.97
Nov. 12	3.3	0.51	0.015	0.127	104	0.91	12.9	0.54	4.160	11.36	88	0.82
2010												
Jan. 29	5.3	0.87	0.004	0.016	57	0.60	14.7	0.63	0.140	4.41	144	0.98
Mar. 8	5.3	0.85	0.018	0.073	45	0.85	n/a	n/a	n/a	n/a	n/a	n/a
Mar. 9	4.3	0.76	0.011	0.083	84	0.91	11.2	0.64	0.003	0.97	181	0.98
Mar.15	4.9	0.66	0.006	0.035	60	0.81	13.3	0.78	0.124	3.45	193	0.99
Apr. 22	3.1	0.27	0.005	0.016	89	0.84	13.2	0.56	0.133	6.00	155	0.99
Jul. 14	1.1	0.85	0.023	0.167	151	0.97	10.8	0.49	0.010	6.53	196	0.99
Oct. 4	4.3	0.62	0.022	0.205	134	0.98	14.7	0.66	0.680	6.01	156	0.99
Dec. 13	6.1	0.16	0.012	0.052	68	0.90	13.8	0.65	0.074	2.44	131	0.97
2011												
Mar. 1	4.1	0.53	0.005	0.040	56	0.69	13.1	0.56	0.486	4.31	110	0.87
Mar. 11	5.1	0.48	0.006	0.033	86	0.80	13.2	0.74	0.247	1.90	158	0.98
May 5	3.8	0.42	0.001	0.021	49	0.83	12.3	0.68	0.195	4.23	181	0.98
Jul. 6	1.7	0.56	0.038	0.080	132	0.94	13.7	0.57	0.649	5.89	181	0.99
Aug. 30	4.8	0.52	0.034	0.379	168	0.98	15.9	0.63	0.321	5.94	150	0.99
2012												
Jan. 5	5.9	0.10	0.002	0.011	50	0.55	11.2	0.48	0.353	3.05	173	0.99

† Linear relationship between NO_3-N and downstream distance.
‡ Measurement error or variability at scales < 10 m.
* Linear relationship between semi-variance and spherical model.
§ Maximum semi-variance (i.e., where semi-variance levels off).
$^{\infty}$ Distance over which NO_3-N concentration is spatially dependent.

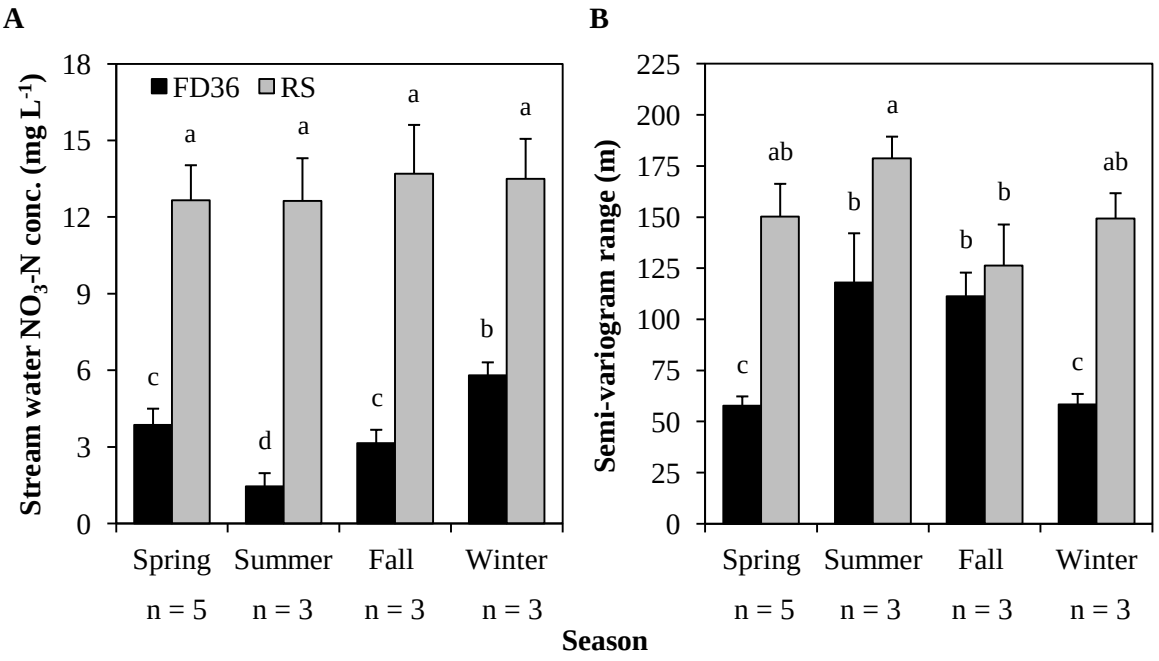

Figure 4.4

(A) Baseflow stream water NO_3-N concentrations from FD36 and RS (Apr. 2009 – Jan. 2012). Seasons were defined as spring (Mar. – May), summer (Jun. – Aug.), fall (Sept. – Nov.), and winter (Dec. – Feb.). (B) Spatial patterns in baseflow stream water NO_3-N concentrations from FD36 and RS. Semi-variogram range values indicate the distance over which stream water NO_3-N concentrations are spatially dependent. Error bars represent one standard error. Letters above bars denote statistical significance ($p < 0.05$).

and downstream distance on all sampling dates ($p < 0.001$) (Table 4.2). Pearson correlation coefficients (R^2) ranged from 0.10 to 0.87 and 0.49 to 0.68 in FD36 and RS, respectively. Overall variability in stream water NO_3-N concentration, measured by the coefficient of variation (CV), ranged from 4% to 94% in FD36 and 7% to 36% in RS (data not shown). Mean overall variability in FD36 was significantly greater in the summer (CV = 65%) compared to the spring and winter (CV = 10% and 6%, respectively) ($p = 0.003$). Variability in RS was similar across all seasons (CV = 18% to 26%).

Spherical models were fit to the experimental semi-variogram on all baseflow sampling dates to quantify spatial patterns in stream water NO_3-N concentrations (Table 4.2). Stream water NO_3-N concentrations in both FD36 and RS showed spatial patchiness within the scale of the survey; however, the range where concentrations became spatially dependent was significantly

less in FD36 compared to RS ($p < 0.001$). Mean patch sizes in NO_3-N concentration of 82 and 151 m were observed for FD36 and RS, respectively. Over the study period, patch sizes in FD36 varied between 45 and 151 m, while patch sizes in RS were between 88 and 196 m (Table 4.2). Spatial patterns of stream water NO_3-N concentrations varied in both catchments with season ($p = 0.027$) (Figure 4.4b). In FD36, patch sizes of NO_3-N concentrations were significantly larger during the summer and fall (118 and 111 m, respectively) compared to spring and winter (57 and 58 m, respectively). Patch sizes of NO_3-N concentrations in RS were significantly larger in the summer (179 m) compared to the fall (126 m). Semi-variogram nugget values were relatively low compared to the sill on all baseflow sampling dates, which resulted in high structural variance (i.e., variance attributed to autocorrelation) (data not shown). Values for structural variance were between 0.52 and 0.99 for both catchments and averaged 0.85. This suggests that only 15% of the observed variability in stream water NO_3-N concentration was either due to measurement error or variability at lag distances less than 10 m.

Stormflow

Storm events did not significantly impact mean stream water NO_3-N concentration in either FD36 or RS (Table 4.2). Compared to baseflow NO_3-N concentrations before the storm event, NO_3-N concentrations following storm events were slightly lower on average (FD36, 3.3 vs. 3.2 mg L^{-1}; RS, 13.4 vs. 12.6 mg L^{-1}). There was also a strong linear relationship between NO_3-N concentration and downstream distance on all storm sampling dates in both FD36 and RS ($p < 0.001$). Overall variability of stream water NO_3-N concentrations tended to decrease during storm events compared to baseflow (data not shown). Storm events occurring in the summer decreased overall variability more than storm events in the spring. For example, in FD36, the CV changed by less than 1% following spring storm events compared to summer events in which the

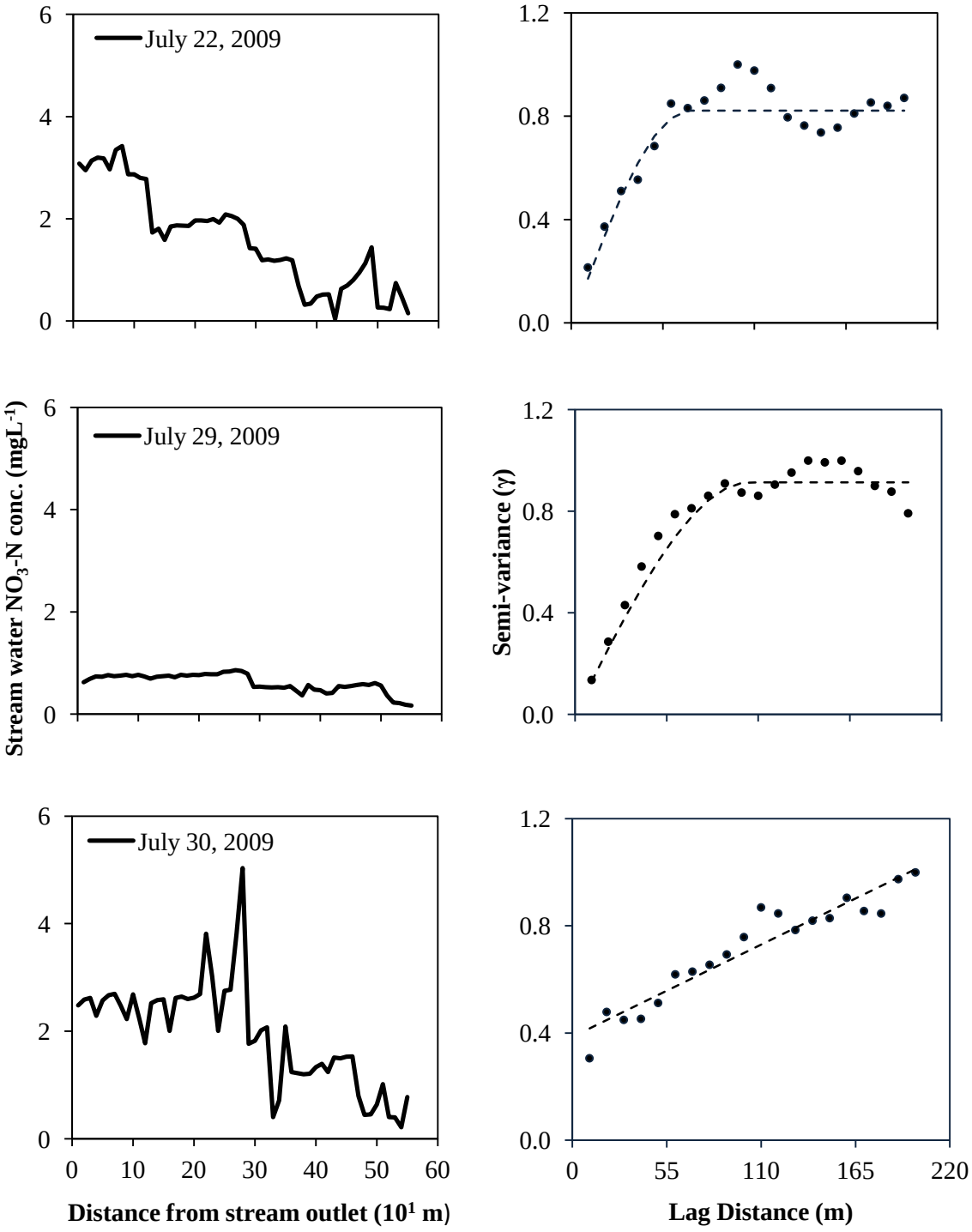

Figure 4.5

Stream water NO_3-N concentration (left column) and semi-variograms (right column) from FD36 before (July 22), immediately following (July 29), and 24 h after (July 30) a storm event (2.9 cm). Spherical models were fit to the July 22 and 29 semi-variograms. A linear model was used to describe the July 30 semi-variogram. Semi-variance was standardized by dividing through by its maximum value on each date. Indices of spatial variability are given in Table 4.2.

CV decreased by more than 30%. Figure 4.5 shows how stream water NO_3-N concentration and spatial patterns changed from baseflow, to immediately following a summer storm, to 24 h after the storm in FD36.

Spherical models were fit to storm event semi-variograms on all dates in both FD36 and RS except for July 30, 2009, which resembled a linear model (Figure 4.2). The range where stream water NO_3-N concentration became spatially dependent was generally greater following a storm event compared to baseflow conditions prior to the storm (Table 4.2). In FD36, the mean patch size of stream water NO_3-N concentration increased from 71 m at baseflow to 111 m immediately following the storm event, while an increase from baseflow to stormflow of 151 to 157 m was observed in RS. This indicated that stream water NO_3-N concentrations became less spatially variable following a storm event. However, one day following a summer storm event (July 2009), NO_3-N concentrations in FD36 became continuously more different along the reach (Figure 4.5), suggesting that concentrations were highly variable compared to baseflow and immediately following the storm event.

Seep NO_3-N Concentration Variability

The number of groundwater-fed seeps identified and sampled in FD36 and RS ranged from 2 and 13 seeps on all sampling dates (Table 4.3). The mean number of seeps sampled on each date was significantly greater in FD36 compared to RS ($p < 0.001$). On each sampling date, 8.7 seeps were sampled in FD36 on average, whereas a mean of 5.0 seeps were sampled in RS (Table 4.3). Conversely, seep water NO_3-N concentrations in FD36 were significantly less than NO_3-N concentrations measured in RS ($p < 0.001$). Mean seep water NO_3-N concentrations of 4.7 and 13.4 mg L^{-1} were observed in FD36 and RS, respectively (Table 4.3). Seep water NO_3-N concentrations were also significantly different among seasons in FD36 ($p = 0.03$), but not in RS

(data not shown). In FD36, mean seep water NO_3-N concentrations were less during the summer (3.3 mg L^{-1}) compared to the winter (6.0 mg L^{-1}). Seep water NO_3-N concentration in individual seeps over the study period ranged from 0.1 to 13.1 mg L^{-1} in FD36 and 1.2 to 29.5 mg L^{-1} in RS (Table 4.3). Storm events did not have a significant effect on seep NO_3-N concentrations in either catchment, but seep concentrations tended to decrease following storm events compared to baseflow (Table 4.3).

Table 4.3 Seep NO_3-N concentrations and variability from FD36 and RS (April 2009 to January 2012). Highlighted rows indicate sampling dates that coincided with storm events.

	FD36				RS			
Date	**n**[†]	**Mean**	**Min.**	**Max.**	**n**[†]	**Mean**	**Min.**	**Max.**
		mg L^{-1}				mg L^{-1}		
2009								
Apr. 29	8	4.8	0.1	11.8	4	13.6	1.2	24.1
May 15	9	3.5	0.1	9.6	5	12.9	1.6	23.9
Jul. 22	7	2.9	0.7	7.3	3	15.7	10.0	24.7
Jul. 29	10	2.8	0.1	10.4	n/a	n/a	n/a	n/a
Jul. 30	12	4.4	0.1	12.1	4	15.7	6.4	22.8
Oct. 9	6	4.6	0.4	11.1	4	14.9	10.1	22.5
Nov. 12	7	5.4	0.6	10.6	6	13.7	2.5	24.0
2010								
Jan. 29	9	5.6	2.1	9.7	6	13.7	3.2	27.5
Mar. 8	11	5.7	1.7	13.1	n/a	n/a	n/a	n/a
Mar. 9	12	4.6	0.1	10.5	6	12.0	2.9	22.1
Mar. 15	13	5.5	0.1	10.5	7	11.4	3.6	24.2
Apr. 22	8	4.2	0.1	9.9	5	12.9	2.1	23.2
Jul. 14	3	2.6	0.8	3.7	3	10.1	8.8	17.6
Oct. 4	5	6.1	1.2	8.9	4	16.2	10.0	21.3
Dec. 13	10	7.5	4.5	12.4	7	14.5	4.4	29.5
2011								
Mar. 1	11	5.6	0.4	10.1	6	11.5	3.1	23.0
Mar. 11	13	5.5	1.1	10.3	9	10.4	2.4	24.0
May 5	10	3.9	0.1	8.7	4	11.7	2.3	21.7
Jul. 6	3	4.4	0.7	4.9	2	16.3	10.4	22.2
Aug. 30	5	3.7	1.4	7.3	6	15.7	10.4	26.8
2012								
Jan. 5	11	4.9	0.1	8.6	4	12.2	8.6	17.8

[†] Number of seeps sampled on each date.

The Influence of Seeps on Stream Water NO_3-N Concentrations and Variability

Estimated seep contributions to streamflow based on stream and seep Cl^- concentrations were between 41% and 136% on all sampling dates (Table 4.4). Seep contributions greater than 100% of streamflow were possible, as losing conditions were often observed during dry periods along the stream in FD36. Over the entire study period, seeps contributed an estimated 69% and 63% to streamflow in FD36 and RS, respectively. Seep contributions to streamflow were

Table 4.4 Estimated seep contributions to streamflow in FD36 and RS (April 2009 to January 2012). Estimations are based on stream and seep water chloride concentrations. Highlighted rows indicate sampling dates that coincided with storm events.

Date	FD36 Estimated seep contributions to streamflow	RS Estimated seep contributions to streamflow
	%	%
2009		
Apr. 29	63	56
May 15	44	52
Jul. 22	136	91
Jul. 29	75	n/a
Jul. 30	80	63
Oct. 9	109	76
Nov. 12	84	68
2010		
Jan. 29	62	67
Mar. 8	49	n/a
Mar. 9	43	58
Mar. 15	41	61
Apr. 22	58	69
Jul. 14	83	62
Oct. 4	72	58
Dec. 13	71	49
2011		
Mar. 1	46	51
Mar. 11	41	47
May 5	80	68
Jul. 6	95	71
Aug. 30	76	76
2012		
Jan. 5	58	63

significantly greater during baseflow compared to stormflow in FD36 ($p = 0.04$), but not in RS (Table 4.4). On average, seeps comprised 76% and 54% of stream discharge during baseflow and stormflow, respectively. Seeps in FD36 also comprised a larger portion of stream baseflow during the summer (105%) compared to the spring and winter (61% and 63%, respectively) ($p = 0.04$). Mean seep contributions in RS were consistent across seasons and averaged 59% to 75%.

Downstream changes in NO_3-N concentrations for stream segments (10 m) with and without seeps (i.e., non-seep) are shown in Figure 4.6. In both FD36 and RS, seeps resulted in an increase in stream water NO_3-N concentrations. During baseflow, mean increases of 0.24 and 0.26 mg L^{-1} NO_3-N were observed for stream segments with seeps in FD36 and RS, respectively. Mean increases in NO_3-N concentration as a result of seep inputs were significant across all seasons in FD36, but only during the spring and summer in RS (Figure 4.6). In FD36, increases in stream water NO_3-N concentrations due to seep inputs were greater during the summer and fall (0.74 and 0.37 mg L^{-1}, respectively) compared to the spring and winter (0.11 and 0.13 mg L^{-1}, respectively). The influence of seeps on changes in stream water NO_3-N concentrations was also significant during stormflow in both FD36 and RS (Figure 4.6). Seeps increased stream water NO_3-N concentrations by 0.15 and 0.19 mg L^{-1} in FD36 and RS, respectively. In contrast to stream segments with seeps, non-seep stream segments had a mean downstream decrease in NO_3-N concentrations during baseflow in both FD36 and RS, and during stormflow in RS (Figure 4.6). Mean decreases in NO_3-N concentrations for non-seep stream segments were not significantly different from zero change in concentration and averaged 0.01 and 0.03 mg L^{-1} in FD36 and RS, respectively. One non-seep stream segment in RS, however, consistently resulted in large increases in stream water NO_3-N concentration of up to 6.0 mg L^{-1} (data not shown). Since there were no visible additions of water at this location, it was assumed that groundwater high in NO_3-N concentration was discharging directly into the stream channel.

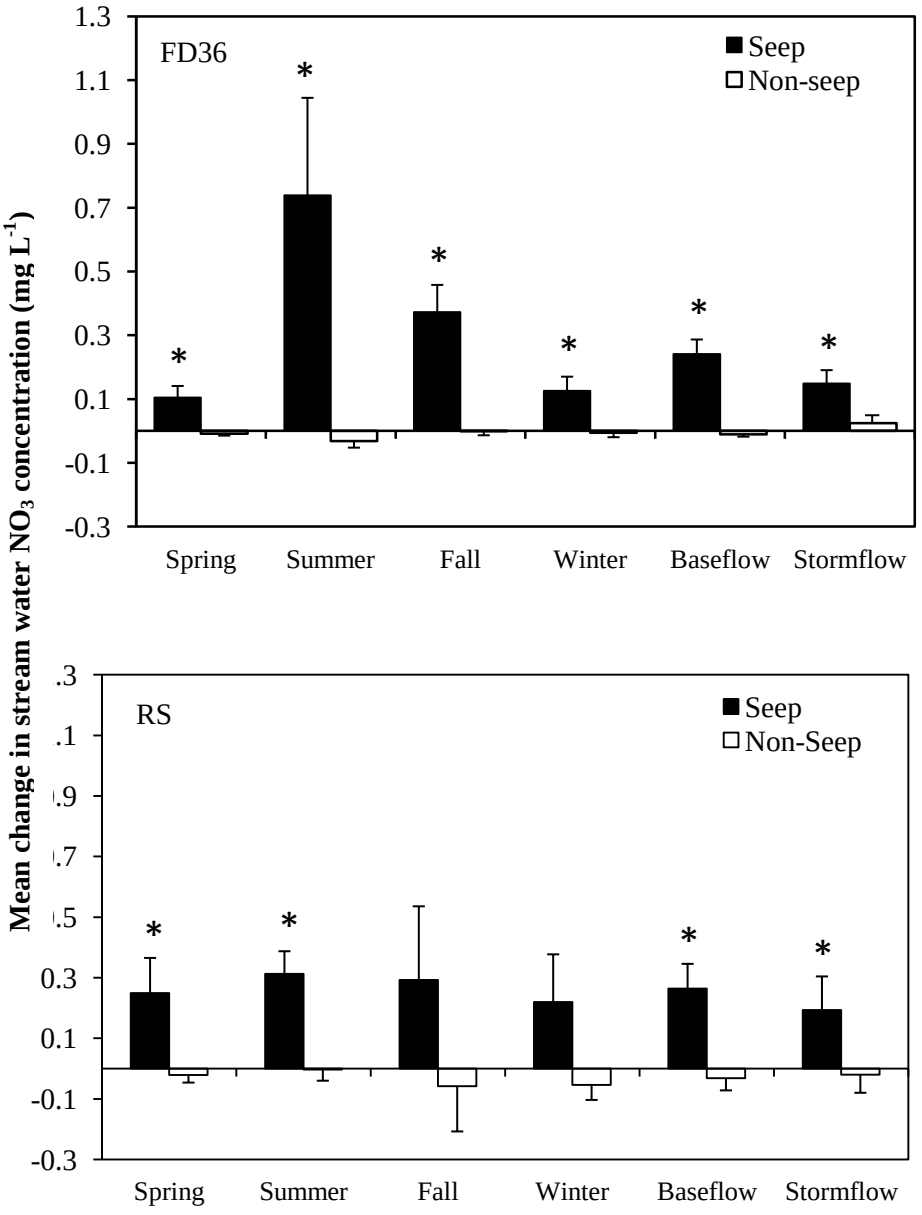

Figure 4.6

Changes in stream water NO_3-N concentration in FD36 and RS. Seasons were defined as spring (Mar.-May), summer (Jun.-Aug.), fall (Sept.-Nov.), and winter (Dec.-Feb.). Seasonal data only includes baseflow sampling. Changes were calculated over a 550 and 490 m stream reach in FD36 and RS, respectively, at 10 m intervals. Stream segments with seep inputs were classified as 'seep' and all other stream segments as 'non-seep'. Error bars represent one standard deviation. Asterisks indicate that the change was significantly different from zero ($p < 0.05$).

The number of seeps sampled during each stream survey significantly influenced spatial patterns in stream water NO_3-N concentration throughout both FD36 and RS (Figure 4.7). A significant linear relationship was observed between the number of seeps sampled on each date and the semi-variogram range for stream water NO_3-N concentration ($p < 0.001$); however, the relationship varied between baseflow and stormflow. Pearson correlation coefficients of 0.82 and 0.69 were found for baseflow and stormflow, respectively. During baseflow and stormflow, the more seeps that were sampled, the smaller the semi-variogram range (or patch size) (Figure 4.7). Therefore, an increase in the number of point inputs from seeps yielded more spatial variability in stream water NO_3-N concentrations.

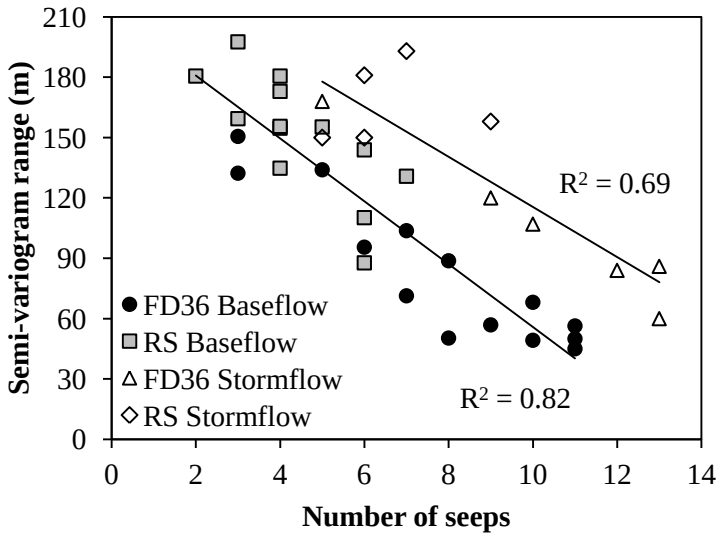

Figure 4.7

Number of seeps sampled on each date compared with the semi-variogram range (m) for stream water NO_3-N concentration. Both baseflow and stormflow comparisons are shown. The range indicates the distance over which stream water NO_3-N concentrations were spatially dependent.

Discussion

Variability of NO_3-N in Stream and Seep Waters

Results from longitudinal monitoring of stream reaches in FD36 and RS suggest that NO_3-N additions primarily occurred where seep discharge entered the stream. Seeps essentially function as a drainage outlet for larger areas of the catchment (although the extent of this area is difficult to determine); therefore, they have the potential to deliver large volumes of agriculturally influenced groundwater to the stream (*Angier and McCarty, 2008*). In FD36 and RS, stream segments with seeps comprised between 5% and 16% of the total stream length, but we estimated that seeps were supplying between 41% and 136% of streamflow. Since NO_3-N concentrations measured in seep discharge were greater than stream water NO_3-N concentrations, the addition of seep discharge to the stream resulted in significant increases in stream water NO_3-N concentrations downstream of the seep input. Stream segments that were not receiving seep inputs exhibited small decreases in NO_3-N concentration indicating that in-stream uptake and/or denitrification were likely occurring along the stream channel (*Peterson et al., 2001; Alexander et al., 2007*). The influence of in-stream NO_3-N removal mechanisms, however, was minimal compared to seep NO_3-N inputs as stream water NO_3-N concentrations increased downstream during all stream surveys.

Nitrate-N concentrations varied substantially among individual seeps in FD36 and RS. On a single sampling date (April 29, 2009), seeps had an absolute range in NO_3-N concentration of 11.7 and 22.9 mg L^{-1} in FD36 and RS, respectively. Variations in seep water chemistry have also been documented in a forested catchment in Pennsylvania (*O'Driscoll and DeWalle, 2010*) and in the Catskill Mountains of New York (*Burns et al., 1998*). Seep water NO_3-N concentrations in these forested catchments, however, had a much smaller absolute range (< 2 mg L^{-1}) of concentration compared to FD36 and RS. Variability in seep water NO_3-N concentrations

has been attributed to differences in physical, chemical, and biological processes occurring in the upslope contributing area (*e.g., Cirmo and McDonnell, 1997*). In addition to differences in biogeochemical processes among the areas draining to seeps, N application rates and land use in agricultural catchments often vary at the field-scale. Nitrogen application rates in areas draining to seeps are likely related to seep NO_3-N concentrations, but there is little research on this potential link. We hypothesize that in agricultural catchments differences in N management determine seep NO_3-N concentration, whereas in forested catchments, differences in biogeochemical processes likely play a larger role in seep NO_3-N concentration.

Once groundwater is discharged from a seep, flow paths and residence times within the seep can also affect the chemistry of seep water entering the stream (*Hill, 1996*). A tracer study in New Zealand pasture demonstrated that approximately 24% of NO_3-N could be removed along a seep surface flow path (*Rutherford and Nguyen, 2004*). Groundwater and NO_3-N transported in these flow paths, however, are more likely to bypass the mitigating features of the riparian zone (*Warwick and Hill, 1988; Angier et al., 2002, 2005*). In contrast, NO_3-N concentrations in shallow groundwater have been reported to decrease by 90% to 95% due to high denitrification rates in saturated riparian zone soils (*Peterjohn and Correll, 1984; Lowrance, 1992*). Since both surface and subsurface flow paths occur along the length of a seep, it is possible that a single seep could function as both a conduit and barrier for NO_3-N fluxes. In FD36, seep NO_3-N concentrations were greater during the winter and spring compared to the summer. During the winter and spring, higher seep discharge could lead to more of the downseep flow being transported along rapid surface flow paths as opposed to slower, subsurface paths. This would decrease the potential for NO_3-N removal and result in higher concentrations delivered to the stream (*Gold et al., 2001*). Alternatively, during the summer, lower seep discharge and longer residence times could promote NO_3-N removal.

Effects of Seeps on Stream Water NO_3-N Variability

Differences in the number of seeps and their NO_3-N concentrations among sampling dates resulted in spatial patterns of stream water NO_3-N concentrations that reflected the variability of seep inputs. Semi-variogram analysis showed that stream water NO_3-N concentrations in FD36 and RS were not only spatially dependent at small scales (i.e., semi-variance increased with increasing lag distance), but also patchy within the scale of the survey. Given the unidirectional flow of stream water, it is not surprising that NO_3-N concentrations at nearby locations were more similar than locations separated by longer distances. We found mean patch sizes of stream water NO_3-N concentration were 82 and 151 m in FD36 and RS, respectively, which suggests that NO_3-N in FD36 was more spatially variable than RS. This coincided with FD36 having more seeps (8.7), on average, compared to RS (5.0). In addition, the greater the number of seeps in both catchments on a single sampling date, the greater the spatial variability of stream water NO_3-N concentrations (i.e., decreased patch size). This suggests that in FD36 and RS, spatial patterns of stream water NO_3-N concentrations were tightly coupled with variable inputs of NO_3-N from seeps.

Stream water NO_3-N concentrations in FD36 and RS exhibited a substantial amount of longitudinal variation over the study period. For example, the annual variation in NO_3-N concentrations at the outlet of FD36 determined by weekly sampling (*Zhu et al., 2011*) was 2 to 3 times less than the variation we observed over the 550 m stream reach during the summer (annual [2009] CV = 32% for 50 samples; CV on July 22, 2009 and July 6, 2011 = 61% and 94%, respectively, for 55 samples). Few studies, however, have quantitatively assessed spatial patterns in stream water NO_3-N concentrations. Dent and Grimm (1999) found that patch sizes of stream water NO_3-N concentrations were approximately 400 m in length, but their study was conducted on a much larger desert stream in Arizona. Although the size of the stream was much larger in the

study by Dent and Grimm (1999), the controls on spatial patterns of stream water NO_3-N concentrations were similar to the finding from FD36 and RS reported herein. Dent and Grimm (2001) found that localized groundwater upwelling zones within the stream had a strong influence on spatial patterns of NO_3-N, which is similar to the effects of point inputs from seepage zones.

Research on spatial patterns of nutrients in soils can also provide a useful comparison to the observations obtained from stream water sampling in FD36 and RS. For example, research has shown that most nutrients in forest soils are spatially dependent from 2 to 5 m (*Palmer, 1990; Lechowicz and Bell, 1991*), whereas in agricultural soils, nutrients are found to be spatially dependent over distances of up to 100 m (*Robertson et al., 1997*). The high spatial variability of nutrient concentrations found within terrestrial soils is likely not reflected in seep discharge as areas draining to seeps tend to integrate the effects of different land uses, flow paths, and biogeochemical processes. Stream water NO_3-N concentration observed in FD36 and RS would therefore be expected to be less variable than soil NO_3-N concentrations within each catchment. In addition, downstream transport of NO_3-N may lengthen the distance over which concentrations are spatially dependent compared to soils by carrying products away from where they are formed or enter the stream (*Wagener et al., 1998*).

Influence of Storm Events on In-stream NO_3-N Variability

Nitrate-N concentrations in stream water became less spatially variable immediately following storm events compared to baseflow in FD36 and RS. Although the number of flowing seeps increased following storm events, patch sizes also increased following storm events. The diminished influence of seeps on spatial patterns in stream water NO_3-N concentrations immediately following storm events compared to baseflow coincided with reduced seep contributions to streamflow and decreased changes to stream water NO_3-N concentrations where

seep water entered the stream. During storm events, rain falling directly into the stream channel and surface runoff from the landscape increased stream discharge and most likely diluted stream water NO_3-N concentrations (*Pionke et al., 1988*). Increased stream discharge also resulted in more turbulent streamflow and greater mixing of the stream water, which would have homogenized NO_3-N concentrations throughout the reach. Similar findings to FD36 and RS have been reported in both aquatic and terrestrial environments. For example, flooding of a desert stream decreased NO_3-N concentration variability (*Dent and Grimm, 1999*). In addition, the distance over which soil nutrient concentrations are spatially dependent is typically greater for cultivated (i.e., well mixed) agricultural fields compared to undisturbed fields (*Robertson et al., 1993*).

The increased patch sizes of stream NO_3-N concentrations that were observed immediately following a small summer storm event in FD36 (July 29, 2009; Figure 4.5), however, were reversed one day following the event as stream water NO_3-N concentrations became continuously more different along the entire reach (July 30, 2009; Figure 4.5). As streamflow cycled from rainfall-diluted and surface runoff dominated flow to subsurface discharge dominated flow (*Pionke et al., 1988*), the influence of seeps on spatial patterns of stream water NO_3-N concentration likely reached its maximum. During this time period, the number of seeps discharging groundwater was at its greatest and stream discharge was decreasing back to baseflow. It is also likely that stream water NO_3-N concentrations would become less variable and patch sizes would return to baseflow values as time passed after the storm and seep discharge declined.

Conclusions

The results of this study showed that seeps in FD36 and RS contributed large volumes of agriculturally-influenced groundwater to the stream. While the magnitude of seep water NO_3-N concentrations varied between catchments and among individual seeps due to differences in hydrologic and biogeochemical processes and variable N inputs across the landscape, seep discharge generally resulted in increased in stream water NO_3-N concentrations. We found that stream water NO_3-N concentrations, on average, increased by 0.25 mg L^{-1} over a 10 m distance when seeps were present compared to a decrease of 0.02 mg L^{-1} when seeps were not present. The influence of seeps on stream NO_3-N concentrations was further reflected in longitudinal patterns of stream water NO_3-N. We found that as the number of seeps increased, the amount of longitudinal variability (i.e. patchiness) in stream water NO_3-N concentration increased. The influence of seeps on stream water NO_3-N concentrations and variability decreased immediately following a storm event compared to baseflow. This was likely due to increased stream discharge and rainfall directly into the stream channel, which decreased the relative contributions of seep water to stream flow and homogenized NO_3-N concentrations over the entire reach. As stream discharge drained back to baseflow, however, the influence of seeps on stream water quality likely reached a maximum, as the number of seeps discharging groundwater into the stream was at its peak. In FD36 and RS, seeps are a significant source of NO_3-N to the stream and play a substantial role in determining N fluxes from these catchments during both baseflow and stormflow conditions.

References

Alexander, R.B., E.W. Boyer, R.A. Smith, G.E. Schwarz, and R.B. Moore. 2007. The role of headwater streams in downstream water quality. *J. Am.Water Resour. As.* 43:41-59.

Angier, J.T., and G.W. McCarty. 2008. Variations in baseflow nitrate flux in a first order stream and riparian zone. *J. Am. Water Resour. Assoc.* 44:367-380.

Angier, J.T., G.W. McCarty, and K.L. Prestegaard. 2005. Hydrology of a first-order riparian zone and stream, mid-Atlantic coastal plain, Maryland. *J. Hydrol.* 309:149-166.

Angier, J.T., G.W. McCarty, C.P. Rice, and K. Bialek. 2002. Influence of a riparian wetland on nitrate and herbicides exported from a field applied with agrochemicals. *Journal of Agriculture and Food Chemistry*. 50:4424-4429.

Boyer, C., A.R. Roy, and J.L. Best. 2006. Dynamics of a river channel confluence with discordant beds: flow turbulence bed load sediment transport and bed morphology. *J. Geophys. Res. – Earth Surface* 111: DOI: 10.102912005/2005JF000458.

Bryant, R.B., T.L. Veith, G.W. Feyereisen, A.R. Buda, C.D. Church, G.J. Folmar, J.P. Schmidt, C.J. Dell, and P.J.A. Kleinman. 2011. U.S. Department of Agriculture Agricultural Research Service Mahantango creek watershed, Pennsylvania, United States: phsiography and history. *Water Resour. Res.* 47: DOI: 10.1029/2010WR010056.

Buda, A.R., T.L. Veith, G.J. Folmar, G.W. Feyereisen, R.B. Bryant, C.D. Church, J.P. Schmidt, C.J. Dell, and P.J.A. Kleinman. 2011. U.S. Department of Agriculture Agricultural Research Service Manhantango creek watershed, Pennsylvania, United States: long-term precipitation database. *Water Resour. Res.* 47: DOI: 10.1029/2010WR010058.

Burns, D.A., P.S. Murdoch, G.B. Lawrence, and R.L. Michel. 1998. Effects of groundwater springs on NO_3^- concentration during summer in Catskill Mountain streams. *Water Resour. Res.* 34:1987-1996.

Carpenter, S.R., N.F. Caraco, D.L. Correll, R.W. Howarth, A.N. Sharpley, and V.H. Smith. 1998. Nonpoint pollution of surface waters with phosphorus and nitrogen. *Ecol. Appl.* 8: 559-568.

Cirmo, C.P., and J.J. McDonnell. 1997. Linking hydrologic and biogeochemical controls of nitrogen transport in near-stream zones of temperate-forested catchments: a review. *J. Hydrol.* 1999:88-120.

Cooper, S.D., L. Barmuta, O. Sarnelle, K. Kratz, and S. Diehl. 1997. Quantifying spatial heterogeneity in streams. *J. N. Am. Benthol. Soc.* 16:174-188.

Craig, J.P., and R.R. Weil. 1993. Nitrate leaching to a shallow mid-Atlantic coastal plain aquifer as influenced by conventional no-till and low-input sustainable grain production systems. *Water. Sci. Technol.* 28:691-700.

Cressie, N. 1985. Fitting variogram models by weighted least squares. *Math. Geol.* 17:563-586.

Davis, S.N., G.M. Thomson, H.W. Bently, and G. Stiles. 2006. Groundwater tracers: a short review. *Groundwater*. 18:14-23.

Dent, C.L., and N.B. Grimm. 1999. Spatial heterogeneity of stream water nutrient concentrations over successional time. *Ecology* 80:2283-2298.

Dent, C.L., N.B. Grimm, and S.G. Fisher. 2001. Multiscale effects of surface-subsurface exchange on stream water nutrient concentrations. *J. N. Am. Benthol. Soc.* 20:162-181.

Fraser, D.F., J.F. Gilliam, and T. Yip-Hoi. 1995. Predation as an agent of population fragmentation in a tropical watershed. *Ecology* 76:1461-1472.

Gardner, B., P.J. Sullivan, and A.J. Lembo. 2003. Predicting stream temperatures: geostatistical model comparison using alternative distance metrics. *Can. J. Aquatic Sci.* 60:344-351.

Gold, A.J., P.M. Groffman, K. Addy, D.Q. Kellogg, M. Stolt, and A.E. Rosenblatt. 2001. Landscape attributes as controls on groundwater nitrate removal capacity of riparian zones. *J. Am. Water Res. Assoc*. 37:1457-1464.

Haggard, B.E., D.E. Storm, and E.H. Stanley. 2001. Effect of a point source input on stream nutrient retention. *J. Am. Water Resour. Assoc.* 37:1291-1299.

Hill, A.R. 1996. Nitrate removal in stream riparian zones. *J. Environ. Qual.* 25: 743-755.

Lechowicz, M.J., and G. Bell. 1991. The ecology and genetics of fitness in forest plants. II. Microspatial heterogeneity of the edaphic environment. *J. Ecol.* 79:687-696.

Legendre, P., and M.J. Fortin. 1989. Spatial pattern and ecological analysis. *Vegetatio* 80:107-138.

Lowrance, R.R. 1992. Groundwater nitrate and denitrification in a coastal riparian forest. *J. Environ. Qual.* 21:401-405.

Marti, E., J. Aumatell, L. Gode, M. Poch, and F. Sabatar. 2004. Nutrient retention efficiency in streams receiving inputs from waste water treatment plants. *J. Environ. Qual.* 33:285-293.

Needlelman, B.A. 2002. Surface runoff hydrology and phosphorus transport along two agricultural hillslopes with contrasting soils. Ph.D. Thesis. The Pennsylvania State University, University Park, PA.

O'Driscoll, M.A., and D.R. DeWalle. 2010. Seeps regulate stream nitrate concentration in forested Appalachian catchments. *J. Environ. Qual.* 39:420-431.

Palmer, M.W. 1990. Spatial scale and patterns of species-environment relationships in hardwood forest of the North Carolina piedmont. *Coenoses* 5:79-87.

Patton, C.J., and J.R. Kryskalla. 2003. Methods of analysis by the U.S. Geological Survey National Water Quality Laboratory: evaluation of alkaline persulfate digestion as an alternative to Kjeldahl digestion for determination of total dissolved nitrogen and phosphorus in water. U.S. Geological Survey water resources investigations report 03-4174, 33 p.

Peterjohn, W.T., and D.L. Correll. 1984. Nutrient dynamics in an agricultural watershed: observations on the role of a riparian forest. *Ecology* 65:1466-1475.

Peterson, B.J., W.M. Wolheim, P.J. Mulholland, J.R. Webster, J.L. Meyer, J.L. Tank, E. Marti, W.B. Bowden, H.M. Valett, A.E. Hershey, W.H. McDowell, W.K. Dodds, S.K. Hamilton, S. Gregory, and D.D. Morrall. 2001. Control of nitrogen export from watersheds by headwater streams. *Science* 292:86-90.

Peterson, E.E., A.A. Merton, D.M. Theobald, and N.S. Urquhart. 2006. Patterns of spatial autocorrelation in stream water chemistry. *Environ. Monit. Assess.* 121:571-596.

Pionke, H.B., J.R. Hoover, R.R. Schnabel, W.J. Gburek, J.B. Urban, and A.S. Rogowski. 1988. Chemical-hydrologic interactions in the near-stream zone. *Water Resour. Res.* 24:1101-1110.

R Development Core Team. 2011. R: a language and environment for statistical computing. R Foundation for Statistical Computing, Vienna, Austria.

Robertson, G.P., K.M. Klingensmith, M.J. Klug, E.A. Paul, J.R. Crum, and B.G. Ellis. 1997. Soil resources, microbial activity, and primary production across an agricultural ecosystem. *Ecol. Appl.* 7:158-170.

Rossi, R.E., D.J. Mulla, A.G. Journel, and E.H. Franz. 1992. Geostatistical tools for modeling and interpreting ecological spatial dependence. *Ecol. Monogr.* 62:277-314.

Rutherford, J.C., and M.L. Nguyen. 2004. Nitrate removal in riparian wetlands: interactions between surface flow and soils. *J. Environ. Qual.* 33:1133-1143.

Scanlon, T.M., S.M. Ingram, and A.L. Riscassi. 2010. Terrestrial and in-stream influences on the spatial variability of nitrate in a forested headwater catchment. *J. Geophys. Res.* 115: G02022, DOI: 10.1029/2009JG001091.

Shabaga, J.A., and A.R. Hill. 2010. Groundwater-fed surface flow path hydrodynamics and nitrate removal in three riparian zones in southern Ontario, Canada. *J. Hydrol.* 388:52-64.

Tesoriero, A.J., H. Liebsecher, and S.E. Cox. 2000. Mechanisms and rate of denitrification in an agricultural watershed: electron and mass balance along groundwater flow paths. *Water Resour. Res.* 36:1545-1559.

U.S. Environmental Protection Agency. 2008. National water quality inventory: 2008. Washington, DC.

Ver Hoef, J.M., E. Peterson, and D. Theobald. 2006. Spatial statistical models that use flow and stream distance. *Environ. Ecol. Stat.* 13:449-464.

Wagener, S.M., M.W. Oswood, and J.P. Schimel. 1998. Rivers and soils: parallels in carbon and nutrient processing. *BioScience* 48:104-108.

Warwick, J., and A.R. Hill. 1988. Nitrate depletion in the riparian zone of a small woodland stream. *Hydrobiologia* 157:231-240.

Zhu, Q., J.P. Schmidt, and R.B. Bryant. 2011. Hot moments and hot spots of nutrient losses from a mixed land use watershed. *J. Hydrol.* 414:393-404.

CHAPTER 5

Linking Nitrogen Management, Seep Chemistry, and Stream Water Quality in Two Agricultural Headwater Catchments

Abstract

Groundwater-fed seeps or seepage zones have been shown to contribute substantially to streamflow and increase nitrogen (N) concentrations, especially nitrate-N (NO_3-N), in stream reaches of agricultural catchments. Knowledge of the factors that influence seep NO_3-N concentrations, however, is still lacking. The objective of this study was to quantify the effects of N management throughout two headwater catchments and NO_3-N retention and removal within seep surface flow paths on NO_3-N concentrations in seep water. In addition, we sought to examine the effect of seeps on stream water quality at the catchment outlet. Nitrate-N retention within seeps was evaluated over a 2-year period (May 2010 – April 2012) by measuring the change in NO_3-N concentration along 20 seeps in FD36 and RS, two small agricultural headwater catchments in the Appalachian Valley and Ridge region of central Pennsylvania. Stream water samples at the catchment outlets were collected concurrently with seep water. Annual farmer surveys were also used to collect N management data at the field-scale. Results showed that the mean N application rate in FD36 (133 kg ha^{-1}) was significantly less than the mean N application rate in RS (200 kg ha^{-1}). Mean N application rate along groundwater flow paths to seeps in both catchments was significantly correlated (R^2 = 0.79) to mean seep top (i.e., emergence point) NO_3-N concentration. Nitrate-N concentration from the seep top generally decreased downseep suggesting that most seeps retained NO_3-N. Mean NO_3-N retention within

seep surface flow paths was 0.8 (16%) and 0.2 (1%) mg L^{-1} in FD36 and RS, respectively; although, NO_3-N retention varied seasonally (-3 to 41%) in FD36. Seasonal variability in seep NO_3-N retention in FD36 was related to both stream discharge (R^2 = 0.53) and air temperature (R^2 = -0.64). Mean seep bottom NO_3-N concentration was significantly correlated to stream NO_3-N concentration at the catchment outlet in both FD36 and RS with seeps accounting for 80% and 79%, respectively, of the variability in stream NO_3-N concentration. The results of this study suggest that while some NO_3-N retention occurs within seep surface flow paths, the primary factor controlling NO_3-N delivery from seeps to streams is N management throughout the catchment. Thus, in agricultural catchments with seeps, management practices that decrease the potential for NO_3-N leaching have the potential to improve stream water quality.

Introduction

Discharge from groundwater-sustained wetlands, slope wetlands, springs, or emergent groundwater seeps (hereafter referred to as seeps) in both forested (*Burns et al., 1998; O'Driscoll and DeWalle, 2010*) and agricultural (*Shabaga and Hill, 2010*) headwater catchments represents a potentially significant source of water and nitrogen (N) to many streams. Recent work by West et al. (2001) and Williams (Chapter 4) also points to the importance of seeps as variable sources of N inputs to headwater streams. Indeed, Williams (Chapter 4) found that variable inputs of nitrate-N (NO_3-N) from seeps in two agricultural headwater catchments in Pennsylvania influenced downstream variations in stream water NO_3-N concentration. Variability in seep NO_3-N concentration may arise due to variable sources of N applied across the catchment, N processing along groundwater flow pathways, or a combination thereof. Few studies, however, have looked at how these factors might influence seep inputs of N to headwater streams.

Research has shown that groundwater N chemistry is generally a reflection of the land use, the type of N source (i.e., fertilizer, atmospheric deposition, etc.), and the distribution of N inputs across a catchment (*Howarth et al., 1996; Sharpley et al., 1998; Boyer et al., 2002*). For example, in many non-glaciated areas in the northeast U.S., catchments are underlain by bedrock that is severely weathered at a shallow depth as a result of stress-relief fracturing (*Gburek and Folmar, 1999*). Water quality within these shallow fractured aquifers has been shown to be affected directly by the overlying and immediately upgradient land use (*Pionke and Urban, 1985*). Differences in management therefore have the potential to result in significant spatial and temporal variability of seep N concentrations. For instance, O'Driscoll and DeWalle (2010) monitored 15 seeps in an Appalachian forested headwater catchment and found that NO_3-N concentrations in seeps varied, ranging from 0.1 to 2.15 mg L^{-1}. In contrast, Williams (Chapter 4) monitored 17 seeps in two Appalachian agricultural headwater catchments and found that NO_3-N concentrations ranged from 0.1 to 29.5 mg L^{-1}. Notably, the primary N input in forested catchments is atmospheric deposition, which is uniformly distributed across small headwater catchments. Absent any effects of N transformations along groundwater flow pathways, one would expect little variability in seep NO_3-N concentrations. In contrast, agricultural catchments are typically managed on a field by field basis, and as a result, N application can be quite variable across the catchment. This variable management can translate to variable seep NO_3-N concentrations (*Williams, Chapter 4*).

The primary flow pathway for N delivery to seeps in many non-glaciated areas in the northeast U.S. is a highly conductive fractured aquifer that can support lateral saturated flows (*Lindsey et al., 2003; Williams, Chapters 2 and 3*). Williams (Chapters 2 and 3) found that this shallow fractured aquifer supplied 53% to 75% of groundwater to seeps. Several studies have also shown that most NO_3-N transported in the shallow fractured aquifer system is not altered by processing along the flow pathway due to short (i.e., several months to 2 years) water residence

times (*Pionke and Urban, 1985; McGuire et al., 2002; Lindsey et al., 2003*). Denitrification in this setting is mostly confined to a deeper aquifer (*Lindsey et al., 2003*), which does not contribute water at the scale of headwater (i.e., first-order) catchments (*Gburek and Folmar, 1999*). This suggests that management is the main factor influencing the water quality of seeps (a hypothesis we hope to test), and that any processing of NO_3-N is limited to the seep surface flow pathway.

Seeps often discharge groundwater to the surface in the riparian zone, which flows over land via concentrated flow paths before entering the stream at discrete points along the channel (*Pionke et al., 1988; Rutherford and Nyugen, 2004; O'Driscoll and DeWalle, 2010*). Hydrologic and biogeochemical processes can either result in NO_3-N retention or removal from seep water or facilitate NO_3-N delivery to the stream. For example, seep surface flow paths have the potential to function as biogeochemical hotspots in the riparian zone (*McCain et al., 2003*), promoting conditions that are often favorable for high denitrification rates and vegetative uptake. Dense vegetation, saturated soils with suitable redox conditions, and large fluxes of electron donors and acceptors all occur with seeps. In contrast, seep surface flow paths may be transport hotspots (*McCain et al., 2003*) and exhibit disproportionately high discharge rates relative to adjacent areas of the riparian zone. Higher discharge rates can result in decreased interaction between seep water and riparian soils along surface flow paths (*Rutherford and Nyguen, 2004*). Inconsistent results from previous research on NO_3-N retention along seep surface flow paths underscore this paradox. Several studies have reported substantial removal of NO_3-N along seep surface flow paths through the riparian zone (*Brusch and Nilsson, 1993; Blackwell et al., 1999; Rutherford and Nyguen, 2004; O'Driscoll and DeWalle, 2010*). Others, however, have found that surface seep flow paths deliver high NO_3-N concentration groundwater directly into the stream, essentially short-circuiting the remedial benefits of the riparian zone (*Warwick and Hill, 1988; Hill, 1990; Angier et al., 2002, 2005*).

In this study, we explore the effects of field-scale N management along groundwater flow paths to seeps and N retention within seeps on seep NO_3-N concentrations and delivery to streams. Seep and stream water in two small agricultural headwater catchments in central Pennsylvania (FD36 and RS) were monitored for two years in order to quantify NO_3-N retention within seeps and the relationship between N management within the catchment and seep water NO_3-N concentrations. The objectives of this study were to (1) determine the relationship between agricultural N management and seep NO_3-N concentrations; (2) quantify NO_3-N retention within seeps and identify potential factors that influence NO_3-N retention; and (3) examine seep contributions to stream water NO_3-N concentrations at the catchment outlet.

Materials and Methods

Site Location and Characteristics

The study was conducted in FD36 (40 ha) and RS (45 ha), which are headwater catchments within the non-glaciated, folded and faulted, Appalachian Ridge and Valley Physiographic region of central Pennsylvania (Figure 5.1). FD36 and RS are two of 15 sub-catchments that form WE-38, a primary research site of the USDA – Agricultural Research Service since 1968 (*Bryant et al., 2011*). The dominant land use in FD36 and RS is agriculture, which comprises 56% and 75% of the land area in each catchment, respectively (Figure 5.1). Common crop rotations include three- to four-year sequences of corn, small grains, hay, and soybeans. Crops are planted on upslope fields in both catchments and the riparian zones in each catchment are variable in width (2 – 20 m) and planted with grasses. Two contrasting soil groups are also found within FD36 and RS (*Needelman et al., 2002*). Well-drained residual soils that are typically stony, silt loams (Leck Kill, Calvin, and Berks series) line the hillslopes, while colluvial soils (Albrights and Hustontown series) are distributed along the stream and valley floor. The

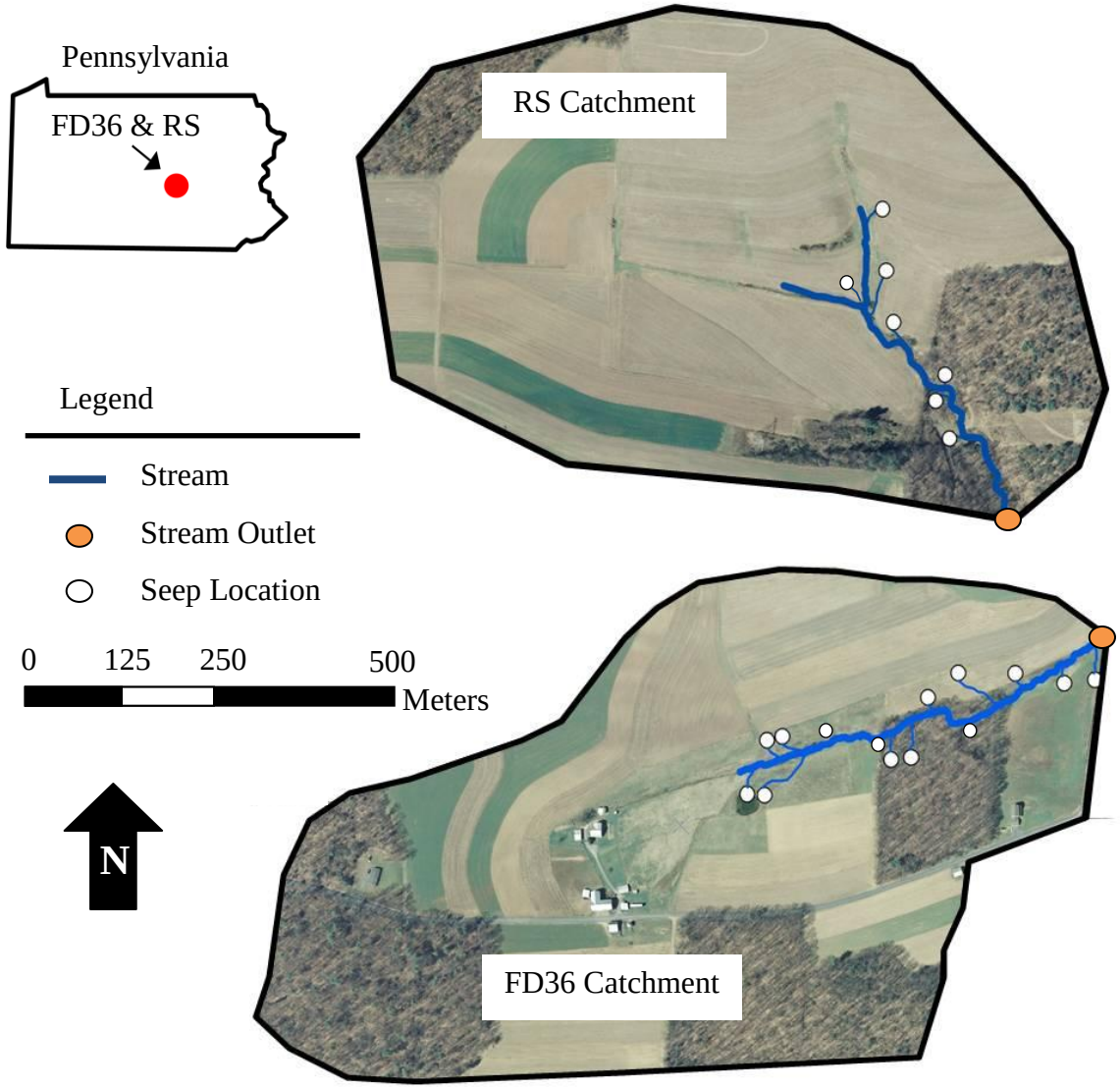

Figure 5.1

Aerial photo of FD36 and RS with locations of groundwater-fed seeps shown. FD36 and RS are small agricultural sub-catchments of WE-38 (7.3 km^2), which is located in central Pennsylvania and has been a primary research site of the USDA-Agricultural Research Service for over 40 years. Stream water leaving WE-38 flows into East Mahantango Creek, which flows into the Susquehanna River and ultimately the Chesapeake Bay.

Albrights and Hustontown soils in the riparian zone have a moderately well-developed fragipan beginning at a depth of 0.5 to 0.7 m and have low permeability.

The climate in FD36 and RS is temperate and humid with annual precipitation averaging 1080 mm yr^{-1} (*Buda et al., 2011*). Previous research in FD36 has shown that groundwater from a

fractured aquifer provides the majority (60% - 80%) of the annual streamflow (*Gburek et al., 1996; Pionke et al., 1996*) and that the surface and subsurface flow systems are predominantly self-contained at the catchment-scale (*Gburek and Folmar, 1999*). Annual catchment N budgets in FD36 indicate that 75% of NO_3-N and 65% of total N are exported in baseflow (*Zhu et al., 2011*), with most of the NO_3-N losses occurring in the pre- (January – April) and post-growing (October – December) seasons. In addition, annual farmer surveys have been conducted across WE-38 since 1994. This database includes information on field management practices such as crop type and yield, tillage type and timing, fertilizer and manure application rate, method, and timing, as well as pesticide type and application rate.

Seeps in FD36 and RS are generally found within the riparian zone; although, some seep surface flow paths extend into upland agricultural areas. Seep surface flow path lengths in both catchments range from 2 to 75 m and flow paths in FD36 tend to be more diffuse and have gentler gradient than flow paths in RS. Results from a previous study show that NO_3-N concentrations in seep water are variable (0.1 to 29.5 mg L^{-1}) and have been shown to influence patterns in stream water NO_3-N concentration (*Chapter 4*). Two studies in seep areas of FD36 also found that the majority (53% - 75%) of seep discharge was from groundwater upwelling through the fragipan from a shallow fractured aquifer (*Chapters 2 and 3*). The upwelling groundwater from the shallow fractured aquifer to seeps had higher (5.7 mg L^{-1}) NO_3-N concentrations relative to groundwater perched on top of the fragipan (0.6 mg L^{-1}).

Seep and Stream Water Sampling

Seep and stream water samples were collected every two weeks between May 2010 and April 2012. Initially, 16 and 7 seeps were identified in FD36 and RS, respectively. We focused our sampling efforts on 13 seeps in FD36 and 7 seeps in RS, all of which flowed consistently and

were regularly sampled (Figure 5.1). Seep sampling followed the approach described by O'Driscoll and DeWalle (2010). Briefly, water samples were collected at the top of each seep (i.e., seep top, emergence point) and at the bottom of each seep (i.e., seep bottom, 0.5 m upseep of the confluence with the stream channel). For seeps with surface flow paths less than 3 m, only seep bottom samples were collected. Seeps were labeled based on their distance from the stream outlet and orientation relative to the stream channel (e.g., 8S, 80 m from the outlet on the south side of the stream; 11N, 110 m from the outlet on the north side of the stream). Several rock drains were also identified in FD36 and RS and were sampled concurrently with seep water. Seep discharge was not measured during water quality sampling due to difficulties associated with accurate discharge measurements in poorly defined, shallow channels. Stream discharge throughout the study period was continuously monitored (5-min intervals) using a recording H-flume at the outlet of FD36. While no stream discharge measurements were made in RS, its close proximity to FD36 as well as its similar size and land use suggests that streamflow in FD36 was representative of streamflow in RS. Stream water samples at the outlet of both catchments were collected every other week throughout the study period.

Water Quality Analysis

All water samples were analyzed for ammonium-N (NH_4-N), NO_3-N, total N, and chloride (Cl^-). Water samples were first filtered (0.45 µm) and then analyzed with a Lachat QuikChem FIA+ autoanalyzer (QuikChem Methods FIA+ 8000 Series, Lachat Instruments, Loveland, Colorado) to determine concentrations of NO_3-N, NH_4-N, and chloride. Total N was determined on unfiltered samples following alkaline persulfate digestion (*Patton and Kryskalla, 2003*). Concentrations of NH_4-N in seep and stream water on all sampling dates were low and often below the analytical detection limit (0.1 mg L^{-1}). As a result, we do not to report these

values in the paper. The main focus of the paper is NO_3-N, which comprised, on average, 95% of total N.

Statistics and Data Analysis

In order to link field-scale N management to seep NO_3-N concentrations, we combined a simple geospatial assessment of seep flow pathways with the detailed land management data available through annual farmer surveys in FD36 and RS. Topographic groundwater flow paths draining to seeps in FD36 and RS were delineated using land surface contour maps that were created from high-resolution LiDAR elevation data (0.5 m horizontal resolution; data collected in Mar. 2007). All analyses were completed in ArcGIS 10.0 (Esri, Inc). We extended groundwater flow paths from the seep emergence point upslope to the catchment boundary in FD36 and RS, which is consistent with observations by Williams (Chapters 2 and 3) that the main source of water to emergent seeps is from the fractured aquifer system that is recharged in upslope landscape positions in both catchments (*Gburek and Folmar, 1999*). While we recognize that surface and subsurface flow paths are not always the same, surface topography is often used to describe groundwater flow paths when there is little information available on subsurface gradients related to the bedrock topography (*Freer et al., 1997*).

Nitrogen application rates from annual farmer surveys were averaged over a 5-year period (2007 – 2011) at the field-scale and then were overlain on the delineated groundwater flow paths. Weighted average N application rates along individual flow paths were then calculated. Given the propensity for recharge, and hence NO_3-N leaching, to be concentrated in well-drained upslope soils, we used a simple inverse distance weighting function that gave progressively more weight to N applied in these regions and less weight to N applied in the near-stream zone. A least squares estimation method was then performed to obtain a Pearson correlation coefficient to

measure the strength of the linear relationship between weighted mean N application rate along the groundwater flow paths draining to seeps and seep top (or seep bottom, if seep length < 3 m) NO_3-N concentrations.

We also sought to evaluate the potential for NO_3-N retention in seeps from the point of emergence to discharge in streams. To determine the amount of NO_3-N retention in seeps, downseep changes in NO_3-N concentration (seep bottom – seep top) were calculated for seeps with lengths greater than 3 m (following O'Driscoll and DeWalle (2010)). Changes in NO_3-N concentrations from seep top to bottom were compared to zero change in concentration with a one-sample t-test. Mean monthly seep top and bottom NO_3-N concentrations were also compared with a paired t-test to evaluate whether seeps functioned as NO_3-N sources or sinks at the catchment scale. Pearson correlation coefficients were calculated between stream discharge, air temperature (recorded at a meteorological station in FD36), and NO_3-N concentration change along seeps to determine factors that were influencing NO_3-N transport in seeps. In addition, Pearson correlation coefficients were calculated for monthly seep bottom NO_3-N concentrations (all seeps and rock drains in the catchment) and stream (catchment outlet) NO_3-N concentrations to evaluate the relationship between seep and stream NO_3-N concentrations. All statistical analyses were completed in *R* statistical software package (*R Foundation for Statistical Computing, 2011*). A probability level of 0.05 was used to evaluate statistical significance in all analysis.

Results

Nitrogen Management in FD36 and RS

Annual farmer surveys showed that N application occurred in both the spring and fall in FD36 and RS. A combination of commercial fertilizers, dairy manure, and swine manure was the

primary source of applied N in both catchments. From 2007 through 2011, farmer surveys showed that N was applied to an average of 14.5 and 24.8 ha in FD36 and RS, respectively, which is equivalent to 36% and 55% of the drainage area in each catchment (Table 5.1). The mean annual N application rate over the 5-yr period was significantly less in FD36 (133 kg ha^{-1}) than in RS (200 kg ha^{-1}) ($p < 0.001$; Table 5.1); although, N application rates in individual fields varied substantially in both catchments from year to year. Nitrogen application rates in RS were significantly greater than FD36 because large amounts of swine manure were applied twice a year from a nearby confined animal feeding operation. Nitrogen application rates did not vary significantly by season (spring or fall) in either catchment.

Nitrogen Application Rate along Groundwater Flow Paths to Seeps

Mean annual N application rate in individual fields of FD36 and RS ranged from 0 to 250 kg ha^{-1} from 2007 through 2011 (Figure 5.2). In FD36, higher mean annual N application rates (150 to 200 kg ha^{-1}) were found on the north side of the stream compared to mean annual N applications rates (0 to 100 kg ha^{-1}) on the south side of the stream. In RS, mean annual N

Table 5.1 Nitrogen management data from FD36 and RS (2007 – 2011). Data were collected from annual farmer surveys in both catchments. The amount of N applied in FD36 and RS was a combination of commercial fertilizer, dairy manure, and swine manure. Nitrogen content in dairy and swine manure was determined using typical compositions reported in the Penn State Agronomy Guide (2011).

	FD36			RS		
Year	**N applied**	**Area of N application**	**Mean N application rate**	**N applied**	**Area of N application**	**Mean N application rate**
	kg	ha	kg ha^{-1}	kg	ha	kg ha^{-1}
2007	2182	15.4	142	3982	19.6	203
2008	2279	15.0	152	5796	27.3	212
2009	1773	12.8	139	4773	22.5	212
2010	1456	14.0	104	6011	28.2	213
2011	2148	15.3	140	4228	26.6	159

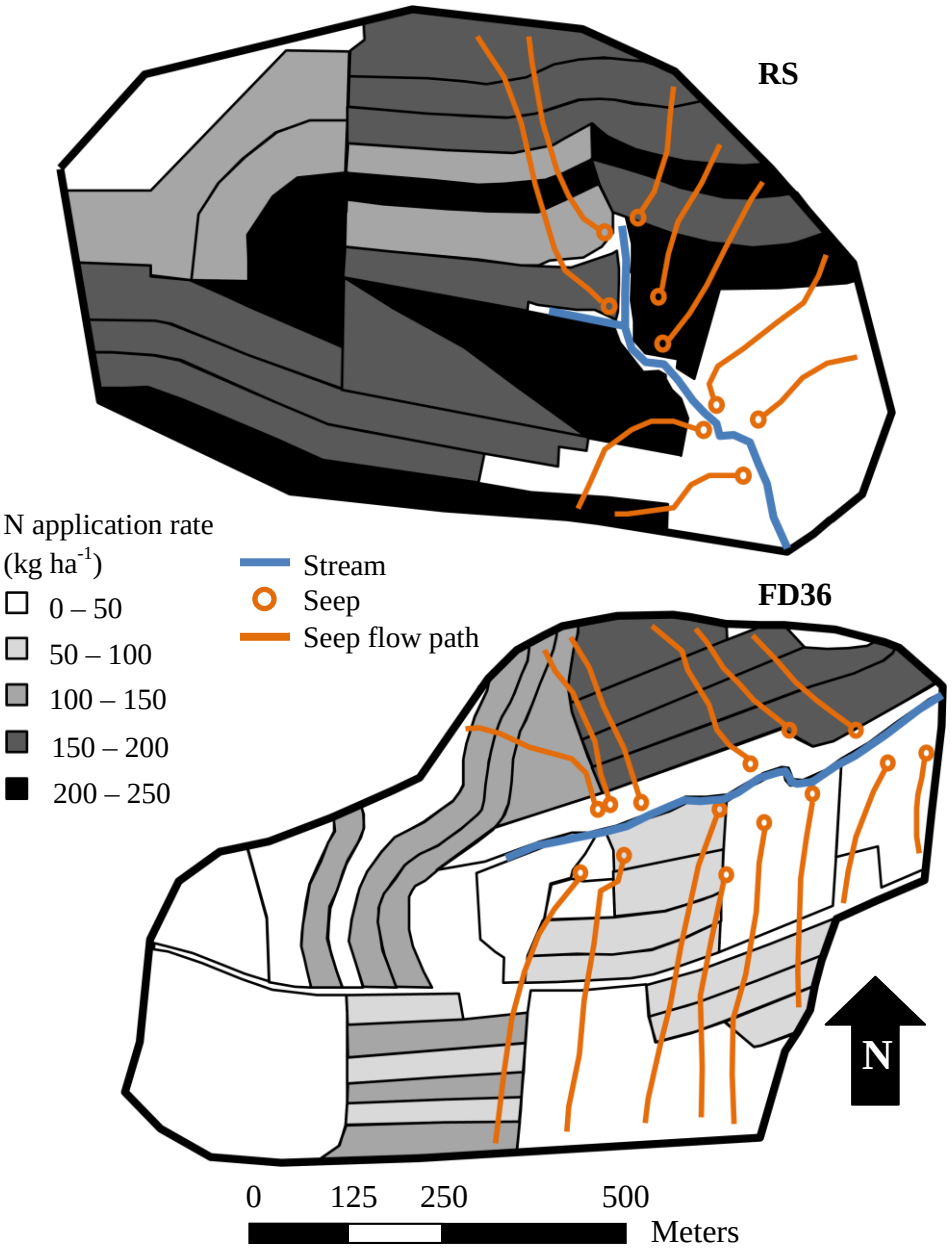

Figure 5.2

Mean N application rates in FD36 and RS from 2007 through 2011. Data were collected from annual farmer surveys in both catchments. The amount of N applied in FD36 and RS was a combination of commercial fertilizer, dairy manure, and swine manure. Nitrogen content in dairy and swine manure was determined using typical compositions reported in the Penn State Agronomy Guide (2011).Seep flow paths were delineated using surface topography and extended from the seep discharge location to the catchment boundary.

application rates were relatively uniform throughout the entire catchment, excluding areas that were forested (Figure 5.2). Nitrogen application rates along groundwater flow paths to seeps were calculated using the weighted mean N application rates from individual fields that intersected these pathways. Nitrogen application rates from individual fields were inversely weighted based on their distance from the stream channel to the catchment divide since most groundwater recharge in FD36 and RS occurs on the well-drained residual hillslope soils (*Gburek and Folmar, 1999*). Using this approach, mean N application rates along groundwater flow paths to seeps were found to range from 0 to 140 kg ha^{-1} in FD36, and 0 to 214 kg ha^{-1} in RS.

Nitrogen application rates along groundwater flow paths to seeps were compared to seep top (or seep bottom if seep length < 3 m) NO_3-N concentrations (Figure 5.2). Nitrate-N concentrations of seeps in FD36 and RS are shown in Table 5.2. A significant positive correlation was found between N application rate and seep NO_3-N concentration in both FD36 and RS (R^2 =

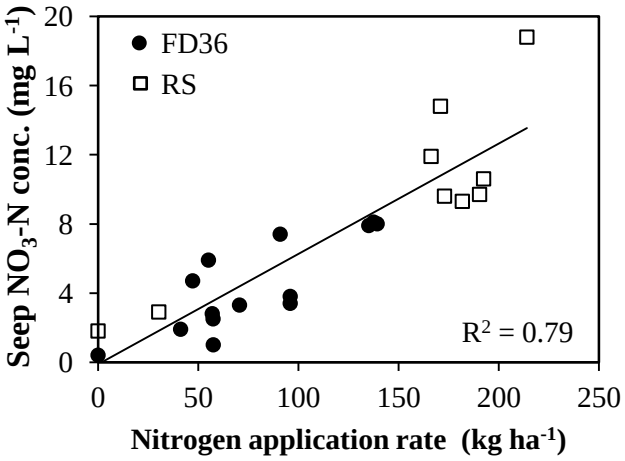

Figure 5.3

Mean N application rate in FD36 and RS compared with seep NO_3-N concentration ($p < 0.001$). Nitrogen application rates from individual fields were used to calculate the mean N application rate along flow paths. Nitrogen application rates were inversely weighted along topographic flow paths from the seep outlet to the catchment divide. Seep NO_3-N concentrations were from the seep top (i.e., emergence point) when seep length > 3m; otherwise, concentrations represent the seep bottom.

0.79; $p < 0.001$; Figure 5.3). Higher mean N application rates in RS compared to FD36 resulted in seeps in RS having higher NO_3-N concentrations. Thus, N application rates upslope of the seep discharge point influenced seep NO_3-N concentrations.

NO_3-N Retention in Seeps

Seep top groundwater in FD36 and RS had higher mean NO_3-N concentration than seep bottom water, suggesting that NO_3-N retention occurred in seeps (Table 5.2 and 5.3). In FD36, mean NO_3-N concentrations of 5.1 and 4.3 mg L^{-1} were observed in seep top and seep bottom water (16% retention), whereas, NO_3-N concentrations of 16.0 and 15.8 mg L^{-1} were found in seep top and seep bottom water in RS (1% retention). Most seeps were NO_3-N sinks over the study period and mean seep top NO_3-N concentration was greater than seep bottom NO_3- N concentration for the majority of seeps (88%) (Table 5.2). Significant decreases in NO_3-N concentrations were observed for 70% and 33% of the seeps (flow paths > 3 m) in FD36 and RS, respectively (Table 5.2). Longer surface flow paths did not always result in greater NO_3-N retention. The slope of seep surface flow paths, however, may have influenced the amount of NO_3-N retention between catchments, as slopes were significantly less along seep surface flow paths in FD36 compared to RS ($p < 0.001$; Table 5.2). Seep surface flow path slopes were 4% and 13% in FD36 and RS, respectively. Overall, mean NO_3-N retention within individual seeps with flow paths greater than 3 m ranged from -25% to 37%.

The greatest magnitude reduction in downseep NO_3-N concentration (retention) occurred during the growing season in FD36 and RS (Table 5.3). In FD36, mean downseep NO_3-N reduction was 2.2 mg L^{-1} during June 2010 and July 2011. Based on paired t-tests, significantly greater NO_3-N concentrations ($p < 0.05$) were measured in seep top water relative to seep bottom water for 8 months (40%) of the study period in FD36 (Table 5.3). While most of the significant

Table 5.2 Seep characteristics from FD36 and RS including site, number of samples, length, slope, bypass events, percentage of sampling events that were bypass events, mean top and bottom seep NO_3-N concentration, and downseep NO_3-N concentration change. Nitrate concentration data were collected from both catchments between May 2010 and April 2012.

				Bypass events[‡]		Upslope annual N appl. rate	NO_3-N concentration		
Site	**n**[†]	**Length**	**Slope**	**n**	**%**		**Top**	**Bottom**	**Change**
		m	m m^{-1}			kg ha^{-1}		mg L^{-1}	
FD36									
2S	12	33	0.028	7	58	0	0.3	0.4	+0.1
8S	26	12	0.051	5	19	57	3.2	2.8	*-0.4*
11N	25	8	0.076	3	12	139	9.5	8.0	*-1.5*
14N	15	55	0.030	0	0	135	10.6	7.9	*-2.7*
22S	6	3				58		1.0	
28N	23	2				148		8.1	
31S	25	29	0.045	4	16	57	3.0	2.5	*-0.5*
35S	26	20	0.041	9	35	47	5.0	4.7	-0.3
[*]36S	32	n/a				65		5.9	
43N	6	2				96		3.8	
46S	14	76	0.012	4	29	41	3.0	1.9	*-1.1*
47N	11	35	0.030	3	27	85	4.8	3.4	*-1.4*
49N	31	17	0.045	8	26	119	7.7	7.4	*-0.3*
53S	30	17	0.027	13	43	71	3.4	3.3	-0.1
RS									
9W	30	8	0.114	12	40	200	14.9	14.8	-0.1
12E	3	19	0.084	0	0	0	2.2	1.8	-0.4
17W	30	10	0.091	14	47	215	18.8	18.8	0.0
19E	24	2				30		2.9	
29E	25	14	0.214	5	20	182	10.6	10.2	*-0.4*
33E	6	64	0.156	3	50	166	9.3	8.7	-0.6
[*]37W	30	n/a				190		11.9	
47E	8	22	0.130	0	0	173	9.7	9.5	*-0.2*
[*]48W	29	n/a				171		9.6	

[†] n is the number of sampling events at each individual seep. It is < 32 and < 30 for sites that ceased to flow for a portion of the study period in FD36 and RS, respectively.

[‡] Seep bypass events occurred when seep NO_3-N concentration remained stable or increased downseep. Seep top samples were not collected for seeps with a length < 3 m.

[§] p Value is for one-sample t-test between the change in seep NO_3-N concentration and zero change in concentration. Values in italics represent significant NO_3-N concentration changes downseep ($p < 0.05$). Seep concentration change calculated as seep bottom concentration minus seep top concentration.

[*] Rock drain that discharges into the stream.

Table 5.3 Mean monthly NO_3-N concentration at the top and bottom of seeps in FD36 and RS, and the downseep change in NO_3-N concentration between May 2010 and April 2012.

Date	FD36 Top	FD36 Bottom	FD36 Change†	RS Top	RS Bottom	RS Change†
	mg L^{-1}					
2010						
May	4.1	3.0	*-1.1*	18.6	18.6	0.0
June	5.4	3.2	*-2.2*	19.8	20.3	+0.4
Oct.	5.9	5.5	-0.4	19.6	19.3	-0.3
Nov.	6.6	6.0	-0.6	20.4	20.5	+0.1
Dec.	7.4	7.1	-0.3	17.3	17.2	-0.1
2011						
Jan.	7.0	6.9	-0.1	21.1	21.4	+0.3
Feb.	6.1	5.3	-0.8	13.9	13.9	0.0
Mar.	5.5	4.9	*-0.6*	13.0	12.7	-0.3
Apr.	4.6	3.6	*-1.0*	13.1	12.7	-0.4
May	4.8	3.2	*-1.6*	12.2	11.7	-0.5
June	5.9	4.2	*-1.7*	16.7	16.5	-0.2
July	6.9	4.7	-2.2	20.4	20.4	0.0
Sept.	4.4	3.5	-0.9	15.6	15.6	0.0
Oct.	4.8	4.2	*-0.6*	14.1	13.8	-0.3
Nov.	4.0	3.8	-0.2	14.7	14.4	-0.3
Dec.	3.8	3.2	-0.6	12.0	11.9	-0.1
2012						
Jan.	3.8	3.9	+0.1	14.4	14.5	+0.1
Feb.	5.1	4.7	-0.4	13.2	13.1	-0.1
Mar.	3.9	3.7	-0.2	15.8	15.6	-0.2
Apr.	3.4	2.8	*-0.8*	16.9	16.8	-0.1
All Dates	5.1	4.3	*-0.8*	16.0	15.8	*-0.2*

†Seep concentration change calculated as seep bottom concentration minus seep top concentration. Values in italics represent significant NO_3-N concentration changes downseep ($p < 0.05$)

NO_3-N retention occurred between April and June in FD36, there was also significant retention in the months before (March) and following (July – October) this period depending on the year. Although NO_3-N retention was also observed in RS, no significant monthly downseep changes in NO_3-N concentrations were found (Table 5.3).

Seep bypass events occurred when NO_3-N concentrations in seep water remained constant downseep (*see Gold et al., 2001; O'Driscoll and DeWalle, 2010*). Seep bottom NO_3-N concentrations were greater or equal to seep top NO_3-N concentrations for 56 of 215 paired samples (26%) in FD36 and 34 of 102 paired samples (33%) in RS (Table 5.2). Site 2S in FD36 and site 17W in RS had the greatest percentage of dates when they functioned as bypass sites (58% and 47%, respectively) (Table 5.2). The frequent occurrence of seep NO_3-N bypass events resulted in a net annual increase in downseep NO_3-N concentration at site 2S. Bypass events in both catchments, however, varied seasonally (Figure 5.4). In both FD36 and RS, the greatest percentage of seep bypass events occurred during the winter (41% and 47%, respectively), which was associated with lower air temperatures and high discharge periods (Figure 5.4). During the summer, when NO_3-N retention in seeps was the greatest, bypass events occurred less frequently (11% and 10% in FD36 and RS, respectively) (Figure 5.4).

Chloride concentrations in seep top and seep bottom water in FD36 and RS were not significantly different on any sampling date and mean concentrations were typically within 0.1 mg L^{-1} of each other (data not shown). This suggests that during periods of NO_3-N retention in seeps, downseep changes in NO_3-N concentration were not due to dilution (Table 5.3). The lack of a downseep change in chloride concentration indicated that NO_3-N was either retained or transformed within the seep surface flow path. To further identify factors that affected NO_3-N concentration in seep surface flow paths, we compared mean monthly seep NO_3-N concentration and downseep NO_3-N concentration changes with seep NO_3-N concentration, air temperature, and log stream discharge (*Q*) using an approach similar to that of O'Driscoll and DeWalle (2010) (Table 5.4). In FD36, mean NO_3-N concentration change was significantly correlated with log *Q* (R^2 = 0.53) and air temperature (R^2 = -0.64). Seep top NO_3-N concentration in FD36 was not correlated with log *Q* or air temperature, but seep bottom NO_3-N concentration was significantly correlated with temperature (R^2 = -0.28). In RS, both seep top and bottom were significantly

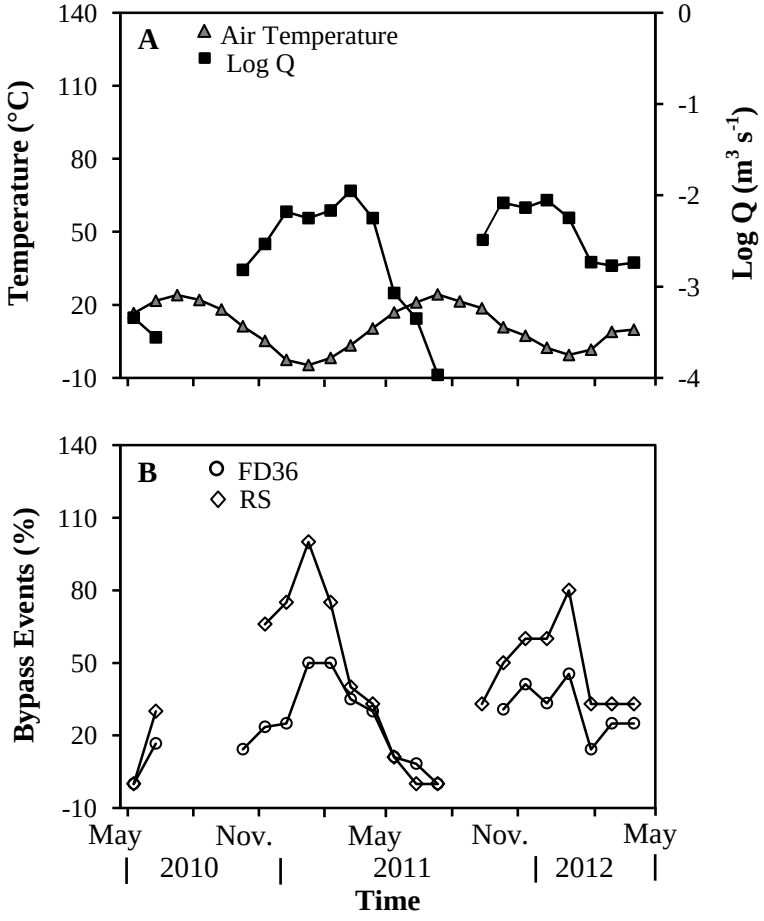

Figure 5.4

(A) Air temperature and log Q (stream discharge) at the catchment outlet of FD36. (B) Percentage of seeps exhibiting NO_3-N bypass events. Seep NO_3-N bypass occurred when NO_3-N concentration remained constant or increased downseep. Gaps in seep data are from times of the year when no seep flow occurred.

correlated with log *Q* (R^2 = -0.25 and -0.23, respectively); however, NO_3-N concentration change was not correlated to either temperature or log *Q*.

Stream NO_3-N Concentration at the Catchment Outlet

Stream water NO_3-N concentrations over the study period were significantly less in FD36 compared to RS ($p < 0.001$, data not shown). Nitrate-N concentration in FD36 ranged from 1.6 to

Table 5.4 Pearson correlation coefficients and p values (in parentheses) for correlations among seep NO_3-N concentration, air temperature, and log Q (stream discharge at the catchment outlet). Italics indicate correlation is significant at $p < 0.05$.

		Seep NO_3-N (mg L^{-1})		
		Top	**Bottom**	**NO_3-N Change†**
FD36				
Seep Bottom NO_3-N	mg L^{-1}	*0.79 (<0.001)*		
NO_3-N Change†	mg L^{-1}	-0.02 (0.541)	0.09 (0.197)	
Air Temperature	°C	-0.04 (0.432)	*-0.28 (0.016)*	*-0.64 (<0.001)*
Log Q (discharge)	m^3 s^{-1}	-0.01 (0.736)	0.06 (0.283)	*0.53 (<0.001)*
RS				
Seep Bottom NO_3-N	mg L^{-1}	*0.99 (<0.001)*		
NO_3-N Change†	mg L^{-1}	-0.11 (0.160)	-0.18 (0.072)	
Air Temperature	°C	0.05 (0.353)	0.04 (0.423)	0.05 (0.366)
Log Q (discharge)	m^3 s^{-1}	*-0.25 (0.027)*	*-0.23 (0.037)*	-0.01 (0.843)

† Seep concentration change calculated as seep bottom concentration minus seep top concentration.

6.7 mg L^{-1}, whereas NO_3-N in RS ranged from 11.3 to 15.7 mg L^{-1}. Nitrate-N concentration was also significantly different among seasons in FD36 ($p = 0.005$), but not in RS (data not shown). In FD36, mean stream water NO_3-N concentration was less during the summer (1.5 mg L^{-1}) compared to the spring and fall (3.8 and 3.1 mg L^{-1}, respectively), and winter (5.8 mg L^{-1}).

Monthly mean stream water NO_3-N concentrations at the catchment outlet in FD36 and RS were compared to monthly mean seep bottom NO_3-N concentrations (Figure 5.5). In FD36, significant correlations existed between NO_3-N concentrations at the stream outlet and nine seep bottoms (64%) (data not shown). Similarly, in RS, significant correlations were also found between NO_3-N concentrations at the stream outlet and four seep bottoms (44%). Monthly mean seep bottom NO_3-N concentration was similar to monthly mean stream NO_3-N concentration in both FD36 and RS for most of the year (within 2 mg L^{-1}) (Figure 5.5). Monthly mean seep bottom NO_3-N concentration in FD36 was on average 0.7 mg L^{-1} greater than stream outlet NO_3-N concentration and could explain 80% of the variability in stream outlet NO_3-N concentrations over the study period (Figure 5.5). In contrast, monthly mean seep bottom NO_3-N concentration

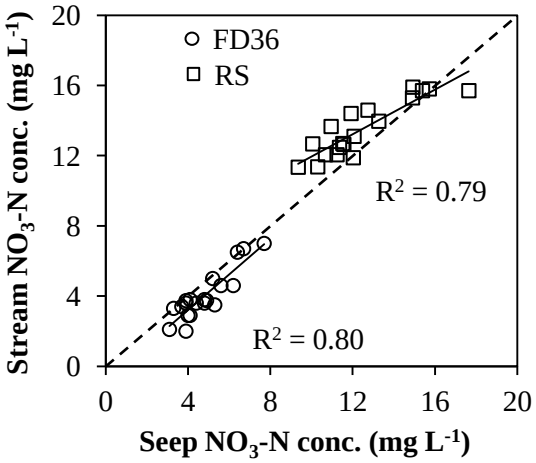

Figure 5.5

Monthly mean seep bottom NO_3-N concentration plotted against monthly mean stream NO_3-N concentration during the study period ($p < 0.001$). The dashed line represents a 1:1 relationship between seep bottom and stream NO_3-N concentration.

in RS was on average 0.9 mg L^{-1} less than monthly mean stream outlet NO_3-N concentration, but could explain 79% of the variability in stream outlet NO_3-N concentration (Figure 5.5). The deviation from a 1:1 line in Figure 5.5 was different between FD36 and RS. The slope of the relationship between monthly mean seep and stream NO_3-N concentrations for FD36 was 1.01, which suggests that stream outlet NO_3-N concentration reflected NO_3-N concentrations in seeps with minimal in-stream alteration. In RS, the slope of the relationship was 0.63, indicating that the NO_3-N concentration at the stream outlet was 27% lower than what the seeps were contributing . Thus, in-stream processing or other mechanisms may be occurring in RS.

Discussion

Seep Characteristics and Hydrology

The presence of seeps in FD36 and RS appeared to be associated with the location of fragipan-containing soils (Albrights and Hustontown series) that occur at the toeslope, where the

uplands transition to the riparian zone. Fragipans have low permeability, often impede the vertical movement of water (*Walter et al., 2000*), and have been shown to influence the amount of surface runoff generation at both hillslope- (*Buda et al., 2009*) and catchment-scales (*Gburek et al., 2006*). However, preferential groundwater upwelling through the fragipan has been found to contribute 53% to 75% of water to seeps in FD36 (*Williams, Chapter 2*). In addition, electrical resistivity imaging (ERI) data from the same sites are also consistent with this interpretation (*Williams, Chapter 3*). Other studies have shown that soil-bedrock contacts and bedrock factures were also possible mechanisms for groundwater upwelling to seeps (*O'Driscoll and DeWalle, 2010*).

Once upwelling groundwater discharged onto the land surface, there was substantial variation in seep surface flow paths through the riparian zone in FD36 and RS. In FD36, seep surface flow paths tended to be diffuse and ill-defined. Surface flow path depths were very shallow and tended to be spread over a larger wet area compared to flow in small channels or rivulets; although during high discharge periods (i.e., winter and spring), defined channels were observed. In contrast, seep surface flow paths in RS were well-defined in small channels from the seep emergence point to the stream. Seep surface flow paths in RS were also steeper than flow paths in FD36. Variability in seep surface flow paths between catchments and among seeps can influence the degree to which seep water interacts with riparian zone soils and vegetation. Riparian zones with different surface flow patterns can exhibit large differences in NO_3-N removal (*Shabaga and Hill, 2010*).

Nitrogen Application Rates and Seep NO_3-N Concentration

In general, when N application rates exceed crop demands in agricultural landscapes, NO_3-N can leach to groundwater. Many studies have shown a high correlation between

agricultural land use and NO_3-N concentrations in groundwater (*Hallberg and Keeney, 1993; Ator and Ferrairi, 1997; Harter et al., 2002*). For example, Gold et al. (1990) monitored groundwater NO_3-N concentrations under several land uses including forest, residential, and agriculture. They found that NO_3-N concentrations from agricultural landscapes were always greater than 10 mg L^{-1}, whereas NO_3-N concentrations from forested landscapes were less than 2 mg L^{-1}. In FD36 and RS, most N applied to agricultural fields is from manure, which can significantly increase the N content of soil (*Paul and Zebarth, 1997*). Mineralization of organic-N from recently applied manure is often a source of NO_3-N leaching to groundwater (*Hii et al., 1999*) and the water quality effects can persist long after reductions in N loading occur (*Carey, 2002*). This time lag is related to the mean residence time of groundwater, which at the scale of FD36 and RS, can be on the order of several months to two years (*McGuire et al., 2002; Lindsey et al., 2003*).

Many studies have found relationships between land use and groundwater quality at larger scales (i.e., forested vs. agricultural catchments), but few studies have shown a link between field-scale N application rates across a catchment to seep NO_3-N concentrations. In this study we found that as N application rates along groundwater flow paths to seeps increased, seep NO_3-N concentrations also increased (Figure 5.3). The variability in N management across FD36 and RS resulted in seep NO_3-N concentrations that ranged from 0.3 to 18.8 mg L^{-1}, and this variability imparted longitudinal variations in NO_3-N in streams in FD36 and RS (*Williams, Chapter 4*). Previous research in FD36 has shown that most groundwater recharge occurs on upslope soils (Leck Kill, Calvin, and Berks series) that are well drained (*Gburek and Folmar, 1999*). Therefore, the potential for NO_3-N leaching was also greater from these landscape positions (*Pionke et al., 2000*). The challenge in connecting N application rates and areas of NO_3-N leaching across the catchment to seep NO_3-N concentrations is identifying the groundwater flow paths from the source of N to the seep discharge point. In this study, we used surface

topography to delineate potential groundwater flow paths and assumed that the majority of recharge, and hence NO_3-N leaching, occurred on the upslope soils as opposed to poorly drained soils closer to the seep discharge locations. Other studies have used the duration of seep flow (*Burns et al., 1998*) and bedrock topography (*Freer et al., 1997*) as potential indicators of groundwater flow paths to seeps. While the duration of seep flow may provide an estimate on the size of the area draining to a seep, it provides little information on the location of these areas. Collecting detailed bedrock topography over an 85 ha area in FD36 and RS with a geophysical tool, such as ground penetrating radar (GPR), may have also yielded better estimates of groundwater flow paths compared to using surface topography as a proxy (*Freer et al., 1997*), but it was beyond the scope of this study.

NO_3-N Retention in Riparian Zone Seeps

Spatial variability in NO_3-N retention among seep surface flow paths (-25% to 37%) in FD36 and RS was similar to NO_3-N retention reported along surface flow paths in other studies. While several studies have shown that seeps retain or remove NO_3-N (*Brusch and Nillson, 1993; Burns et al., 1998; O'Driscoll and DeWalle, 2010*), others have found no measurable NO_3-N retention (*Warwick and Hill, 1988; Hill, 1990*) or NO_3-N increases (*Steinheimer et al., 1998*). The amount of interaction between seep water and groundwater along surface flow paths through the riparian zone may, in part, elucidate some of the conflicting findings for seep NO_3-N retention from the literature and within FD36 and RS. At one end of the continuum, seep water can be transported in small rivulets quickly across the riparian zone surface or in shallow pipe networks that have short water residence times and limited interaction with riparian soils. At the other extreme are sites with diffuse surface flow where repeated exchanges of water between surface flow and areas of slower flowing water increase residence times. Research has shown that

subsurface residence times on the order of one day are sufficient to achieve significant NO_3-N reductions (*e.g., Rutherford and Nguyen, 2004*). Therefore, vertical exchange between seep surface water, soil water, and shallow groundwater along seep flow paths would allow seep water to spend more time in the subsurface environment and increase the potential for biotic assimilation of N or denitrification. In FD36, seep surface flow paths were less steep and more diffuse compared to surface flow paths in RS. Thus, longer residence times along more tortuous surface flow paths in FD36 likely resulted in seeps retaining more NO_3-N compared to RS.

Nitrate-N retention along seep surface flow paths also varied seasonally in FD36 (-3% to 41%) with the greatest amount of retention occurring in the growing season. Retention in FD36 was significantly correlated with both air temperature and stream discharge, which suggests that hydrological and biogeochemical mechanisms were primarily responsible for downseep NO_3-N concentration changes. While the specific mechanisms for NO_3-N retention were not determined as part this study, we hypothesize that denitrification and vegetative uptake could explain the seasonal NO_3-N concentration declines along seep surface flow paths. During the spring and summer in FD36, low flows may result in increased interaction between seep water and groundwater along the surface flow path. In addition, warm air temperatures resulted in increased growth of grasses and algae along surface flow paths in the riparian zone. Work by Chapman et al. (1996) points to the importance of increased uptake of NO_3-N along surface flow paths as growth of macrophytes and microflora increases. Indeed, Cooper and Cooke (1984) also showed that NO_3-N retention in the riparian zone was influenced by both vegetative uptake (75%) and denitrification (25%). In contrast to FD36, while biogeochemical mechanisms undoubtedly affect seasonal NO_3-N retention in RS, faster flows and steeper seep flow paths may not allow sufficient time for substantial NO_3-N removal to occur.

Overall, NO_3-N concentrations declined by 16% and 1% from seep top to bottom over the study period in FD36 and RS, respectively, which suggested that seeps can function as NO_3-N

sinks at the catchment-scale. Nitrate-N retention along seep surface flow paths in FD36 and RS (0.8 and 0.2 mg L^{-1}, respectively) was similar in magnitude to other studies examining seep NO_3-N retention even though NO_3-N concentrations were much greater. This suggests that characteristics of seeps, such as groundwater upwelling and surface flow paths, may restrict or limit the ability of seeps to remove NO_3-N. As a result, NO_3-N removal potential in seeps is substantially less than NO_3-N removal potential in shallow groundwater flow paths reported in the literature. For example, Peterjohn and Correll (1984) found that 90% to 98% of NO_3-N was removed along groundwater flow paths in a deciduous riparian forest. In addition, NO_3-N concentrations in groundwater were decreased by 90% or more when flow paths were sufficiently long (6 – 176 m) and the riparian aquifer had anaerobic zones and adequate carbon supplies (*Vidon and Hill, 2006*). However, since little (if any) NO_3-N removal occurs along groundwater flow paths through the shallow fractured aquifer system in small headwater catchments like FD36 and RS (*Pionke and Urban, 1985; Gburek and Folmar, 1999; Lindsey et al., 2003*), the riparian zone is the main area where NO_3-N processing can occur before NO_3-N is lost to stream water. Since stream baseflow in headwater catchments is often supplied by seeps, NO_3-N processing along seep surface flow pathways can therefore have a significant effect on stream NO_3-N concentrations (*Williams, Chapter 4*).

Seep Controls on Catchment-scale NO_3-N

Nitrate-N concentrations have been shown to increase downstream in FD36 and RS as a result of seep inputs to the stream (*Williams, Chapter 4*). In a previous study, Williams (Chapter 4) found that stream segments (10 m) with seeps increased in NO_3-N concentration by 0.25 mg L^{-1} during baseflow compared to a 0.02 mg L^{-1} decrease in stream water NO_3-N concentration when seeps were not present. In the current study, we found that mean monthly seep bottom NO_3-N

concentrations were significantly correlated with mean monthly stream NO_3-N concentrations at the catchment outlet of both FD36 and RS, which further suggests that headwater stream NO_3-N concentrations are strongly affected by NO_3-N delivery from seep inputs.

Even though seeps comprise a small fraction of the land area in a catchment, seeps transport agriculturally-influenced water to the stream more rapidly than slower groundwater flow paths (*Srinivasan et al., 2002; Morley et al., 2011*). Nitrate-N concentrations at the catchment outlet in FD36 tended to be less than NO_3-N concentrations in seep water indicating that other flow paths (e.g., shallow groundwater) and processes (e.g., in-channel transformations and hyporheic exchange) may also influence stream NO_3-N concentrations, but to a much lesser extent than seeps (*Scanlon et al., 2010*). In contrast, NO_3-N concentrations at the catchment outlet in RS tended to be greater than NO_3-N concentrations in seep water. Previous research in RS has shown that NO_3-N concentration in groundwater within RS is the highest of all sub-catchments that comprise WE-38 (*Gburek and Folmar, 1999*), indicating that groundwater contributions directly into the stream channel may also influence stream NO_3-N concentration. The effect of seeps on stream water quality observed in this study has also been shown to occur in other catchments. O'Driscoll and DeWalle (2010) found that seeps were important for determining NO_3-N fluxes at the catchment outlet of a forested catchment in central Pennsylvania with low NO_3-N concentrations (< 1 mg L^{-1}). Therefore, regardless of the magnitude of seep NO_3-N concentration, seeps can be one of the primary factors controlling stream water quality in headwater catchments.

Since surface seep flow paths are a significant source of NO_3-N to streams, they also have the potential to be areas on the landscape where implementation of best management practices (BMPs) may lead to improvements in stream water quality. In FD36 and RS, both N management across the catchment and NO_3-N retention within seeps were shown to influence seep delivery to streams. Although the design and implementation of BMPs that increase

residence times within seeps in order to promote NO_3-N removal is feasible, changes to N management throughout the catchment, which is the ultimate source of NO_3-N to seeps and streams, may be a better approach. There is currently a suite of BMPs available, such as winter cover crops, that promote increased crop uptake and decrease the potential for NO_3-N leaching (*e.g., Kou et al., 2001*). While N management practices within agricultural catchments need to be assessed on a field by field basis, decreasing NO_3-N loss to groundwater through implementation of BMPs can decrease the amount of NO_3-N transported in seep surface flow paths and improve stream water quality in agricultural headwater catchments.

Conclusions

The objective of this study was to quantify the effects of N management throughout two agricultural headwater catchments and NO_3-N retention within seep surface flow paths on seep water NO_3-N concentrations. In addition, we sought to examine the effect of seeps on stream water quality at the catchment outlet. Using data from annual farmer surveys in FD36 and RS, we found that N application rates along groundwater flow paths to seeps were highly correlated with seep NO_3-N concentrations. As the mean annual N application rate along a groundwater flow path increased, seep NO_3-N concentration also increased. Once groundwater discharged from seeps to surface flow, NO_3-N retention along individual seep surface flow paths varied widely over the study period; however, at the catchment-scale, seeps generally functioned as NO_3-N sinks. We found that NO_3-N concentrations decreased by a mean of 16% and 1% from seep top to seep bottom in FD36 and RS, respectively. Downseep declines in NO_3-N concentration were not due to dilution, but instead appeared to result from retention or transformation within seeps. Results suggest that during periods of high discharge, seep water will be transported rapidly across the riparian zone surface, which will result in channelized flow, short water residence

times, and limited potential for NO_3-N retention. In contrast, when seep discharge is low and air temperatures are warm (i.e., summer), increased vertical exchange among seep water, soil water, and groundwater increase water residence times and the potential for vegetative uptake and denitrification to occur.

Results suggested that seeps in FD36 and RS played a key role in determining N fluxes at the catchment outlet. We found that surface seeps in FD36 and RS were a significant source of NO_3-N to streams and that both N application rates along groundwater flow paths to seeps and NO_3-N retention within seeps ultimately influenced stream water NO_3-N concentrations at the catchment outlet. Therefore, seeps have the potential to be areas on the landscape where implementation of BMPs may lead to improvements in stream water quality. Although the design and implementation of BMPs that increase residence times within seeps in order to promote NO_3-N removal is feasible, changes to N management throughout the catchment, which is the ultimate source of NO_3-N to seeps and streams, may be a better approach. While N management practices in agricultural catchments need to be assessed at the field-scale, decreasing NO_3-N loss to groundwater through implementation of BMPs can decrease the amount of NO_3-N transported in seep surface flow paths and improve stream water quality in agricultural headwater catchments.

References

Angier, J.T., G.W. McCarty, and K.L. Prestegaard. 2005. Hydrology of a first-order riparian zone and stream, mid-Atlantic coastal plain, Maryland. *J. Hydrol.* 309:149-166.

Angier, J.T., G.W. McCarty, C.P. Rice, and K. Bialek. 2002. Influence of a riparian wetland on nitrate and herbicides exported from a field applied with agrochemicals. *Journal of Agriculture and Food Chemistry*. 50:4424-4429.

Ator, S.W., and M.J. Ferrari. 1997. Nitrate and selected pesticides in ground water of the mid-Atlantic region. U.S. Geological Survey, Water-Resources Investigation Report 97-4139.

Blackwell, M.S.A., D.V. Hogan, and E. Maltby. 1999. The use of conveniently and alternatively located buffer zones for the removal of nitrate from diffuse agricultural run-off. *Water Sci. Technol.* 39:157-164.

Boyer, E.W., C.L. Goodale, N.A. Jaworski, and R.W. Howarth. 2002. Anthropogenic nitrogen sources and relationships to riverine nitrogen export in the northeastern USA. *Biogeochemistry* 57:137-169.

Brüsch, W., and B. Nilsson. 1993. Nitrate transformation and water movement in a wetland area. *Hydrobiologia* 251: 103-111.

Bryant, R.B., T.L. Veith, G.W. Feyereisen, A.R. Buda, C.D. Church, G.J. Folmar, J.P. Schmidt, C.J. Dell, and P.J.A. Kleinman. 2011. U.S. Department of Agriculture Agricultural Research Service Mahantango creek watershed, Pennsylvania, United States: phsiography and history. *Water Resour. Res.* 47: DOI: 10.1029/2010WR010056.

Buda, A.R., P.J.A. Kleinman, M.S. Srinivasan, R.B. Bryant, and G.W. Feyereisen. 2009. Factors influencing surface runoff generation from two agricultural hillslopes in central Pennsylvania. *Hydrol. Process.* 23:1295-1312.

Buda, A.R., T.L. Veith, G.J. Folmar, G.W. Feyereisen, R.B. Bryant, C.D. Church, J.P. Schmidt, C.J. Dell, and P.J.A. Kleinman. 2011. U.S. Department of Agriculture Agricultural Research Service Manhantango creek watershed, Pennsylvania, United States: long-term precipitation database. *Water Resour. Res.* 47: DOI: 10.1029/2010WR010058.

Burns, D.A., P.S. Murdoch, G.B. Lawrence, and R.L. Michel. 1998. Effect of ground water springs on NO3- concentration during summer in Catskill Mountain streams. *Water Resour. Res.* 34:1987-1996.

Carey, B.M. 2002. Effects of land application of manure on ground water at two dairies over the Sumas-Blaine surficial aquifer. Washington Department of Ecology, Publication No. 02-03-007.

Chapman, P.J., B. Reynolds, and H.S. Wheater. 1996. Experimental investigation of potassium and nitrate dynamics in a headwater stream in mid-Wales. *Chem. Ecol.* 13:1-19.

Cooper, A.B., and J.G. Cooke. 1984. Nitrate loss and transformation in 2 vegetated headwater streams. *N. Z. J. Mar. Freshwater Res.* 18:441-450.

Freer, J., J. McDonnell, K.J. Beven, D. Brammer, D. Burns, R.P. Hooper, and C. Kendal. 1997. Topographic controls on subsurface stormflow at the hillslope-scale for two hydrologically distinct small catchments. *Hydrol. Process*. 11:1147-1352.

Gburek, W.J., A.N. Sharpley, and H.B. Pionke. 1996. Identification of critical source areas for phosphorus export from agricultural catchments. *In: Advances in hillslope processes*. M.G. Anderson and S.M. Brooks (Editors) Vol. 1. John Wiley and Sons, New York, NY, pp. 263-282.

Gburek, W.J., and G.J. Folmar. 1999. Patterns of contaminant transport in a layered fractured aquifer. *J. Contam. Hydrol.* 37:87-109.

Gburek, W.J., B.A. Needelman, M.S. Srinivasan. 2006. Fragipan controls on runoff generation: hydropedological implications at landscape and watershed scales. *Geoderma* 131:330-344.

Gold, A.J., P.M. Groffman, K. Addy, D.Q. Kellogg, M. Stolt, and A.E. Rosenblatt. 2001. Landscape attributes as controls on groundwater nitrate removal capacity of riparian zones. *J. Am. Water Res. Assoc*. 37:1457-1464.

Hallberg, G.R., and D.R. Keeney. 1993. Nitrate. *In: Regional ground-water quality.* W.M. Alley (Editor). U.S. Geological Survey, Van Nostrand Reinhold, New York, NY, pp 297-321.

Harter, T., H. Davis, M. Mathews, and R. Meyer. 2002. Shallow groundwater quality on dairy farms with irrigated forage crops. *J. Contamin. Hydrol.* 55:287-315.

Hii, B., H. Liebscher, M. Mazalek, and T. Tuominen. 1999. Ground water quality and flow rates in the Abbotsford aquifer, British Columbia. Environmental Canada, Vancouver, B.C.

Hill, A.R. 1990. Groundwater flow paths in relation to nitrogen chemistry in the near-stream zone. *Hydrobiologia* 206:39-52.

Howarth, R.W., G. Billen, D. Swaney, A. Townsend, N. Jaworski, K. Lajtha, J.A. Downing, R. Elmgren, N. Caraco, T. Jordan, F. Berendse, J. Freney, V. Kudeyarov, P. Murdoch, and Z. Zhao-Liang. 1996. Regional nitrogen budgets and riverine N and P fluxes for the drainages to the North Atlantic Ocean: natural and human influences. *Biogeochemistry* 35:75-139.

Kou, S., B. Huang, and R. Bembenek. 2001. Effect of winter cover crops on soil nitrogen availability, corn yield, and nitrate leaching. *Sci. World J.* 2:22-29.

Lindsey, B.D., S.W. Phillips, C.A. Donnelly, G.K. Speiran, L.N. Plummer, J.K. Bohlke, M.J. Focazio, W.C. Burton, and E. Busenberg. 2003. Residence times and nitrate transport in groundwater discharging to streams in the Chesapeake Bay watershed. U.S. Geological Survey Water Resources Investigations Report 03-4035.

McClain, M.E., E.W. Boyer. C.L. Dent, S.E. Gergel, N.B. Grimm, P.M. Groffman, S.C. Hart, J.W. Harvey, C.A. Johnson, E. Mayorga, W.H. McDowell, and G. Pinay. 2003. Biogeochemical hotspots and hot moments at the interface of terrestrial and aquatic ecosystems. *Ecosystems* 6:301-312.

McGuire, K.J., D.R. DeWalle, and W.J. Gburek. 2002. Evaluation of mean residence time in subsurface waters using oxygen-18 fluctuations during drought conditions in the mid-Appalachians. *J. Hydrol.* 261:132-149.

Morley, T.R., A.S. Reeve, and A.J.K Calhoun. 2011. The role of headwater wetlands in altering streamflow and chemistry in a Maine, USA catchment. *J. Am. Water. Resour. Assoc.* 47:337-349.

Needlelman, B.A. 2002. Surface runoff hydrology and phosphorus transport along two agricultural hillslopes with contrasting soils. Ph.D. Thesis. The Pennsylvania State University, University Park, PA.

O'Driscoll, M.A., and D.R. DeWalle. 2010. Seeps regulate stream nitrate concentration in forested Appalachian catchments. *J. Environ. Qual.* 39:420-431.

Patton, C.J., and J.R. Kryskalla. 2003. Methods of analysis by the U.S. Geological Survey National Water Quality Laboratory: evaluation of alkaline persulfate digestion as an alternative to Kjeldahl digestion for determination of total dissolved nitrogen and phosphorus in water. U.S. Geological Survey water resources investigations report 03-4174, 33 p.

Paul, J.W., and B.J. Zebarth. 1997. Denitrification and nitrate leaching during the fall and winter following dairy cattle slurry application. *Canadian J. Soil Sci.* 77:231-240.

Peterjohn, W.T., and D.L. Correll. 1984. Nutrient dynamics in an agricultural watershed: observations on the role of a riparian forest. *Ecology* 65:1466-1475.

Pionke, H.B., and J.B. Urban. 1985. Effect of agriculture land use on ground-water quality in a small Pennsylvania watershed. *Groundwater*. 23:68-80.

Pionke, H.B., J.R. Hoover, R.R. Schnabel, W.J. Gburek, J.B. Urban, and A.S. Rogowski. 1988. Chemical-hydrologic interactions in the near-stream zone. *Water Resour. Res.* 24:1101-1110.

Pionke, H.B., W.J. Gburek, and A.N. Sharpley. 2000. Critical source area controls on water quality in an agricultural watershed located in the Chesapeake basin. *Ecol. Eng.* 14:325-335.

Pionke, H.B., W.J. Gburek, and R.R. Schnabel. 1996. Flow and nutrient transport patterns for an agricultural hill-land watershed. *Water Resour. Res.* 32:1795-1804.

R Development Core Team. 2011. R: a language and environment for statistical computing. R Foundation for Statistical Computing, Vienna, Austria.

Rutherford, J.C., and M.L. Nguyen. 2004. Nitrate removal in riparian wetlands: interactions between surface flow and soils. *J. Environ. Qual.* 33:1133-1143.

Scanlon, T.M., S.M. Ingram, and A.L. Riscassi. 2010. Terrestrial and in-stream influences on the spatial variability of nitrate in a forested headwater catchment. *J. Geophysic. Res.* 115: doi: 10.1029/2009JG001091.

Shabaga, J.A., and A.R. Hill. 2010. Groundwater-fed surface flow path hydrodynamics and nitrate removal in three riparian zones in southern Ontario, Canada. *J. Hydrol.* 388:52-64.

Sharpley, A.N., J.J. Meisinger, A. Breeuswma, J.T. Sims, T.C. Daniel, and J.S. Schepers. 1998. Impacts of animal manure management on groundwater and surface water quality. *In:*

Animal manure management: effective use of manure as a soil resource. J.L. Hatfield and B.A. Stewart (Editors) CRC Press LLC, Boca Raton, FL, pp. 173-230.

Srinivasan, M.S., W.J. Gburek, and J.M. Hamlett. 2002. Dynamics of stormflow generation - a hillslope-scale field study in east-central Pennsylvania, USA. *Hydrol. Process.* 16:649-665.

Steinheimer, T.R., K.D. Scoggin, and L.A. Kramer. 1998. Agricultural chemical movement through a field-size watershed in Iowa: surface hydrology and nitrate losses in discharge. *Environ. Sci. Technol.* 32:1048-1052.

Vidon, P.G.F., and A.R. Hill. 2006. A landscape-based approach to estimate riparian hydrological and nitrate removal functions. *J. Am. Water Resour. Assoc.* 42:1099-1112.

Walter, M.T., M.F. Walter, E.S. Brooks, T.S. Steenhuis, J. Boll, and K. Weiler. 2000. Hydrologically sensitive areas: variable source area hydrology implications for water quality assessment. *J. Soil Water Conserv.* 3:277-284.

Warwick, J., and A.R. Hill. 1988. Nitrate depletion in the riparian zone of a small woodland stream. *Hydrobiologia* 157:231-240.

West, A.J., S.E. Findlay, D.A. Burns, K.C. Weathers, and C.M. Lovett. 2001. Catchment-scale variation in the nitrate concentration of groundwater seeps in the Catskill Mountains, New York, USA. *Water Air Soil Poll.* 132:389-400.

Zhu, Q., J.P. Schmidt, and R.B. Bryant. 2011. Hot moments and hot spots of nutrient losses from a mixed land use watershed. *J. Hydrol.* 414:393-404.

CHAPTER 6

Nitrogen Transport in Riparian Zone Seeps: Conclusions and Future Research

Excess nitrogen (N) in terrestrial and aquatic ecosystems has resulted in numerous water quality problems throughout the U.S. and across the world, which emphasizes the need to develop effective management plans to deal with N pollution. Previous research has identified emergent groundwater-fed seeps as a potentially significant source of water and N, especially nitrate-N (NO_3-N), to streams in headwater catchments, yet few studies have evaluated NO_3-N transport in seeps and their influence on stream water quality. The four studies in this dissertation evaluated seep zone formation, hydrology, and biogeochemistry in order to gain an improved understanding of NO_3-N transport in seeps and their effects on stream water quality in two small headwater agricultural catchments (FD36 and RS) located in central Pennsylvania. The major findings and conclusions from the four studies are summarized in this final chapter and future research needs are addressed. In addition, the results from the four studies are used to evaluate the potential effectiveness of several management practices aimed at improving water quality in agricultural headwater catchments with seeps.

Summary of Major Findings and Conclusions

The objective of the first study, chapter two, was to compare hydrological processes and NO_3-N transport in seep areas to adjacent areas of the riparian zone without seeps (i.e., non-seep areas). Using an extensive network of nested piezometers at three paired study sites in FD36, we

found that seep areas had a greater NO_3-N transport potential than non-seep areas. Spatial patterns in water table depth indicated that groundwater flow paths in non-seep areas were dominated by uniform, lateral flow through the subsurface. Lateral subsurface flow is characterized by longer residence times in which groundwater can interact with riparian soils and vegetation, which promote NO_3-N removal and uptake. In contrast, water table depth in the seep areas was highly variable with some regions having positive vertical gradients (e.g. groundwater upwelling), which suggested that preferential flow was an important flow pathway for groundwater in seep areas. Preferential flow paths can limit NO_3-N removal because groundwater typically has a shorter residence time within the subsurface. A two-component mixing model also showed that the groundwater in seep and non-seep areas were from different sources. Water in seep areas was primarily (53% – 75%) from a shallow fractured aquifer (6-m deep monitoring wells), whereas, the water in non-seep areas was primarily (58% – 82%) from perched water on top of the fragipan (1-m deep monitoring well). The upwelling of groundwater from the shallow fractured aquifer in seep areas, which had high NO_3-N concentrations relative to water perched on top of the fragipan, resulted in seep areas with significantly greater NO_3-N concentrations compared to non-seep areas. Thus, seep areas were shown to be a potentially significant source of NO_3-N to the stream in FD36.

The results of chapter two provided compelling evidence for varying hydrology and NO_3-N transport potential between seep and non-seep areas of the riparian zone. Chapter three built upon these results by using electrical resistivity imaging (ERI) to visualize subsurface hydrologic processes in a seep and non-seep area over a series of precipitation events. Results showed that the seep area of the riparian zone in FD36 was much more complex in terms of hydrology and N transport compared to the non-seep area. In the seep area, preferential flow paths through the fragipan served as a location to discharge groundwater to the surface. Upwelling groundwater in these localized regions created an area of the riparian zone that was extremely hydrologically

dynamic. For example, in the seep area, only a small amount of precipitation (41 mm) was required to activate groundwater flow. While the size of the saturated area and the amount of water table rise likely depend on the storm event duration and intensity, the seep area will remain active until another storm event or series of storm events continues to expand the seep area or the groundwater drains to the stream during dry conditions. We found that as the seep area became active, the NO_3-N transport potential was high due to groundwater and NO_3-N bypassing the remedial benefits of the riparian zone via preferential flow paths. At saturation, however, groundwater flow in the seep area was found to be a mixture of sources (groundwater from the shallow fractured aquifer and water perched on top of the fragipan), which resulted in the dilution of NO_3-N concentration. In contrast to the seep area, results from the non-seep area showed that it remained hydrologically inactive for substantial periods of time and required a large amount of precipitation (141 mm) to activate. The potential for the non-seep area to deliver NO_3-N to the stream was low since it was disconnected from the high NO_3-N source (i.e., shallow fractured aquifer) and groundwater likely had increased interaction with riparian soils as it moved laterally toward the stream.

The purpose of the third study, chapter four, was to determine if the potential for NO_3-N delivery from seeps that was observed in the previous two studies, chapters two and three, was transferred into measurable effects on stream water quality. We found that while the magnitude of seep water NO_3-N concentration varied between FD36 and RS and among individual seeps in both catchments, seep discharge resulted in an increase in stream water NO_3-N concentration. Results showed that stream water NO_3-N concentration increased by 0.25 mg L^{-1} over a 10 m reach when seeps were present compared to a decrease of 0.02 mg L^{-1} when no seeps were present. The influence of seeps on stream NO_3-N concentration was further reflected in longitudinal patterns of stream water NO_3-N in FD36 and RS. We found that as the number of seeps increased, the amount of longitudinal variability (i.e., patchiness) in stream water NO_3-N

concentration increased. Results also showed that the influence of seeps on stream water NO_3-N concentration and variability decreased immediately following precipitation events compared to baseflow. This was likely due to increased stream discharge and rainfall directly into the stream channel, which decreased the relative contributions of seep water to streamflow and homogenized NO_3-N concentrations over the entire reach. As stream discharge drained back to baseflow, however, the influence of seeps on stream water quality likely reached a maximum, as the number of seeps discharging groundwater into the stream was at its peak. Thus, the results of this study showed that in FD36 and RS, seeps were a significant source of NO_3-N to the stream and played a substantial role in determining N fluxes from these catchments during both baseflow and stormflow conditions.

Chapter five, the final study, was completed in order to determine what factors influenced seep NO_3-N delivery to streams and how seeps contributed to NO_3-N fluxes at the catchment outlet. Results showed that N application rates along groundwater flow paths to seeps were significantly correlated to seep top (i.e., emergence point) NO_3-N concentration. We found that as the mean N application along the groundwater flow path to a seep increased, seep top NO_3-N concentration increased. We also found that N retention within seeps influenced seep NO_3-N delivery to streams. Nitrate-N concentration in seep surface flow paths decreased downseep (i.e., seep top to seep bottom) by 0.8 (16%) and 0.2 (1%) mg L^{-1} in FD36 and RS, respectively; although NO_3-N retention varied seasonally (-3% to 41%) in FD36. The seasonal variability in seep NO_3-N retention in FD36 was found to be related to both stream discharge and air temperature, suggesting that both hydrological and biogeochemical processes affected NO_3-N retention within seeps. At the catchment-scale, mean seep bottom NO_3-N concentration was significantly correlated to stream NO_3-N concentration at the stream outlet in both FD36 and RS. Seeps accounted for 80% and 79% of the variability in stream NO_3-N concentration in FD36 and RS, respectively. The results of this study suggested that while some NO_3-N retention occurred

within seep surface flow paths, the primary factor controlling NO_3-N delivery from seeps to streams and ultimately NO_3-N concentrations at the catchment outlet was N management throughout the catchment. Thus, in agricultural catchments with seeps, adjusting management practices in order to decrease the probability of NO_3-N leaching has the potential to decrease NO_3-N concentrations in seeps and improve stream water quality.

Potential Effectiveness of BMPs in Agricultural Catchments with Seeps

Manure and Fertilizer N Management

N Application Rate

The results from Williams (Chapter 5) suggest that NO_3-N concentrations in seep water were significantly correlated to the N application rate along the groundwater flow path draining to the seep. Therefore, one way to decrease NO_3-N concentrations in seep water is to decrease the amount of N applied across the landscape. Indeed, many studies have reported that elevated N application rates increase the potential for NO_3-N leaching (*Zvomuya et al., 2003; Guo et al., 2006*). The potential effectiveness of decreasing N application rates was also demonstrated in chapter 5 where areas of FD36 and RS receiving little or no N application had seep NO_3-N concentrations that were very low. Similarly, in a study by O'Driscoll and DeWalle (2010), a forested catchment with no N inputs had seeps with NO_3-N concentrations that were often less than 1 mg L^{-1}. Nitrogen inputs are essential for crop growth in agricultural catchments, but reducing the N application rate may produce a significant change in stream water quality. For example, the mean N application rate in FD36 and RS was 133 and 200 kg ha^{-1}, respectively, and mean sep NO_3-N concentrations were 4.7 and 13.4 mg L^{-1}. Thus, a 35% reduction in N application rate in RS (200 to 133 kg ha^{-1}) could result in a potential decrease of 65% in the mean seep NO_3-N concentration. Reductions in N application rate have the potential to be one of the

most effective BMPs in agricultural catchments because it is targeting the source of N. While farmers may be hesitant to reduce N application rates for fear that crop yield will decline, altering the timing and method of N application may also decrease the potential for NO_3-N leaching (*Power and Schepers, 1989*).

Timing of N Application

In order to decrease the risk of NO_3-N leaching, the timing of N application should coincide with crop N demand. Therefore, spring application of N is typically recommended because the N is available when the crops need it for growth. In FD36 and RS (and in many other catchments), manure and fertilizer is applied during both the spring and fall. Most of the N in FD36 and RS is lost during the non-growing season (*Zhu et al., 2011; Williams, Chapters 4 and 5*), which indicates that N application in the fall may be a significant source of N to seeps. Several studies have shown that fall application can lead to excess NO_3-N leaching (*Cookson et al., 2002; Gupta et al., 2004*). In a soil column study, Williams et al. (2012) found that the timing of manure application in the fall determined the amount of NO_3-N lost in leachate. The authors showed that when manure was applied at soil temperatures greater than 10°C in the early-fall, the potential for NO_3-N leaching is significantly increased compared to when the soil temperature is less than 10°C. Thus, altering the timing of manure application in the fall could decrease the potential for NO_3-N leaching and ultimately seep NO_3-N concentrations.

In the spring, splitting N applications and applying N in phase with crop demand may also minimize the risk for NO_3-N leaching (*Power et al., 1998*). Split applications with pre-sidedress nitrogen tests (PSNT) have been shown to increase N use efficiency (*Musser et al., 1995*). While it is not practical for farmers to split manure applications, lower pre-planting manure application rates could be used with supplemental sidedress mineral fertilizer as

determined by PSNT. Thus, this practice would provide as much N to the crop with less total N applied.

Method of N Application

The potential for NO_3-N leaching and ultimately NO_3-N delivery to seeps may also be influenced by the method of N application (i.e., surface vs. subsurface). Incorporation technologies, such as shallow disk injection, often reduce volatile N losses, but leave large pools of ammonium-N (NH_4-N) in the soil, which can nitrify and potentially leach if not taken up by the crop (*Dell et al., 2012*). However, there have only been a few studies that have compared NO_3-N leaching losses following surface and subsurface N application. Misselbrook et al. (1996) did not find any significant differences between surface application and shallow knife injection of cattle slurry. Similarly, no differences in NO_3-N leaching were found after shallow injection and surface band application of liquid swine manure (*Weslien et al., 1998*). However, while Powell et al. (2011) found that NO_3-N leaching losses were similar with shallow shank injection and surface broadcasting, manure incorporation with an aerator increased leaching relative to both. The results from these studies suggest that the method of N application may be less important in terms of the potential for NO_3-N leaching compared to the application rate and timing of application.

Soil Management

Tillage

In FD36 and RS, the majority of farmers practice no-till farming. Several studies have shown that differences in tillage (no-till vs. conventional tillage) may play a role in the potential for NO_3-N leaching. Conventional tillage has been shown to lead to elevated oxidation of soil

organic matter and mineralization of soil N compared to no-till systems (*Randall et al., 1997*). However, conventional tillage could lead to less NO_3-N leaching compared to no-till (*Kanwar et al., 1993; Weed et al., 1996*). In no-till systems, large soil macropores can form and increase the risk NO_3-N leaching (*Di and Cameron, 2002*). In contrast, Rasmussen (1999) found that NO_3-N leaching increased with more intensive cultivation (i.e., conventional tillage). While, the results from these studies are inconsistent, altering the type of tillage could influence the potential for NO_3-N leaching depending on the soil type and climate.

Crop Management

Cover Crops

Growing cover crops, such as rye or oats, is another BMP that has been successful in reducing the risk of NO_3-N leaching. As mentioned previously, most of the N loss in FD36 and RS occurs during the non-growing season. However, most of the fields are left fallow during this time. Cover crops planted immediately after harvest or double cropped can take up excess N remaining in the soil before the winter when the majority of NO_3-N loss occurs. Studies have shown that planting cover crops can reduce NO_3-N leaching over the winter (*Shrestha and Ladha, 1998*) and even reduce the potential for NO_3-N leaching from the next crop (*Delgado et al., 2001*). For example, planting ryegrass in November reduced NO_3-N leaching by 1.4 to 4.3 g N m^{-2} yr^{-1}, but did not affect grain yield the following year (*Thomsen, 2005*). Similarly, wheat, rye, and rapeseed planted after sweet corn and incorporated in the spring had a positive effect on the subsequent potato crop and reduced NO_3-N leaching over the winter (*Weinert et al., 2002*). Thus, cover crops could be incorporated into the crop rotations in FD36 and RS (and other catchments) in order to reduce NO_3-N leaching and potentially decrease seep NO_3-N concentrations.

Diversified Crop Rotations

In addition to cover crops, maintaining a diversified crop rotation can help retain N in the soil and decrease the risk of NO_3-N leaching. Several studies have shown that differences in residue, rooting depths, and soil-plant-water dynamics among various plant species can influence NO_3-N leaching potential (*Randall et al., 1997; Malpassi et al., 2000*). For example, including alfalfa in a rotation has been shown to be effective in reducing NO_3-N leaching because of its deep rooting depth and high water usage (*Owens, 1987*). Diversified crop rotations also have been shown to reduce N application rates over the course of a rotation compared to continuous corn (*Ju et al., 2007*). Indeed, including N-fixing legumes in a crop rotation can provide a gradual release of N into the soil that is often better synchronized with subsequent plant needs compared to single applications of fertilizer or manure.

Edge of Stream Management

Riparian Zones

The establishment and conservation of riparian zones can provide many environmental benefits in agricultural headwater catchments, such as increased wildlife habitat and decreased stream water temperatures (*e.g., Hill, 1996; Cirmo and McDonnell, 1997*). Research has also shown that riparian zones can decrease nutrient concentrations entering the stream by greater than 90% (*e.g., Peterjohn and Correll, 1984*). Results from this dissertation, however, suggest that in catchments with seeps, riparian zones may not be an effective management practice to decrease NO_3-N delivery to the stream. Water and NO_3-N in seep discharge often flow in surface pathways. Rapid transport of water and NO_3-N through the riparian zone was therefore commonly observed in FD36 and RS. The results from chapter five indicate that NO_3-N removal in seep surface flow paths through the riparian zone in FD36 and RS was minimal. Riparian

zones are also established or conserved over an entire stream reach, whereas seeps only represent small areas on the landscape. Thus, riparian zones do not specifically target areas on the landscape, like seeps, for nutrient removal.

In FD36 and RS, riparian zones were not effective at removing NO_3-N in seep surface flow paths; however, altering the riparian zone characteristics has the potential to increase their effectiveness. For example, in FD36 and RS, the riparian zone often did not extend to the seep top (i.e., groundwater emergence point). Portions of many seep surface flow paths as a result were actively farmed (e.g., received nutrient applications, planted with crops, etc). Increasing the width of the riparian zone to include the entire flow path has the potential to increase the NO_3-N removal potential.

Bioreactors

Bioreactors are designed to remove NO_3-N in water by increasing the amount of denitrification (*e.g., Janes et al., 2008*). Bioreactors have been successfully used in catchments with tile drainage, where wood-chips, peat, pine bark, and almond and walnut shells are used as a carbon source in a bioreactor that is installed at the outlet of the tile drain (*e.g., Blowes et al., 1994*). Water and NO_3-N from the tile drain is then routed through the bioreactor, which promotes NO_3-N removal, prior to the water entering the stream channel. Seeps in ways are similar to tile drains, in that they drain areas of a catchment to a single point on the landscape where water and NO_3-N are delivered directly to the stream channel. Thus, bioreactors have the potential to target seep areas on the landscape similar to tile drains. To our knowledge, however, the use of bioreactors to mitigate NO_3-N concentrations in seep discharge has not been done previously.

If the location of a seep upwelling location was known, like in FD36 and RS, a bioreactor could be installed at this location. The upwelling groundwater, which is high in NO_3-N concentration, would pass through the wood chips on its way to the surface and NO_3-N would be removed via denitrification. The downside of using a bioreactor is that they can be expensive to implement and require some maintenance in order to function properly. In addition, in catchments like FD36 and RS, it is highly unlikely that a bioreactor could be installed at all seep locations. However, the seeps with the highest NO_3-N concentrations could be targeted in order to have the largest impact on stream water quality.

Future Research

Results from this dissertation have shown that seeps are an important source of N, especially NO_3-N, to agricultural headwater streams. Seeps also play a large role in determining N fluxes at the catchment outlet. The complexity of seep formation, hydrology, and biogeochemistry described in FD36 and RS has lead to further questions on seeps and their influence stream water quality. In this section, the need for future research on seeps is discussed.

The top priority and most challenging need is the development of new methods to identify the locations of groundwater-fed seeps or zones of seepage. Currently the only accurate method for determining the location of a seep is to walk the entire length of a stream under wet conditions. Surface topography can also been used to identify possible locations of seeps (e.g., concave landscape positions), but seeps occurred at a variety of landscape positions in FD36 and RS. In order to asses the impact of seeps at larger scales, we need a better way of not only determining how many seeps are likely to be found within a catchment, but also the location of the seeps in relation to different land management practices. In addition to identifying where seeps occur, more research is needed on seep discharge. Several research questions include 1)

under what conditions (i.e., antecedent soil moisture, rainfall depths, seasons, etc.) are seeps contributing groundwater to streams?; 2) how long does seepage continue after a storm event?; and 3) how do changes in seep discharge influence N concentration? Results from this dissertation suggest that there is a time lag between a storm event and seep response; therefore, more detailed sampling over several storm events is needed in order to better understand seep formation and hydrology.

More research is also needed on N transport with seep surface flow paths. We found that NO_3-N is removed along seep surface flow paths, but did not isolate the specific mechanisms responsible for the removal. Both denitrification and vegetative uptake are likely removal mechanisms along seep surface flow paths. In order to design BMPs that enhance the NO_3-N removal potential in the riparian zone, we need to understand the N cycling and biogeochemistry along seep flow paths. Several studies have shown that residence time is an important factor in determining the amount of NO_3-N removal. Thus, more research is needed on residence times of water and NO_3-N along seep surface flow paths.

References

Blowes, D.W., W.D. Robertson, C.J. Ptacek, and C. Merkley. 1994. Removal of agricultural nitrate from tile drain effluent using in line bioreactors. *J. Contam. Hydrol.* 15:207-221.

Cirmo, C.P., and J.J. McDonnell. 1997. Linking the hydrologic and biogeochemical controls of nitrogen transport in near-stream zones of temperate-forested catchments: a review. *J. Hydrol.* 199:88-120.

Cookson, W.R., I.S. Cookson, and J.S. Rowarth. 2002. Winter soil temperature (2-15C) effects on nitrogen transformations in clover green manure amended or unamended soils: a laboratory and field study. *Soil Biol. Biochem.* 34:1401-1415.

Delagado, A. 2001. Potential use of innovative nutrient management alternatives to increase nutrient use efficiency, reduce losses, and protect soil and water quality. *J. Communication Soil Sci. Plant Analysis.* New York: Marcel Dekker Inc.

Dell, C.J., P.J.A. Kleinman, J.P. Schmidt, and D.B. Beegle. 2012. Low-disturbance manure incorporation effects on ammonia and nitrate loss. *J. Environ. Qual.* 41:928-937.

Di, H.J., and K.C. Cameron. 2002. Nitrate leaching in temperate agroecosystems: sources, factors, and mitigating strategies. *Nutrient Cycling in Agroecosystems* 46:237-256.

Guo, Y., H. Li, Y. Zhang, X. Zhang, and A. Lu. 2006. Effects of water table and fertilization management on nitrogen loading to groundwater. *Ag. Water Manag.* 82:86-98.

Gupta, S.C., E. Munyankusi, J.F. Moncrief, F. Zvomuya, and M. Hanewall. 2004. Tillage and manure application effects on mineral nitrogen leaching from seasonally frozen soils. *J. Environ. Qual.* 33:1238-1246.

Hill, A.R. 1996. Nitrate removal in stream riparian zones. *J. Environ. Qual.* 25: 743-755.

Janes, D.B., T.C. Kapar, T.B. Moorman, and T.B. Parkin. 2008. In situ bioreactors and deep drain-pipe installation to reduce nitrate loss in artificially drained fields. *J. Environ. Qual.* 37:429-436.

Ju, T., Q. Gao, P. Christie, and S. Zhang. 2007. Changes in soil environment from excessive application of fertilizers and manures to two contrasting intensive cropping systems on the North China Plain. *Environ. Pollut.* 146:534-542.

Kanwar, S., E. Stolenberg, R. Pfeiffer, L. Karlen, S. Colvin, and W. Simpkins. 1993. Transport of nitrate and pesticides to shallow groundwater systems as affected by tillage and crop rotation practices. pp. 270-273. *In* Proceedings of the Conference, Feb. 21-24, Minneapolis, MN, USA. ISBN 10 0935734341.

Malpassi, N., C. Kasper, B. Parkin, A. Cambardella, and A. Nubel. 2000. Oat and rye root decomposition effects on nitrogen mineralization. *Soil Sci. Soc. Am. J.* 64:208-215.

Misselbrook, T.H., J.A. Laws, and B.F. Pain. 1996. Surface application and shallow injection of cattle slurry on grassland: nitrogen losses, herbage yields and nitrogen recoveries. *Grass Forage Sci.* 51:51-57.

O'Driscoll, M.A., and D.R. DeWalle. 2010. Seeps regulate stream nitrate concentration in forested Appalachian catchments. *J. Environ. Qual.* 39:420-431.

Owens, B. 1987. Nitrate leaching losses from monolith lysimeters as influenced by nitrapyrin. *J. Environ. Qual.* 16:34-38.

Peterjohn, W.T., and D.L. Correll. 1984. Nutrient dynamics in an agricultural watershed: observations on the role of a riparian forest. *Ecology* 65:1466-1475.

Powell, J.M., W.E. Jokela, and T.H. Misselbrook. 2011. Dairy slurry application method impacts ammonia emission and nitrate leaching in no-till corn silage. *J. Environ. Qual.* 40:383-392.

Power, F., and S. Schepers. 1998. Nitrate contamination of groundwater in North America. *Ag. Ecosyst. Environ.* 26:165-187.

Randall, W., R. Huggins, P. Russell, J. Fuchs, W. Nelson, and L. Anderson. 1997. Nitate losses through subsurface tile drainage in conservation reserve program, alfalfa, and row crop systems. *J. Environ. Qual.* 26:1240-1247.

Rasmussen, J. 1999. Impact of ploughless soil tillage on yield and soil quality: a Scandinavian review. *Soil Till. Res*. 53:3-14.

Shrestha, K., and K. Ladha. 1998. Nitrate in groundwater and integration of nitrogen-catch crop in rice-sweet pepper cropping system. *Soil Sci. Soc. Am. J.* 62:1610-1619.

Thomsen, K. 2005. Nitrate leaching under spring barley is influenced by the presence of a ryegrass catch crop: results from a lysimeter experiment. *Ag. Ecosyst. Environ.* 111:21-29.

Weed, J. and S. Kanwar. 1996. Nitrate and water present in and flowing from root-zone soil. J. Environ. Qual. 25:709-719.

Weinert, L., L. Pan, R. Moneymaker, S. Santo, and G. Stevens. 2002. Nitrogen recycling of nonleguminous winter cover crops to reduce leaching in potato rotations. *Agronomy J.* 94:365-372.

Weslien, P.L., L. Klemedtsson, L. Svensson, B. Galle, A. Kasimir-Klemedtsson, and A. Gustafson. 1998. Nitrogen losses following application of pig slurry to arable land. *Soil Use Manage.* 14:200-208.

Williams, M.R., G.W. Feyereisen, D.B. Beegle, and R.D. Shannon. 2012. Soil temperature regulates nitrogen loss from lysimeters following fall and winter manure application. *T. ASABE* 55: 861-870.

Zhu, Q., J.P. Schmidt, and R.B. Bryant. 2011. Hot moments and hot spots of nutrient losses from a mixed land use watershed. *J. Hydrol.* 414:393-404.

Zvomuya, F., J. Rosen, R. Russell, and C. Gupta. 2003. Nitrate leaching and nitrogen recovery following application of polyolefin-coated urea to potato. *J. Environ. Qual.* 32:480-489.

APPENDIX A

Groundwater Table and Piezometer Data for Chapter Two

This appendix contains the water table and piezometer data from three seep and three adjacent non-seep areas of the riparian zone that are presented in chapter two. There are two sections in this appendix: 1) groundwater table depth measured in piezometers; and 2) piezometer ammonium-N (NH_4-N), nitrate-N (NO_3-N), and chloride (Cl^-) concentrations. Other data in chapter two, such as stream discharge as well as groundwater, seep water, and stream concentrations, are shown in Appendix D. The figures in each section of this appendix are formatted to display the data and are not meant to show the differences among sampling dates (i.e., the y-axis varies for each figure); thus, caution must be taken if comparing two sampling dates or differences between seep and non-seep areas.

Groundwater Table Depth

The x-axis is the piezometer identification number (1 to 40) and the y-axis is the depth of the groundwater table below (or above) the land surface (cm). The piezometers were installed at two depths (20 and 60 cm). The black circles represent the 60 cm piezometers and the white squares represent the 20 cm piezometers. The dashed line at 0 cm represents the relative location of the land surface. The dotted line shows the depth of the 20 cm piezometers.

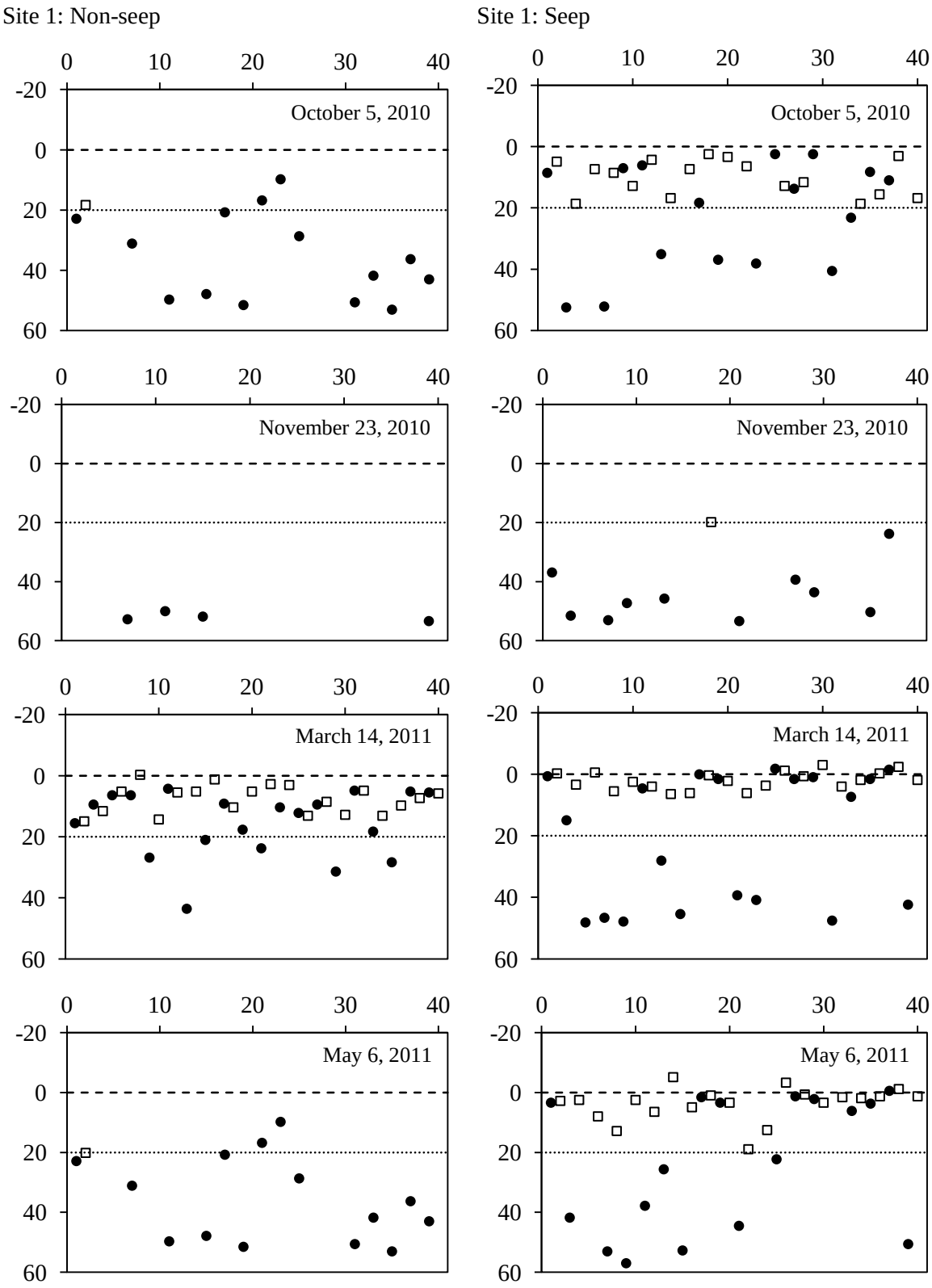
Site 1: Non-seep
Site 1: Seep
October 5, 2010
November 23, 2010
March 14, 2011
May 6, 2011
0
10
20
30
40
-20
0
20
40
60

Site 1: Non-seep (cont.)

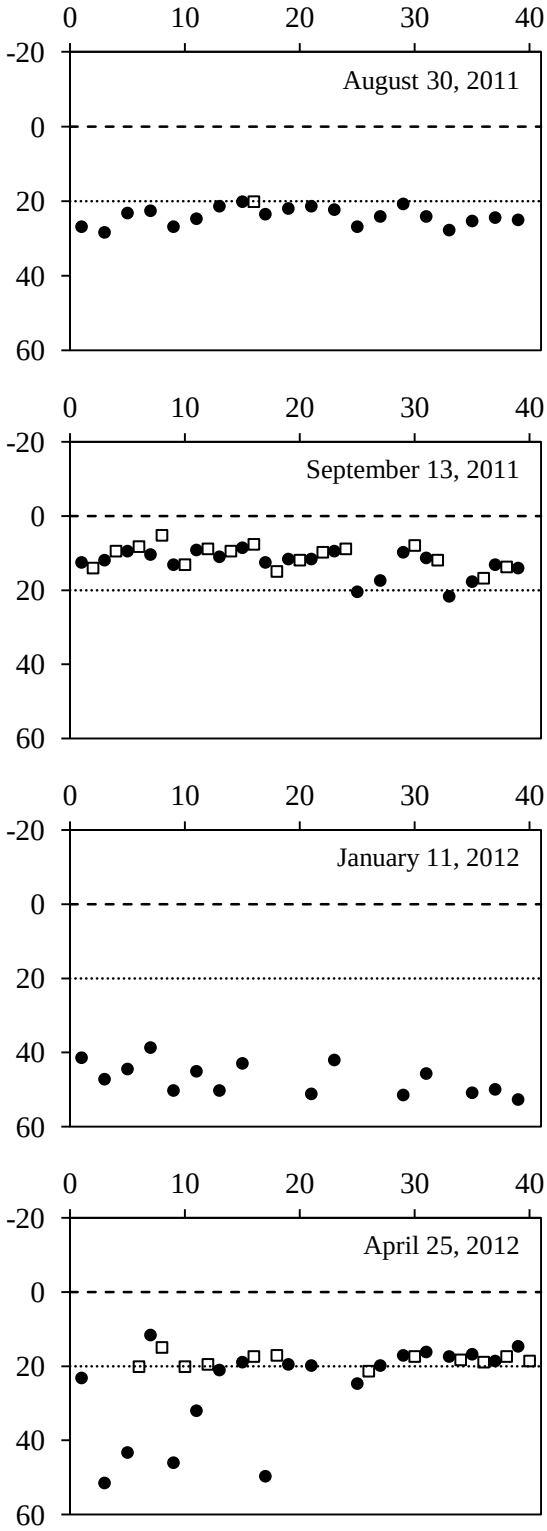

Site 1: Seep (cont.)

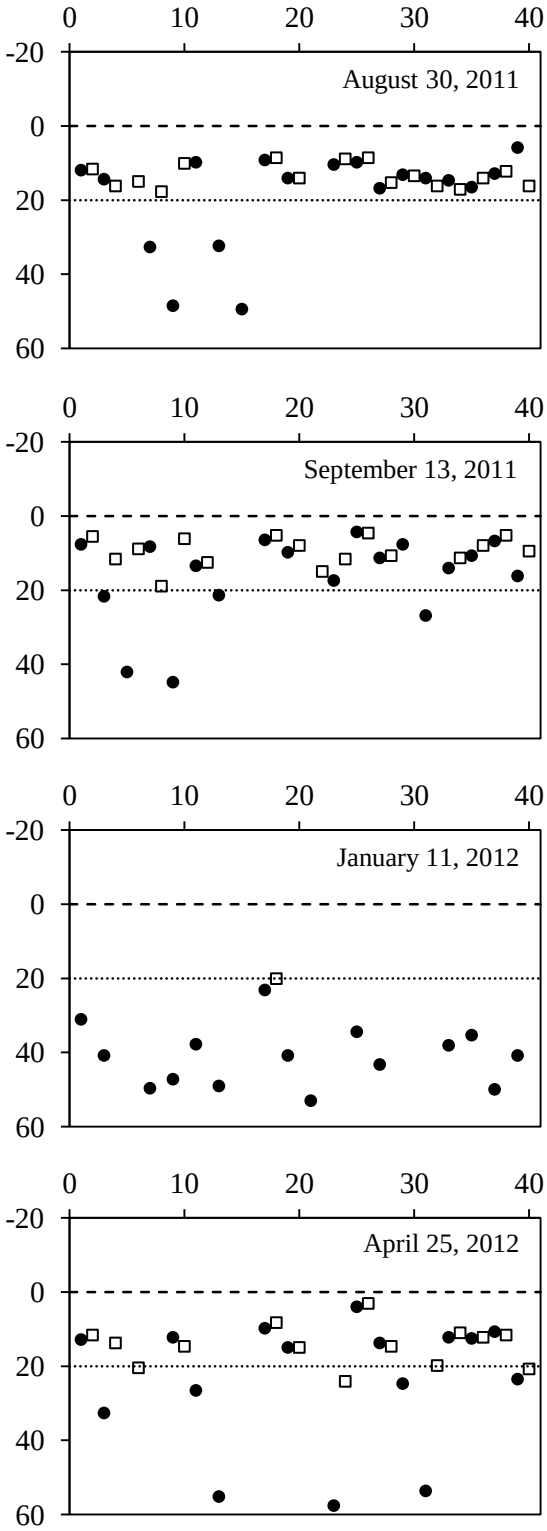

Site 1: Non-seep (cont.)

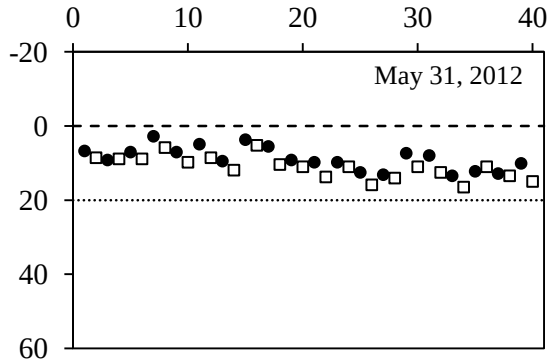

Site 1: Seep (cont.)

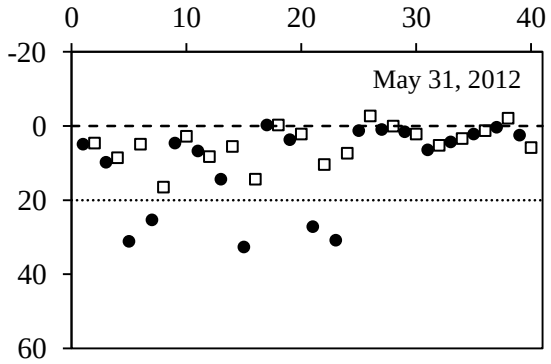

Site 2: Non-seep

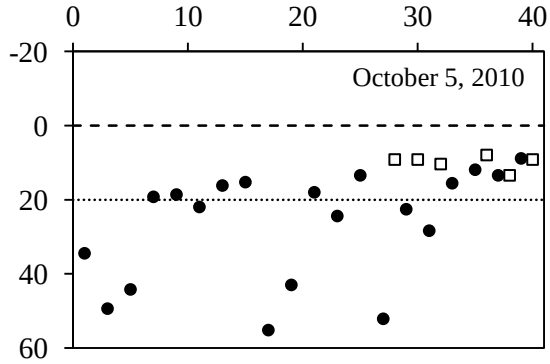

Site 2: Seep

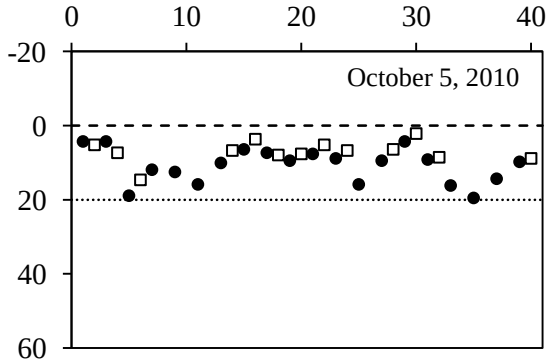

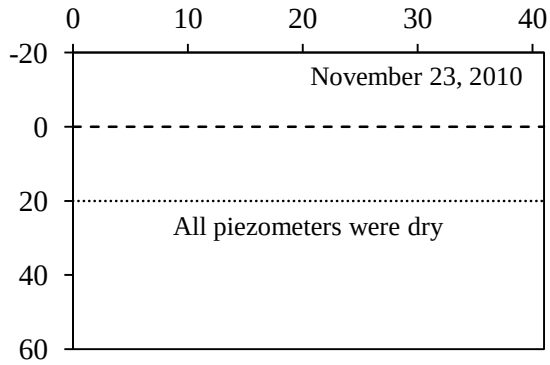

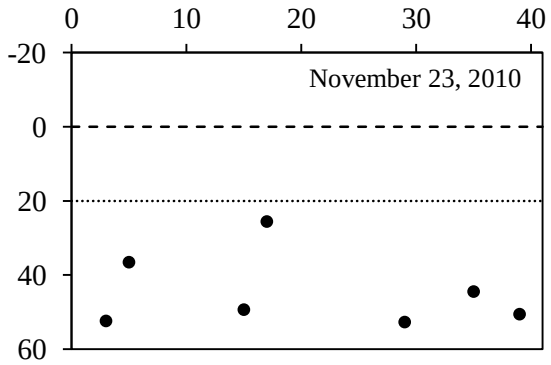

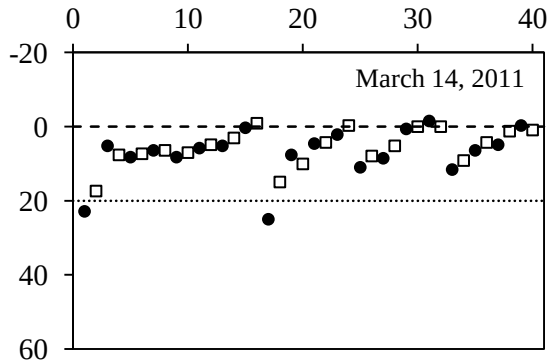

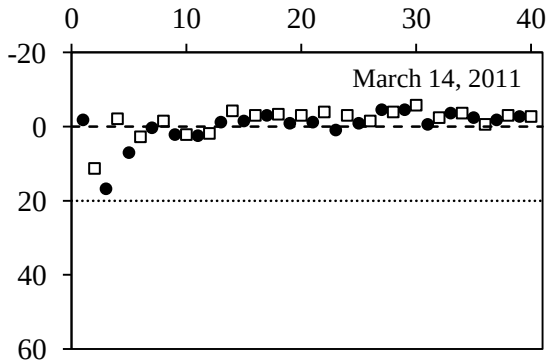

Site 2: Non-seep (cont.)

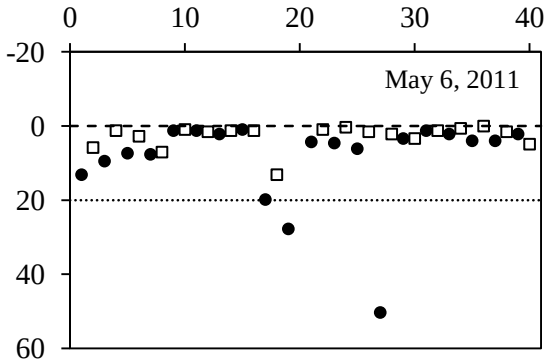

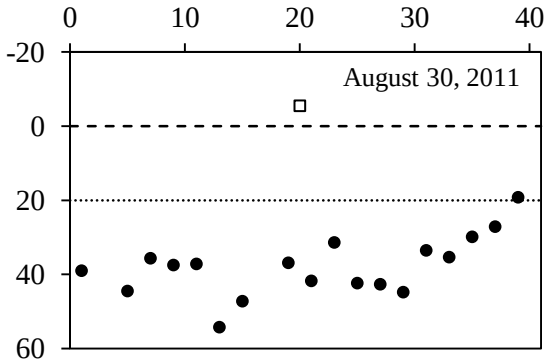

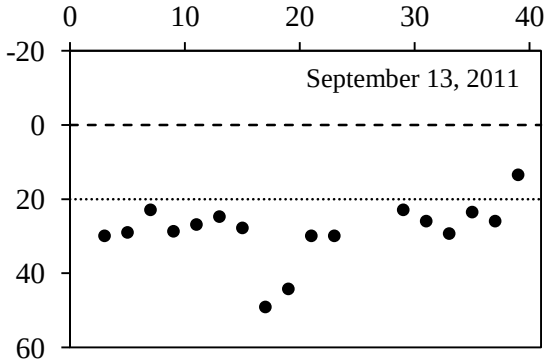

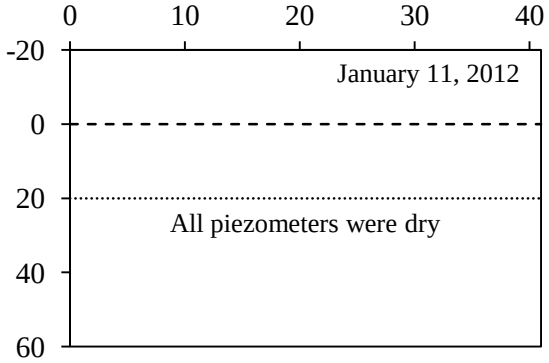

Site 2: Seep (cont.)

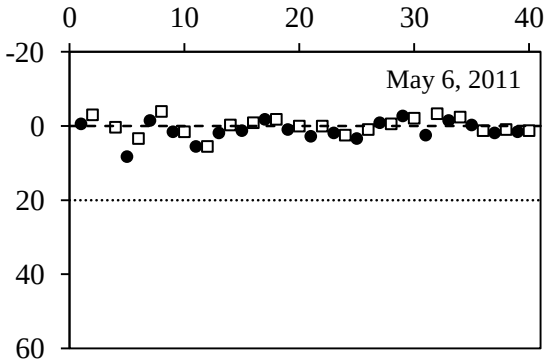

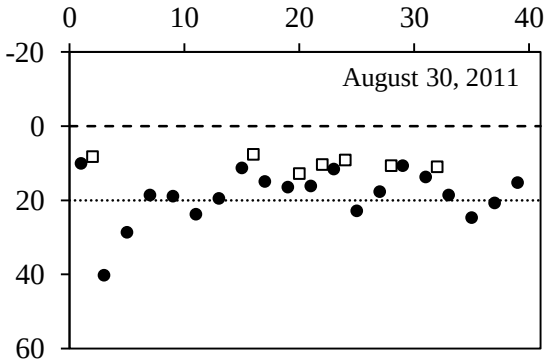

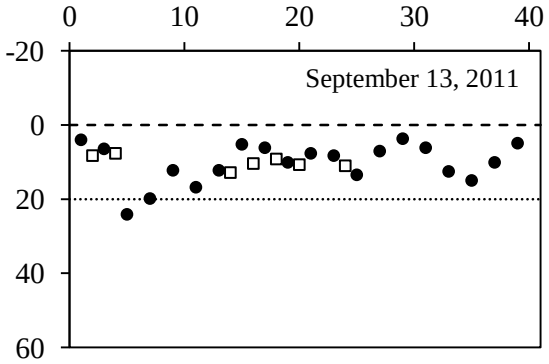

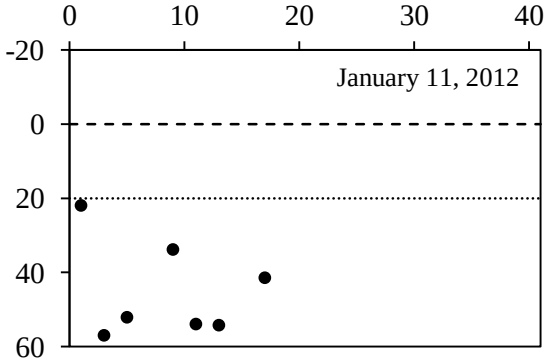

Site 2: Non-seep (cont.)

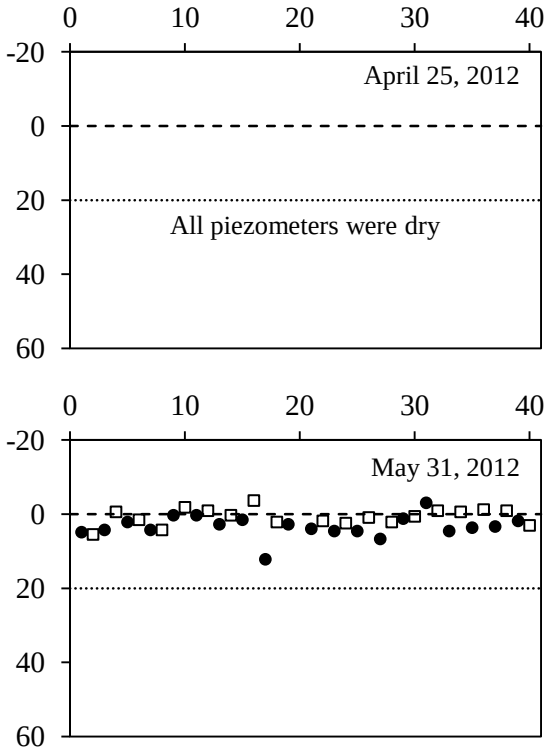

Site 2: Seep (cont.)

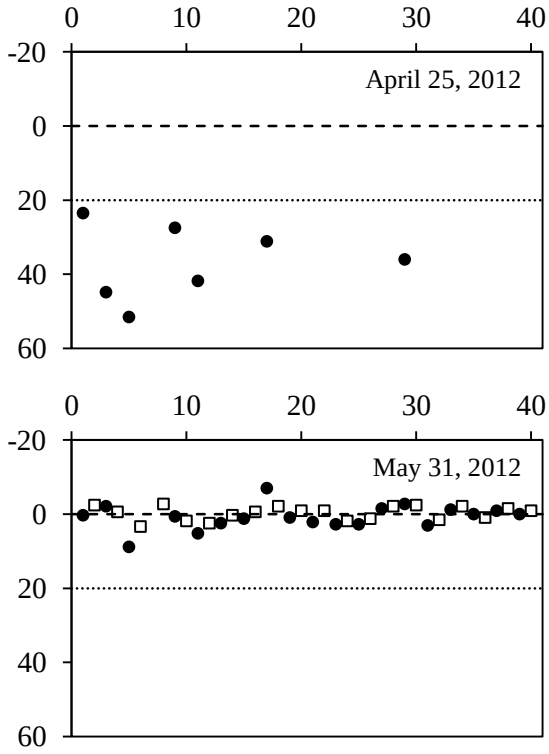

Site 3: Non-seep

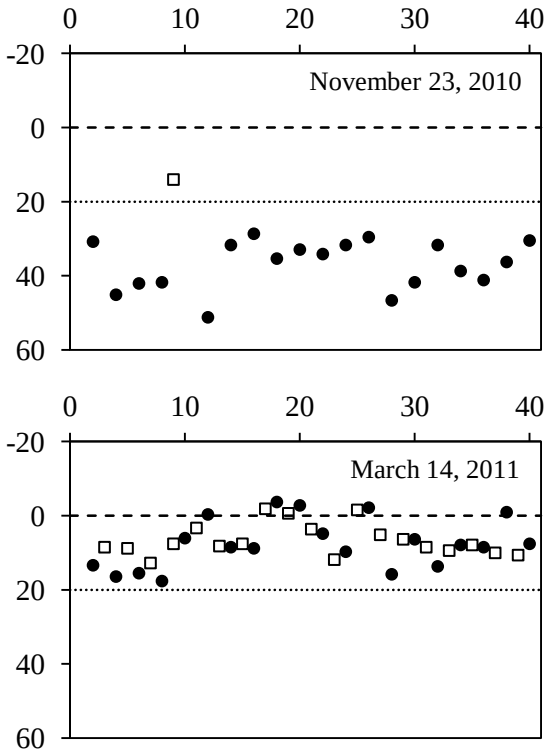

Site 3: Seep

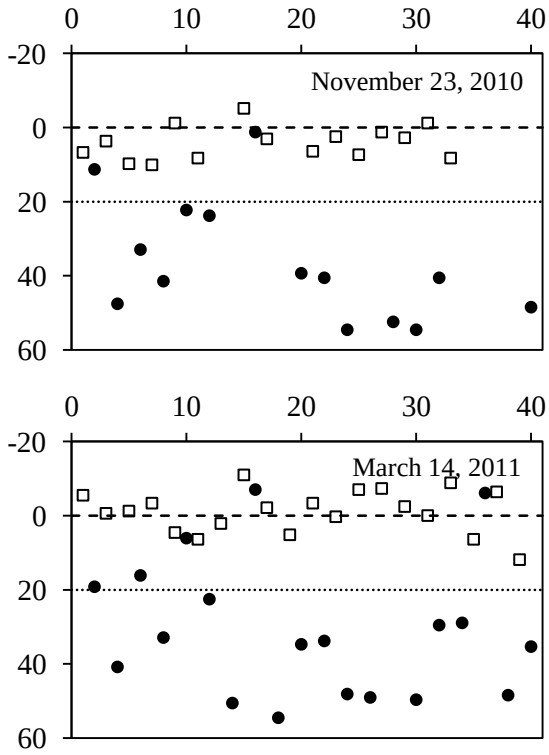

Site 3: Non-seep (cont.)

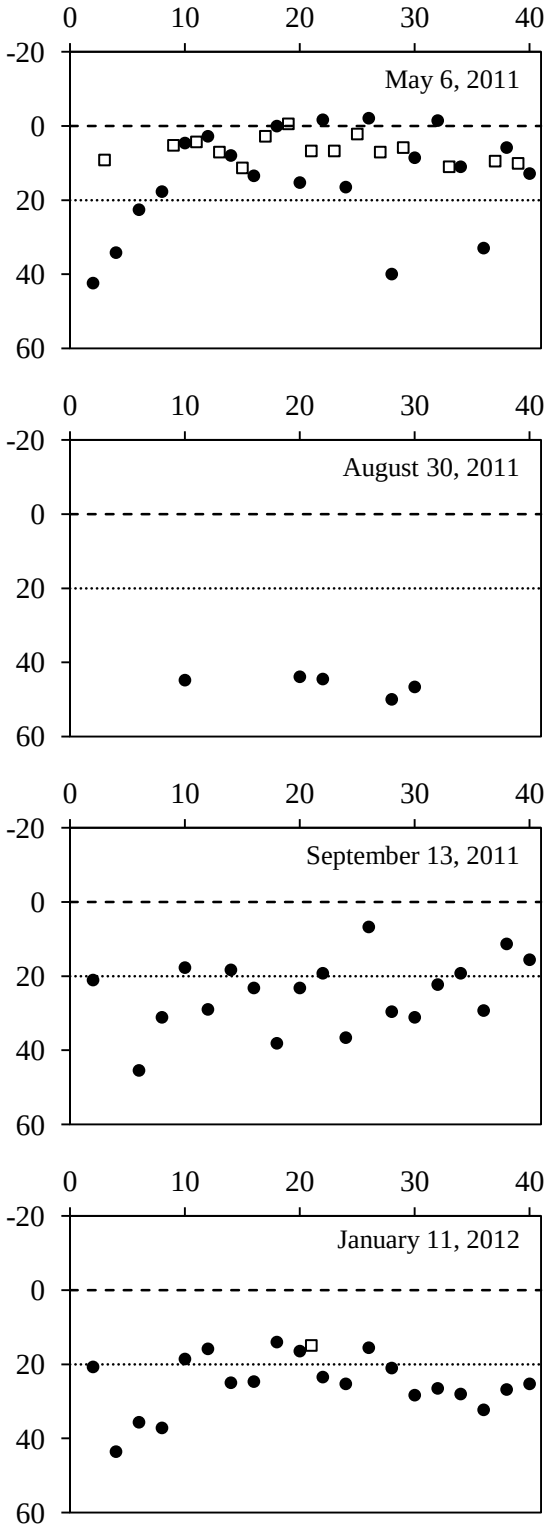

Site 3: Seep (cont.)

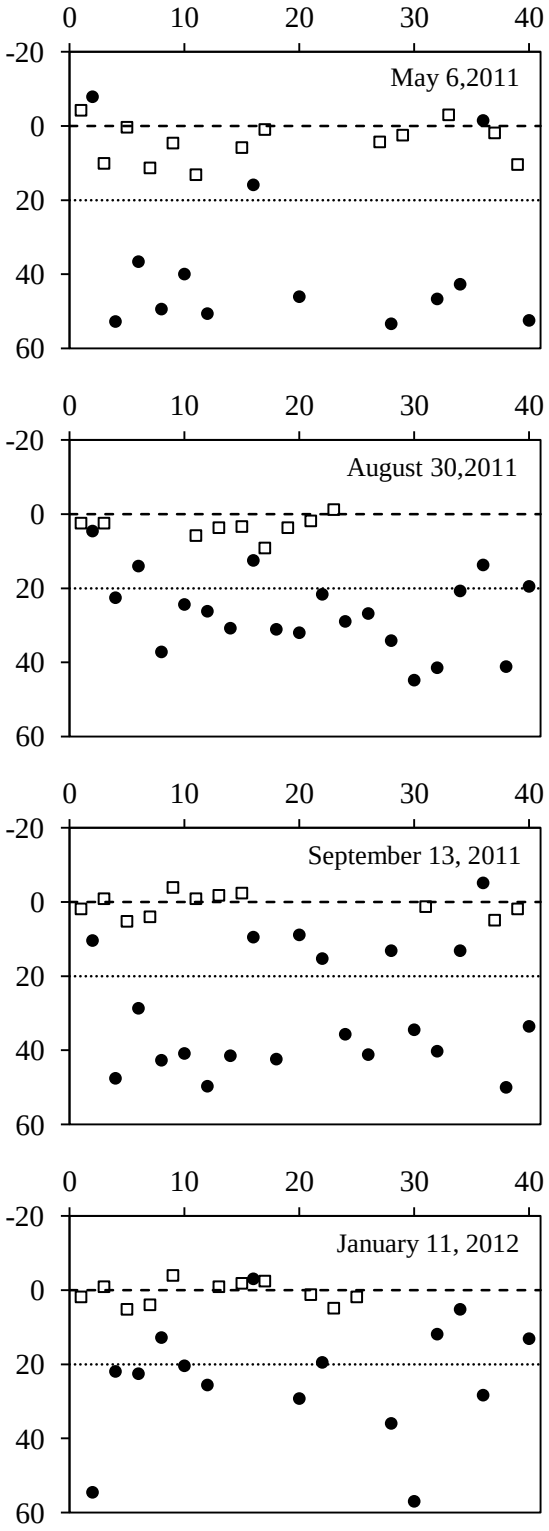

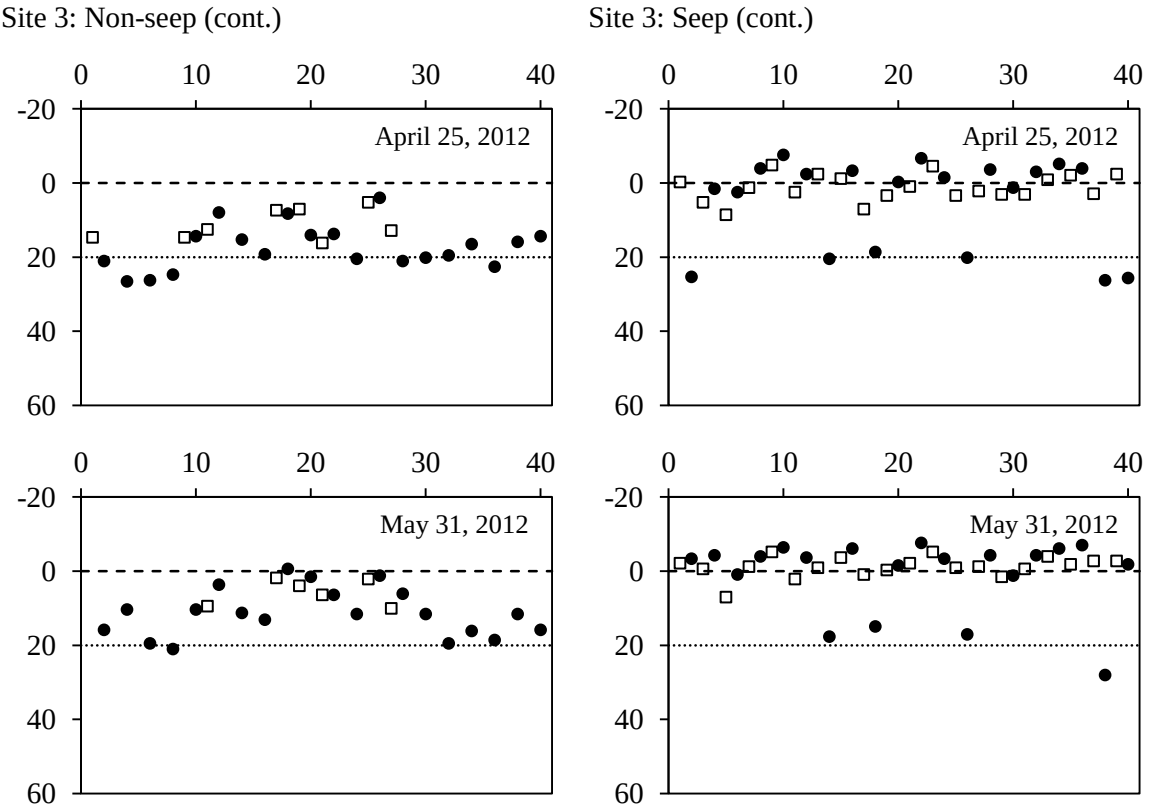

Piezometer NH_4-N, NO_3-N, and Cl^- Concentrations

NH_4-N Concentrations

The x-axis is the piezometer identification number (1 to 40) and the y-axis is NH_4-N concentration in mg L^{-1}. The piezometers were installed at two depths (20 and 60 cm). The odd numbered piezometers are 60 cm deep and the even numbered piezometers are 20 cm deep. The black circles represent study site 1, the white squares represent study site 2, and the grey triangles represent study site 3. No samples were collected from study site 3 on Oct. 5, 2010.

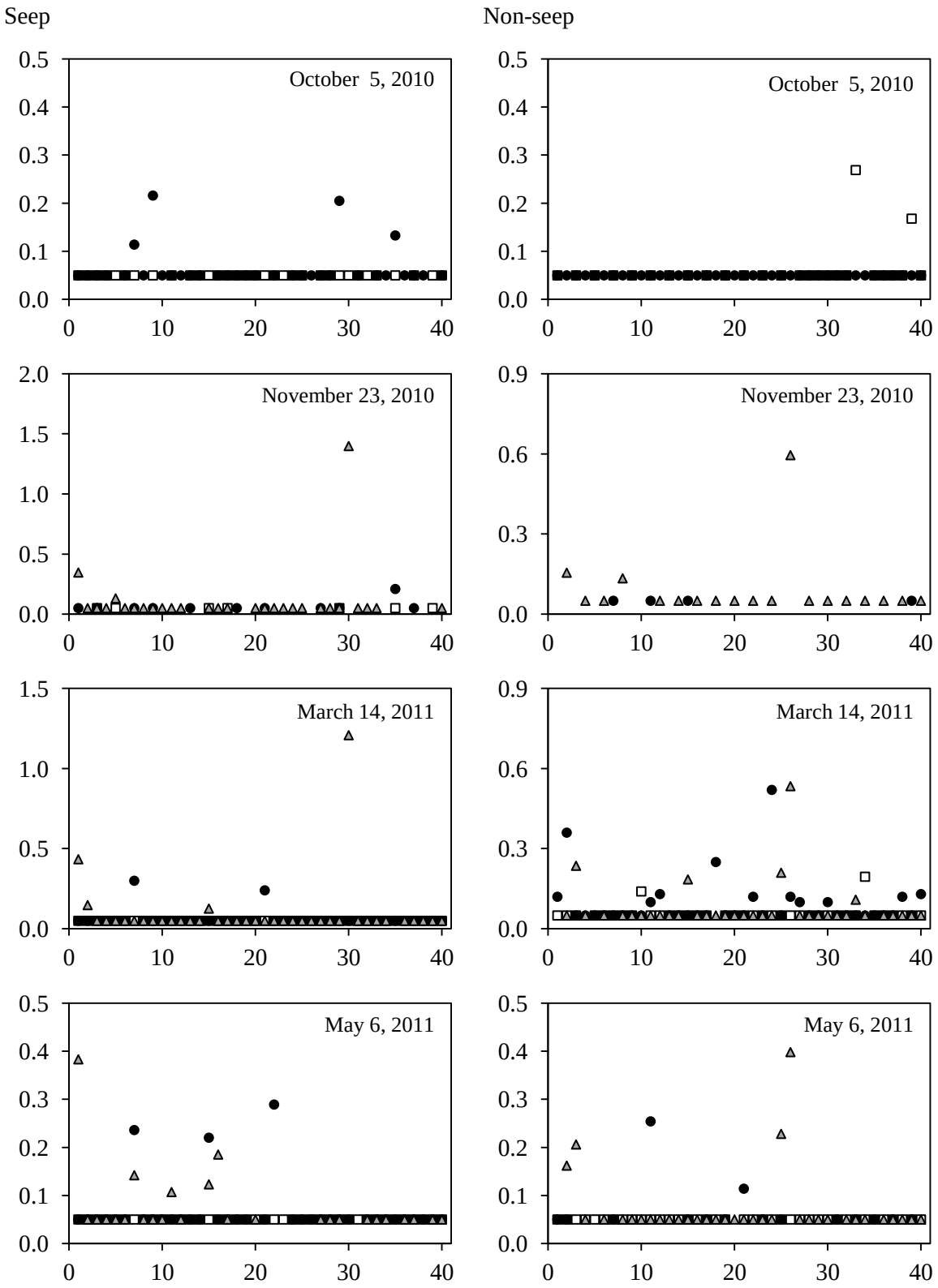
Seep
Non-seep
October 5, 2010
November 23, 2010
March 14, 2011
May 6, 2011

Seep (cont.)

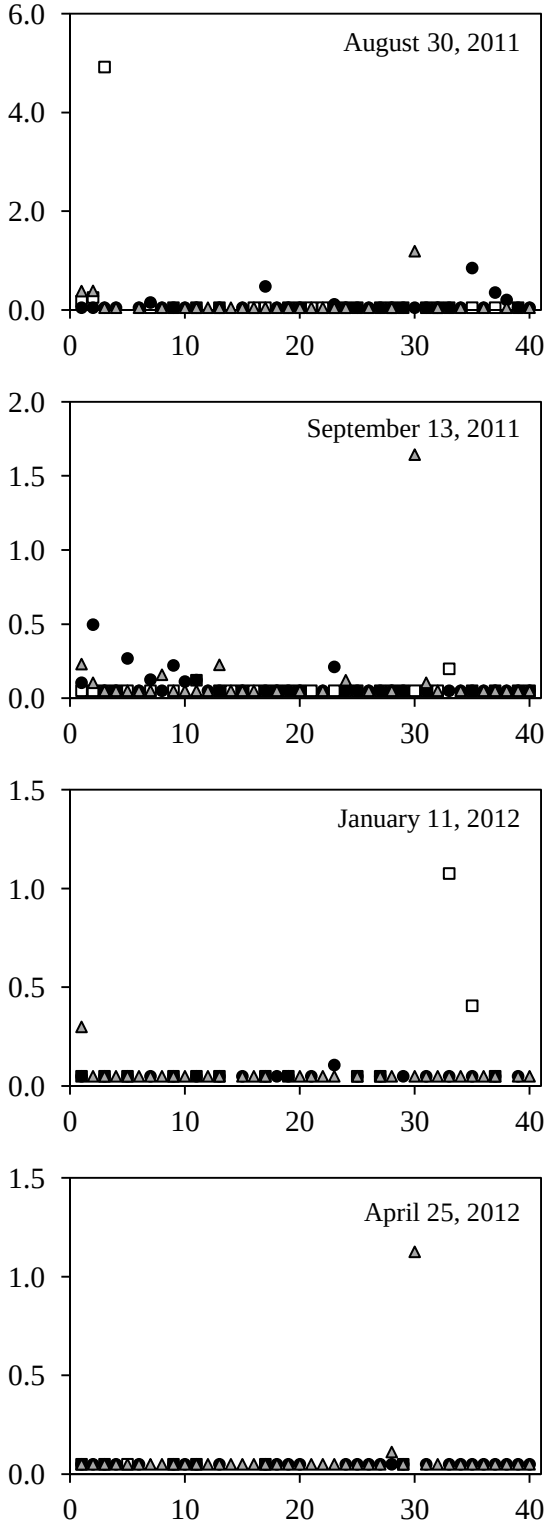

Non-seep (cont.)

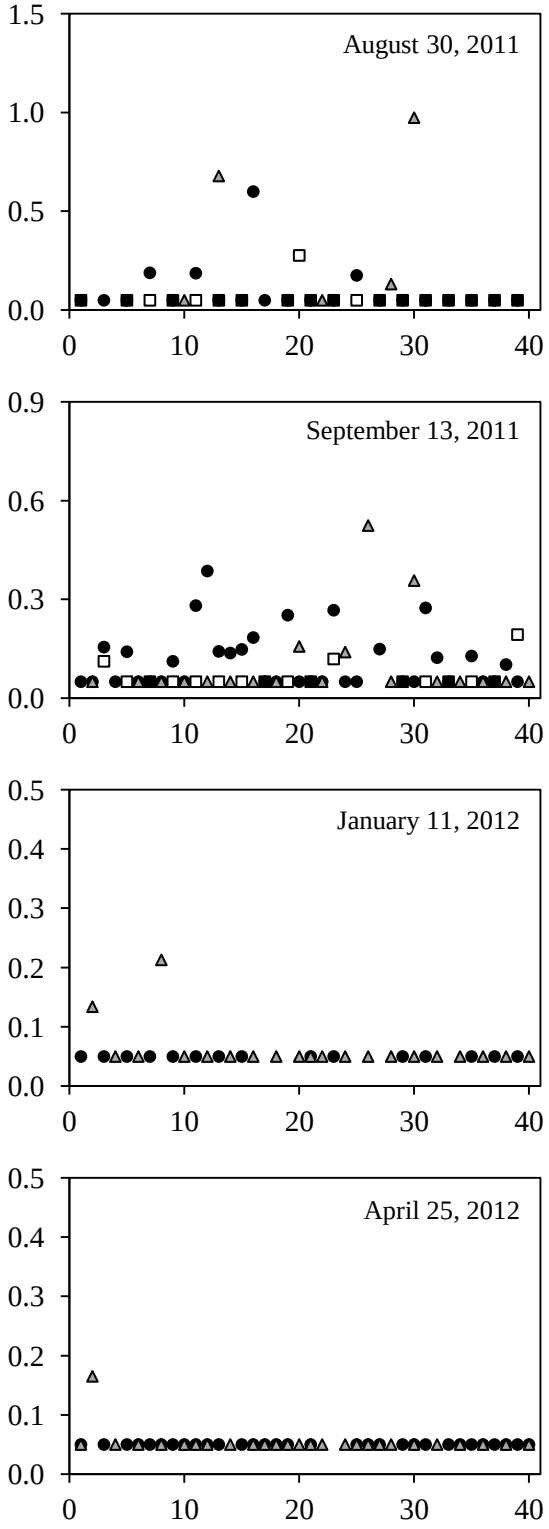

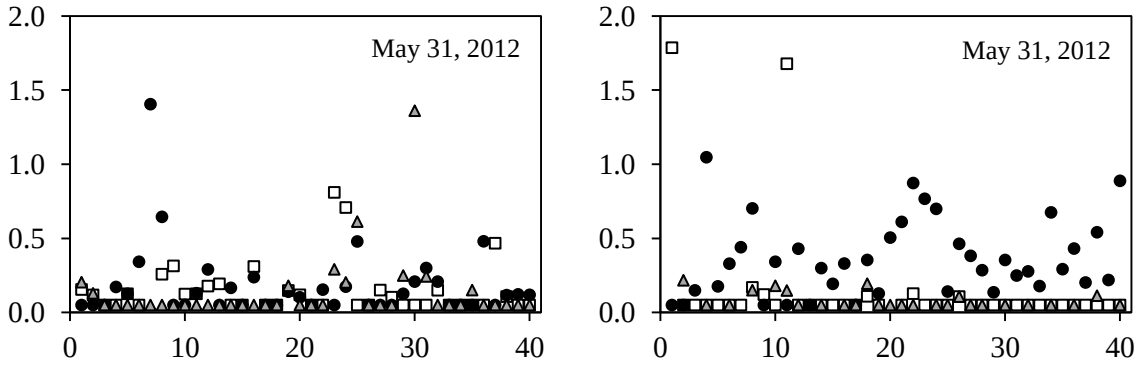

NO_3-N Concentrations

Similar to the previous section, the x-axis is the piezometer identification number (1 to 40) and the y-axis is NO_3-N concentration in mg L^{-1}. The black circles represent study site 1, the white squares represent study site 2, and the grey triangles represent study site 3.

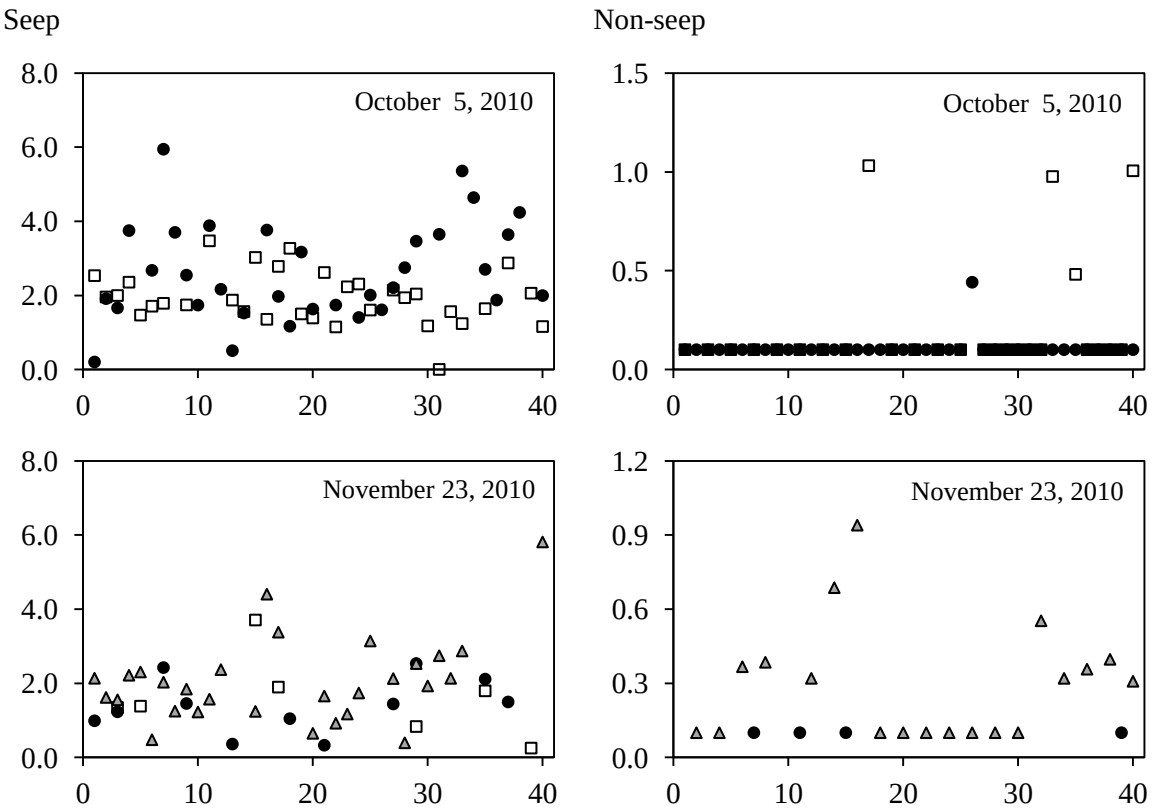

Seep (cont.)

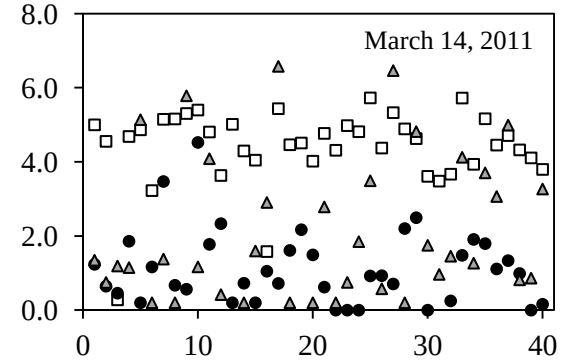

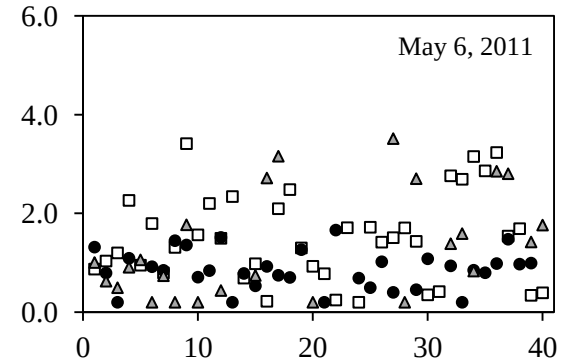

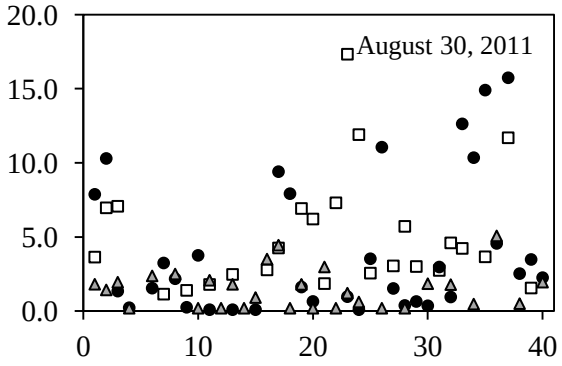

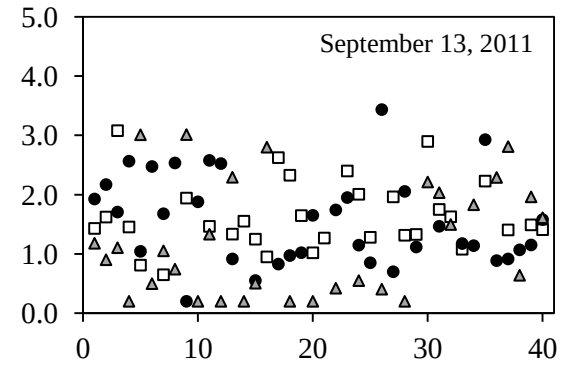

Non-seep (cont.)

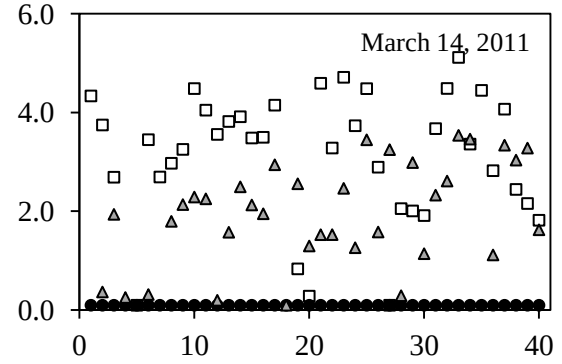

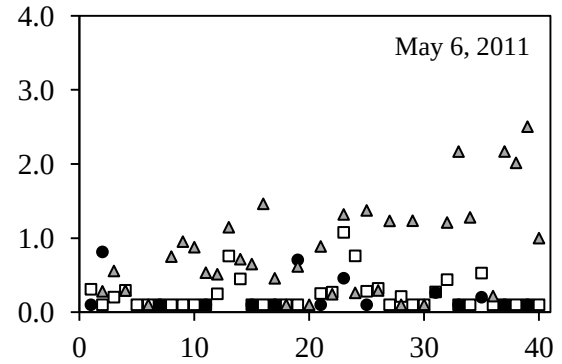

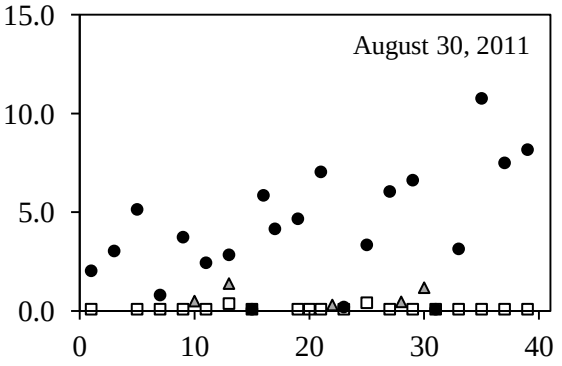

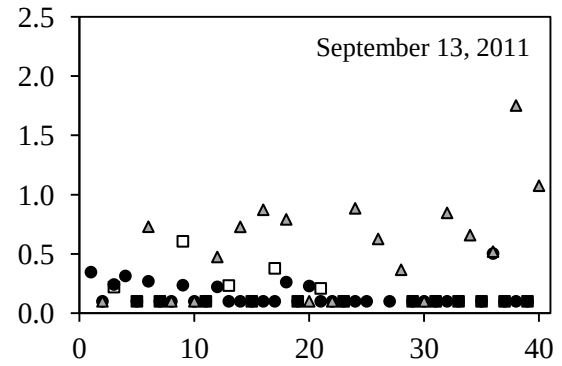

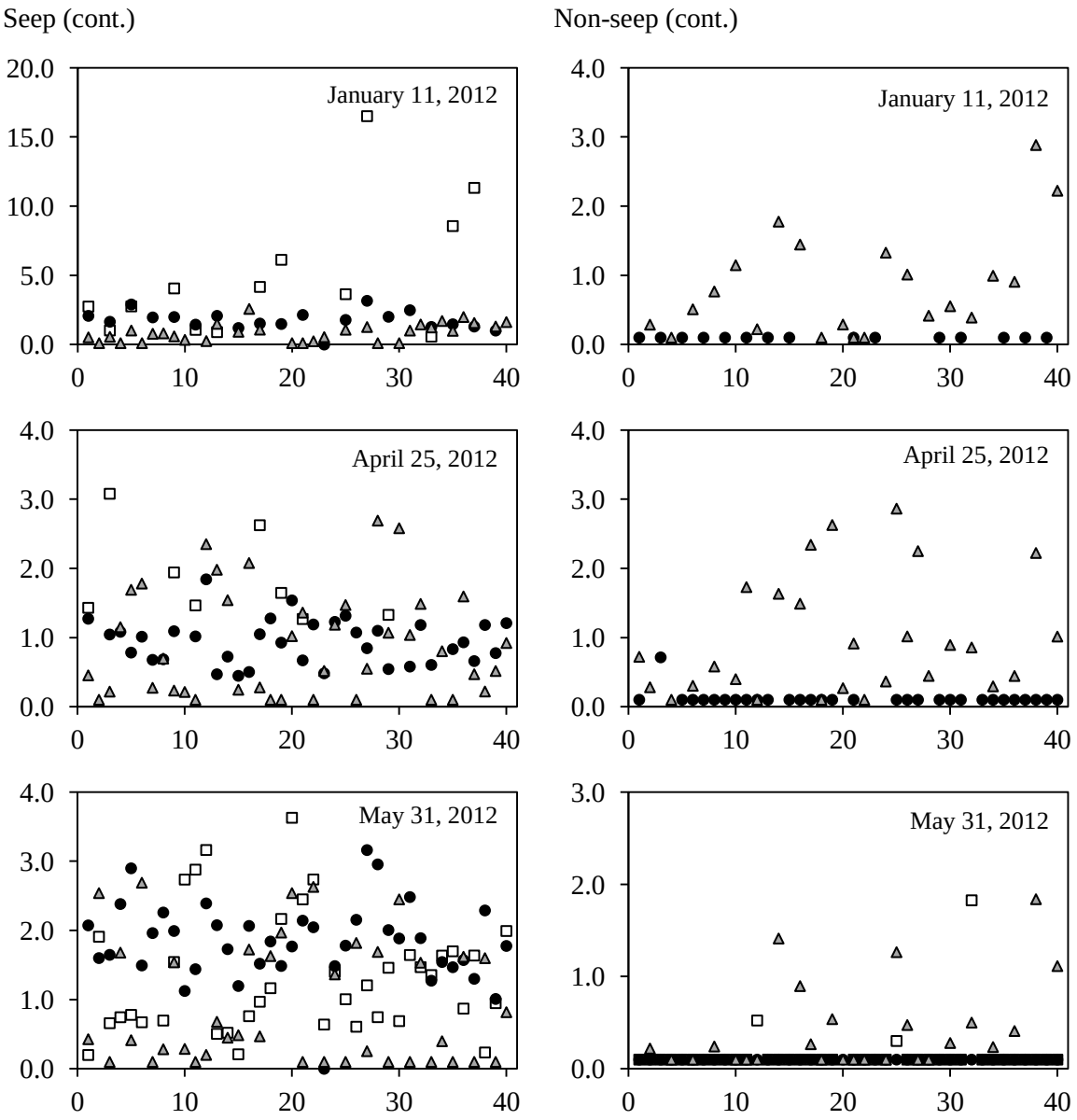

Cl^- Concentrations

Similar to the previous two sections, the x-axis is the piezometer identification number (1 to 40) and the y-axis is Cl^- concentration in mg L^{-1}. The black circles represent study site 1, the white squares represent study site 2, and the grey triangles represent study site 3.

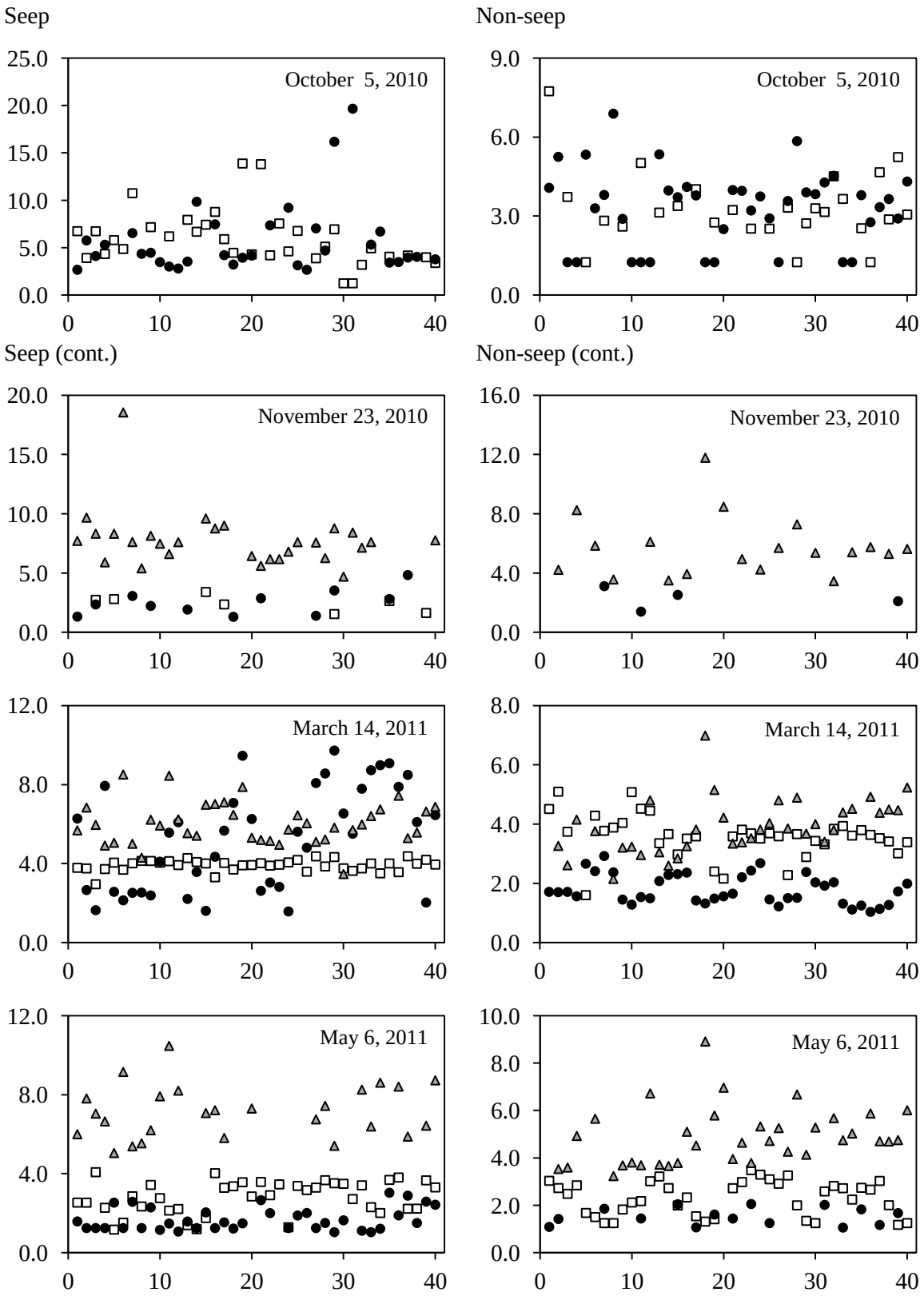
Seep
Non-seep
October 5, 2010
October 5, 2010
Seep (cont.)
Non-seep (cont.)
November 23, 2010
November 23, 2010
March 14, 2011
March 14, 2011
May 6, 2011
May 6, 2011

Seep (cont.)

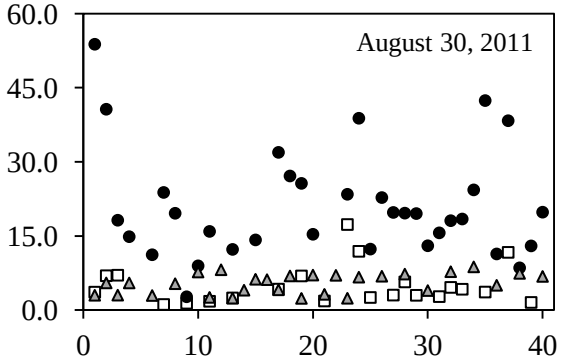

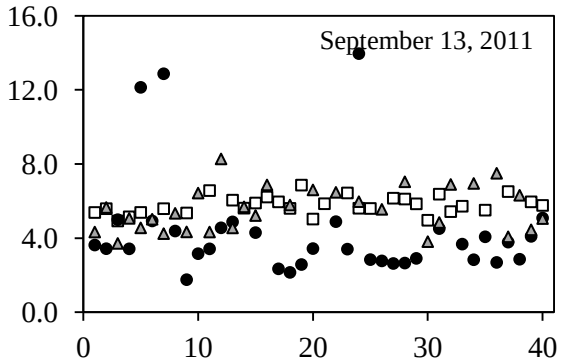

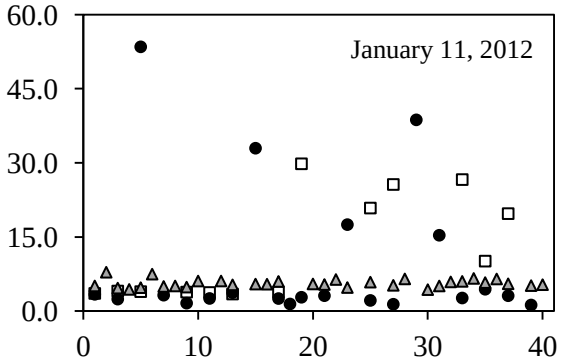

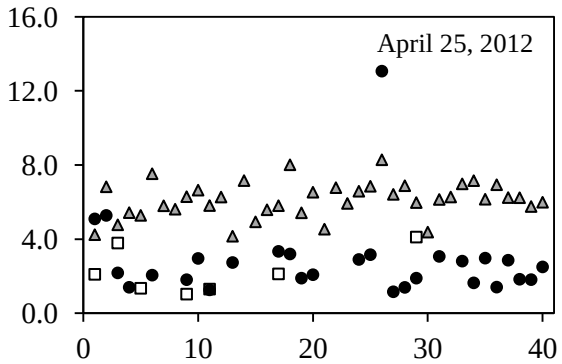

Non-seep (cont.)

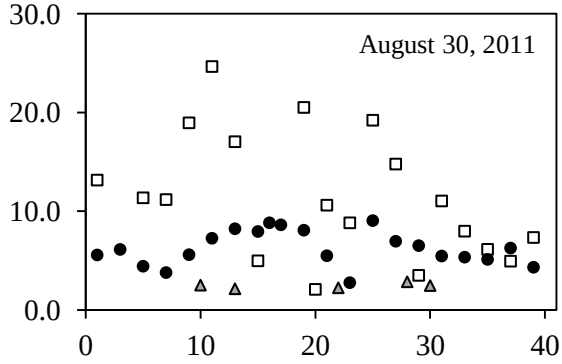

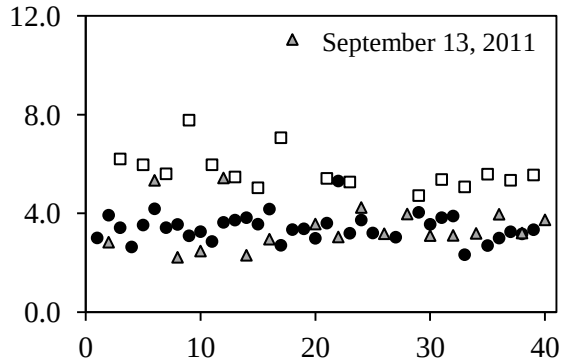

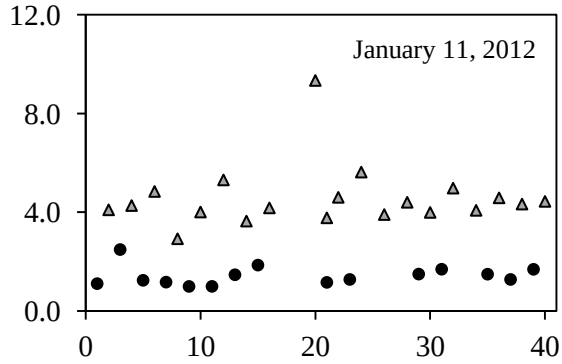

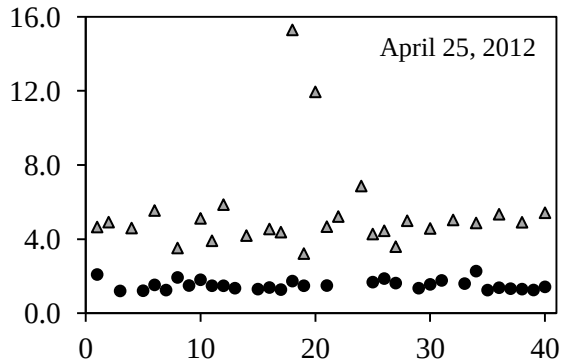

Seep (cont.)

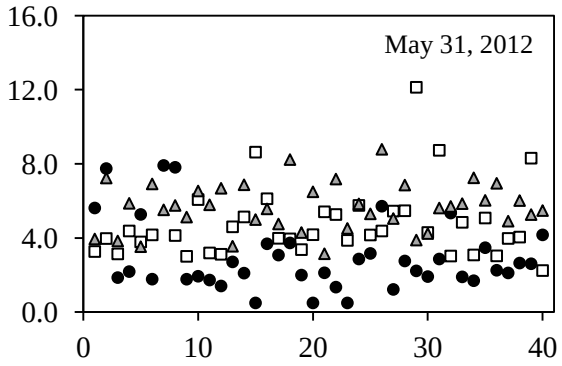

Non-seep (cont.)

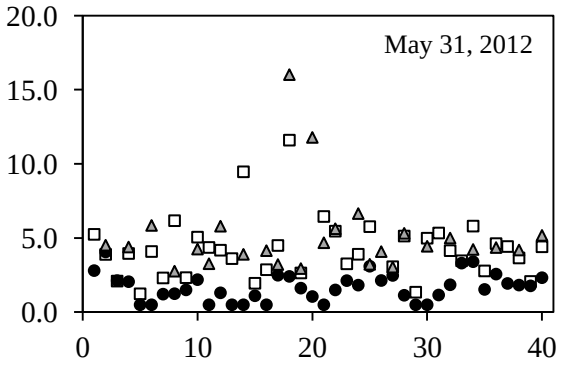

APPENDIX B

Groundwater Table, Piezometer, and Electrical Resistivity Imaging Data for Chapter Three

This appendix contains the water table, piezometer, and electrical resistivity imaging (ERI) data from a seep and an adjacent non-seep area of the riparian zone that are presented in chapter three. There are five sections in this appendix: 1) groundwater table depth measured in piezometers; 2) non-seep apparent resistivity and inverted resistivity sections; 3) seep apparent resistivity and inverted resistivity sections; 4) piezometer nitrate-N (NO_3-N) concentration; and 5) piezometer chloride (Cl^-) concentration. The figures in each section of this appendix are formatted to display the data and are not meant to show the differences among sampling dates (i.e., the y-axis varies for each figure); thus, caution must be taken if comparing two sampling dates or differences between seep and non-seep areas.

Groundwater Table Depth

The x-axis is the piezometer identification number (1 to 20) and the y-axis is the depth of the groundwater table below (or above) the land surface (cm). The piezometers were installed at a depth of 60 cm. The black circles represent water table measurements from the seep area and the white squares represent water table measurements from the non-seep area. The dashed line at 0 cm represents the relative location of the land surface. On April 21 and April 22, 2012, the water table depth was greater than 60 cm in both the seep and non-seep areas; therefore, the data are not shown.

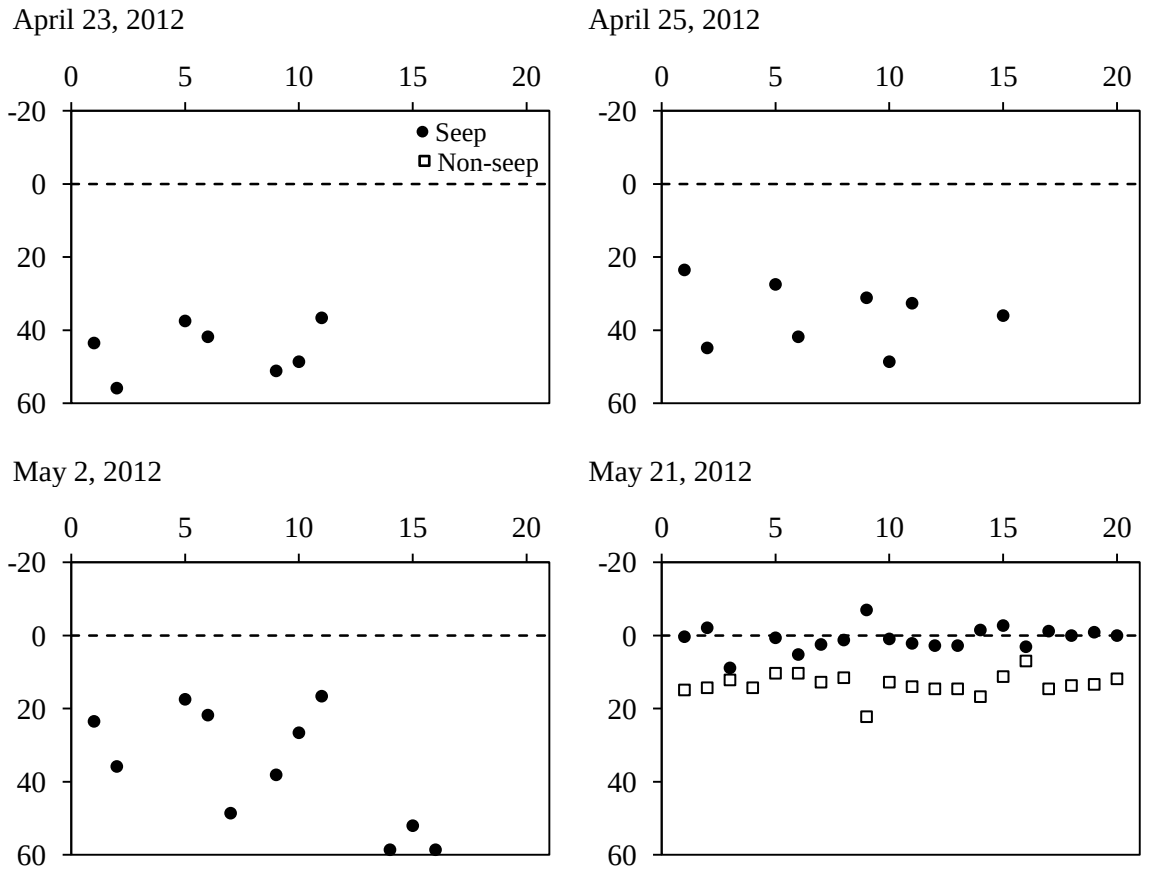

Non-seep Electrical Resistivity

The first set of figures in this section is apparent resistivity data that were collected in the field using the IRIS Syscal Pro Resistivity Meter with a dipole-dipole electrode geometry (32 electrodes at 0.5 m interval spacing). Apparent resistivity is defined as the resistivity of an electrically homogeneous and isotropic half-space that would yield the measured relationship between the applied current and the potential difference for a particular arrangement and spacing of electrodes. The second set of figures is the result of data inversion with EarthImager2D (Advanced Geosciences, Inc.). The x-axis and y-axis are depth and distance measured in m, respectively. Resistivity values are reported in Ωm.

Apparent Resistivity

April 21, 2012

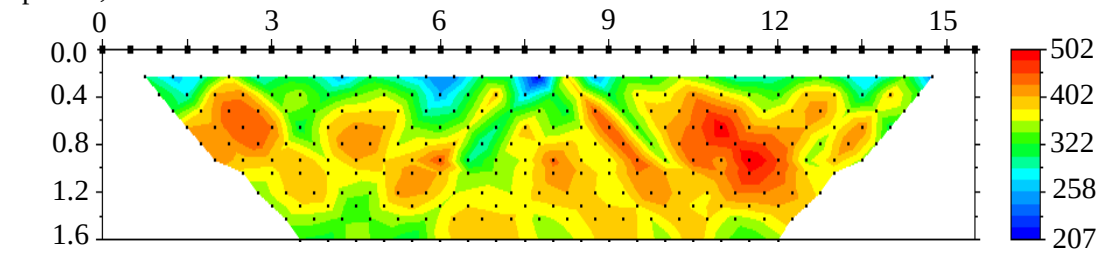

April 22, 2012

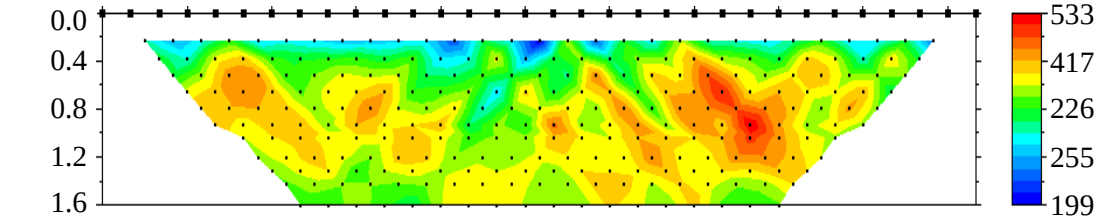

April 23, 2012

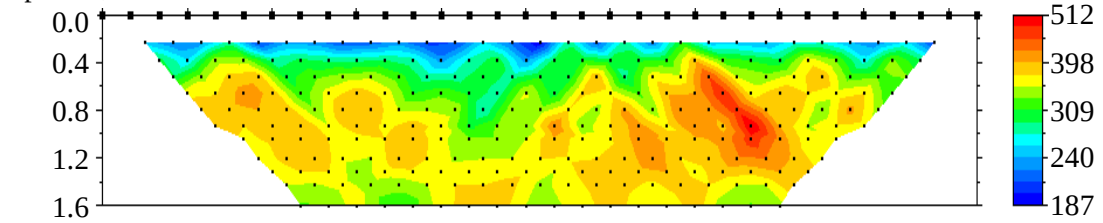

April 25, 2012

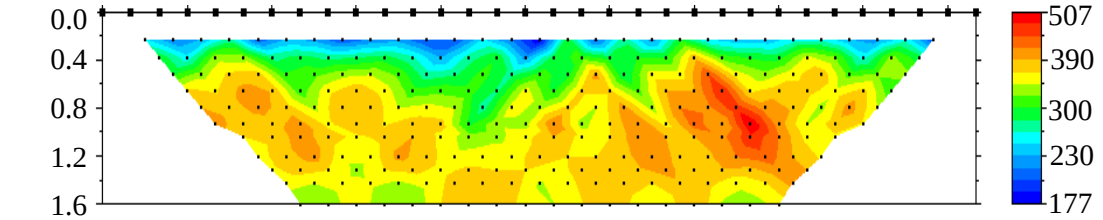

May 2, 2012

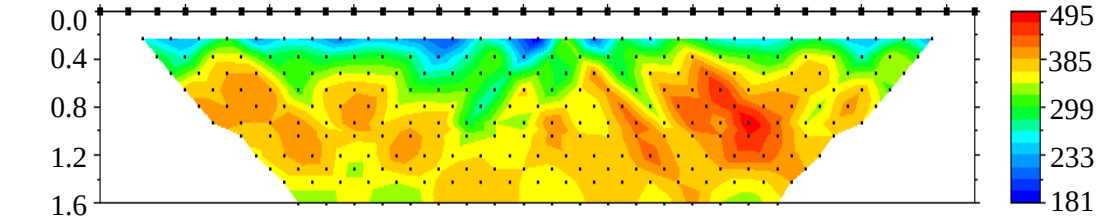

May 21, 2012

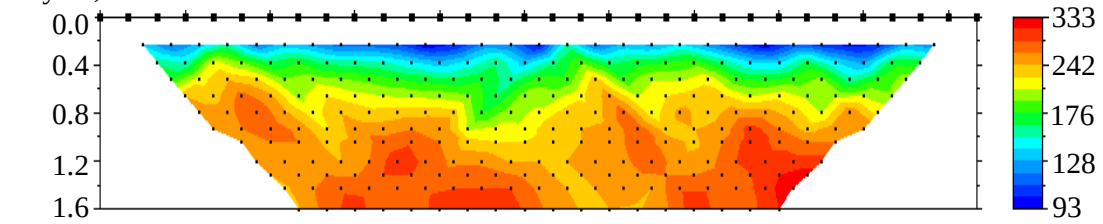

Inverted Resistivity Section

April 21, 2012

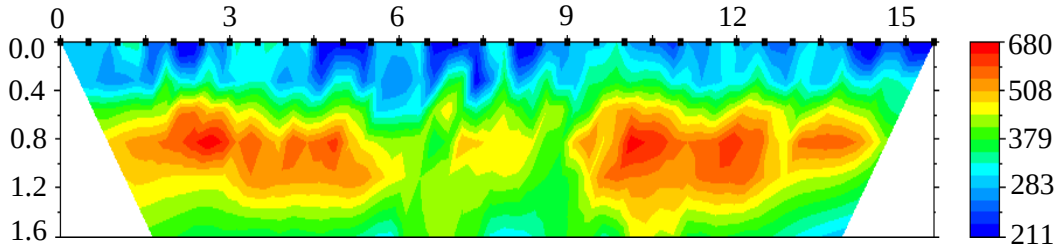

April 22, 2012

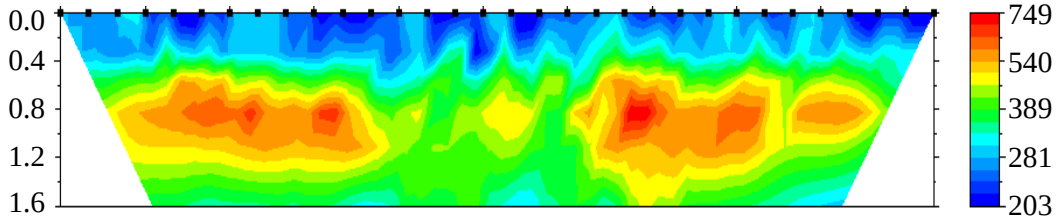

April 23, 2012

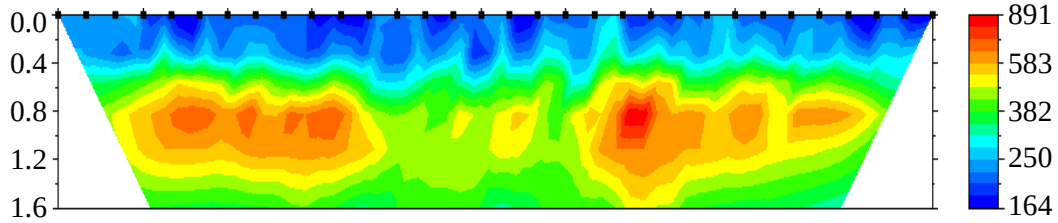

April 25, 2012

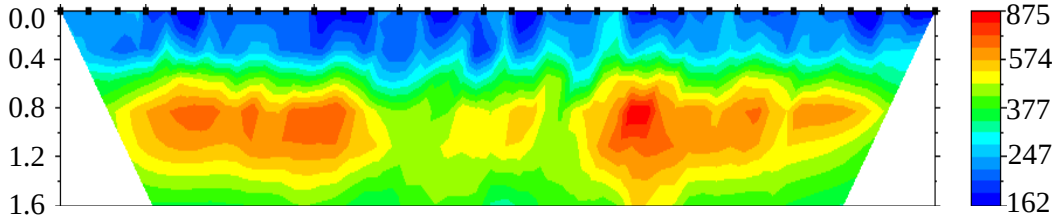

May 2, 2012

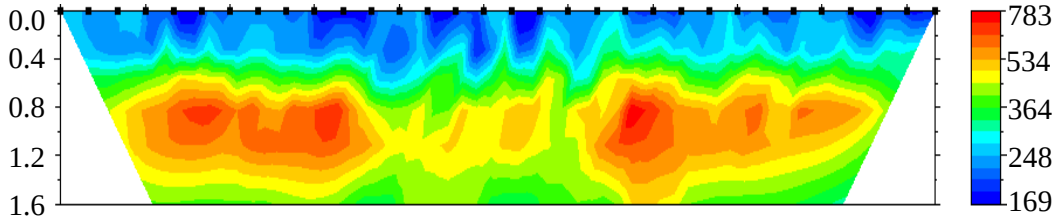

May 21, 2012

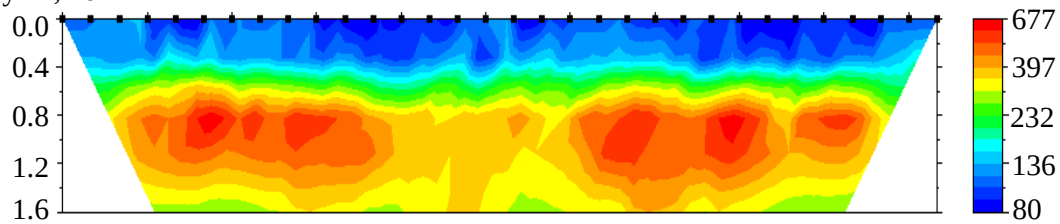

Seep Electrical Resistivity

Similar to the previous section of this appendix, the first set of figures in this section is apparent resistivity data that were collected in the field using the IRIS Syscal Pro Resistivity Meter with a dipole-dipole electrode geometry (32 electrodes at 0.5 m interval spacing). The second set of figures is the result of data inversion with EarthImager2D (Advanced Geosciences, Inc.). The x-axis and y-axis are depth and distance measured in m, respectively. Resistivity values are reported in Ωm.

Apparent Resistivity

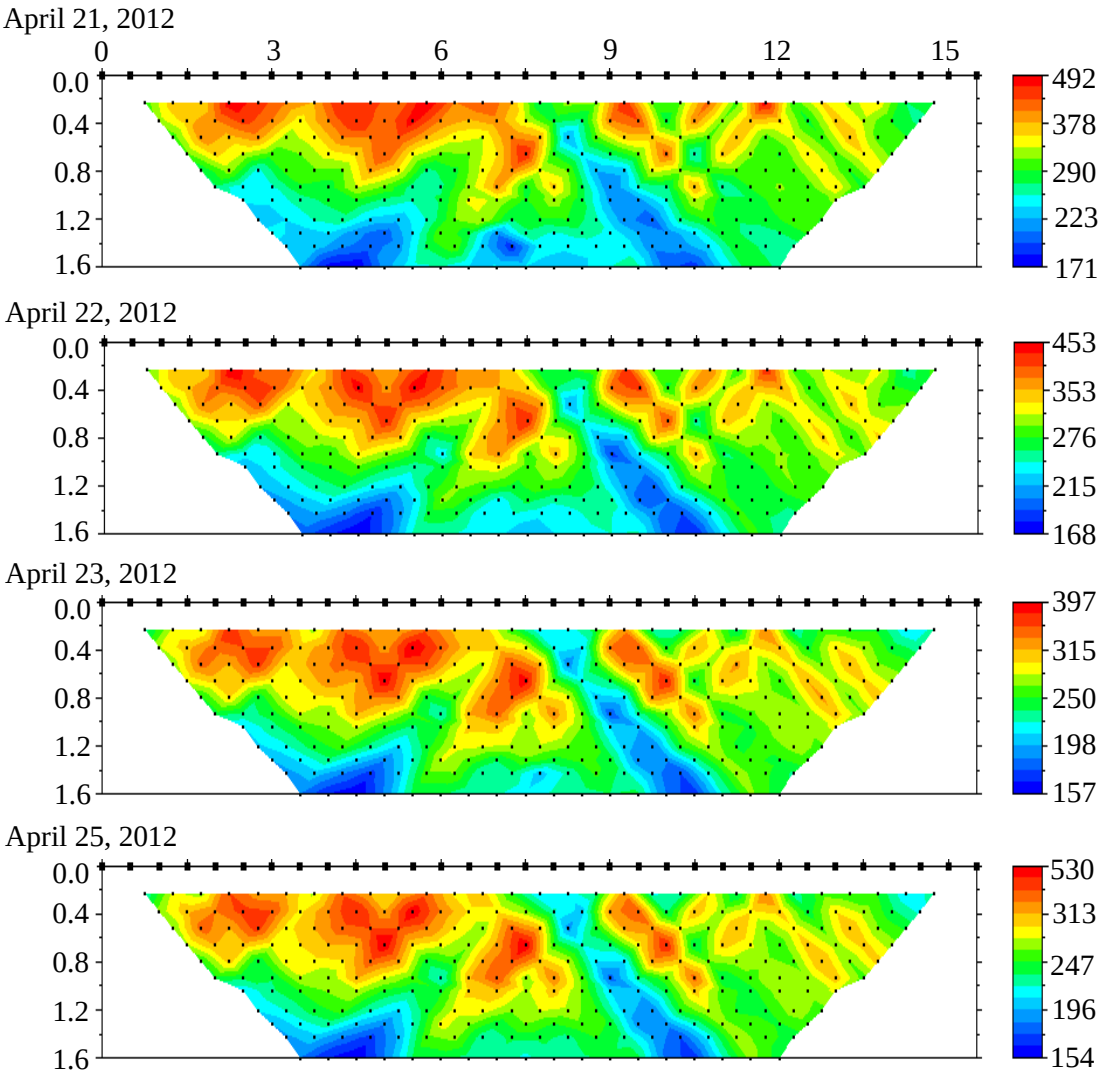

May 2, 2012

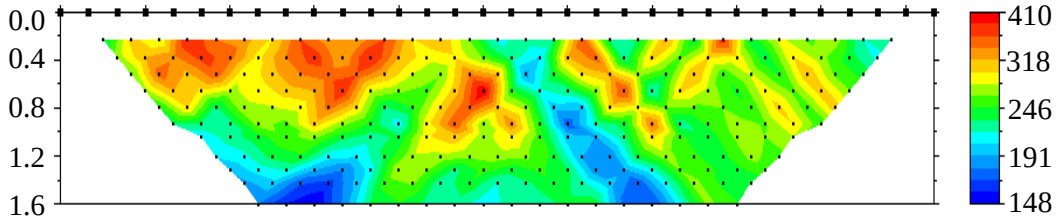

May 21, 2012

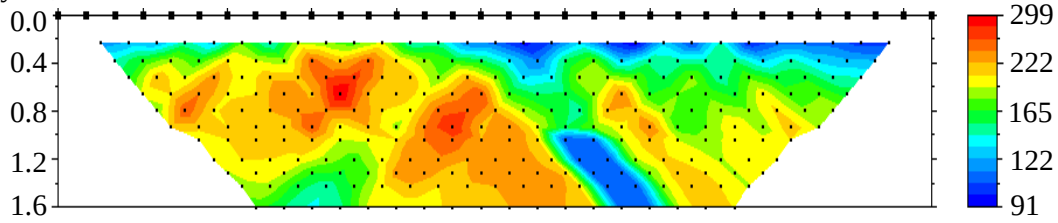

Inverted Resistivity Section

April 21, 2012

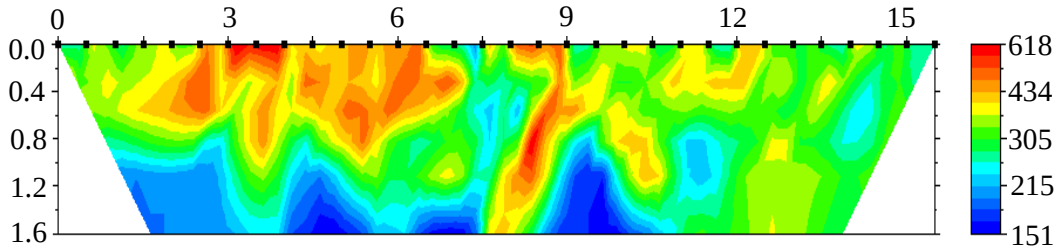

April 22, 2012

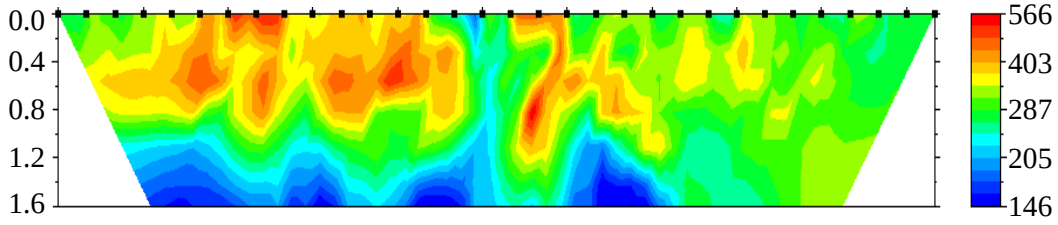

April 23, 2012

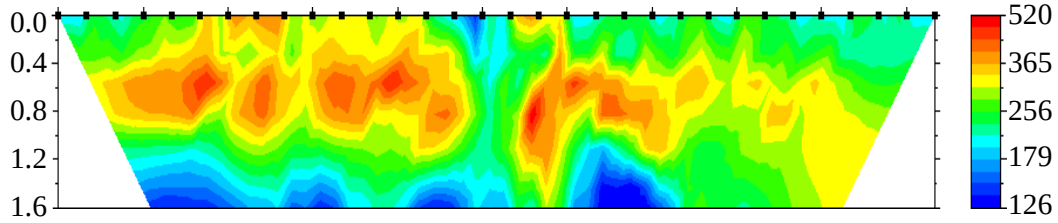

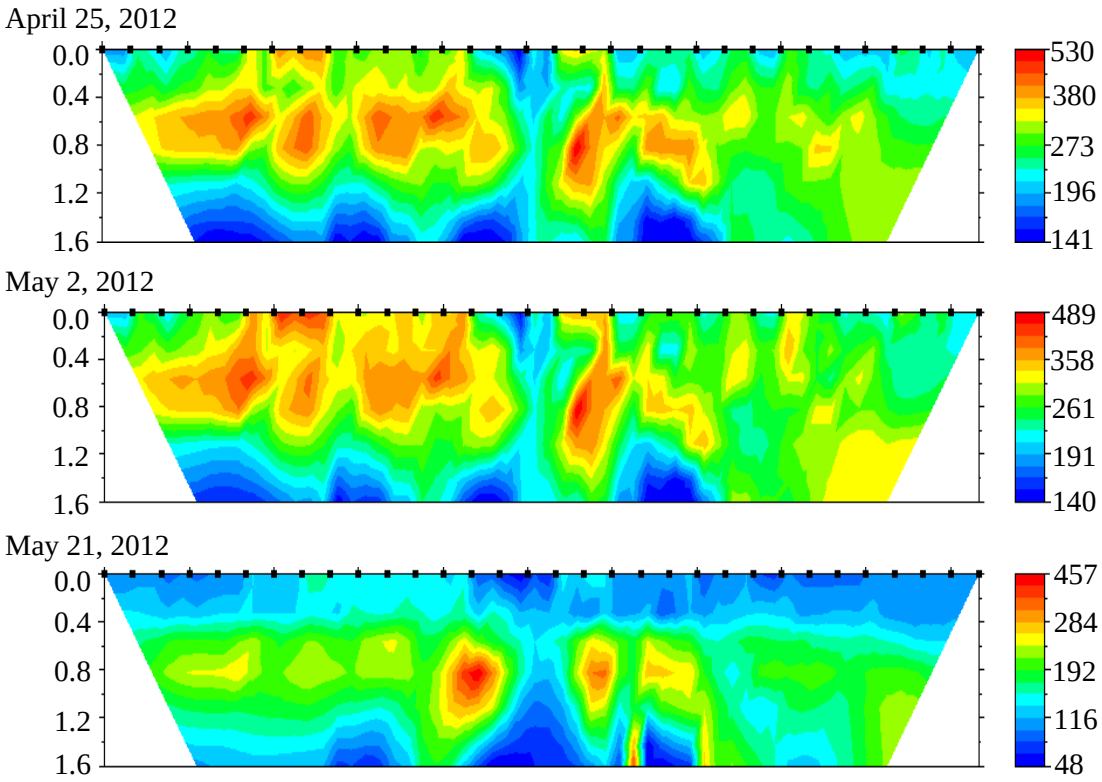

Piezometer NO_3-N Concentration

The x-axis is the piezometer identification number (1 to 40) and the y-axis is NO_3-N concentration (mg L^{-1}). The piezometers were installed at two depths (20 and 60 cm). On April 21 and April 22, no water samples were collected from either the seep or non-seep area.

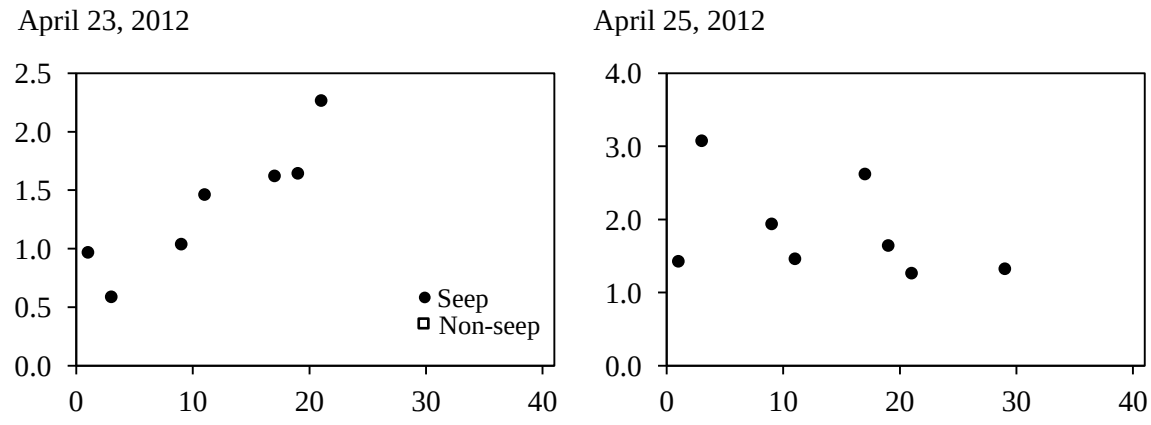

May 2, 2012

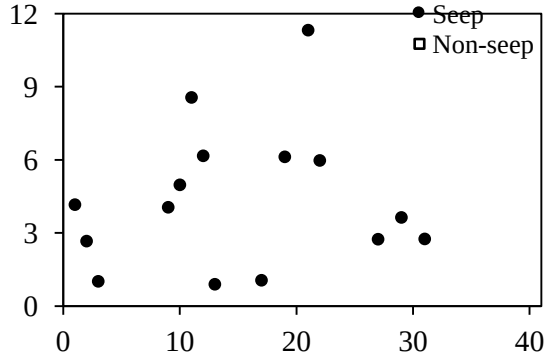

May 21, 2012

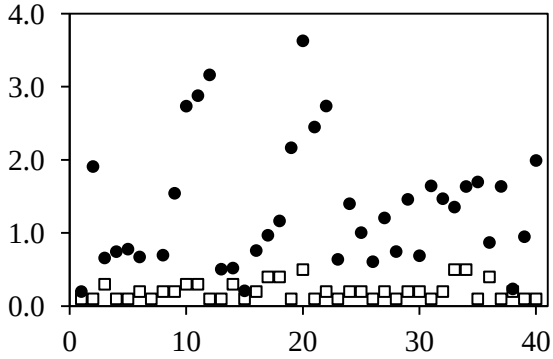

Piezometer Cl^- Concentration

The x-axis is the piezometer identification number (1 to 40) and the y-axis is Cl^- concentration (mg L^{-1}). The piezometers were installed at two depths (20 and 60 cm). On April 21 and April 22, no water samples were collected from either the seep or non-seep area.

April 23, 2012

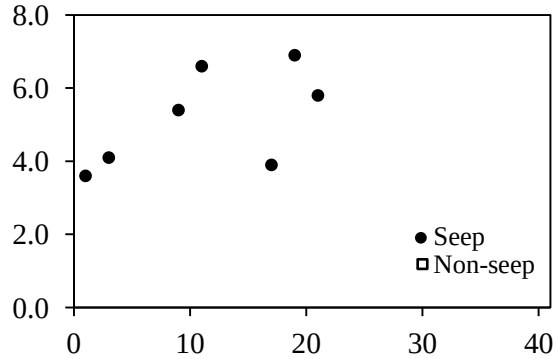

April 25, 2012

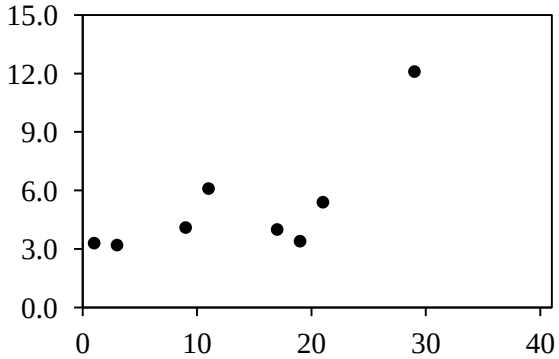

May 2, 2012

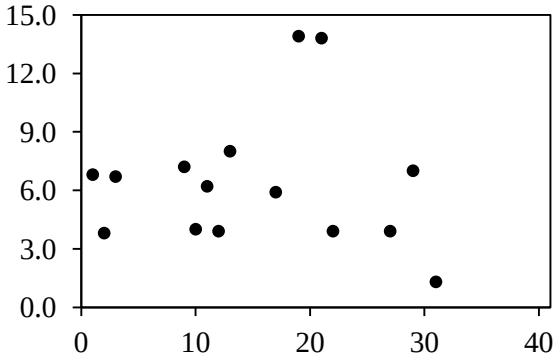

May 21, 2012

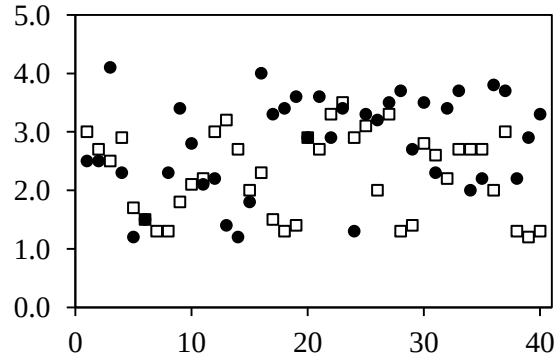

APPENDIX C

Stream and Seep Nitrate Data for Chapter Four

This appendix contains the stream and seep data that are presented in chapter four. There are three main sections of this appendix: 1) baseflow stream and surface seep nitrate-nitrogen (NO_3-N) concentrations in FD36 and RS; 2) stream and seep NO_3-N concentrations measured during and following storm events; and 3) semi-variogram analysis of stream NO_3-N concentration. The figures in each section are formatted to display the data and are not meant to show the differences among sampling dates (i.e., the y-axis varies for each figure); thus, caution must be taken if comparing two sampling dates or differences between FD36 and RS.

Baseflow Stream and Seep NO_3-N Concentrations

The x-axis is the distance (m) from the stream outlet and the y-axis is NO_3-N concentration (mg L^{-1}). Seep location and NO_3-N concentration (mg L^{-1}) are also labeled.

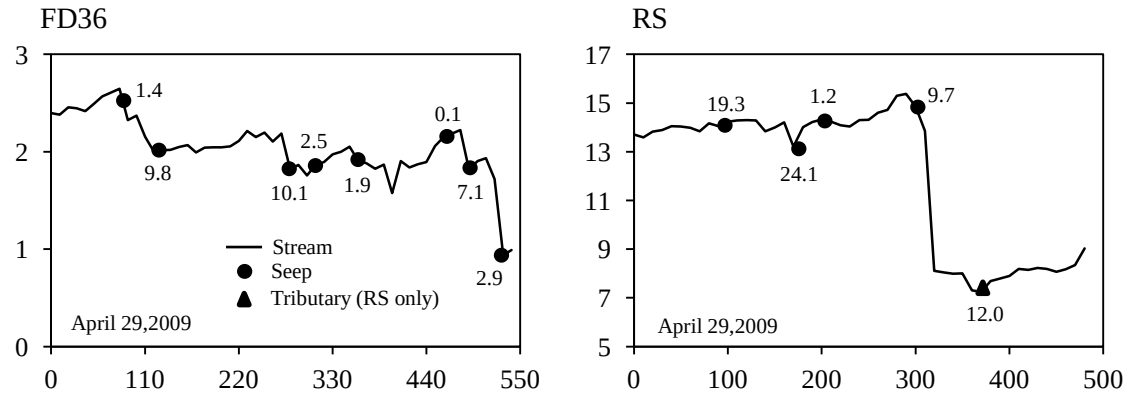

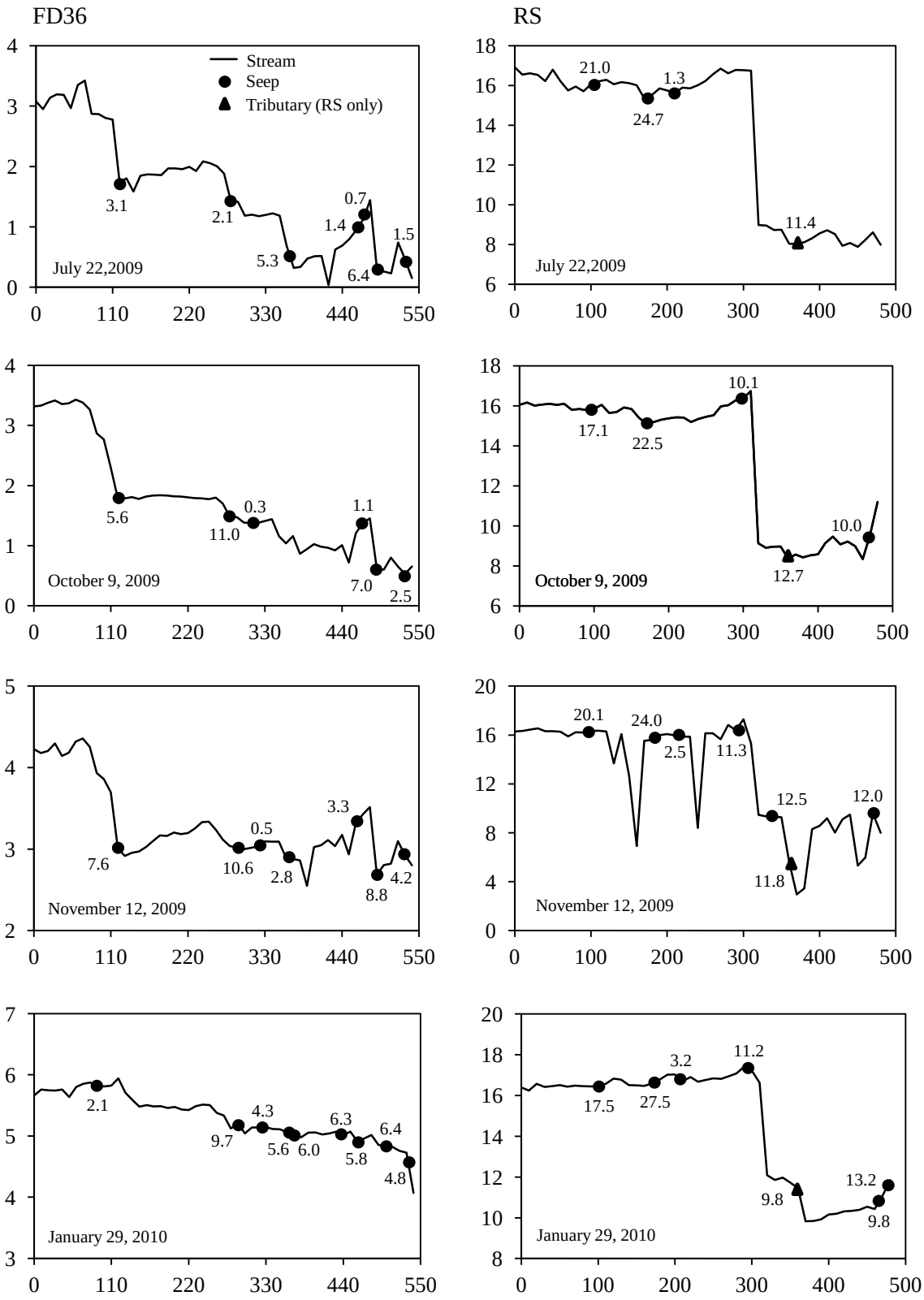
FD36
RS
Stream
Seep
Tributary (RS only)
July 22,2009
3.1
2.1
5.3
1.4
0.7
6.4
1.5
July 22,2009
21.0
1.3
24.7
11.4
October 9, 2009
5.6
11.0
0.3
7.0
1.1
2.5
October 9, 2009
17.1
22.5
10.1
12.7
10.0
November 12, 2009
7.6
10.6
0.5
2.8
3.3
8.8
4.2
November 12, 2009
20.1
24.0
2.5
11.3
11.8
12.5
12.0
January 29, 2010
2.1
9.7
4.3
5.6
6.0
6.3
5.8
6.4
4.8
January 29, 2010
17.5
27.5
3.2
11.2
9.8
13.2
9.8

FD36

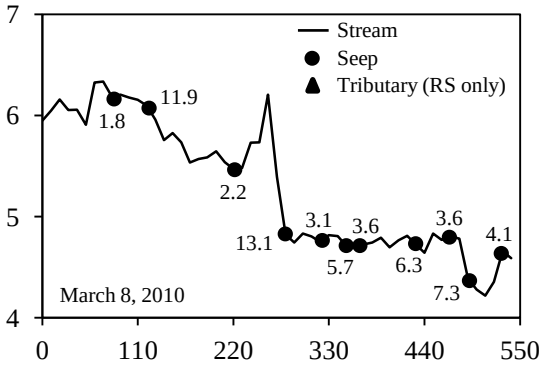

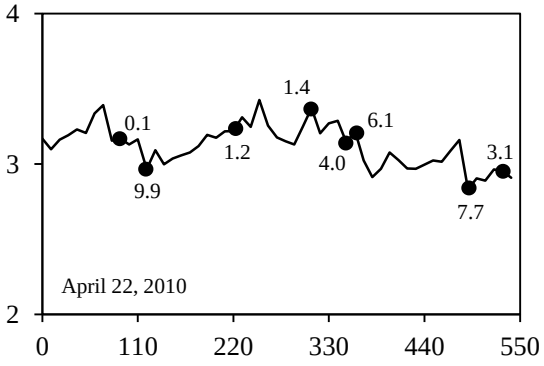

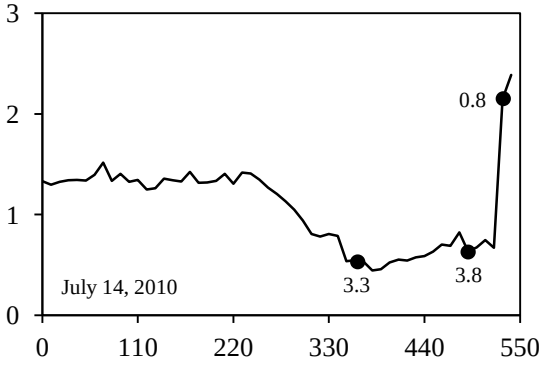

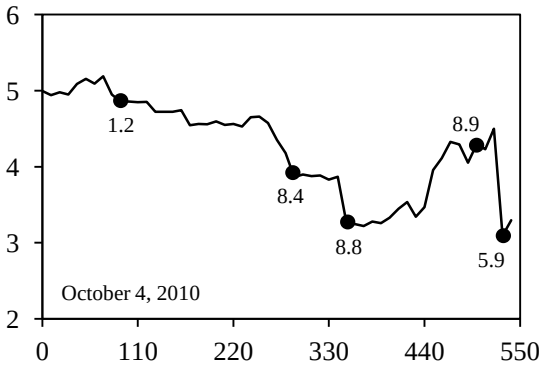

RS

No Data Collected

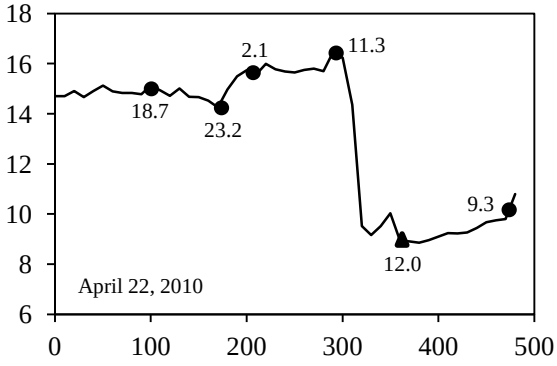

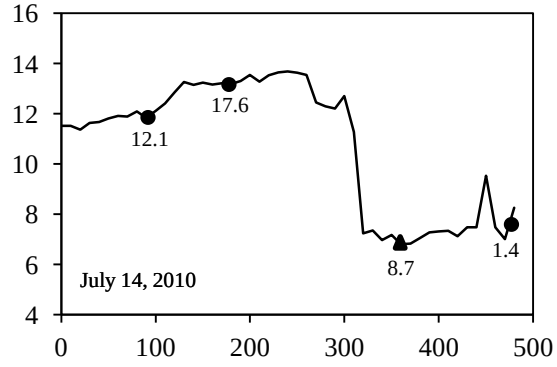

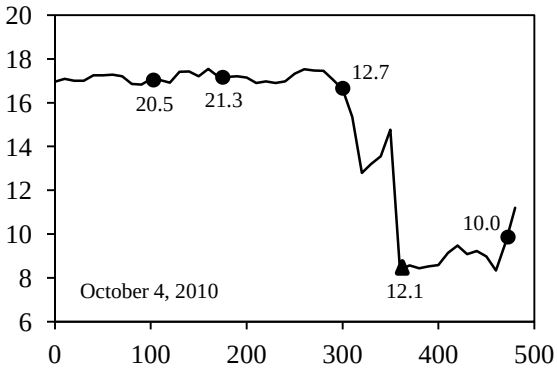

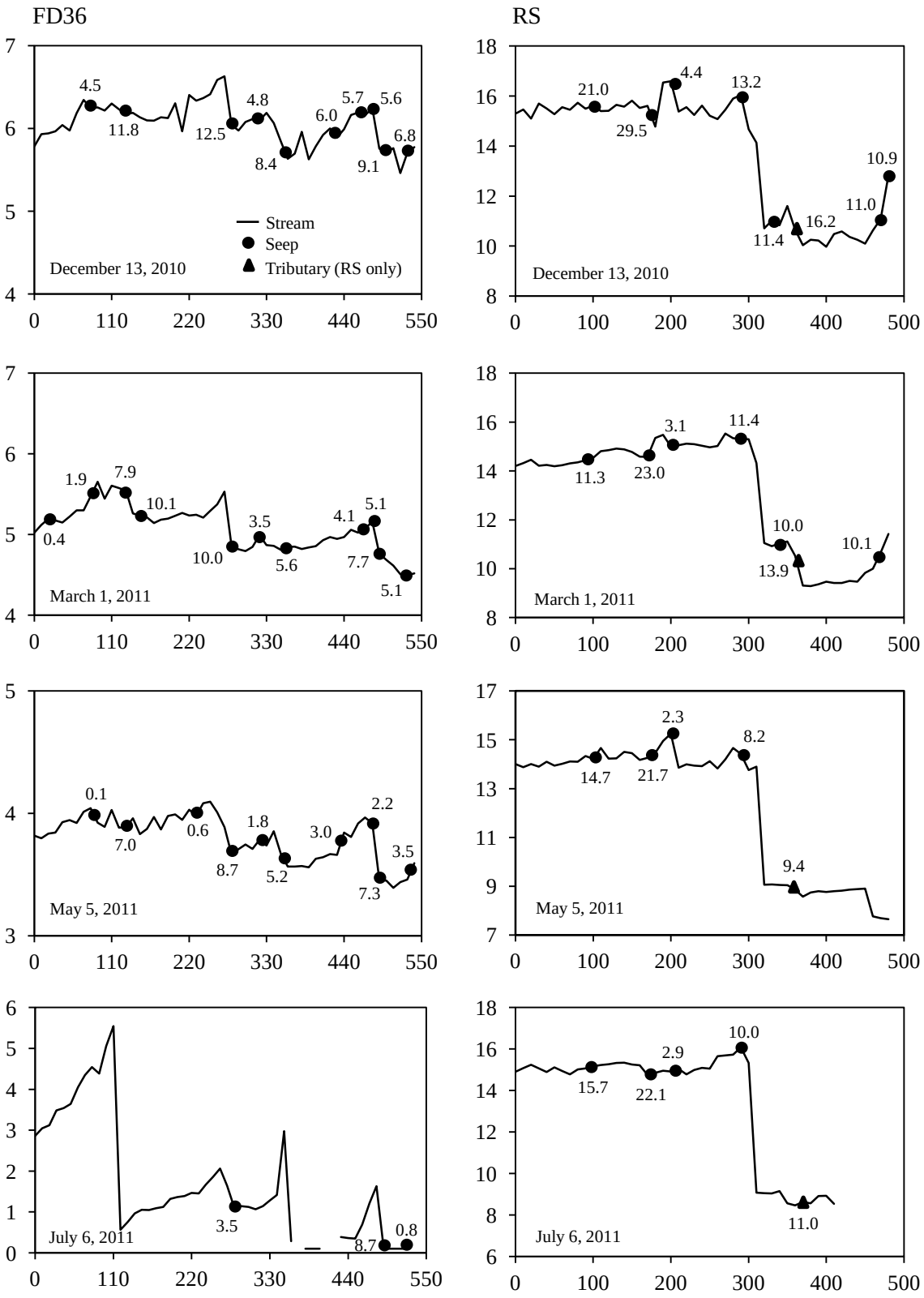
FD36
RS
Stream
Seep
Tributary (RS only)
December 13, 2010
March 1, 2011
May 5, 2011
July 6, 2011
4.5
11.8
12.5
4.8
8.4
6.0
5.7
9.1
5.6
6.8
21.0
29.5
4.4
13.2
11.4
16.2
11.0
10.9
1.9
7.9
10.1
0.4
10.0
3.5
5.6
4.1
7.7
5.1
5.1
11.3
23.0
3.1
11.4
13.9
10.0
10.1
0.1
7.0
0.6
8.7
1.8
5.2
3.0
7.3
2.2
3.5
14.7
21.7
2.3
8.2
9.4
15.7
22.1
2.9
10.0
11.0
3.5
8.7
0.8

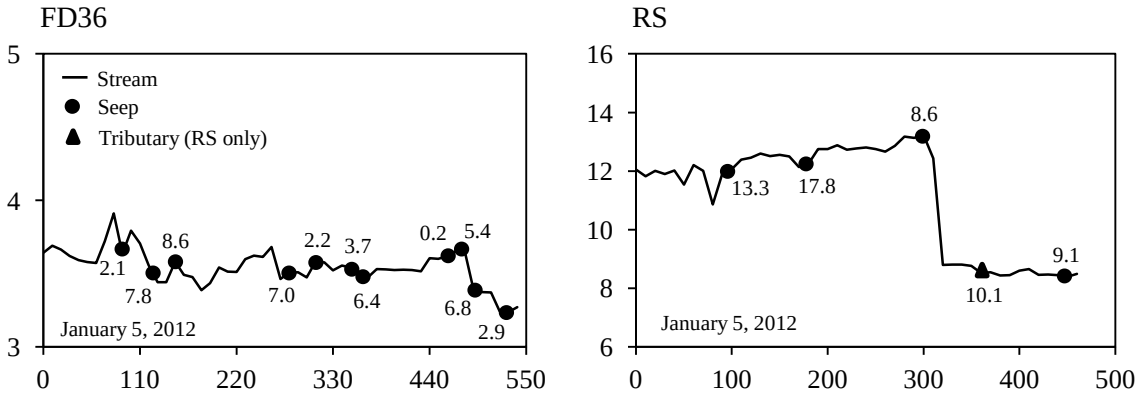

Storm Event Stream and Seep NO_3-N Concentrations

Similar to the previous section on baseflow NO_3-N concentration, the x-axis is the distance (m) from the stream outlet and the y-axis is NO_3-N concentration (mg L^{-1}). Seep location and NO_3-N concentration (mg L^{-1}) are also labeled.

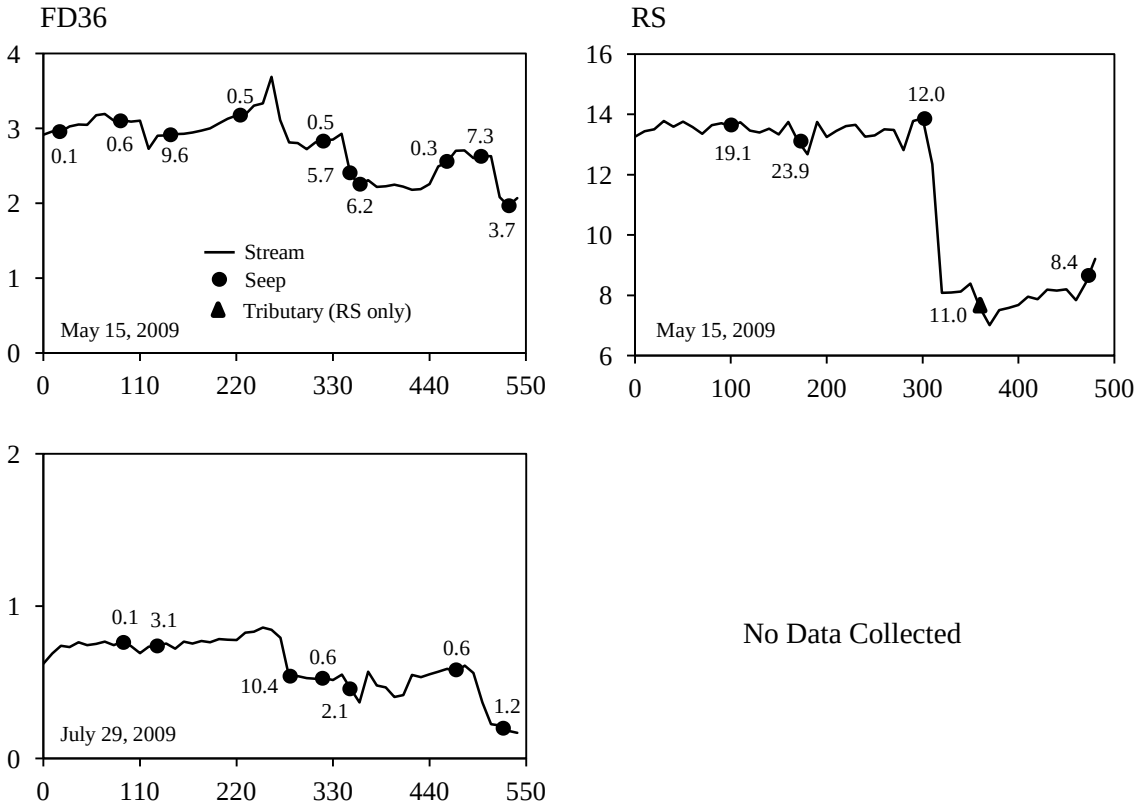

No Data Collected

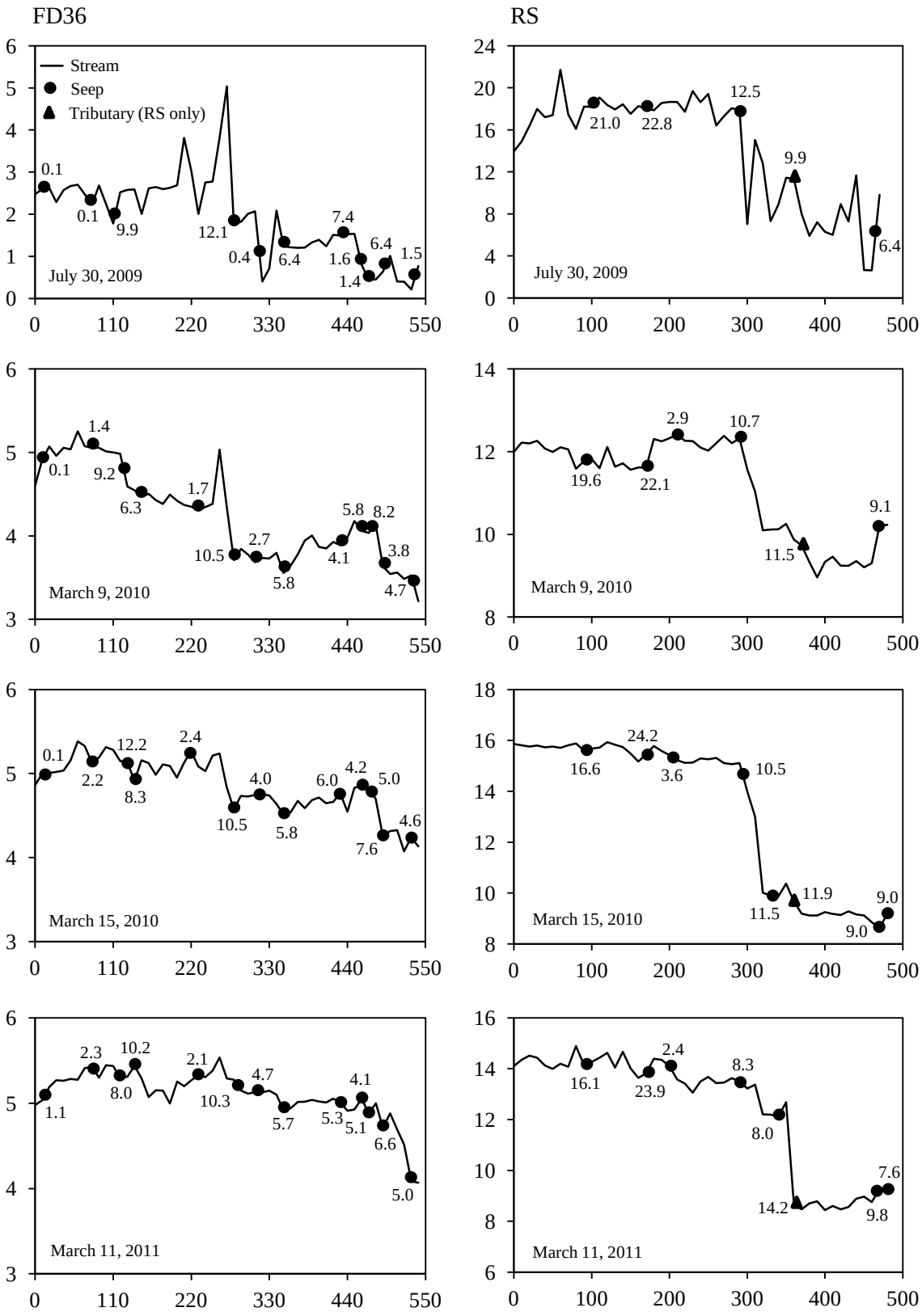
FD36
RS
Stream
Seep
Tributary (RS only)
July 30, 2009
March 9, 2010
March 15, 2010
March 11, 2011

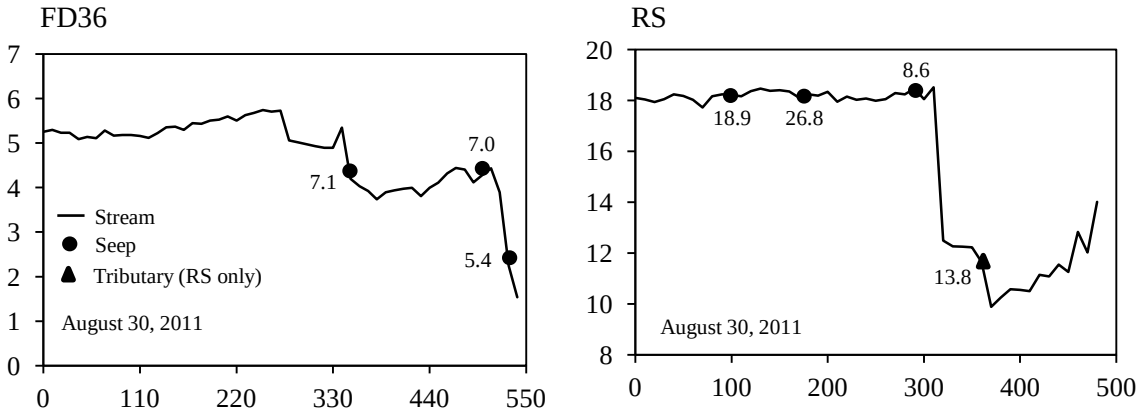

Semi-variogram Analysis of Stream NO_3-N Concentration

The x-axis is the lag distance (m) (i.e., the distance between two sample locations) and the y-axis is the semi-variance (i.e., half the average, squared difference between pairs of points) of stream NO_3-N concentration. Spherical models were fit to the data on all sampling dates (except July 30, 2009; linear model) to quantify the semi-variogram range (i.e., average patch size) and sill. The apparent y-intercept, called the nugget, represents measurement error or variability occurring at scales smaller than the sampling grain. We used a lag interval of 10 m and extended our analysis to a lag of 200 m.

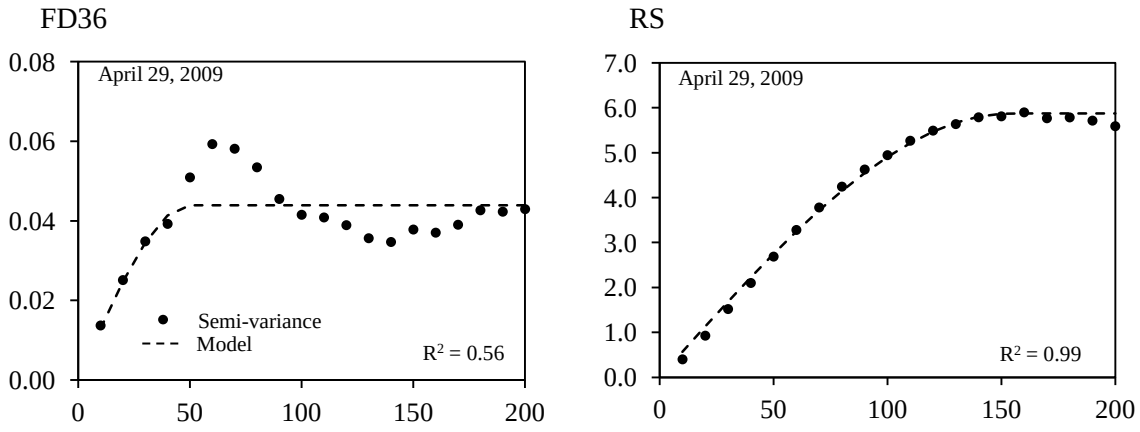

FD36

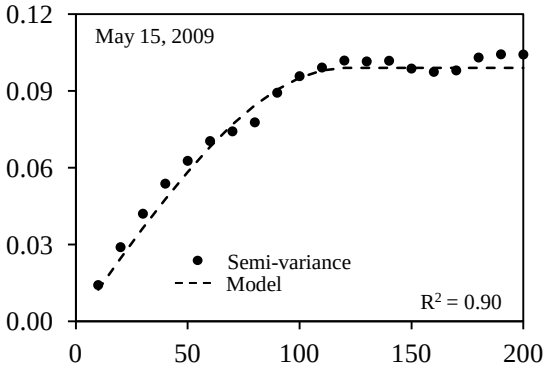

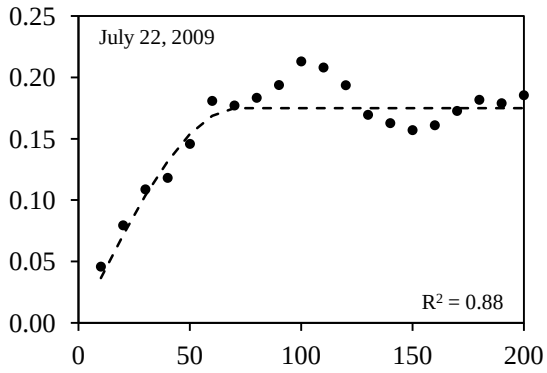

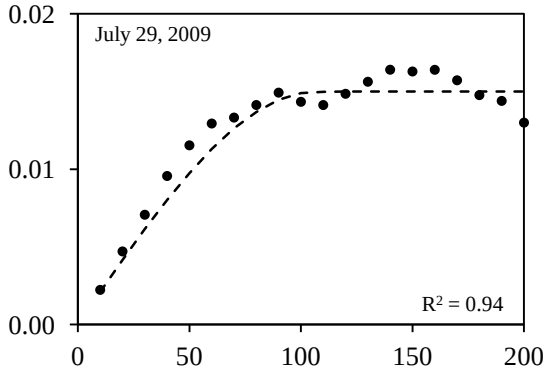

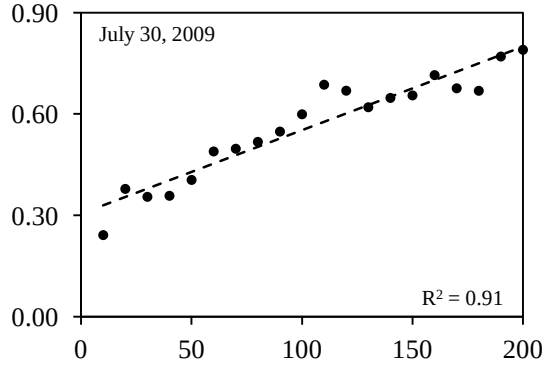

RS

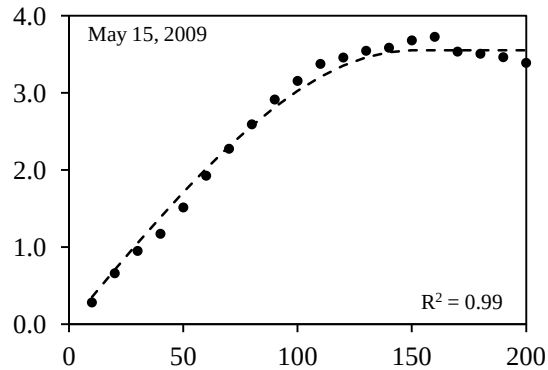

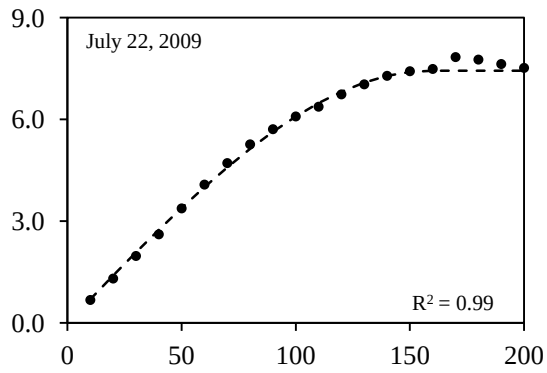

No Data Collected

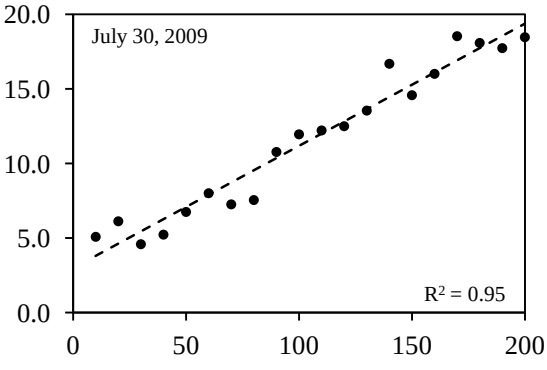

FD36

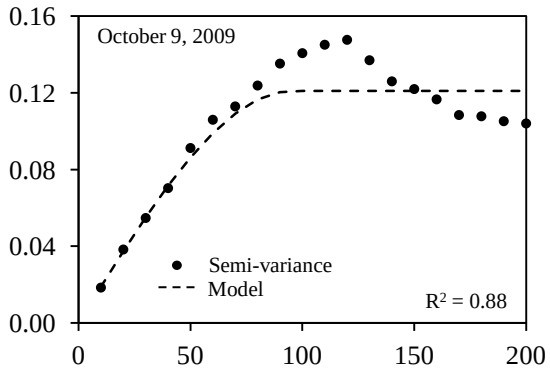

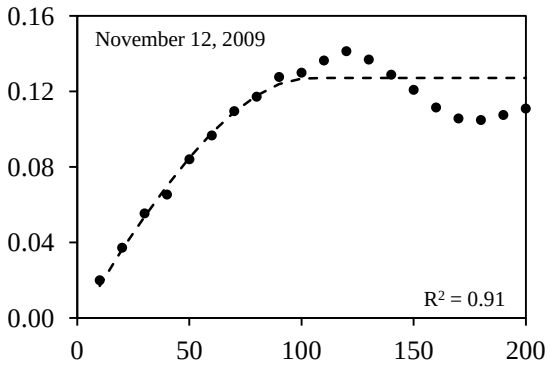

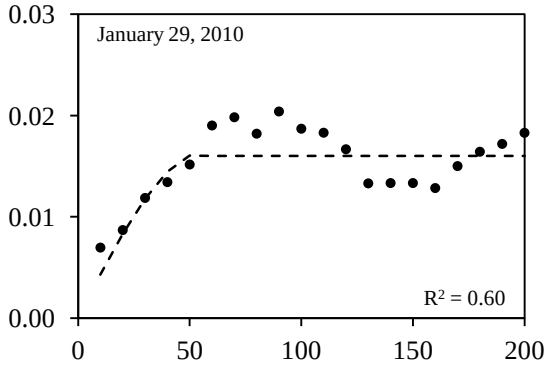

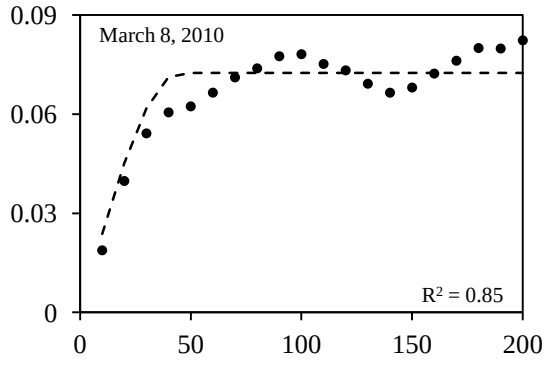

RS

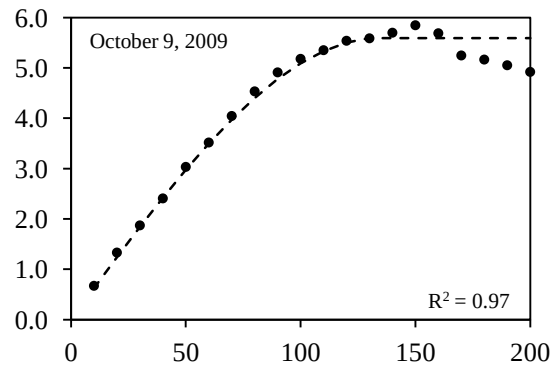

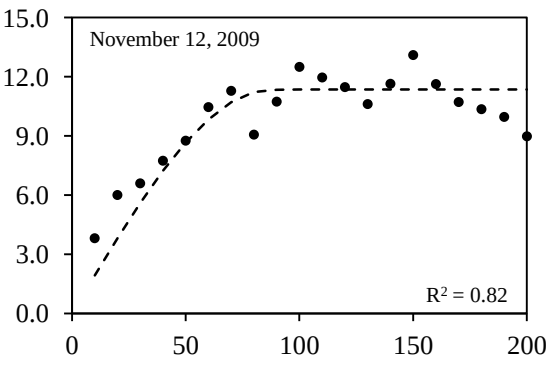

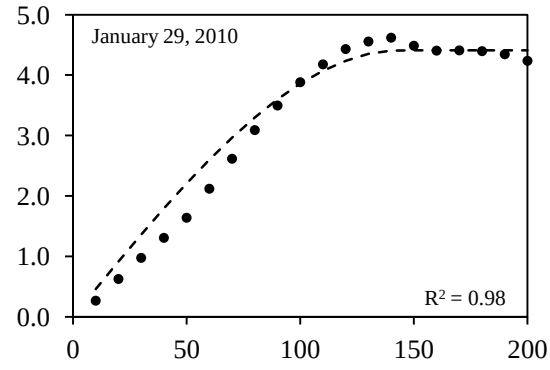

No Data Collected

FD36

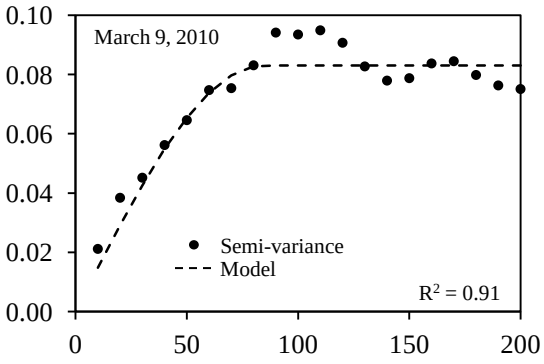
March 9, 2010
Semi-variance
Model
R² = 0.91
0.10
0.08
0.06
0.04
0.02
0.00
0
50
100
150
200

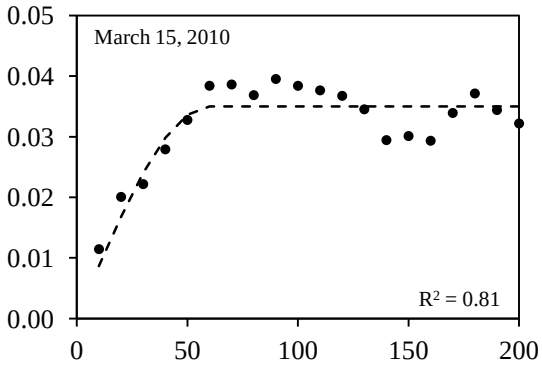
March 15, 2010
R² = 0.81
0.05
0.04
0.03
0.02
0.01
0.00
0
50
100
150
200

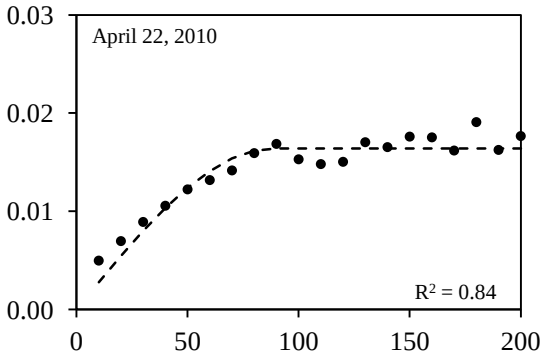
April 22, 2010
R² = 0.84
0.03
0.02
0.01
0.00
0
50
100
150
200

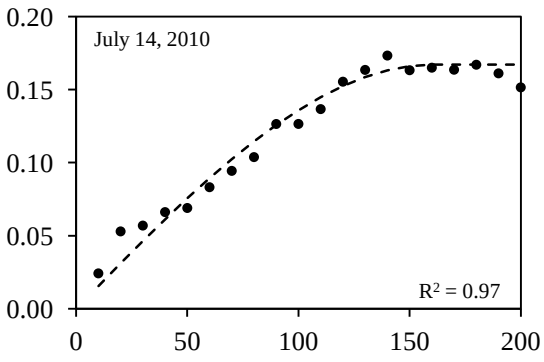
July 14, 2010
R² = 0.97
0.20
0.15
0.10
0.05
0.00
0
50
100
150
200

RS

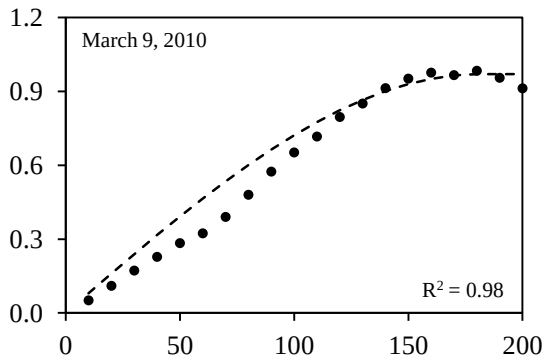
March 9, 2010
R² = 0.98
1.2
0.9
0.6
0.3
0.0
0
50
100
150
200

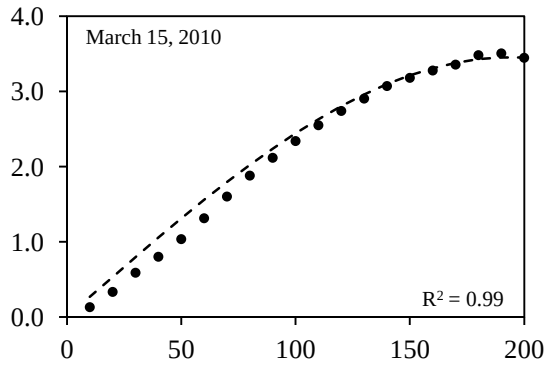
March 15, 2010
R² = 0.99
4.0
3.0
2.0
1.0
0.0
0
50
100
150
200

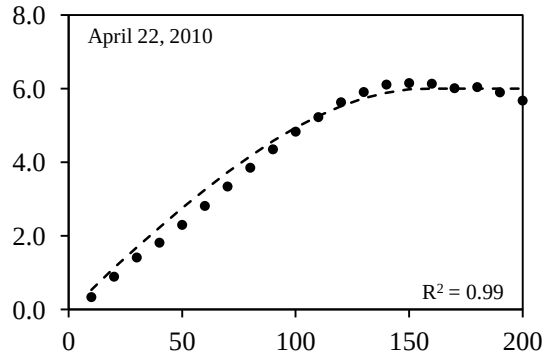
April 22, 2010
R² = 0.99
8.0
6.0
4.0
2.0
0.0
0
50
100
150
200

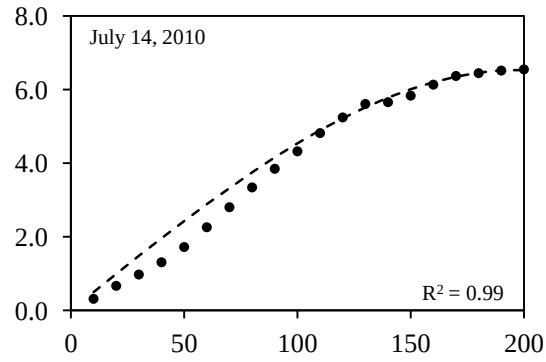
July 14, 2010
R² = 0.99
8.0
6.0
4.0
2.0
0.0
0
50
100
150
200

FD36

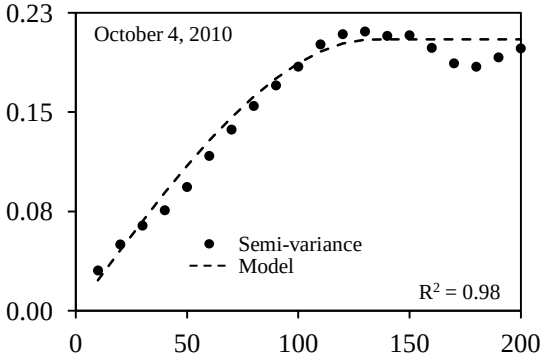
October 4, 2010
Semi-variance
Model
R² = 0.98
0.23
0.15
0.08
0.00
0
50
100
150
200

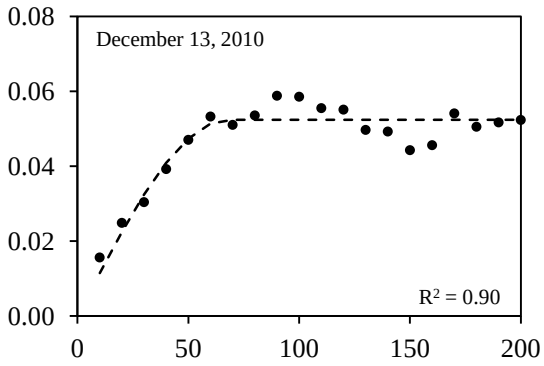
December 13, 2010
R² = 0.90
0.08
0.06
0.04
0.02
0.00
0
50
100
150
200

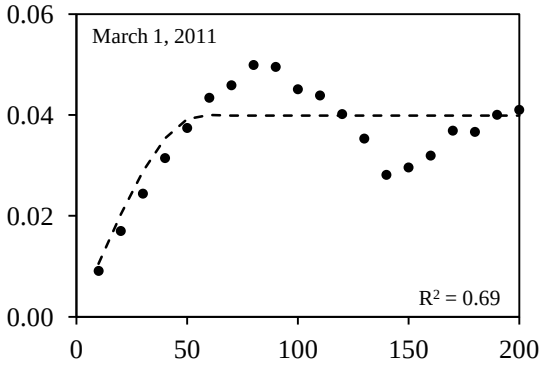
March 1, 2011
R² = 0.69
0.06
0.04
0.02
0.00
0
50
100
150
200

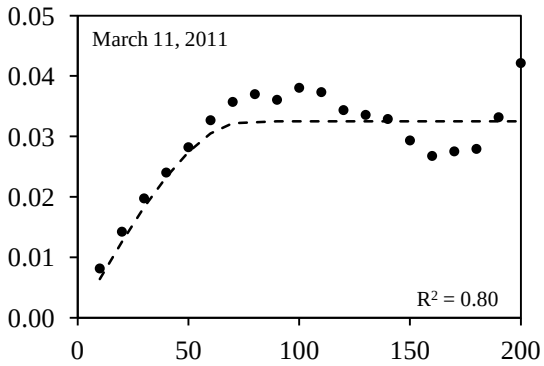
March 11, 2011
R² = 0.80
0.05
0.04
0.03
0.02
0.01
0.00
0
50
100
150
200

RS

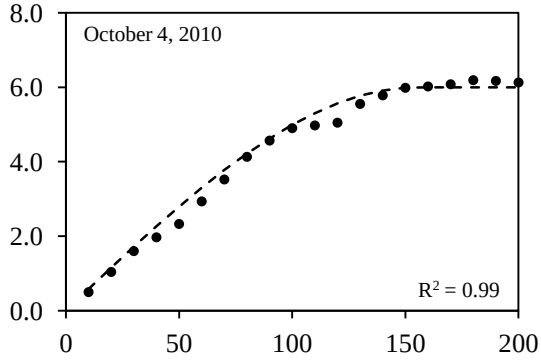
October 4, 2010
R² = 0.99
8.0
6.0
4.0
2.0
0.0
0
50
100
150
200

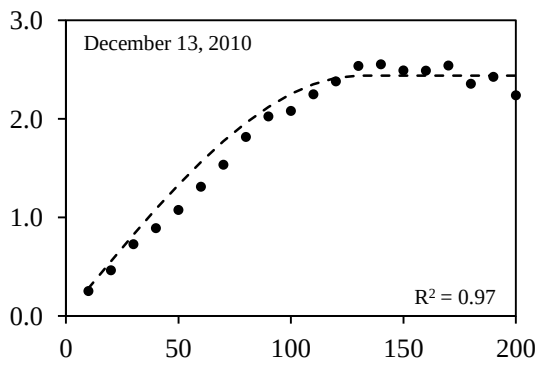
December 13, 2010
R² = 0.97
3.0
2.0
1.0
0.0
0
50
100
150
200

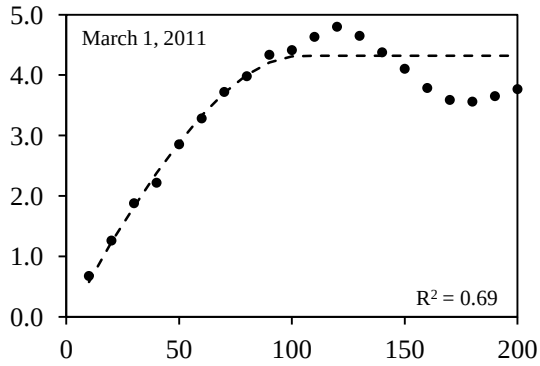
March 1, 2011
R² = 0.69
5.0
4.0
3.0
2.0
1.0
0.0
0
50
100
150
200

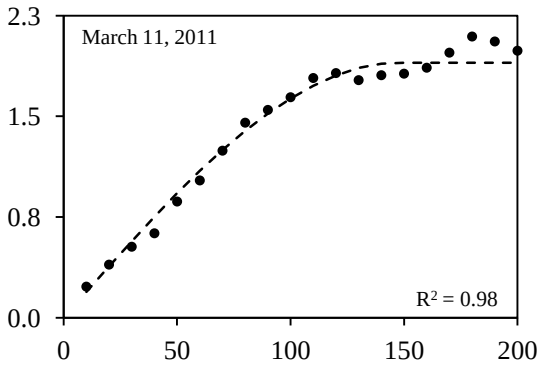
March 11, 2011
R² = 0.98
2.3
1.5
0.8
0.0
0
50
100
150
200

FD36

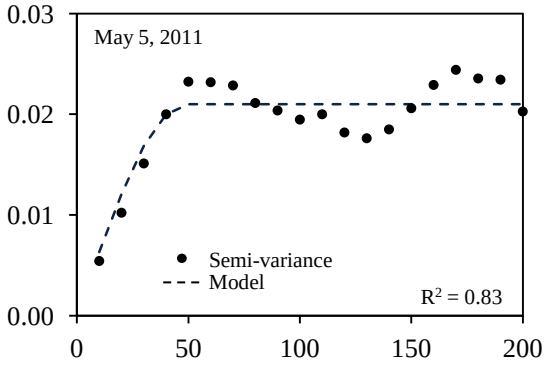
May 5, 2011
Semi-variance
Model
R² = 0.83

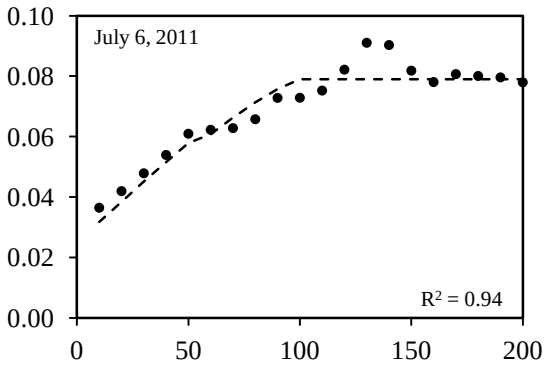
July 6, 2011
R² = 0.94

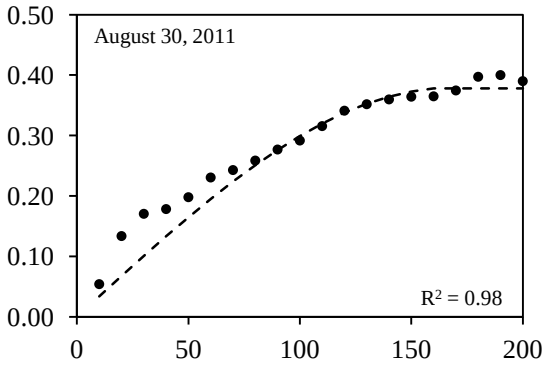
August 30, 2011
R² = 0.98

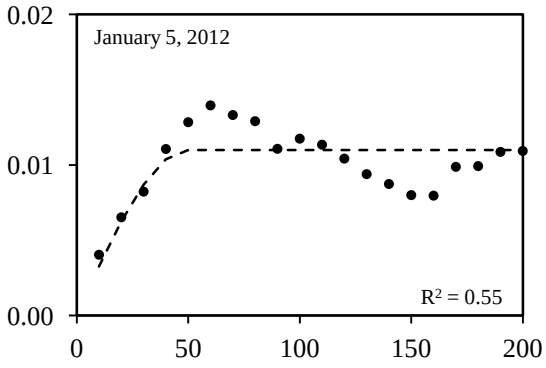
January 5, 2012
R² = 0.55

RS

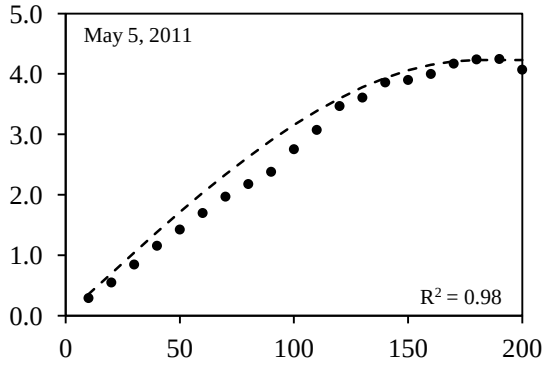
May 5, 2011
R² = 0.98

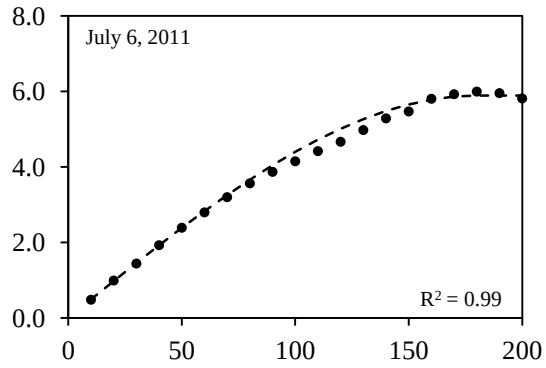
July 6, 2011
R² = 0.99

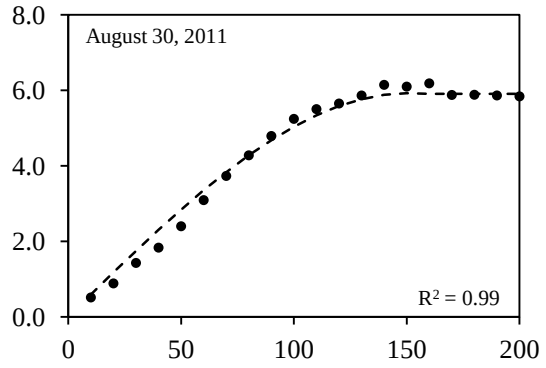
August 30, 2011
R² = 0.99

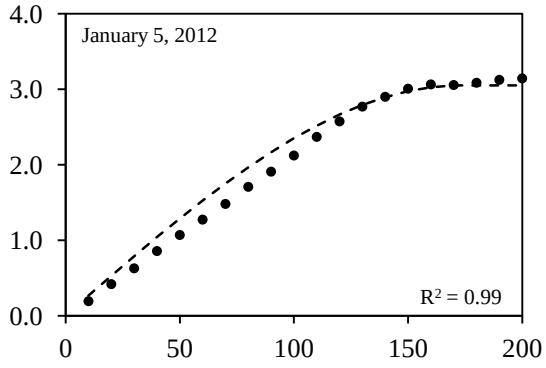
January 5, 2012
R² = 0.99

APPENDIX D

Stream, Seep, Groundwater, and Nitrogen Management Data for Chapter Five

This appendix contains the stream, seep, groundwater, and N management data that are presented in chapter five. There are six sections in this appendix: 1) nitrate-nitrogen (NO_3-N) concentrations at the seep top and bottom; 2) chloride (Cl^-) concentrations at the seep top and bottom; 3) stream discharge; 4) stream NO_3-N concentration; 5) monitoring well NO_3-N concentration; and 6) N management data. The figures in each section are formatted to display the data and are not meant to show the differences among sampling dates.

Seep Top and Bottom NO_3-N Concentrations

The x-axis is time (d) and the y-axis is NO_3-N concentration (mg L^{-1}). The seep top is where groundwater emerges onto the land surface and the bottom is 0.5 m from the stream.

Seep: 20-S

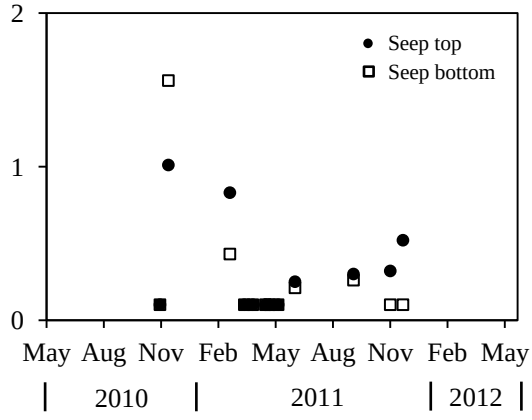

Seep: 80-S

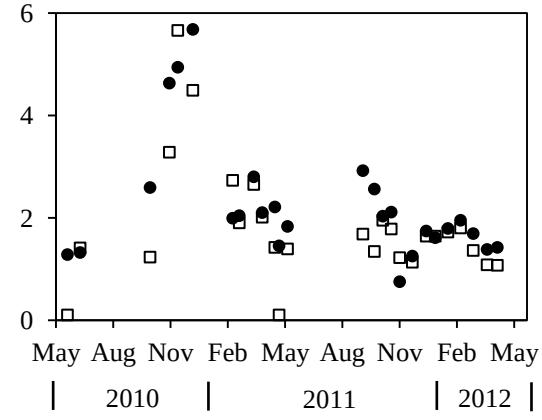

Seep: 120-N

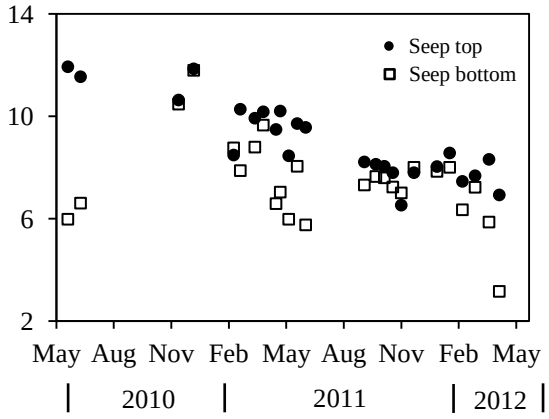

Seep: 140-N

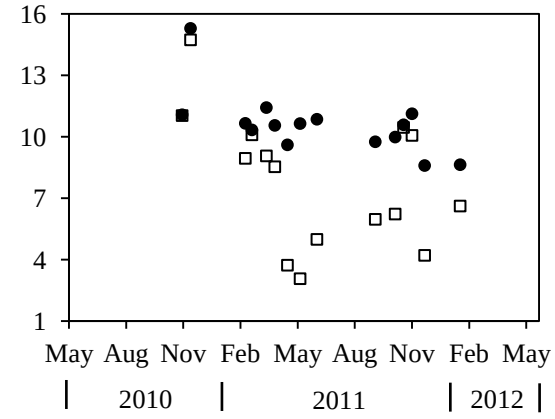

Seep: 220-S

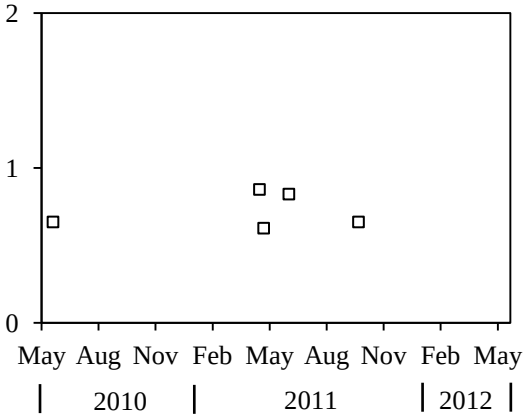

Seep: 280-N

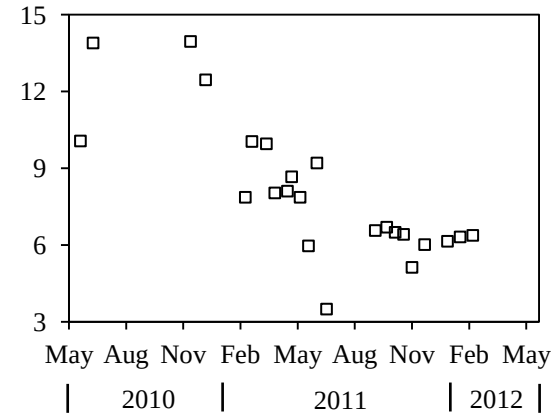

Seep: 310-S

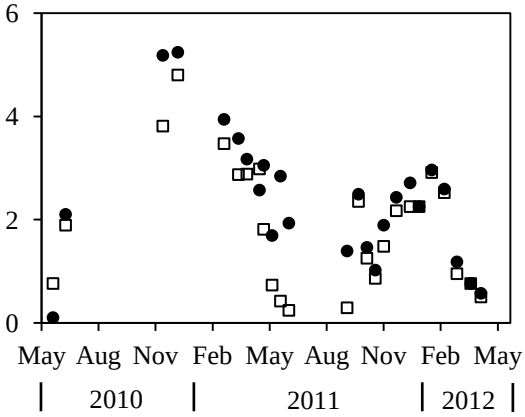

Seep: 350-S

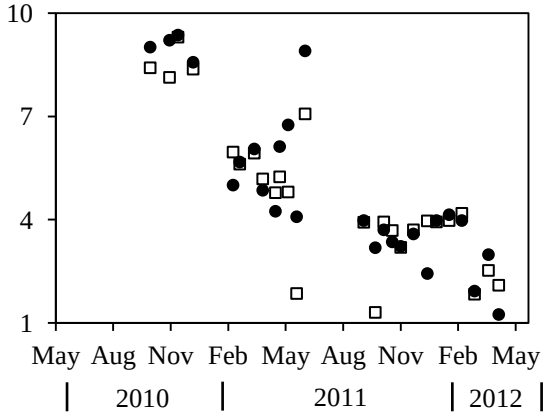

Rock Drain: 360-S

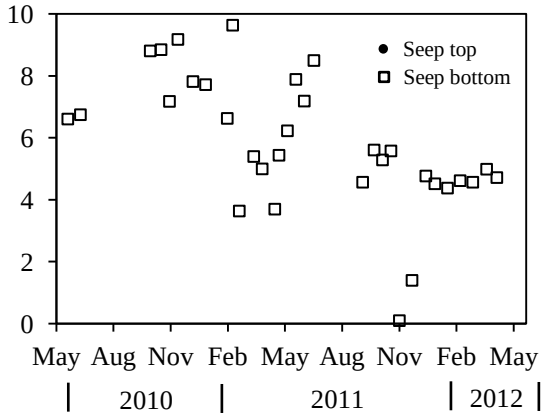

Seep: 430-N

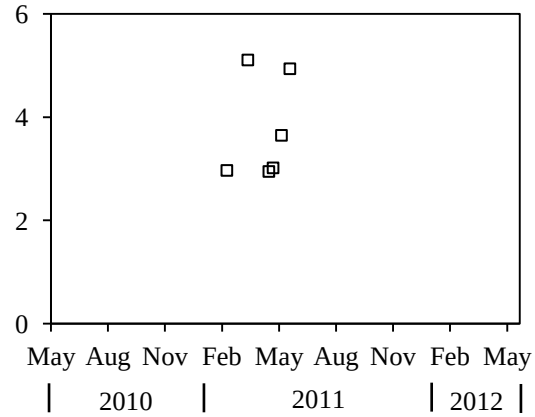

Seep: 460-S

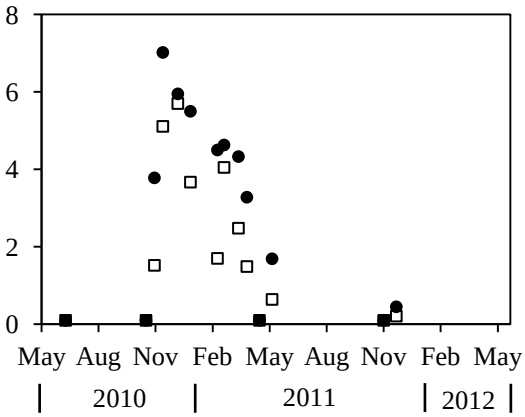

Seep: 470-N

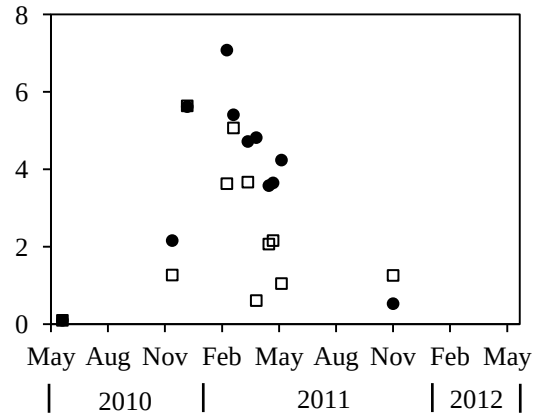

Seep: 490-N

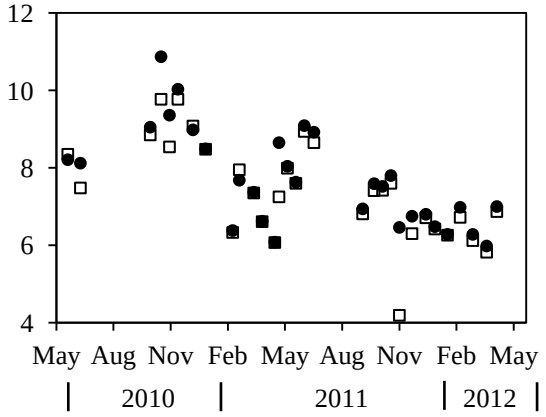

Seep: 530-S

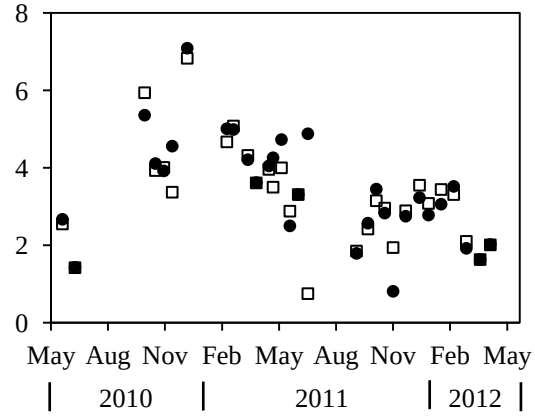

Seep Top and Bottom Cl^- Concentrations

The x-axis is time (d) and the y-axis is Cl^- concentration (mg L^{-1}).

Seep: 20-S

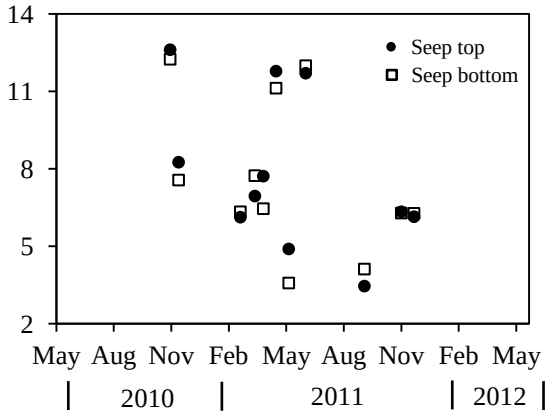

Seep: 80-S

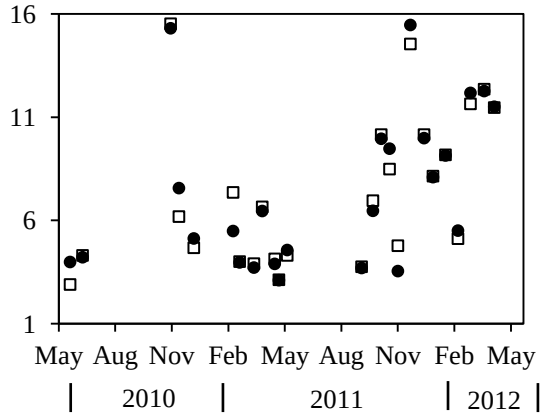

Seep: 120-N

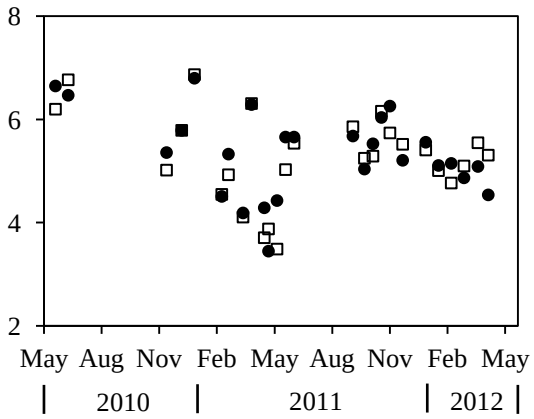

Seep: 140-N

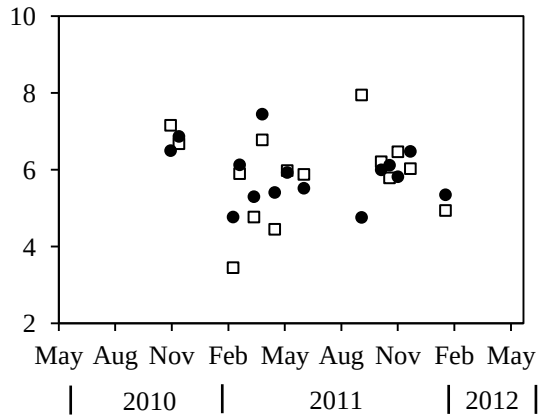

Seep: 220-S

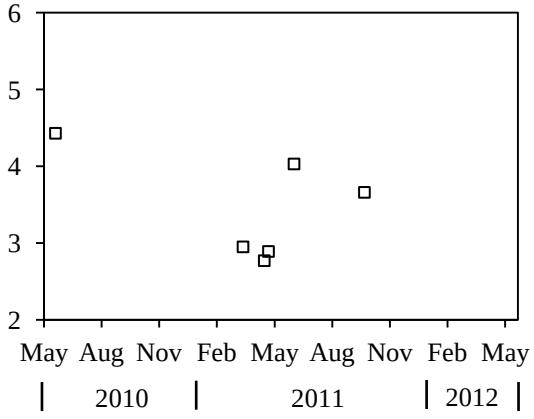

Seep: 280-N

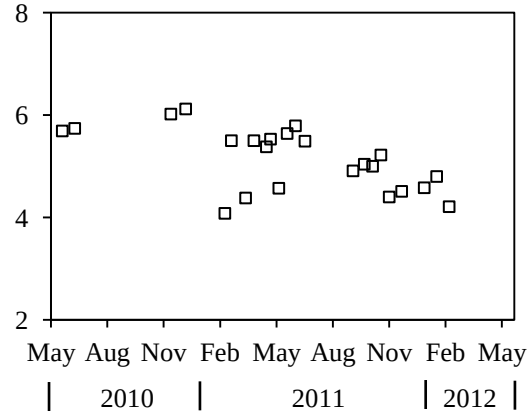

Seep: 310-S

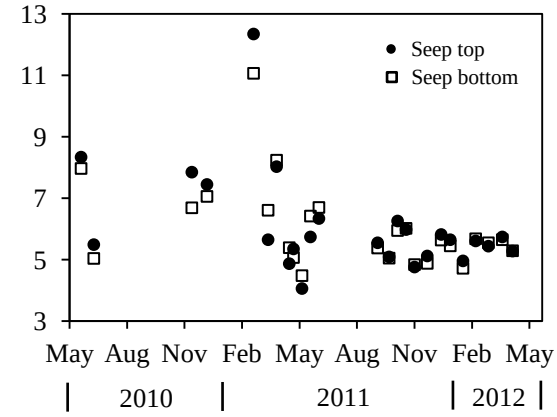

Seep: 350-S

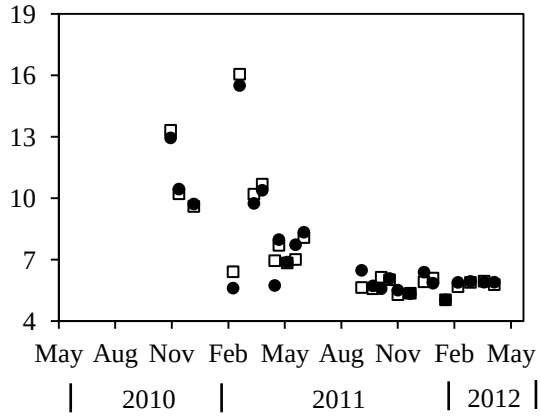

Rock Drain: 360-S

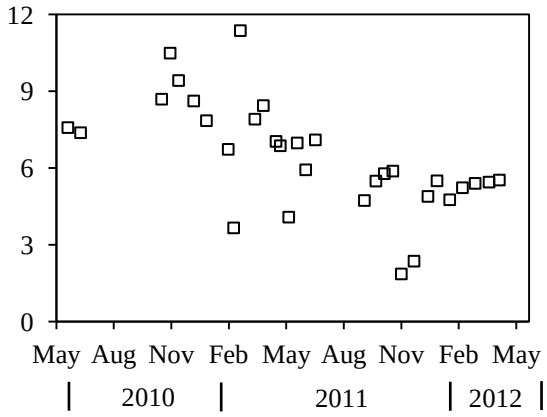

Seep: 430-N

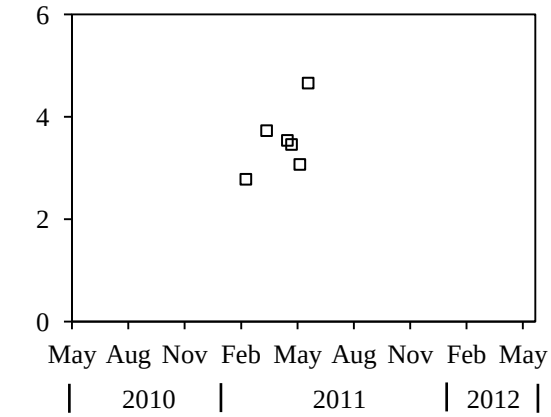

Seep: 460-S

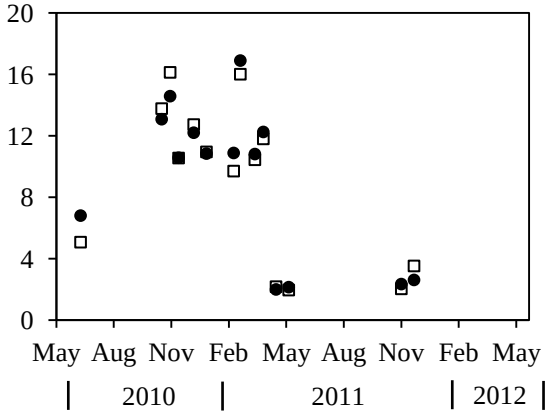

Seep: 470-N

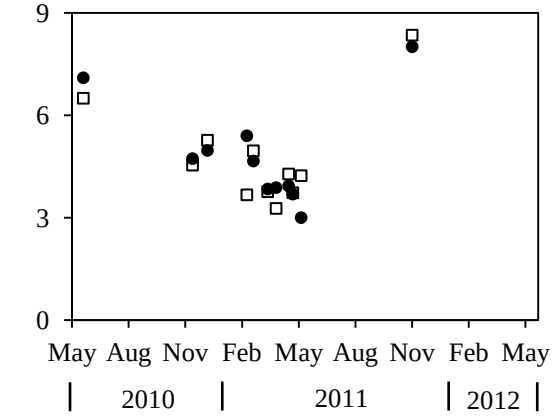

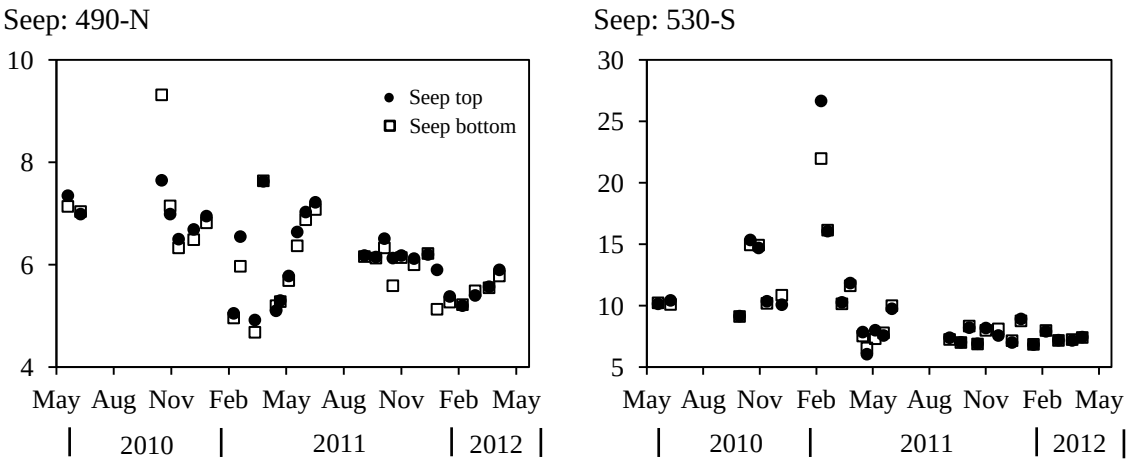

Stream Discharge

The x-axis is time (d) and the y-axis is stream discharge ($m^3 s^{-1}$). Stream discharge is collected every five minutes with recording H-flumes. The five minute data was used to calculate daily average discharge for each flume. A large storm on September 7, 2011 destroyed flumes 2 and 3; therefore, no data was recorded until they could be fixed in April 2012. Also, flumes 2, 3, and 4 often freeze during the winter; thus, the data collected is not accurate and has been removed. Seep sampling dates are labeled on the figure for flume 1.

Flume 1

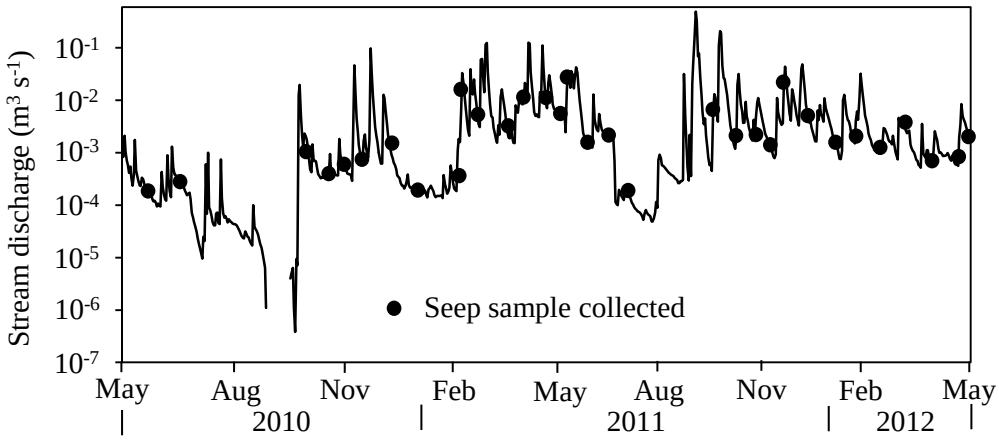

Flume 2

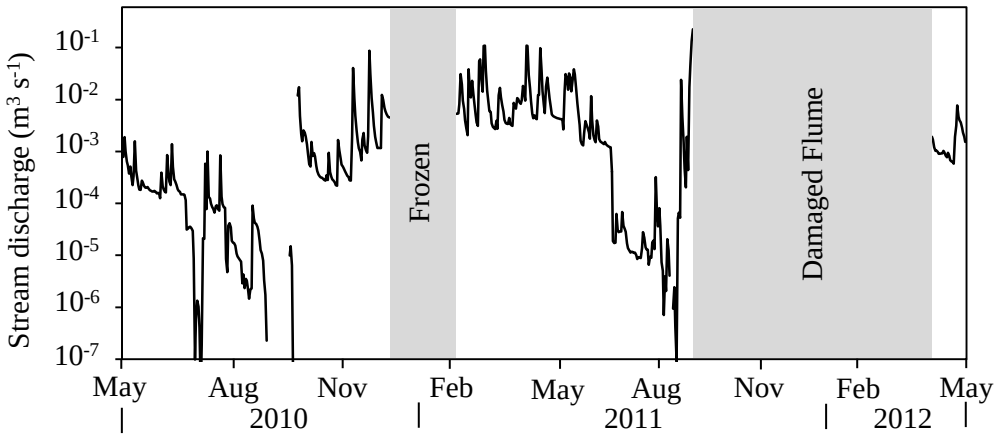

Flume 3

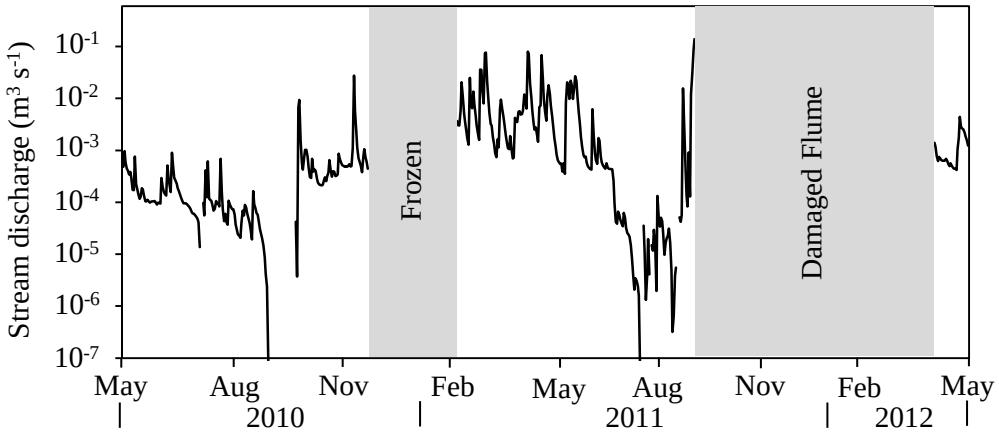

Flume 4

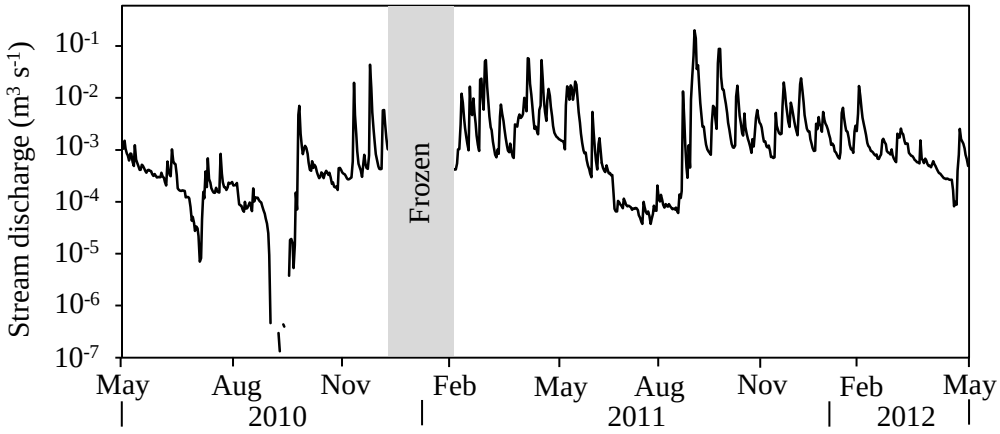

Stream NO_3-N Concentration

The x-axis is time (d) and the y-axis is stream NO_3-N concentration (mg L^{-1}). Stream NO_3-N concentration was sampled from the flumes in FD36 weekly. Flumes 2, 3, and 4 often freeze during the winter; thus, no data is collected during these time periods.

Flume 1

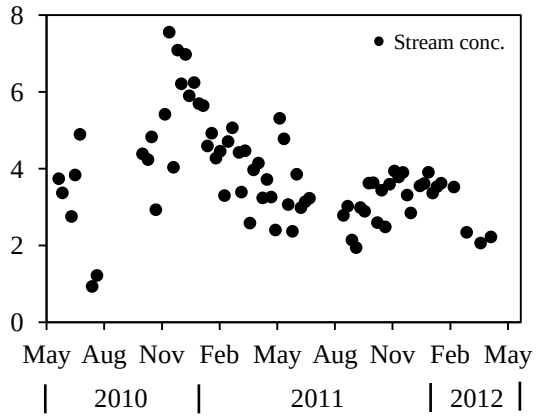

Flume 2

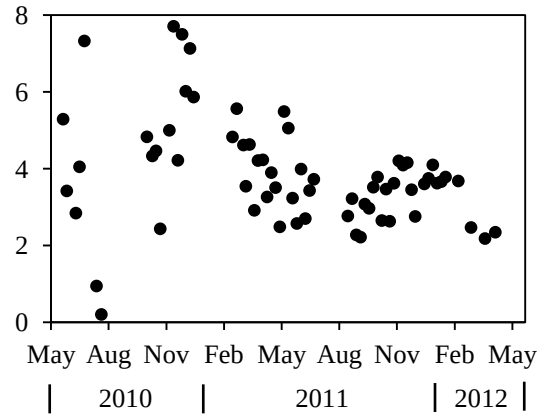

Flume 3

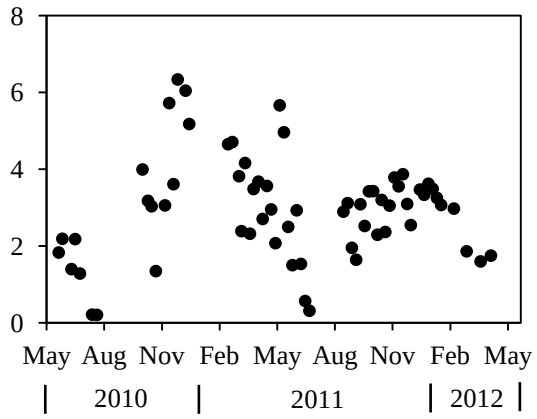

Flume 4

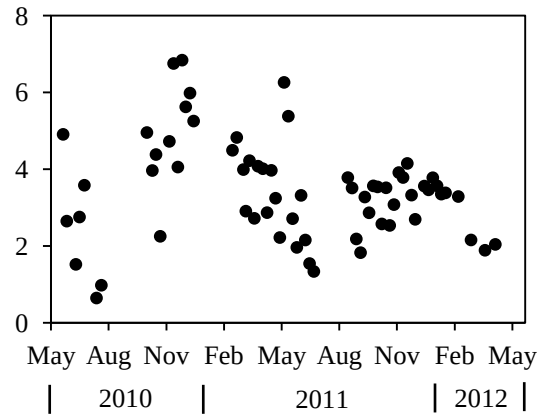

Monitoring Well NO_3-N Concentration

The x-axis is time (d) and the y-axis is monitoring well NO_3-N concentration (mg L^{-1}). Groundwater was sampled from piezometers at two depths (1 m, shallow; 6 m, deep).

Piezometer nest 1

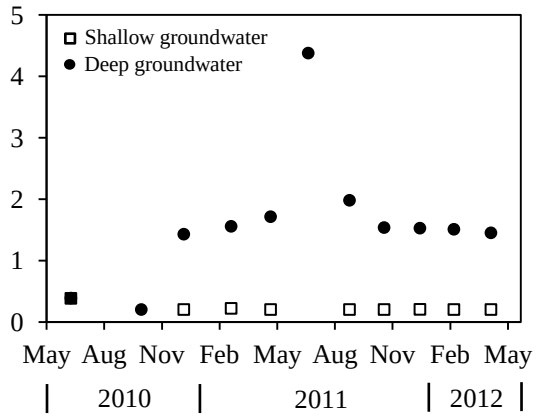

Piezometer nest 2

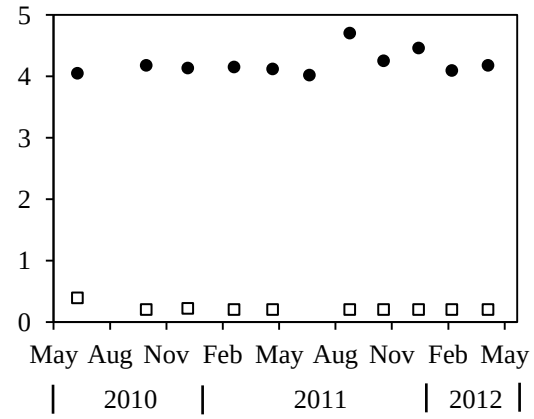

Piezometer nest 3

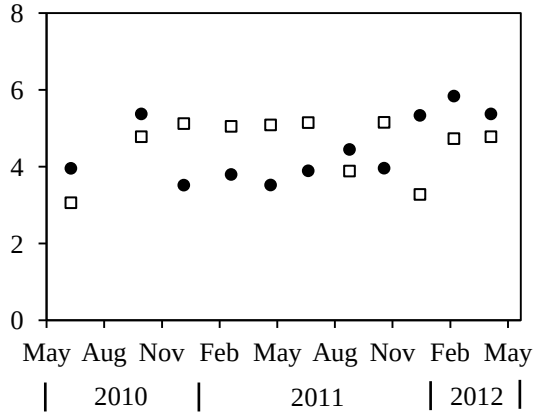

Piezometer nest 4

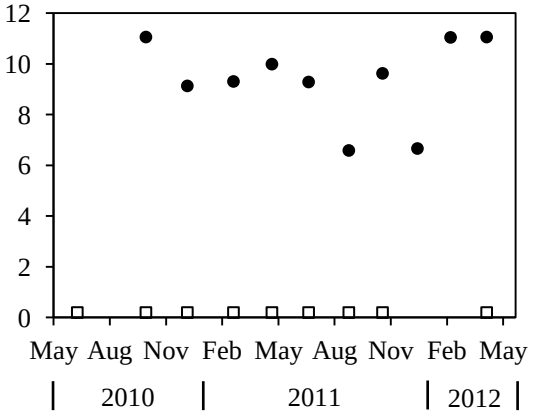

Piezometer nest 5

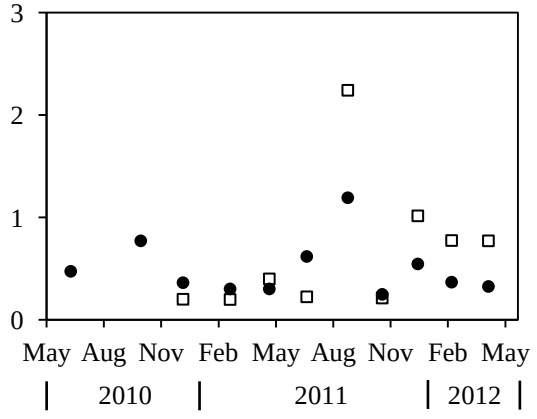

FD36 Annual N Application rates

2007

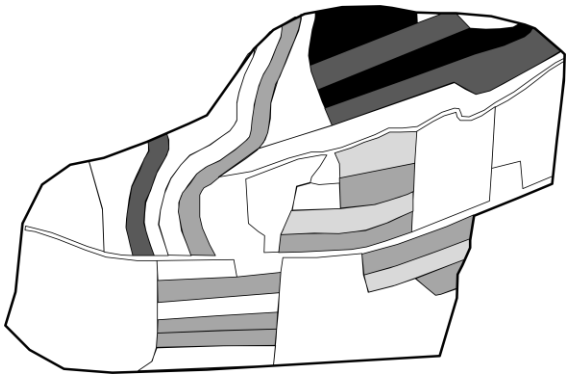

2008

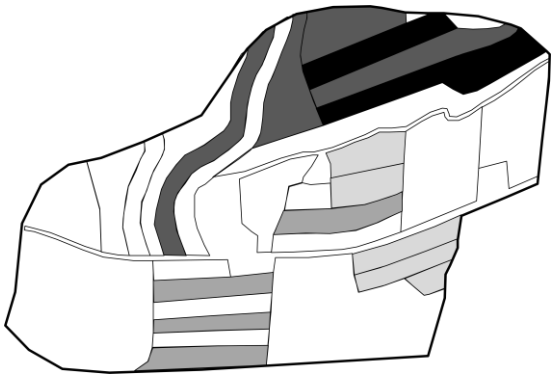

2009

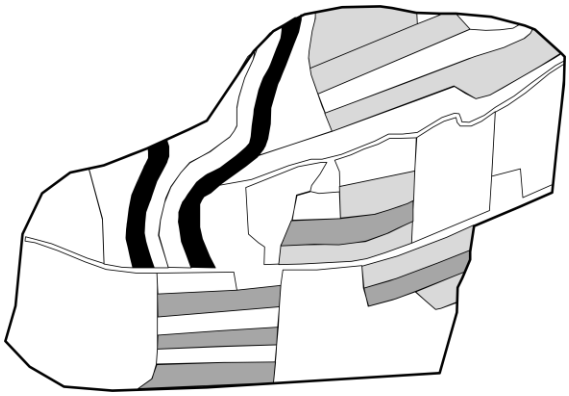

2010

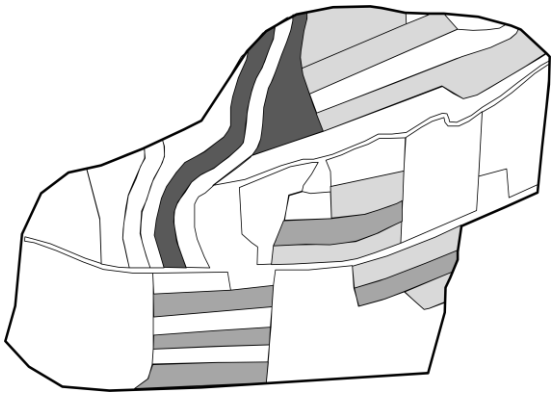

2011

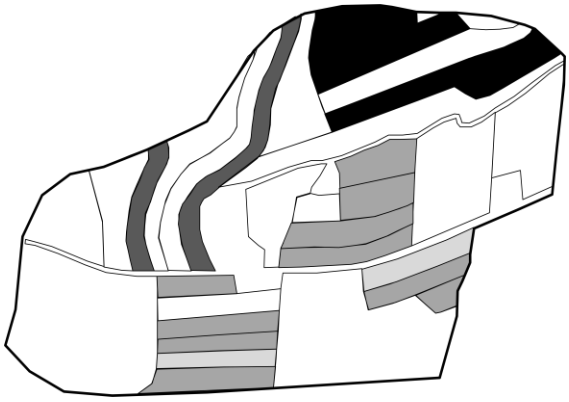

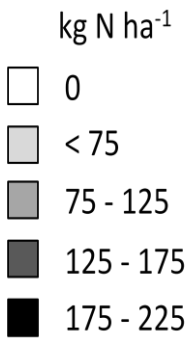

RS Annual N Application rates

2007

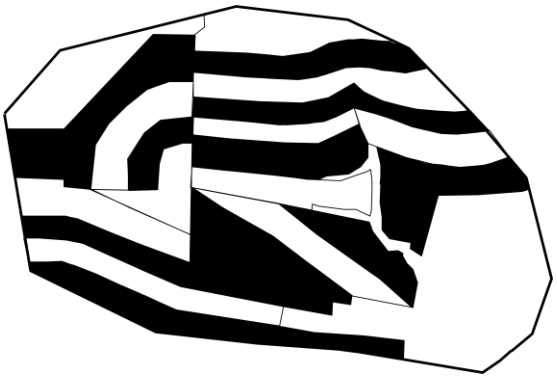

2008

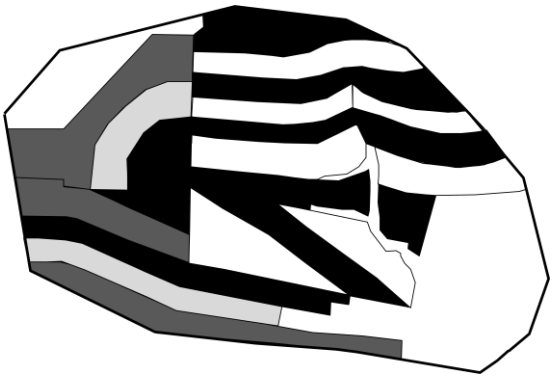

2009

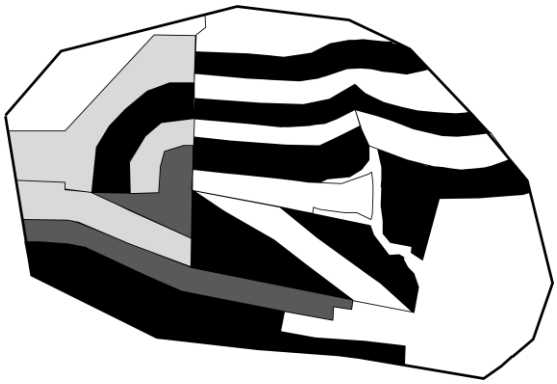

2010

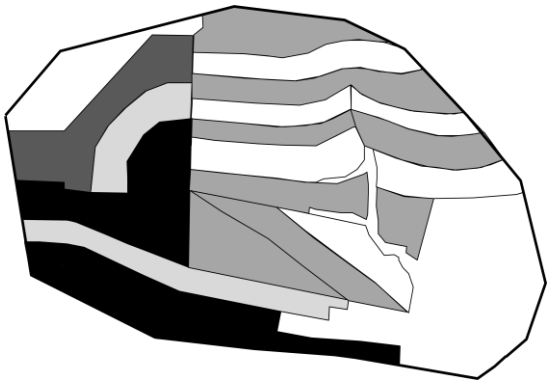

2011

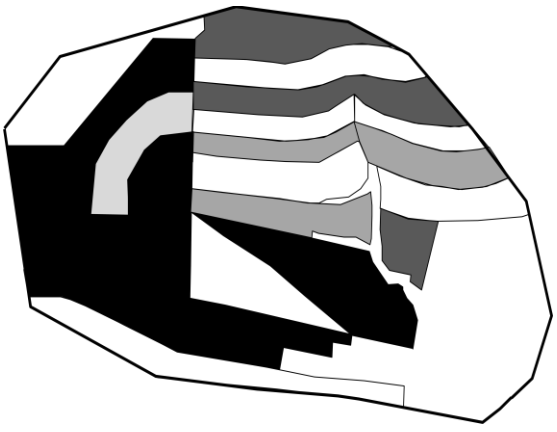

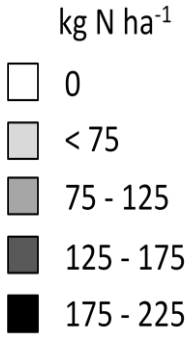

Curriculum Vitae

MARK R. WILLIAMS

EDUCATION

Doctor of Philosophy in Agricultural and Biological Engineering, The Pennsylvania State University, Department of Agricultural and Biological Engineering, University Park, PA, 2013. DISSERTATION: *Spatial and Temporal Variability of Nitrogen Transport in Riparian Zone Seeps*

Master of Science in Agricultural and Biological Engineering, The Pennsylvania State University, Department of Agricultural and Biological Engineering, University Park, PA, 2010. THESIS: *Manure Application Under Winter Conditions*

Bachelor of Science in Environmental Resource Management, The Pennsylvania State University, University Park, PA, 2008. SPECIALIZATION: *Soil Science and Watershed and Water Resources Management*

PROFESSIONAL AND ACADEMIC EXPERIENCE

Postdoctoral Research Agricultural Engineer, USDA-ARS, Soil Drainage Research Unit, Columbus, OH, starting June 2013

Graduate Research Assistant, The Pennsylvania State University, Department of Agricultural and Biological Engineering, University Park, PA, 2010-2013

Student Laboratory Technician, USDA-Agricultural Research Service, University Park, PA, 2010

Graduate Teaching Assistant, The Pennsylvania State University, Department of Agricultural and Biological Engineering, University Park, PA, 2008-2010

Student Waste Handler, The Pennsylvania State University, Department of Environmental Health and Safety, 2006-2009.

PUBLICATIONS

Williams, M.R., G.W. Feyereisen, D.B. Beegle, and R.D. Shannon. 2012. Soil temperature regulates phosphorus loss from lysimeters following fall and winter manure application. *Transactions of the ASABE* 55(3): 871-880.

Williams, M.R., G.W. Feyereisen, D.B. Beegle, and R.D. Shannon. 2012. Soil temperature regulates nitrogen loss from lysimeters following fall and winter manure application. *Transactions of the ASABE* 55(3): 861-870.

Williams, M.R., G.W. Feyereisen, D.B. Beegle, R.D. Shannon, G.J. Folmar, and R.B. Bryant. 2011. Manure application under winter conditions: nutrient runoff and leaching losses. *Transactions of the ASABE* 54(3): 891-899.

Williams, M.R., G.W. Feyereisen, G.J. Folmar, and H.S. Lin. 2010. Experimental system for simulating a natural soil temperature profile during freeze-thaw cycles. *Applied Engineering in Agriculture* 26(5): 843-848.